



# **Foresight study on laboratory modelling of wave and ice loads on coastal and marine structures**

**J. Sutherland and K.-U. Evers (Editors)**

**Deliverable D2.3**  
**EC contract no. 261520, HYDRALAB-IV**

**Status:** Public Document  
**Version:** 2.1  
**Date:** Sept 2013



## Document Information

Title	Foresight study on laboratory modelling of wave or ice loads on coastal and marine structures
Lead Authors	J Sutherland and K-U Evers (Editors)
Contributors	W Allsop, D Donnai, J Kirkegaard, S Schimmels, K Ramachandran, M Paul, M le Boulluec, J Ohana, CT Stansberg, B Hofland, P Prinos, F Taveira Pinto, R von Bock und Polach, O Gudmestad & R Guttierrez-Serrat
Distribution	Public document
Document Reference	HYDRALAB-IV Deliverable D2.3. DOI: 10.5281/zenodo.3368939

## Document History

Date	Revision	Prepared by	Organisation	Approved by	Status
April 2013	1.0	J. Sutherland K.-U. Evers	HR Wallingford HSVA	Simone van Schijndel	Restricted Release for comment
Sept. 2013	2.0	J. Sutherland K.-U. Evers	HR Wallingford HSVA	Simone van Schijndel	Incorporates IAHR paper
Aug 2019	2.1	J. Sutherland	HR Wallingford		CC licence & DOI added. Release date remains 2013 as no content changed.

## Acknowledgement



The work described in this publication was supported by the European Community's 7th Framework Programme through the grant to the budget of the Integrated Infrastructure Initiative HYDRALAB-IV, Contract no. 261520.

## Disclaimer

This document reflects only the authors' views and not those of the European Community. This work may rely on data from sources external to the HYDRALAB project Consortium. Members of the Consortium do not accept liability for loss or damage suffered by any third party as a result of errors or inaccuracies in such data. The information in this document is provided "as is" and no guarantee or warranty is given that the information is fit for any particular purpose. The user thereof uses the information at its sole risk and neither the European Community nor any member of the HYDRALAB Consortium is liable for any use that may be made of the information.

## License

This report is licensed under the Creative Commons Attribution 4.0 International License. To view a copy of this license, visit <https://creativecommons.org/licenses/by/4.0/>.



## Abstract

The measurement of wave and / or ice loads on coastal and maritime structures can play an important role in their final design. The number and range of man-made structures that are subject to these loads is increasing – from offshore oil and gas facilities, through ships and, renewable energy devices, to breakwaters, quay walls, bridges and tunnels. This Foresight Study was produced by member of the [HYDRALAB](#) Joint Research Activity 'Hydraulic Response of Structures' (HyReS) on how the physical modelling of the interactions between structures and wave or ice forces may evolve. It starts with a review of the present state-of-the-art, identifies present shortcomings and identifies likely future developments.

The anticipated short-term advances include the development of:

- sampling schemes to allow shorter test series to be run;
- methods for computing the low-frequency response of floating structures;
- wave-generation techniques for tsunamis;
- shallow-water wave generation for wind waves;
- tactile pressure sensors to measure forces that vary in space and time;
- active transducers to reproduce non-linear mooring lines;
- remote sensing of water levels over wide areas;
- optical and acoustic devices for making measurements over surfaces or in 3D volumes; and
- data access through development of met-data and data standards and data-transfer techniques.

The longer-term (more speculative) changes that are anticipated include the:

- development of composite models with full two-way coupling between numerical and physical models in real time;
- drawing together of physical modellers with CFD modellers, who are developing numerical flumes and wave basins, to address similar problems;
- continued reduction in sensor size, improvements in resolution, increases in sampling frequency and improved spatial coverage, leading to much more detailed datasets;
- development of the active laboratory, with many more computer-controlled non-linear devices;
- improved treatment of uncertainty; and
- More open access to data as part of a wider movement towards open science.

## Contents

FORESIGHT STUDY ON LABORATORY MODELLING OF WAVE OR ICE LOADS ON COASTAL AND MARINE STRUCTURES.....		- 1 -
J.Sutherland and K.-U. Evers (Editors).....		- 1 -
1	Introduction.....	- 1 -
1.1	Scope of work.....	- 2 -
1.2	Contents .....	- 2 -
2	Review of topics .....	- 4 -
2.1	Ship moored in a harbour.....	- 4 -
2.1.1	General considerations	- 5 -
2.1.2	Similarity Law, scale of the model and scale effects	- 6 -
2.1.3	The tests	- 6 -
2.2	Moored and free floating structures in deep water.....	- 7 -
2.2.1	Applications and types of structures	- 8 -
2.2.2	Key issues for model testing in waves, current and wind	- 8 -
2.3	Response of fixed structures to waves and currents.....	- 10 -
2.3.1	Vertical breakwaters and crown walls of rubble-mound breakwaters-	- 10 -
2.3.2	Sloping structures - revetments and dykes	- 13 -
2.3.3	Surface-piercing bottom-mounted offshore structures	- 17 -
2.3.4	Submerged offshore structures	- 18 -
2.4	Response of structures to ice.....	- 21 -
2.4.1	General	- 21 -
2.4.2	Mooring systems in ice	- 25 -
2.5	Changes in the use of laboratories .....	- 33 -
2.5.1	From tides to turbulence	- 33 -
2.5.2	The rise of marine renewable energy	- 34 -
2.5.3	Impact of climate change on hydrodynamic load testing	- 34 -
2.5.4	Impact of climate change on ice load testing	- 35 -
3	Establishing the correct environment.....	- 40 -
3.1	Establishing the correct hydrodynamic environment .....	- 40 -
3.1.1	Wave generation and absorption	- 40 -
3.1.2	Wind Generation	- 52 -
3.1.3	Current generation and recirculation	- 53 -
3.1.4	Surface elevation measurement and analysis	- 54 -
3.1.5	Flow velocity measurement	- 61 -
3.1.6	Air content	- 62 -
3.2	Establishing the correct ice conditions.....	- 66 -
3.2.1	Production of model ice sheet	- 66 -
3.2.2	Ice sheet production methods	- 69 -
3.2.3	Ice properties	- 71 -
3.2.4	Modeling of different ice conditions	- 79 -
4	State of the art in modelling techniques.....	- 92 -
4.1	Model construction .....	- 92 -
4.1.1	Stiffness / rigidity	- 92 -
4.1.2	Mooring lines, catenary moorings and fenders	- 92 -
4.1.3	Ballasting and mass distribution in floating bodies	- 96 -
4.1.4	Permeability of rock structures	- 96 -
4.1.5	Dynamic ice friction	- 97 -
4.1.6	Sliding of caissons, blockwork and crown-walls	- 99 -



4.2	Measurement and analysis techniques.....	- 99 -
4.2.1	Load cells (Force Measurements)	- 99 -
4.2.2	Torque measurements	- 104 -
4.2.3	Pressure measurements	- 105 -
4.2.4	Motion detectors	- 106 -
4.2.5	Photography	- 107 -
5	Shortcomings.....	- 110 -
5.1	Statistical nature of response .....	- 110 -
5.1.1	Long duration tests for extreme response	- 110 -
5.1.2	Sampling extreme waves from field measurements	- 110 -
5.1.3	Design wave	- 110 -
5.1.4	Sampled waves	- 111 -
5.1.5	Importance sampling	- 111 -
5.1.6	Scatter and repeatability in impulsive wave events	- 112 -
5.2	Limitations in sensor technology .....	- 112 -
5.2.1	Limited spatial resolution of sensors	- 112 -
5.2.2	Sensor range (Sensor resolution over a large measuring range)	- 113 -
5.2.3	Sensor resolution and signal on noise ratio.	- 113 -
5.2.4	Whole body movement	- 113 -
5.2.5	Mooring lines	- 114 -
5.2.6	Two phase flows	- 114 -
5.2.7	Optical techniques in turbid water	- 114 -
5.2.8	Wave-structure interactions	- 114 -
5.3	Limitations in facilities.....	- 114 -
5.3.1	Wave generation in deep water	- 114 -
5.3.2	Current generation	- 114 -
5.4	Using model results .....	- 114 -
5.4.1	Linking to numerical models	- 114 -
5.4.2	Data management	- 115 -
6	Short-term developments .....	- 116 -
6.1	Sampling Schemes.....	- 116 -
6.2	Quadratic transfer functions .....	- 116 -
6.3	Coupling of Boussinesq model to wave paddle .....	- 117 -
6.4	Tsunami generation.....	- 117 -
6.5	Focused wave generation .....	- 118 -
6.6	Tactile sensors .....	- 119 -
6.6.1	Tekscan sensors	- 119 -
6.6.2	Application in wave flume	- 121 -
6.6.3	Application in ice model testing	- 123 -
6.7	Active transducers for nonlinear loads .....	- 127 -
6.7.1	Traditional representation of non-linear loads	- 127 -
6.7.2	Application of servo-motor	- 128 -
6.7.3	Non-passive effects	- 131 -
6.8	Wave measurements (area).....	- 131 -
6.9	Extension of acoustic and optical measurements to 3D .....	- 133 -
6.10	Data access .....	- 134 -
7	Longer time-scale changes in capabilities .....	- 135 -
7.1	Development of composite models .....	- 135 -
7.2	Learning from CFD .....	- 135 -
7.3	Sensor developments.....	- 135 -
7.4	Facility developments .....	- 136 -

7.4.1	Hybrid facilities: process simulators	- 136 -
7.4.2	Link to geotechnics: modelling clay	- 137 -
7.5	The active laboratory	- 138 -
7.6	Treatment of uncertainty	- 139 -
7.7	Open Science	- 139 -
8	Discussion and conclusions	- 142 -
9	References	- 144 -
10	Appendix A, Contributors to the report	- 165 -
11	Appendix B Catenary mooring	- 166 -
12	Appendix C Foresight Study on the Physical Modelling of Wave and Ice Loads on Marine Structures	- 168 -

### Tables

Table 2.1	Fixed and moored floating offshore structure types	- 23 -
Table 3.1	Wave focusing methods as currently used in physical wave modelling	- 46 -
Table 2.2	Method of model ice production and use of dopants at different ice facilities	- 69 -
Table 3.3	Types of ice floes	- 79 -
Table 6.1	Correlation between load cell and tactile sensor sheet	- 127 -

### Figures

Figure 2.1	Moored ship behaviour tests for enlargements to the ports of Las Palmas (left) and Coruña (right) in Spain	- 5 -
Figure 2.2	Instrumentation for moored ship behaviour tests	- 7 -
Figure 2.3	Examples of vertical breakwaters (Allsop, 2000)	- 11 -
Figure 2.4	Example wave loadings, pulsating and impulsive, on a simple vertical wall with small toe berm, test 10003 from Allsop et al (1996)	- 11 -
Figure 2.5	Idealised rubble mound breakwater with crown wall, after Burcharth (1994)	- 13 -
Figure 2.6	Revetment armour thickness, $t_a$ , for slabs, blocks and rock armour, after McConnell & Allsop (1999)	- 14 -
Figure 2.7	Wave-in-deck loads on an idealised section of a jetty platform supported by piles, after Cuomo et al.(2007)	- 16 -
Figure 2.8	Idealised filtered time history of vertical load acting on an elevated platform	- 16 -
Figure 2.9	Idealised filtered time history of horizontal load acting on an elevated platform	- 16 -
Figure 2.10	Breaking wave impact on bottom mounted cylinder	- 17 -
Figure 2.11	The photo shows two riser segments suspended in the test flume. To the right is shown the setup for a spanning pipeline model test in the same flume.	- 19 -
Figure 2.12	Vortex shedding behind two riser segments	- 19 -
Figure 2.13	Model test of vortex induced vibrations of a pipeline performed in a towing tank	- 20 -
Figure 2.14	Model of tunnel element during installation test	- 21 -
Figure 2.15	Selected different concepts of moored floating structures and vessels tested in ice at HSVA	- 24 -
Figure 2.16	Catenary mooring line arrangement (example)	- 26 -
Figure 2.17	Mooring lines arrangement (a) & components of catenary mooring system (b)	- 26 -
Figure 2.18	Single mooring line characteristic (left) and restoring moment (right)	- 26 -
Figure 2.19	Horizontal restoring force curve (left) and vertical restoring force curve (right) [full scale values]	- 27 -

Figure 2.20	Moored FPU during ice vaning model tests (Evers, 2008).....	- 28 -
Figure 2.21	Different segments of the SPAR model (Evers & Jochmann, 2011).....	- 29 -
Figure 2.22	(a) Schematic diagram of moored SPAR model; (b) SPAR model in the 5 m deep ice tank section (model scale 1:45) , (Evers & Jochmann, 2011).....	- 29 -
Figure 2.23	OIB model with “dry” mooring system (a) ; FPU model in fixed mode connected to the transverse carriage (b) .....	- 30 -
Figure 2.24	Outline of ice-vaning scenarios carried out in level ice and manoeuvring in ridges (Evers, 2011) .....	- 31 -
Figure 2.25	Schematic diagrams and photographs of a “dry” mooring system.....	- 32 -
Figure 2.26	Fixed mode test setup of a floating production unit (FPU).....	- 33 -
Figure 2.27	Changes in sea ice extent .....	- 37 -
Figure 2.28	Dynamic positioning in ice .....	- 39 -
Figure 2.29	Ice failure at a lighthouse and a physical model of the lighthouse.....	- 39 -
Figure 3.1	Wave paddles. (a) Articulated type. (b) Piston type. ....	- 40 -
Figure 3.2	Oblique waves generated by the wave generator to the right. (a) 3D wavemaker at rest. (b) 3D wavemaker in absorbing mode. ....	- 42 -
Figure 3.3	Wave packet registration at different positions (left), instantaneous wave profiles at selected instants (right) (Clauss 2000).....	- 44 -
Figure 3.4	Schematic view of the computer controlled optimization of waves (Clauss, Schmittner 2007) .....	- 45 -
Figure 3.5	Tsunami time series.....	- 47 -
Figure 3.6	Tsunami / bore wave created on shallow foreshore of GLOBEX Hydralab project (Deltares).....	- 49 -
Figure 3.7	N-wave generated in old Delta Flume and overtopping a dike slope (Hofland et al 2013) .....	- 49 -
Figure 3.8	Schematic drawing of the HR Wallingford / UCL Tsunami Generator .....	- 50 -
Figure 3.9	Tsunami Generator mounted within the wave flume, the adjustable outlet is in the foreground under water .....	- 51 -
Figure 3.10	The Mercator time series at 1:50 scale using the HR Wallingford Tsunami Generator .....	- 51 -
Figure 3.11	UK Coastal research facility (courtesy of HR Wallingford).....	- 53 -
Figure 3.12	General purpose flume with variable height tail gate (courtesy of HR Wallingford) .....	- 54 -
Figure 3.13	Resistive wave gauge functional diagram .....	- 55 -
Figure 3.14	Capacitive wave gauge functional diagram and example of set up on a model at Ifremer .....	- 55 -
Figure 3.15	Servo wave gauge functional diagram and example at Ifremer.....	- 55 -
Figure 3.16	Ultrasonic wave gauge functional diagram and example at Ifremer .....	- 56 -
Figure 3.17	Laser wave gauge functional diagram and example at Ifremer .....	- 56 -
Figure 3.18	Starry sky basin at HR Wallingford in 1974 .....	- 56 -
Figure 3.19	Void fraction measurements and photographs of air entrained in a plunging breaker: (a) $t = 9T/40$ , (b) $t = 13T/40$ , and (c) $t = 17T/40$ , where $T$ is the wave period. (Blenkinsopp and Chaplin 2007). ....	- 64 -
Figure 3.20	Dual-tip conductivity probe (a) Probe in operation, flow from bottom left to top right (b) Definition sketch (Murzyn and Chanson 2009).....	- 65 -
Figure 3.21	Voltage output of conductivity probe (Murzyn and Chanson 2009) .....	- 65 -
Figure 3.22	Vertical and horizontal thin sections with microbubble inclusions of HSVA’s model ice .....	- 68 -
Figure 3.23	Water is sprayed under high pressure into the air of the pre-cooled ice tank at HSVA forming crystal nuclei which settle down on the water surface .....	- 69 -
Figure 3.24	History of temperature during a freezing-warming-cycle in the ice tank at HSVA. ....	- 70 -
Figure 3.25	The spraying process at Aalto University .....	- 71 -

Figure 3.26	Flexural strength versus brine volume fraction for sea ice as measured with large beams in field testing (Timco, 1986) .....	- 72 -
Figure 3.27	Point loading beam with LVDT designed by HSVA (upward loading).....	- 74 -
Figure 3.28	In-situ cantilever beam loading (downward loading); load vs. time plot.....	- 74 -
Figure 3.29	3-point loading beam (downward loading).....	- 74 -
Figure 3.30	Determination of strain modulus (plate approach) .....	- 75 -
Figure 3.31	10 kN uni-axial compression testing machine as used at HSVA .....	- 78 -
Figure 3.32	Test setup for ice density tests at HSVA .....	- 79 -
Figure 3.33	Modeling of ice floes .....	- 80 -
Figure 3.34	Ice floe production (left) and ice floe distribution prior to testing (right) .....	- 80 -
Figure 3.35	Picture sequence along the ice tank (example) .....	- 81 -
Figure 3.36	Examples of stitched pictures (a-b), (c) example of binary image .....	- 81 -
Figure 3.37	Preparation of brash ice channel at HSVA.....	- 82 -
Figure 3.38	Production of a brash ice channel at Aalto University .....	- 83 -
Figure 3.39	Brash ice channel (Aalto University).....	- 83 -
Figure 3.40	Ice sheet cut into stripes (left) and steel beam submerging ice when pushed by towing carriage (right).....	- 84 -
Figure 3.41	Geometric characteristics of a pressure ice ridge .....	- 84 -
Figure 3.42	First-year ice ridge modelled at HSVA: (a) ridge embedded in level ice sheet, (b-c) adfrozen ridge fragments from consolidated part of ridge .....	- 85 -
Figure 3.43	Schematic diagram of required cut length & layout for cuts to be prepared ..	- 85 -
Figure 3.44	Location of ridges, level ice and open water in the ice tank (example).....	- 86 -
Figure 3.45	Ridge profiling device to determine keel depth and sail height.....	- 86 -
Figure 3.46	Cross section profiles of a FY- ice ridge.....	- 87 -
Figure 3.47	Test set-up of the punch tests .....	- 87 -
Figure 3.48	Example of ridge punch tests analysis .....	- 88 -
Figure 3.49	Calculated shear stress in a ridge (example) .....	- 89 -
Figure 3.50	The Aalto University ice basin, the carriage and the ridge. Measuring places are marked with arrows (Leiviskä, 1999).....	- 90 -
Figure 3.51	Ice rubble field at HSVA's ice tank (left), moored FPU model entering the ice rubble astern (right) .....	- 91 -
Figure 4.1	Model mooring line in a claw foot arrangement .....	- 93 -
Figure 4.2	Typical performance curves for fenders (Ref. Fentek).....	- 95 -
Figure 4.3	Model of buckling type fender. The graphs show model characteristics compared to prototype.....	- 96 -
Figure 4.4	Side by side tankers with mooring lines, berthing lines and fenders .....	- 96 -
Figure 4.5	(a) Friction testing device; (b) ice sample loaded between load cells.....	- 98 -
Figure 4.6	Schematic diagram of the friction testing apparatus .....	- 98 -
Figure 4.7	Current HR Wallingford three axis rigid force measurement device .....	- 100 -
Figure 4.8	Caisson with rigid force measurement rig (left) & pressure sensors (right) ..	- 100 -
Figure 4.9	Sensors (top row) and large scale force-plates (bottom row) used for measuring overall structure loads .....	- 101 -
Figure 4.10	Fixed mode test setup of a floating production unit (FPU) .....	- 102 -
Figure 4.11	Schematic diagram and photographs of the six component scale.....	- 102 -
Figure 4.12	Instrumented propeller shaft (left) and different HBM torque transducer types (right) .....	- 104 -
Figure 4.13	Icebreaking vessel with POD-drive.....	- 105 -
Figure 4.14	Oqus 300 camera and schematic layout of optical tracking system .....	- 107 -
Figure 4.15	Underwater camera for motion tracking .....	- 107 -
Figure 4.16	Digital photographs used to determine ice flow concentration and movement of elements .....	- 108 -
Figure 4.17	Digital photographs used to document the mode of failure of an ice sheet ..	- 108 -

Figure 4.18	Submerged ice floes under the hull of a moored structure (snapshot from video records)	- 108 -
Figure 4.19	Force and acceleration time history synchronized with video record	- 109 -
Figure 4.20	Synchronized high-speed recording of wave impact on jetty, and force measurements on the structure	- 109 -
Figure 6.1	Example of combination of numerical and physical wave model	- 117 -
Figure 6.2	Water level variation and wave paddle position of tsunami models that can be created in Deltares' new Delta Flume. Left: solitons for water depths of 5 to 8 m. Right: leading-depression N-waves at 8 m water depth with lengths of 100-300 m	- 118 -
Figure 6.3	N-wave generated in old Delta Flume travelling through flume and overtopping a dike slope (Hofland et al 2013)	- 118 -
Figure 6.4	The layout of the tactile sensor (left), typical sensor performance (right)	- 120 -
Figure 6.5	Experimental setup (left), calibration curves (right)	- 120 -
Figure 6.6	Comparison of static and dynamic calibration results	- 121 -
Figure 6.7	Plunging breaking on the dike (left), spatial distribution of the impact pressure recorded by I-Scan (right)	- 122 -
Figure 6.8	Pressure-time history of a breaking wave recorded by I-Scan pressure sensor	- 122 -
Figure 6.9	Line-like ice contact pressure distribution on the model cylinder	- 123 -
Figure 6.10	(a) Line-like ice contact pressure distribution on the model cylinder, (b-d) process of sealing the tactile sensor (source: HSVA)	- 124 -
Figure 6.11	Waterproof protection by plastic films	- 125 -
Figure 6.12	Schematic presentation of the calibration set up at Aalto University	- 126 -
Figure 6.13	Traditional two-stage coil spring representation of mooring lines in physical model	- 128 -
Figure 6.14	the response of servomotor to changes in line load when modeling a mooring line	- 129 -
Figure 6.15	<i>Control logic for servomotor only system</i>	- 130 -
Figure 6.16	<i>Control logic for servomotor and force transducer system</i>	- 131 -
Figure 6.17	The automated trinocular stereo imaging system (ATSIS) and the schematic of a trinocular stereo-imaging mode	- 132 -
Figure 6.18	Particle image velocimetry used to obtain wave elevation field	- 132 -
Figure 6.19	Wave surface near dune face measured by stereo photography (Van Thiel de Vries, 2009)	- 133 -
Figure 6.20	Terrestrial laser scanner wave measurement set-up	- 133 -
Figure 7.1	Pictures of process simulators. Top left: wave impact generator with erosion generated (top right). Bottom left: wave impact generator at sand dike with erosion generated (bottom right)	- 137 -
Figure 7.2	Left erosion of weak clay at small scale. Right erosion of (boulder) clay at full scale (courtesy Deltares)	- 138 -
Figure 11.1	Catenary shape parameters of a line	- 166 -



# FORESIGHT STUDY ON LABORATORY MODELLING OF WAVE OR ICE LOADS ON COASTAL AND MARINE STRUCTURES

J.Sutherland and K.-U. Evers (Editors)

## 1 Introduction

There is a long history of conducting experimental tests of the interactions between water or ice and structures, from Archimedes, through Leonardo da Vinci to the great 19<sup>th</sup> century pioneers such as Froude and Reynolds. The 20<sup>th</sup> century saw the development of many of the great hydraulics and hydrodynamics laboratories that remain in use to this day, such as:

- Hamburgische Schiffbau-Versuchsanstalt GmbH, HSVA (Germany, 1913)
- Delft Hydraulics, now known as Deltares (NL, 1927);
- Waterways Experiment Station (USA, 1929);
- National Research Council Hydraulics Lab, Ottawa (Canada, 1945);
- Port and Harbour Research Institute (Japan, 1946);
- Laboratoire National D'Hydraulique (France, 1946);
- Hydraulics Research Station, now known as HR Wallingford (UK, 1947);
- Centro de Estudios y Experimentación de Obras Públicas, CEDEX (Spain, 1957);
- Danish Hydraulics Institute (Denmark, 1964);
- MARINTEK Large Ocean Basin (Norway, 1981);
- Coastal Research Center - Forschungszentrum Küste (Germany, 1983).

Physical modelling has been used as a design tool for river, coastal and marine structures worldwide since the foundation of the laboratories above, and many others not reported here. Indeed, the prevalence of hydraulics laboratories in Universities and Research Institutes across the world is testimony to the continued importance and influence of physical model testing in hydraulics today. This history and practice of hydraulic modelling has been reported in many books and papers, including the following publications:

1. Yalin (1971) *Theory of Hydraulic Models*.
2. Hudson *et al* (1979) *Coastal Hydraulic Models*.
3. Ivicics (1980) *Hydraulic Models*.
4. Dalrymple (Ed.) (1985) *Physical Modelling in Coastal Engineering*.
5. Martins (Ed.) (1989) *Recent Advances in Hydraulic Physical Modelling*.
6. Hughes (1993) *Physical models and laboratory techniques in coastal engineering*.
7. Chakrabarti (1994) *Offshore Structure Modelling*.
8. Frostick, McLelland and Mercer (Ed.s) (2011) *Users guide to physical modelling and experimentation, experience of the HYDRALAB network*.

The study of wave or ice loads on man-made structures is an important sub-set of physical hydraulic modelling, yet is one which plays only a small role in the references above (with the exception of Chakrabarti, 1994). Mankind has built structures in, around, under or over water since the days of the earliest piers, bridges and enclosed harbours (C 2,500 BC). From offshore oil and gas facilities, through ports, terminals, marinas, quays and breakwaters, to groynes, bridges and pipelines, the number and range of man-made structures that interact with the hydraulic environment is increasing.

The importance of wave and ice loads on structures can be illustrated with a couple of examples. The International Chamber of Shipping estimates that in 2008 the international shipping industry transported over  $7.7 \times 10^9$  tonnes of cargo, equivalent to a total volume of

world trade by sea of over  $3 \times 10^{13}$  billion tonne-miles. These ships, their berths and moorings are subject to loads which must be accounted for in design. Moreover, the IPCC 4<sup>th</sup> Assessment Report (Nicholls *et al*, 2007) reports that coasts are experiencing adverse consequences of hazards related to climate change and sea level, that the risks are expected to increase over coming decades and that the impact of climate change on coasts will be exacerbated by increasing human-induced pressures. An increasing number of people and assets are expected to be put at risk at the coast, due to sea level rise and the increasing development at the coast. Part of the hazard comes from wave and ice loads. Conversely, rising temperatures are leading to a reduction in the area of sea ice. However, this opens up opportunities for sea-borne trade using routes (such as the north-west passage and the northern sea route) that were previously unfeasible and for the exploitation of natural resources (such as oil and gas) in Arctic areas. Therefore there is a continuing (and possibly even increasing) need for research and consultancy work on wave and ice forces on floating and moored structures.

Over the years technology has improved and the tools, techniques and procedures used in wave and ice tests have evolved. The rate of technological change has never been greater and The EC funded HYDRALAB network (see [www.hydralab.eu](http://www.hydralab.eu)) has playing an important role in producing new tools and techniques to improve the range of services offered by hydraulic laboratories. However, there are still gaps in our knowledge and there are also non-explored areas, such as nonlinear wave absorption systems.

## 1.1 Scope of work

This Foresight Study is one of three undertaken by the project HYDRALAB-IV. The others are:

- Foresight study on water and environmental elements (Thomas *et al*, 2010, which draws on a critical review by Johnson *et al*, 2012) and
- Foresight study on water and sediments.

All three Foresight Studies have developed visions of how the physical modelling of water and the elements around it may evolve and indicate the areas where the greatest changes are likely to occur. Each study has also identified what the possible consequences are for the development of our hydraulic laboratories, including instrumentation and facilities. All three foresight studies will be published on the HYDRALAB web site [www.hydralab.eu](http://www.hydralab.eu).

This study therefore provides a state-of-the-art description of topics and methodologies used in laboratory-based physical modelling of the effects of waves or ice on structures. Due to the focus of the laboratories involved, the study will be mainly confined to coastal and marine structures, where waves or ice loads are of greatest concern. It also identifies which significant problems are not addressed well by present techniques and tools; and describes the technological developments that we believe are likely to occur during the next few years, both in the short term (based on on-going developments) and in the longer term, which is necessarily more speculative. The aim of this Foresight Study is therefore to look forward at a European scale and to identify the future research subjects with respect to laboratory modelling of wave and ice interaction with structures.

## 1.2 Contents

This Foresight Study consists of the following sections:

1. Introduction, including scope and contents (this section)

2. Review of topics, which introduces four main classes of problems, (i) ships in harbours, (ii) floating structures in deep water, (iii) response of fixed structures to waves and currents, and (iv) response of structures to ice. The issues that are of greatest importance are described for each class of problem. The section end with some observations in the trends observed in the modelling of particular topics.
3. Establishing the correct environment, which is split into two main sub-sections: (i) establishing the correct hydrodynamic environment and (ii) establishing the correct ice environment. The former includes methods for producing waves, winds and currents, a summary of standard measurement techniques (for measuring surface elevation and velocity) and a section on measuring the air content in breaking waves. The latter includes descriptions of how ice sheets are produced, the measurement of ice properties and the modelling of different ice conditions (such as brash ice and ice ridges).
4. State of the art in modelling techniques. This section is split into two main areas: (i) Model construction and (iii) Measuring and analysis techniques for modelling the forces on structures.
5. Shortcomings, where limitations in our present methods are discussed.
6. Short-term developments, which are advances in techniques that are likely to be delivered within approximately the next five years, based on on-going or planned developments;
7. Longer time-scale changes in capabilities, which represent greater changes from the present day, based on general trends. This section is necessarily more speculative than the previous section; and
8. Discussion and conclusions.

This study report also includes references and Appendices with a list of contributors to the report, some more detailed information and the paper on the foresight study presented at the 35<sup>th</sup> IAHR World Congress (Sutherland and Evers, 2013).



## 2 Review of topics

### 2.1 Ship moored in a harbour

Port activities are significantly influenced by environmental forces. Large amplitude motions induced by wave action on moored ships, for instances, may lead to the interruption of shipping operations or damage to the mooring system, port structures or other ships. The study of the behaviour of moored ships may combine different areas of research, namely: propagation of sea states to the port taking into account nonlinear wave-wave interactions and sub-harmonic generation; hydrodynamic interaction between the ship and waves, taking into account the influence of nearby port structures; simulation of the ship response considering the nonlinear characteristics of its mooring system and other forcing loads (wind, currents, ice, etc.).

Due to the complexity of the phenomena, it is desirable to use an approach that combines physical and numerical modelling with prototype measurements, when possible (Taveira Pinto *et al.*, 2008). Composite modelling allows us to take advantage of the strengths of each approach while trying to avoid their limitations. Efforts should be made to perform systematic data collection in the field as prototype measurements are usually scarce but important for calibration and validation of physical and numerical models.

It is well known that the nonlinear effects in the proximity and inside harbour basins are not negligible: decreasing water depths cause very significant wave transformations (refraction, shoaling, breaking, wave-wave interactions) and nonlinear effects become stronger. Energy transfer to lower frequencies is very important (Battjes *et al.*, 2004; Baldock, 2006), since long wave forcing may lead to significant moored ships responses and disturb harbour operations (Moes, 2004; Shiraishi *et al.*, 2006; Sakakibara and Kubo, 2008a). Therefore, it is imperative to predict accurately those effects when evaluating the response of moored ship.

Well-designed small-scale physical models of port and offshore terminals are a valuable tool to study the response of moored ships to different environmental conditions (waves, currents, wind) and design parameters (type of ship, load condition, mooring layout, water depth). In fact, despite being a simplified reproduction of the reality, physical models can reproduce the phenomena with the greatest influence on the behaviour of moored ships in harbours under wind, current and wave forcing. These include the non-linear effects related to the propagation of waves to shallower waters and their interaction with coastal structures, and to the mooring system. Froude similitude is usually applied as it ensures that the correct relationship is maintained between inertial and gravitational forces when the prototype is scaled to model dimensions.

Numerical models have evolved significantly and gained much importance in recent years (Woo *et al.*, 2004; Wenneker *et al.*, 2006; Van der Molen *et al.*, 2008) but still cannot replace physical modelling. Turbulence, viscous and higher order effects rely on tuning in numerical models (Van der Molen, 2006). Physical modelling is one of the most reliable tools for studying the behaviour of moored ships in ports (Davies *et al.*, 2001; Van der Molen and Moes, 2009), finding application in the design of port facilities, study of downtime and mooring problems (Cornett *et al.*, 1999; Rosa Santos *et al.* 2010) and in the calibration of numerical models (Bingham, 2000), among others.

Physical models can give a valuable insight about phenomena not completely understood and difficult to cope with numerically, but scale and laboratory effects may jeopardize the quality of results. Tests at different scales together with field measurements are the basis for analysing scale effects. Laboratory effects result from inappropriate representations of the forcing actions

or boundary conditions (solid boundaries like wave paddles or sidewalls do not exist as such in the prototype) and also exist in large-scale models. Significant effort is still needed to understand and reduce them, despite developments in the wave generation and active wave absorption techniques (Oumeraci, 2003).

### 2.1.1 General considerations

In order to carry out tests on the operability of a moored ship, the ship movements have to be determined and the force exerted on its moorings and fenders have to be measured and these values must be compared with those considered allowable for the vessel type being studied: “limit values”.

The operability that is obtained as a result of these tests is a more realistic approximation than the one that is determined from a wave disturbance tests, where the “Exceedance Indexes (downtime)” for a specific wave height can only be used for guidance purposes with regard to the general operability of the wharves being tested, because the behaviour of a moored ship does not depend exclusively on the water surface elevation in the wharf, as is measured in these tests.

In some cases, the above-mentioned allowable values -“limit values”- refer to operability situations, whereas in other cases they refer to safety situations. If the operability value limits are exceeded, it can be necessary to stop the loading and unloading activities or continue with these operations, but the productivity is reduced. If the safety limits are exceeded, the ship can no longer remain at its mooring, either because its safety is at risk, the mooring lines or the fenders might be damaged, or because the wharf or the harbour facilities might be in danger.

Both limits are established as allowable ship movement values and allowable mooring and fender stress values. Where movements are concerned and for operability purposes, the AIPCN/PIANC (1995) publication and other domestic standards (such as Puertos del Estado, 1999) contain information about allowable ship movement values, whereas for moorings and fenders, one has to resort to data made available by the manufactures or refer to specific publications (such as OCIMF, 1992).

The ship is modelled out of wood, polyester or other materials and its shape and weight distribution being reproduced. Threads of synthetic materials are used for the moorings and the fenders are simulated with metal strips. Figure 2.1 shows a general view of two models used in this type of tests.

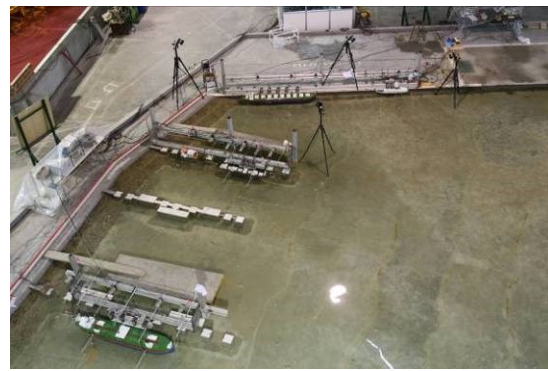
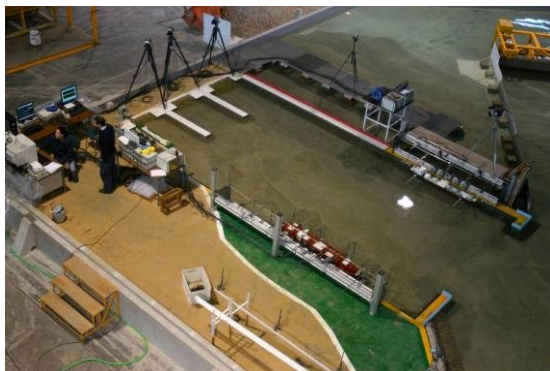


Figure 2.1 Moored ship behaviour tests for enlargements to the ports of Las Palmas (left) and Coruña (right) in Spain

### 2.1.2 Similarity Law, scale of the model and scale effects

“Froude’s Law” is the similarity law applied, this being customary with physical models in maritime engineering, because the forces of gravity predominate over the other forces, i.e. elasticity, surface tension or viscosity.

The models generally used, are without scale distortion and the usual scale range from around 1:100 to 1:150, it being necessary to adopt the smallest scales possible on the basis of the ship models available and the precision of the instrumentation to be used<sup>1</sup>.

To make sure that the forces of viscosity are sufficiently representative in the two tests -wave disturbance and moored ship- it is necessary to check that the model Reynolds number  $[(Re)_m]^2$  reaches values of several hundred in deep water and thousands or greater than  $10^4$  in shallow water.

In the case of the ship, the effect that in its environment the flow might not be turbulent, would be solved by making the hull coarser artificially, but in general with the values of the Reynolds number indicated above the flow turbulence is guaranteed.

### 2.1.3 The tests

The following aspects have to be known when planning the test: the position of the moorings and the location of the bollards and fenders; the types, characteristics and conditions of the ship load (full, average or ballast); the layout, materials, characteristics and types of moorings lines and fenders and, of course, the maritime climate conditions (waves and, where relevant, currents, tides and wind).

The waves generated for the ship operability study are generally a range of typical conditions, whereas extreme waves are reproduced for safety tests.

Once the instrumentation for each test is calibrated, the data (time series) is taken for the stress exerted on the moorings lines and fenders, together with the ship movements (heave, roll, pitch, surge, sway and yaw). A variety of instruments are used to take data, including the following: level gauges for the waves; optical systems, laser emitters-receivers and accelerometers for the movements and extensometers for the mooring and fender stresses. Some of these items of equipment can be seen in Figure 2.2, which shows the details of one such test.

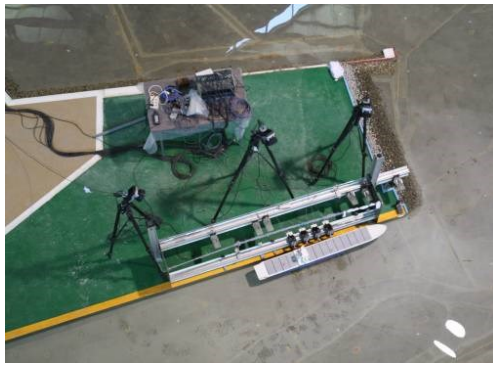
---

<sup>1</sup> Where Froude’s similarity is concerned, the scale of forces varies with the geometrical cube, hence the importance of ensuring that the model is as large as possible, i.e. to enable one to achieve sufficient precision when measuring the forces.

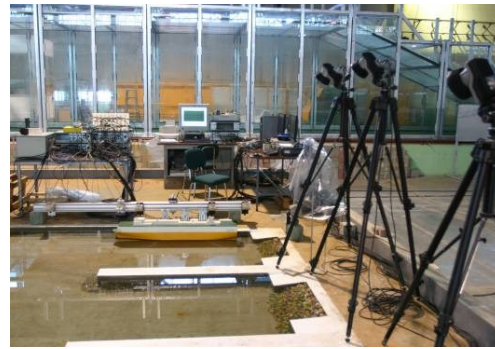
<sup>2</sup> When calculating the Reynolds number for these tests ( $Re = V \cdot L / \nu$ ), the following were adopted:

- $L = h$  at shallow and intermediate depths or  $L = L_o/2$  at undefined depths, where  $h$  is the depth at the model reference zone and  $L_o$  is the wavelength in deep waters.
- $V$  = group waves celerity.





Ship Movements. Optical Systems



Ship Movements. Laser Sensors



Fenders and mooring lines



Figure 2.2 Instrumentation for moored ship behaviour tests

The data recorded -wave height, ship movements and stress affecting moorings lines and fenders- made it possible to establish the operability or the safety of the moored ship, with the limits inherent to the test and the of the hypotheses adopted in the calculation method, which along general lines are explained below for the case of operability.

## 2.2 Moored and free floating structures in deep water

Mooring of ships or other floating structures in open seas needs evaluation of the response around the natural modes. Low frequency horizontal motions response is generally experienced related to the quadratic transfer functions (QTFs). Side by side interaction involves precise modelling of the berthing lines and fenders (Lécuyer *et al*, 2012). Mooring can be part of the energy capture in the marine renewable energy context.

The drift velocity of a free-floating body can be approximated by a simple model based on the equilibrium between the drift forces and drag forces. The drift forces are calculated from the second order QTFs at zero frequency (diagonal of the matrix), and taking into account their

variations with the velocity through the wave drift damping (le Boulluec *et al*, 2008). Drag forces are tuned by a drag coefficient and a development of the square velocity.

Types of testing varies between component testing, where only parts of the total system is tested, and global system verification, where the (hydrodynamically speaking) essential factors for the global behavior are modeled including the vessel with complete moorings etc. in combined waves, wind and current conditions.

For more details on the status in the experimental and numerical modeling of these types of structures we also mention here reports from the International Towing Tank Conference, Ocean Engineering Committee (ITTC 2011, 2008, 2005), and also DNV RP-C205 (DNV, 2010).

## 2.2.1 Applications and types of structures

The main areas can be categorized as:

**Oil and gas**, where structures can be moored ships and FPSOs, Semisubmersibles, Spars and other types of buoys, TLPs, Floating terminals (FLNG), Multibody systems;

**Renewable energy**, where the structure types can be wave energy converters, or floating wind turbines (similarities with small Spar buoys) usually applied in large arrays; and

**Other**, where the structures can be Aquaculture systems (fish net structure), or very large floating structures (VLFS) for floating islands, airports etc.

## 2.2.2 Key issues for model testing in waves, current and wind

### 2.2.2.1 Six DOF rigid body motions & offset, underlying hydrodynamic excitation and damping loads

Second-order low-frequency (LF, slow-drift) load contributions in irregular waves is still an important issue to be studied by model testing. Numerical models exist and are in general use, but there are uncertainties that need to be resolved by verification. It is also important to note that extremes often clearly exceed simple estimates based on Rayleigh statistics. The slow-drift is important in surge, sway and yaw, but also vertical LF motions can be important for large floaters such as semisubmersibles, ultra-large monohulls and large buoys. with extremes often clearly exceeding simple linear estimates. In deep water, the horizontal drift forces are usually calculated from the second order QTFs at zero frequency (diagonal of the matrix), thereby following Newman's approximation, while full QTF matrices are needed for vertical drift forces. (In finite and shallow water, this is not always the case, see e.g. Stansberg & Pakozdi, 2009). Also the corresponding damping is experimentally of interest, consisting of several contributions from both potential and viscous flow theory. Higher-order and viscous drift forces can also be significant in high waves (Berthelsen *et al.*, 2009). Testing in current is done to verify current coefficients, and also to investigate possible vortex-induced motion (VIM) phenomena. Wave-current-structure interaction is another important issue in progress, where in particular the influence on drift forces is an unresolved issue (Stansberg 2008b). Wind modelling in wave basins is important for a final global system verification including waves, wind and current, while detailed wind loads are usually tested in designated wind tunnels.

On the other hand, large-body wave-frequency (WF) contributions are usually quite well understood with the exception of viscous damping (for which a drag component is usually tuned) and in very high waves.

### 2.2.2.2 Extreme mooring line loads

In real moorings, nonlinear effects can lead to much higher loads than one can directly estimate linearly from motions (Fylling *et al.*, 1992). This is especially the case in catenary moorings, where nonlinear line dynamics from viscous drag, combined with nonlinear static restoring

characteristics, represent significant contributions. This is also to some extent present in taut mooring. Combined with the above nonlinear slow-drift motion behavior, the resulting extreme loads can become strongly non-linear, and model testing in realistic mooring can be essential for determining the design. The mooring line drag also contributes significantly to the slow-drift vessel motion damping. For smaller bodies, mooring and riser dynamics can be important for the wave-frequency motion.

#### **2.2.2.3 Riser loads and behavior/VIV**

In general, the including of risers in global verification studies is important mainly because of the effect on global offset and damping. Wave-induced loads on risers may also be important, e.g. at the hang-off point. Furthermore, the riser behavior in current can be particularly important if vortex-induced vibrations (VIV) are experienced; such tests are usually run with separate riser models only and at larger scales.

#### **2.2.2.4 Multi-body interaction problems**

Testing with two or more bodies, such as side-by-side cases, is becoming more and more relevant. This may involve studies of complex hydrodynamic, mechanical as well as operational interaction effects.

#### **2.2.2.5 Marine operations; demonstration of functionality**

This includes such as lifting operations and installations at sea, both at the surface as well as deep-water intervention. Tests are done in still water as well as in waves and in current. It is essential to measure vessel motions in all six degrees of freedom (DOF) and in particular their relative motions. Multi-body problems are often involved. The basic functions of completely new floater concepts or operations are also often studied through initial feasibility tests.

#### **2.2.2.6 Green water (water on deck), air-gap, run-up, wave slamming**

These are strongly nonlinear phenomena that need to be investigated and verified through model testing; sometimes the final design is also directly made from the testing. For ships and FPSO's, observation and measurement of green water on deck and related slamming loads on the flare and deck installation is essential. For platforms, nonlinear air-gap and run-up and possible deck impact is important, as well as breaking wave impact on columns. See also Section 2.3.3 (surface-piercing bottom-fixed structures).

#### **2.2.2.7 Dynamic positioning (DP)**

The performance of self-propelled ships and platforms with DP systems is often studied by model testing. Especially, this testing can be needed in high waves due to limitations in available numerical models. Ship manoeuvrability is a key point for harbour entrance, berthing, channel navigation when crossing other ships in shallow water, fuel consumption, towing and rescue operation, survivability in rough seas (Gourlay, 2009, Ferrant *et al*, 2008).

#### **2.2.2.8 Confined water problems**

The complex dynamical resonant behaviour of confined water volumes excited by waves and/or vessel motions can be difficult to predict by numerical methods due to nonlinear and viscous effects. This includes such as moonpool dynamics and water gaps between adjacent structures. For flexible floating structures such as fish nets with supports, various special issues will be relevant.

Free surface natural periods in tanks or moonpools may be approached by analytical methods for simple shapes such as rectangles (Molin 2001, Faltinsen 2002) or axisymmetric structures (Newman 2003, McIver 2003). Standard diffraction and radiation models (Maisondieu *et al* 2001, Le Boulluec *et al* 2005) can be used for moderate free surface effects. For a correct

evaluation of waves amplitudes between side by side ships some improvement can be found in Chapter 2.2 (Lécuyer et al, 2012).

#### **2.2.2.9 Nonlinear wave loads**

Second-order sum-frequency wave loads, often denoted as "springing" loads, will usually contribute to the loads and responses on structures with natural frequencies close to two times the wave frequencies, such as the tether tension on TLPs. Numerical models exist by use of sum-frequency QTFs, but they need to be verified.

For TLP's in steep and high waves, higher-order wave loads leading to "ringing" phenomena can be important for extreme loads. Here model testing is quite essential.

#### **2.2.2.10 Marine renewable energy device moored in intermediate to deep water**

Modelling of a wave energy converter is based on diffraction and radiation theory coupled to a model of the Power Take Off. A relatively large scale ratio (1/7 geometrical scale in the case of the Pelamis and 1/1000 scale for the power) is needed to correctly represent the PTO (Henderson, 2006). The question of an "equivalent" PTO at smaller scale remains open.

### **2.3 Response of fixed structures to waves and currents**

Fixed structures that are subject to wave and current loading exist from inland of the shoreline (such as building subject to overtopping or flooding) through shallow water depths (from piers and trestles to groynes and breakwaters) right out to deep water (from oil platform jackets to pipelines). These objects may be submerged or emergent and we may be interested in overtopping, impulsive or pulsating pressures and/or forces, movement or run-up limits. Typical laboratory experiments are described in Sections 2.3.1 to 2.3.3.

#### **2.3.1 Vertical breakwaters and crown walls of rubble-mound breakwaters**

##### **2.3.1.1 Vertical breakwaters / seawalls**

A vertical breakwater is a structure of rectangular (or nearly rectangular) cross section having a vertical or nearly vertical front wall extending directly from the seabed or built on top of a (relatively) thin bedding layer (Figure 2.3). A composite breakwater is a combined structure with a main body of rectangular or nearly rectangular cross section placed on a rubble mound that is submerged at all tidal levels. In each instance, the main (vertical) wall is made of masonry or concrete blocks, or a reinforced concrete or sheet steel caisson filled with sand etc. A superstructure formed of in-situ concrete is often constructed on top of it. The cross section of superstructure can differ from a simple rectangular shape, perhaps with a sloped front or other shape. In plan shape, the wall elements are usually rectangular, butted closely together, or keyed together, but some such walls use circular (or part circular) caissons. The rubble foundation will have a protruding berm seaward and landward of the wall element, with berm and slope covered by armour units for protection against erosion.



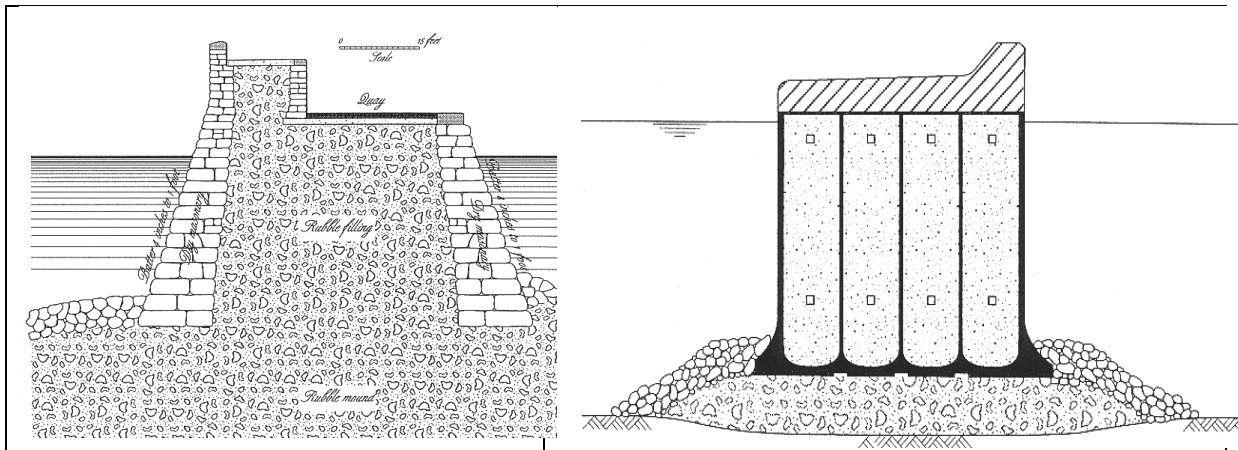


Figure 2.3 Examples of vertical breakwaters (Allsop, 2000)

In some examples, the seaward face may be covered by a mound of concrete armour blocks to reduce the intensity of any impulsive loadings (they do not reduce pulsating wave loads), and to reduce wave reflections. The caisson alternatively may have a perforated front face into a voided chamber to (partially) absorb wave energy and reduce wave reflections from the breakwater.

### 2.3.1.2 Wave loadings on vertical walls

In fully random storm seas, there will inevitably be a wide range of different types of wave breaking, but it has been found convenient to use three categories of wave load / breaking condition, the first two of which are illustrated by example measurements of wave pressures in Figure 2.4 taken from Allsop *et al* (1996):

- Non-breaking or pulsating;
- Impulsive breaking or impact;
- Broken waves

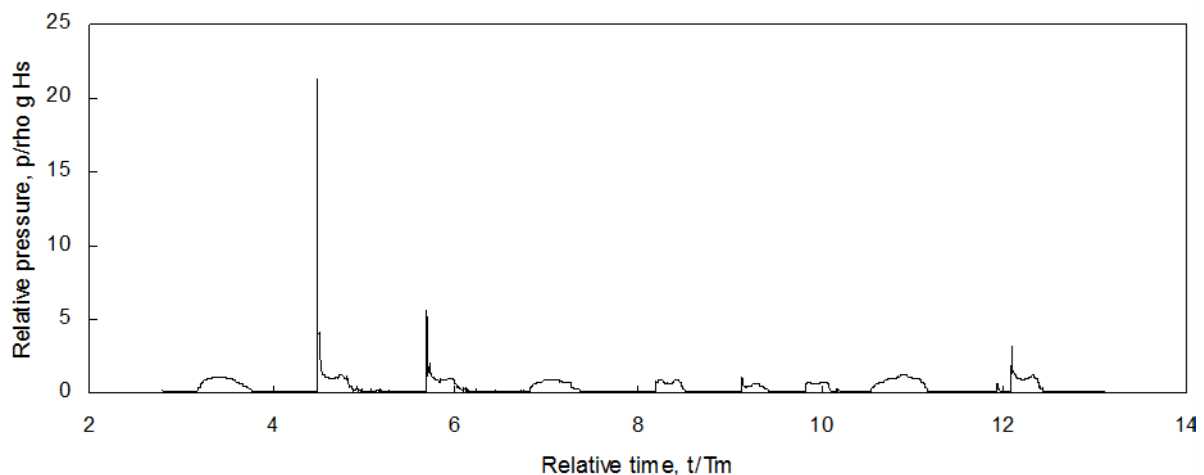


Figure 2.4 Example wave loadings, pulsating and impulsive, on a simple vertical wall with small toe berm, test 10003 from Allsop *et al* (1996)

The least complicated load case is generally when the wave is non-breaking, also termed reflecting or pulsating. For this condition, the wave motion is relatively smooth, and some processes can be predicted by relatively simple wave theories. Much greater wave forces arise



if the wave can break directly against the wall, termed plunging, breaking, impulsive or impact. These conditions are more difficult to predict, and attract significant variability / uncertainty. Rather lower forces arise if waves have already broken before reaching the wall. The wave motion is turbulent, but often highly aerated. More detailed definitions of each load type, and descriptions of methods to predict occurrence of each load type, are described by Allsop (2000). Recent work by Cuomo and co-workers (2010, 2011) has extended the prediction of impulsive loads, and clarified the relationships between high intensity loads and short durations.

In each instance above, horizontal loadings ( $F_h$ ) are established at  $F_{1/250}$  exceedance level (the average of the 1/250 events, as used by Goda, 1985, 2000), or sometimes  $F_{0.1\%}$  (0.1% exceedance), related to random seas of at least 1000 wave duration.

### 2.3.1.3 Rubble mound crown walls

The crest of a rubble mound breakwater or seawall often includes a crown wall, see Figure 2.5. Crown wall elements are generally formed of in-situ concrete with a horizontal roadway with a seaward parapet wall or up-stand. In some such crown walls, a down-stand protrusion reduces wave pressure penetration to the underside of the roadway, and forms a key into the core material to assist sliding resistance. The up-stand element acts to reduce wave overtopping, and the roadway (if correctly designed) can direct overtopping flows away from the rear face of the mound.

Generally the crown wall crest is at or below the armour, but if the crown wall projects above the armour, it may experience impulsive wave loads over its exposed part. The lower (protected) part may only see pulsating wave loads. The crown wall base or roadway will experience wave-induced up-lift forces. Additional up-lift forces may also be generated where the seaward face includes recurve or projecting bull-nose (sometimes included to reduce overtopping). Assessment of the overall stability of the crown wall again requires that the most critical combinations of horizontal and up-lift forces be identified, even though the individual peak loads will not occur at the same moment.

As with composite vertical breakwaters, impulsive pressures on the crown wall will be characterised by high peak pressures of short duration. The influence of impulsive pressures on the overall stability of the crown wall must be evaluated by considering the dynamic response of the crown wall, perhaps as modified by its support conditions. It is likely that significant air inclusions in breaking waves hitting the crown wall may reduce the peak pressures from those measured in small scale models, but will increase the effective durations, see Cuomo et al (2010) for guidance on transforming model test loadings into prototype.

To assess the resistance of the crown wall against sliding / overturning or breakage, load distributions giving the largest tensile stresses in the various parts of the structure must be established from wave-induced pressures, wave and dead loads transmitted through armour units against the wall, and reaction forces from the foundation.

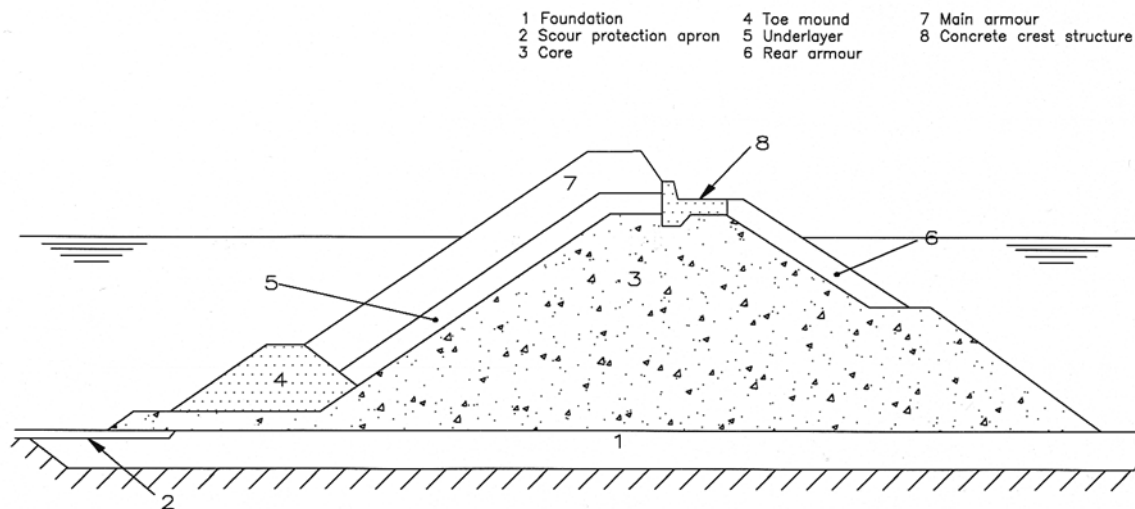


Figure 2.5 Idealised rubble mound breakwater with crown wall, after Burcharth (1994)

### 2.3.2 Sloping structures - revetments and dykes

Coastal dikes are used in many countries like The Netherlands, Denmark, Germany, Vietnam, United Kingdom, United States, and more. During extreme surges the dikes (also termed embankment seawalls or levees) have to withstand high water levels and waves. The main response parameters that are measured in hydraulic facilities are the overtopping behaviour, particularly with respect to crest level, and/or the strength of the dike or revetment facing. Key guides for the design of revetments or the prediction of wave overtopping are given by McConnell (1999) and by Pullen et al (EurOtop, 2007). The major international guide – the International Levee Handbook - is in preparation in 2013.

#### 2.3.2.1 Overtopping

The main function of any dike or seawall is to limit wave overtopping under conditions of high water levels (including surge) and/or large waves. The main methods to predict wave overtopping due to wind waves are based on empirical equation sets, themselves based on hydraulic model tests measuring overtopping discharges under irregular (random) wave conditions. Previous work used wave run-up levels, perhaps as predicted by Hunt (1959) or Battjes (1974) who extended the approach to irregular waves.

Manuals to predict wave overtopping have been developed by Owen (1980), Besley (1999), TAW (1990, 2001), and most recently the EurOtop manual by Pullen et al (2007). The main methods predict the mean overtopping discharge, but some extended methods are described to give individual overtopping volumes.

The maximum individual overtopping volume is probably the key measure for hazard assessment purposes, such as danger to people, or damage to buildings (e.g. EurOtop, 2007; or Allsop et al, 2004, 2005). Still, in most guidelines the quantity most often used to assess overtopping behaviour is the mean overtopping discharge. This is mostly due to the fact that this integral quantity is easy to measure in a model, and substantially more data are available to relate mean overtopping discharges to wave and structure parameters. But the same mean overtopping discharge caused by a large wave height (and higher structure crest) will often lead to more damage than the same overtopping discharge from a lower wave height on a lower crest. Better techniques are therefore strongly required to generate and determine maximum

overtopping volumes. For single waves, Hughes (2004) describes a method for the overtopping volume of single waves using the integrated momentum under the wave crest.

Not all characteristics of the single wave in an irregular wave field that causes the extreme overtopping are known. For vertical structures, Davey (2010) used several parameters to statistically characterize the separate waves that lead to extreme overtopping, which were: the wave crest elevation, the wave trough elevation, the wave period, and the preceding wave crest elevation. However, these do not completely determine the amount of overtopping of a single wave, and it concerned another structure type. The use of the preceding crest by Davey indicates that not only the separate wave must be considered.

### 2.3.2.2 Strength

As the largest hydraulic attack to dikes usually occurs during storm surges, the main protective layers on coastal dykes (revetment armouring) are often constructed above low water level, so that revetment systems requiring close placement like placed block revetments or asphalt layers can be constructed in dry conditions. Blockwork or slabbing may use much less material than conventional rock armour or rip-rap layers. These other revetment systems may be needed in areas where rock armour is not found easily. A comparison of total armour thickness on 1:2 slope revetments using: rock armour or rip-rap; close-fitted stone or concrete blockwork; or slabbing, is shown in Figure 2.6.

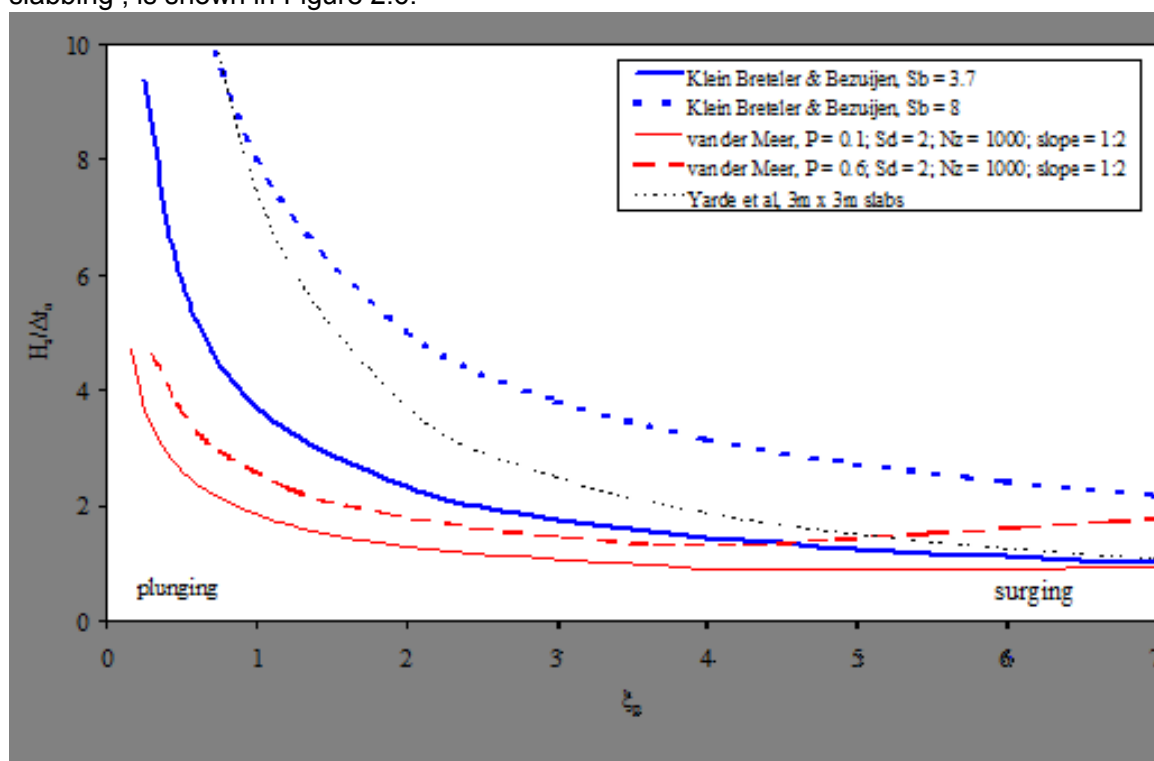


Figure 2.6 Revetment armour thickness,  $t_a$ , for slabs, blocks and rock armour, after McConnell & Allsop (1999)

As blocks, slabs or asphaltic revetments are relatively closed, rather than porous, the load on the revetment is determined by the ratio of the permeability of the top (block) layer, compared to the permeability of the layers underneath, expressed in a parameter called the leakage length. When this parameter is large (i.e. a closed top layer), large pressure differences can occur over the top layer.

For surging waves the wave load is determined by the moment of the largest run-down of the waves. The maximum upward pressure difference between the filter layer under the revetments and the top of the filter layer occurs just up-slope of the wave front. When plunging waves occur, the maximum forces generally occur during a wave impact.

The resistance of the dike armour to loadings may require full-scale or near-full scale tests, as the permeable flow through the filter material underneath the placed block revetment needs to have a high Reynolds number, key geotechnical responses do not scale by Froude.

Wave induced pressures on sloping dike surfaces are likely to be more damped than those on vertical walls. Plunging and surging breakers are typically found at sea dikes and highest impact pressures have been recorded during plunging breakers (Grüne, 1988). Wave pressures on dikes under real sea-state conditions are complicated components from wave impacts and wave run-up are mixed (Grüne & Bergmann, 1994). Klein Breteler & Coeveld (2004) determined the shape of the pressure fields that determine the largest loads. It is not however clear which waves (with which characteristics) create these pressure fields. Just simply taking the largest waves from a record did not always lead to the largest upward pressure differences (Kuiper & Doorn, 2005).

#### **2.3.2.3 Decks and beams**

Hydraulic loads applied by waves to the deck or other projecting elements (beams, fenders) can be defined as “wave-in-deck loads”. These can be summarised as:

- uplift loads on decks;
- uplift loads on beams or other projecting elements;
- downward loads on decks (inundation and suction);
- horizontal loads (both seaward and shoreward) on beams or other projecting elements.

Prediction methods for these loads are described in detail by McConnell et al (2003, 2004), and up-dated by Cuomo et al. 2007, 2009. A sketch of wave-in-deck loads acting on a suspended deck structure is shown in Figure 2.7 (Cuomo et al. 2007, 2009). The nature, occurrence and magnitude of these wave loadings vary significantly for different structures and wave conditions. Horizontal elements such as deck slabs may be subject to large vertical forces upward or downward (especially under conditions that inundate the deck). Vertically faced elements like beams and fenders can experience significant forces horizontally (and vertically if of significant thickness).

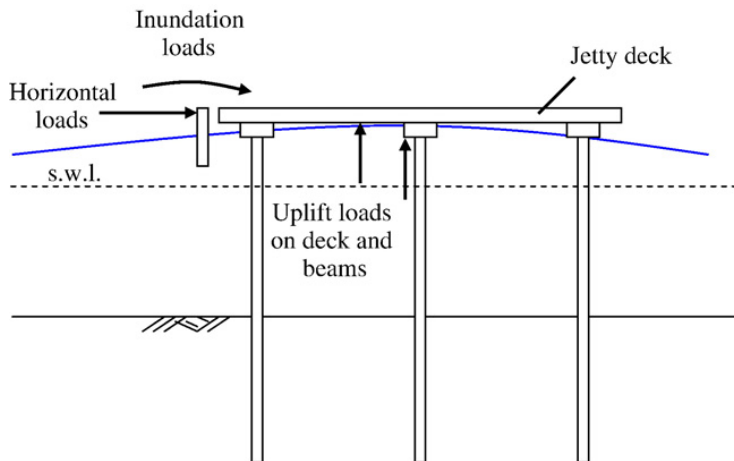


Figure 2.7 Wave-in-deck loads on an idealised section of a jetty platform supported by piles, after Cuomo et al.(2007)

A classic loading pattern showing an impact load followed by a quasi-static (slowly varying) load is shown in Figure 2.8, and a similar idealised time history of horizontal load on a platform is shown in Figure 2.9.

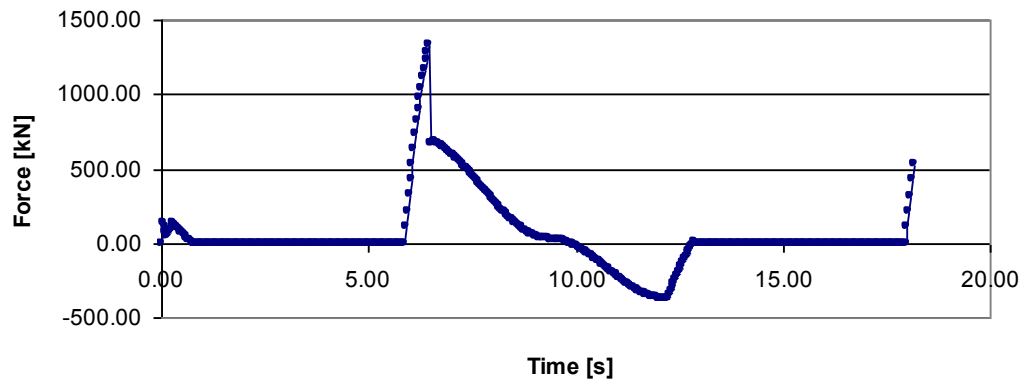


Figure 2.8 Idealised filtered time history of vertical load acting on an elevated platform

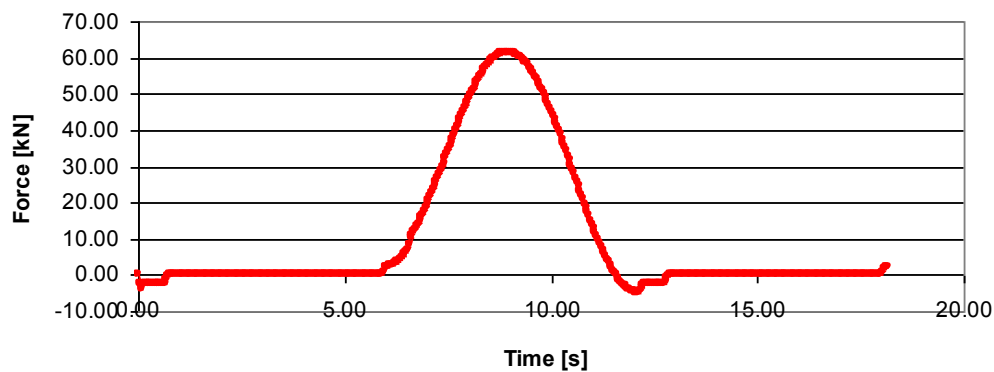


Figure 2.9 Idealised filtered time history of horizontal load acting on an elevated platform

### 2.3.3 Surface-piercing bottom-mounted offshore structures

Forces and responses in waves and current are needed to design surface-piercing bottom mounted structures, which are fixed to the seabed either by gravity, by a caisson or piles driven into the bottom. The bottom depth is usually finite to shallow, but fixed platforms have also been designed for waters deeper than 300m. The objectives of experiments are:

- Determination of the global forces and responses from waves and currents;
- Determination of impact pressures on structural elements – particularly in the splash zone.
- Determination of wave run-up, including diffracted elevations.
- Scour protection of surrounding seabed.

As for the floating structures above, we also refer to reports from the International Towing Tank Conference, Ocean Engineering Committee (ITTC 2005, 2008, 2011).

The model structure is suspended in dynamometers and equipped with pressure gauges at selected positions. Wave run-up is typically recorded by wave gauges mounted on the surface of the structure and by video capture.

The impact pressures and run-up depends on the actual form of the wave front when hitting the structure (Figure 2.6). To obtain representative wave loading it is necessary to use long sequences of irregular waves or alternatively to use focussed wave generation whereby the breaking point of the waves can be accurately predicted (Zang and Taylor, 2010).

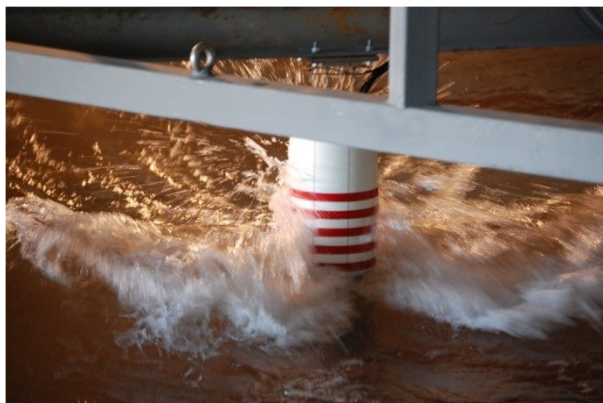


Figure 2.10 Breaking wave impact on bottom mounted cylinder

#### 2.3.3.1 Applications and types of structures:

*Coastal engineering:* Various types of structures (lighthouses, piles and others).

*Renewable energy:* Bottom-fixed wind turbine foundations

*Oil and gas:* GBS platforms, LNG terminals, jacket platforms

*Other:* Artificial islands.

#### 2.3.3.2 Key issues for model testing in waves, current (and wind):

*6 DOF global wave and current forces and responses*

Global forces and responses on single bodies in waves only are usually modelled numerically by linear diffraction models, or by simpler Morison models (DNV 2010) if they are slender, which often work reasonably well in moderate waves. There is still a need to verify systems by model tests to check if anything has been overlooked. Furthermore, in higher waves nonlinear effects may become important. With current added, and /or multiple bodies, there are particular issues that need model testing.



Higher-order wave loads and resulting response oscillations (ringing) can be important in steep and high waves for column-based structures with natural frequencies close to 3 - 4 times the main wave frequencies, which is typically in the range 2 – 5 seconds full scale. This may be an issue that arises in connection with offshore wind turbine foundations in finite water, which have characteristics quite differently from conventional oil and gas applications (Leverette 1994, Stansberg *et al.* 1995, Nestegård *et al.* 1996).

High and steep waves, including breaking waves, may also lead to global wave impact forces (on the hull and /or on the topside) which may be hard to predict, and therefore need to be investigated and / or verified. See e.g. Stansberg *et al.* (2004, 2012).

Quite often, models are designed to be as stiff as possible such that forces are measured more or less directly. Sometimes, however, elastic models are made to also study the detailed response behaviour of the structure.

The relevance from wind for these types of structures is mainly connected with wind turbines.

#### *Wave elevation in surrounding field*

For medium large to large structures model test verification is often needed to check the surrounding wave field.

#### *Run-up; air-gap*

The local nonlinear wave enhancement/upwelling, including run-up, around vertical columns and walls, need to be studied or verified by experiments. Numerical models, including CFD, are in development, but are still immature. Both the elevation and the flow field are of interest (Stansberg & Kristiansen 2006, Stansberg *et al.* 2010, Kendon *et al.* 2010).

#### *Local wave impact; slamming*

Local impact from steep and breaking waves and /or from upwelling/run-up around structures need experimental investigations (Stansberg *et al.* 2012). As for the run-up above, CFD models are in development, but this seems to be even more challenging for the loads than for the flow. The accurate measurement of local loads/pressure, and interpretation of results, are key issues, especially when air entrainment/entrapment occurs.

#### *Measurements of kinematics*

It is difficult to make accurate measurements of the kinematics field including the wave crest, for waves and waves and current combined. Improving knowledge of the kinematics will improve our understanding of the loads.

### **2.3.4 Submerged offshore structures**

Examples of submerged offshore structures are:

- Submarine pipelines and risers
- Ocean outfalls
- Protection structures for valves on pipelines
- Intake structures for cooling water and diffusors on outfalls
- Tunnels and tunnel elements

#### **2.3.4.1 Pipelines and risers**

The fundamental tests of pipelines and pipes resting on the seabed are made on short sections of pipe exposed to waves and/or currents perpendicular to the axis of the pipe. In order to

obtain the best possible model scale and high Reynolds numbers in the test these are often done by moving the pipe model suspended from a carriage in still water rather than oscillating the water around a fixed pipe. In some cases a current may also be generated along the flume to simulate combined wave and current conditions (Branković, et al., 2010).

The pipe is suspended in a two-component dynamometer to provide drag and lift forces on the pipe section and pressure cells inserted in the cylinder surface are used to obtain detailed information on pressure distributions. A similar technique is used for risers as shown in Figures 2.7 and 2.8.

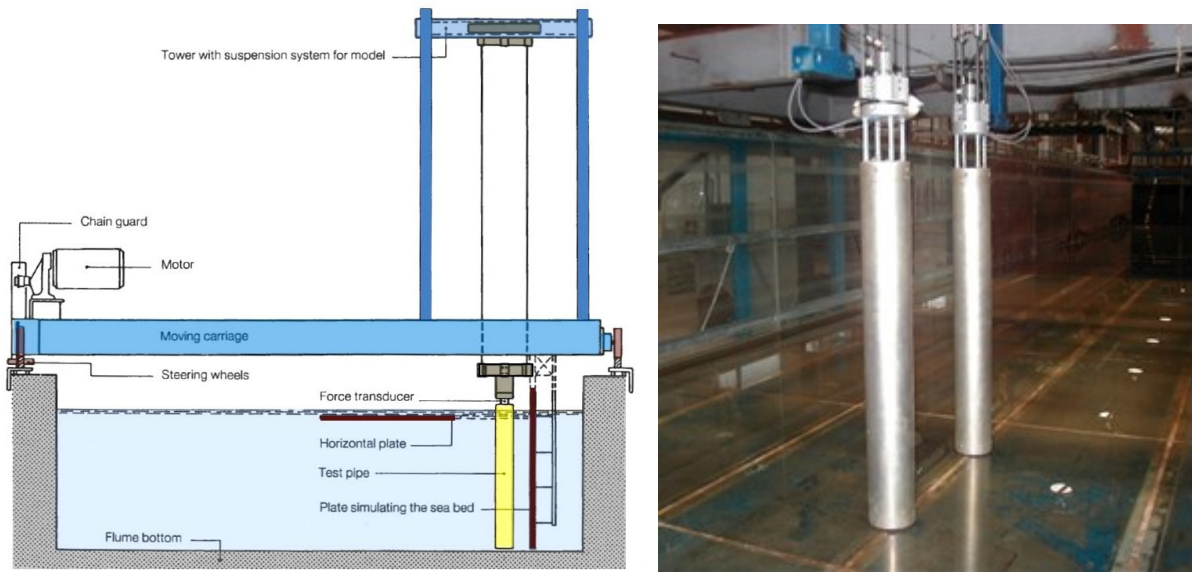


Figure 2.11 The photo shows two riser segments suspended in the test flume. To the right is shown the setup for a spanning pipeline model test in the same flume.

Note that the pipeline is mounted vertically for this test.

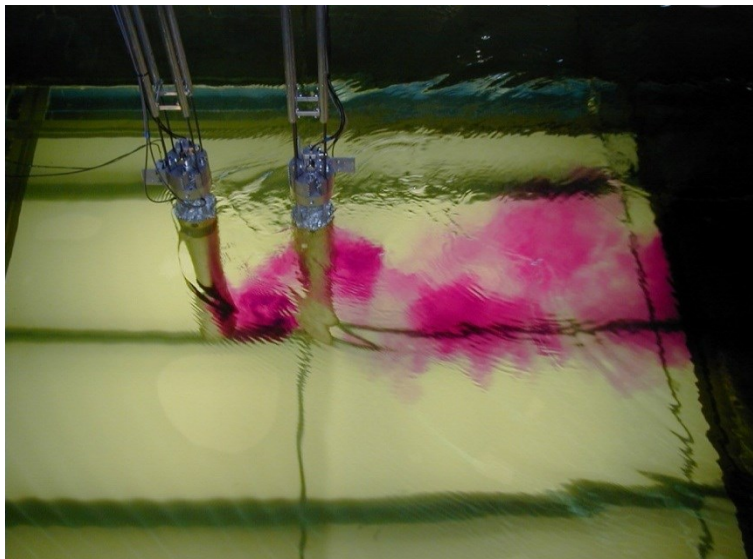


Figure 2.12 Vortex shedding behind two riser segments



This type of testing has been extended to cover scenarios with pipes in trenches and partly buried. The testing has also been applied to study loads and response of pipes suspended above the seabed to due to spanning caused by scour or uneven seabed. In these cases the suspension has been made elastic to model the vortex induced vibrations of pipelines. Design guidelines for submarine pipelines have been developed on the basis of such tests and analysis software for pipeline stability are verified against the results.

Tests as described above are, however, significant simplifications of the exposure in nature. The simplified setup with short pipe sections exposed to lateral loading have been supplemented with larger lengths of pipes whereby the force distribution along the pipe and its relation to the oscillatory behaviour of pipelines could be studied, see Figure 2.9. Studies of this type require large facilities with powerful carriages.



Figure 2.13 Model test of vortex induced vibrations of a pipeline performed in a towing tank

The requirements to the size of facility are even more demanding when exposure to waves and current of different directions have to be made. Such a facility does not exist today for testing in an acceptable scale. Another simplification is that the effect of moveable seabed sediment is not covered. A new and unique facility has been built at the University of Western Australia to study the combined effect of waves, current, moveable sediment and pipeline. This facility makes it possible to assess the stability of a pipeline under the influence of the dynamic process of local erosion.

#### 2.3.4.2 Protection structures, diffusers and intakes

Structures of limited horizontal extent are like pipelines tested for total loads from waves and currents. Models of such structures are typically suspended on force gauges to obtain all relevant components of forces and moments. In addition the designs are often tested for distribution of flow entering or jetted from the structures. The flow is documented by acoustic methods, lasers or micro propellers and also often visualisation techniques such as the injection of tracers.

#### 2.3.4.3 Submerged tunnels

Tunnels are large structures constructed in segments of often 100-200m in length and containing multi-lane roads. The placement of tunnel elements, i.e. lowering the element and placing it on pre-installed saddles or gravel layer on the seabed, is a critical operation as the element is suspended from floating barges, thus influenced by the motions of the complex

system of floating barges, elastic wires and heavy tunnel element. In many cases such structures are located in estuaries or near river mouths where the currents may be very irregular. Similar arguments apply to the placement of caissons from barges.

Testing of such critical marine operations can be done in relatively small scale but the experimental facility must be able to simulate complex wave and current conditions. The objective of the tests is to determine the maximum acceptable environmental forces during the operation, i.e. the characteristics of the weather window for the operation. The tests are made on properly scaled model elements and include forces in wires and motion of the element at various stages of the placing operation (Figure 2.10).

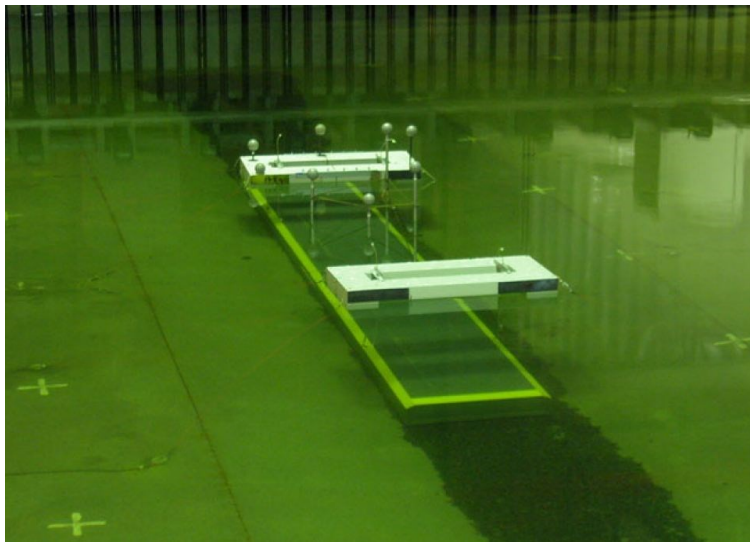


Figure 2.14 Model of tunnel element during installation test.

In Figure 2.10 the element is suspended under two barges. Individual motions of the element and the barges are measured by tracking positions of the spheres attached to the models.

## 2.4 Response of structures to ice

Ice sheets can interact with structures by moving past fixed structures (such as monopiles, bridge piers, artificial islands, fixed or moored oil and gas production units) or by having a ship force a path through it. Typical laboratory experiments include:

- (1) Force on a fixed monopile (e.g. lighthouse),
- (2) Force on fixed inclined structures (e.g. artificial island, conical structures)
- (3) Force on fixed multi-leg structures (jacket platforms)
- (4) Force on semi-submersible platforms
- (5) Force and motions on a ship
- (6) Force on moored vessels (FPU or FPSO)
- (7) Force on moored SPAR buoy
- (8) Dynamic positioning of moored floating structures

### 2.4.1 General

Fixed and floating offshore structures as well as ship navigation in cold regions are subject to loads from different sea ice conditions. For design purpose it is essential to estimate the ice forces acting on the structure and its behaviour in different ice conditions, like level ice, broken

ice, ice ridges and ice rubble fields. Therefore ice model tests are carried out in ice facilities for various types of offshore structures and ships to investigate the ice-structure interaction.

For structures located in an ice environment, it is most important for a number of reasons to understand the ice-structure interaction and the structures' response to the ice:

- Static respectively quasi-static ice loads on structures can be determined by means of analytical calculation methods.
- There is not a proper understanding of the difference between moored structures and fixed structures in ice with respect to ice failure mechanisms, or the loads and parameters that affect the dynamic behaviour of the coupled system. Thus, it is essential for the calculation of the action of ice on a structure to better understand the *failure mechanism of the ice* during the interaction with the structure. The ice is a brittle material that is rather difficult to model and analyze. The formation of the ice around the structure and the failure modes of the ice during interaction cannot easily be understood without proper physical modeling.
- In order to be able to prepare a proper design and carry out necessary modifications the *structure's response modes* must be identified. Traditional modeling and analysis may not be sufficient and ice tank modeling will represent the only substitute to full scale testing. We have seen that unknown failure modes have been detected in the ice tank such that correct modifications can be made on the structure to provide a safe and optimal design.
- The traditional analysis can only help us to answer our known questions. In the ice tank, questions we did not ask may become apparent. As such the ice tank testing will help us to *identify unknowns*, the issues we did not think about, issues that may be critical for the safety of the structure.
- Modern finite element analysis using moving and collapsible finite elements might gradually be developed to predict ice loads. Ice tank testing is, however, and will continue to be, essential to *calibrate the calculation models*. It is, furthermore, believed that ice tank testing also in the future will be needed to calibrate new situations to be modeled with numerical tools.
- For ice tank testing, *realistic "through the ice sheet"* ice properties must be modeled to obtain realistic test results.

Gravity-based structures are suited for up to 100 m water depth in regions with multiyear (MY) ice and to 150 m in first year (FY) ice, respectively. Jacket and jackup type platforms are feasible to water depth of about 60 m in regions like Cook Inlet and the Bering Sea, but may not be suitable for the Beaufort or Chukchi seas. It is possible to construct ice or gravel islands for up to about 12 m water depth. Gravel islands may not be suited for the Chukchi Sea's more dynamic conditions compared to the Beaufort Sea (Ghoneim 2011).

The choice of an appropriate exploration or production system does not only depend on water depth and ice conditions, but also on the ice management and disconnect capabilities commensurate with the arctic region under consideration. The risks associated with the operation and the consequences of failures have to be quantified and understood. Thus feasibility studies are recommended, combined with model testing of concepts with respect to

cost and risk management during design, construction, installation, operation, and decommissioning.

Information on floating structures is given in the ISO/DIS 19906 standard code but the guidance offered is limited. Only generalities are offered in the normative part, involving check lists and general recommendations for design, but no guidance on applicable methods on induced ice actions, including ice scenarios is offered. Ideally one would like a standard/code to include information and guidance on a methodology that is accurate. ISO/DIS 19906 is still weak on guidance for moored structures in ice (Moslet 2010). There are also significant gap areas for *floating systems* that need to be addressed to enable cost-effective design.

In most methods regarding ice loads, the load itself is assumed to be independent of the stiffness characteristics of the structure and the methods are to a very large extent based on measurement and research on fixed structures. For fixed structures there are generally three distinctions made on the structures properties: a) width/diameter, b) rectangular or circular waterline shape and c) slope angle. This should also be analogous to floating structures, but there is one principal difference. The structures response can change the property a) and c) based on the exerted load. This is a classic feedback effect, which may further change the load (Moslet *et al.* 2010).

There is a need for methods that can assess the global loads under various combinations of ice conditions and other environmental forces and especially the response, coupling all degrees of freedom (sway, heave, pitch, accelerations etc.) back to the load calculation.

The standard/code should include in its informative part:

- Examples of how the methodology is applied to a selection of floater types vs. different ice scenarios.
- Guidance on the use of model testing of floating structures in ice basins, including calibration and validity of the test results. This guidance should include a table on the most important model tests to be performed for various structure alternatives.

A consistent methodology for application of the recommended analytical ISO formulas to derive the global ice load as a function of the floater's response is basically needed. In order to obtain reliable design ice loads for these cases ice model tests and numerical simulations are required.

Typical ice tank testing which can be carried out with fixed or moored floating offshore structures is summarized in Table 2.2.

Table 2.1 Fixed and moored floating offshore structure types

<b>Fixed Offshore Structures</b>	<b>Moored floating offshore structures</b>
Caisson	SPAR
Monopile	FPSO
Multi-leg platform	FPU
Cylindrical shaped	Buoy
Conical shaped	Tanker
Rectangular shaped	
sloping	

The assessment of various concepts of fixed and floating exploration and production platforms, offshore loading terminals, floating production units as well as foundation of wind turbines for the operation in Arctic waters is often based on the results achieved from ice model tests. The performance of numerous model test programs with fixed and moored floating structures to support the design with respect to the operability in various ice conditions (i.e. level ice, pressure ice ridges, ice floes, ice rubble fields and managed ice) is reported by Evers & Jochmann (2011).

The choice of a proper scale plays an important role, because the environmental conditions (ice, water depth, current, etc.), dimensions of the structure/vessel, the dimensions of the ice tank, and the configuration of the mooring system are to be considered. For the model test campaign, in general, the full scale situation has to be modelled as accurately as possible. Deviations of modelled test set-up from full scale set-up cannot always be eliminated, because some features have to be simplified and need to be adapted to the available infrastructure.

The dynamic behaviour of the moored vessel and its interaction with the mooring system is of great importance and has to be simulated as accurately as possible in the model tests. For the conceptual design of the vessel and the mooring system the ice forces, restoring forces, mooring line forces, vessel displacement, vessel motions (heave, pitch, roll and yaw) have to be determined. Also the interaction between submerged broken ice floes and the turret respectively mooring lines is of interest.

The first moored floating structure in ice was tested at HSVA about 30 years ago. HSVA was contracted by Gulf Canada Ltd. to develop the design of the hull shape of the conical drilling unit Kulluk in order to deflect submerged broken ice. Subsequently comprehensive ice model tests were conducted in level ice and ridges. Within the following years other concepts (Figure 2.11) like Arctic shuttle tanker, STL, SPM, offloading buoys, SPAR and shallow draft buoys, moored FPU and FPSO were subject of ice model tests.

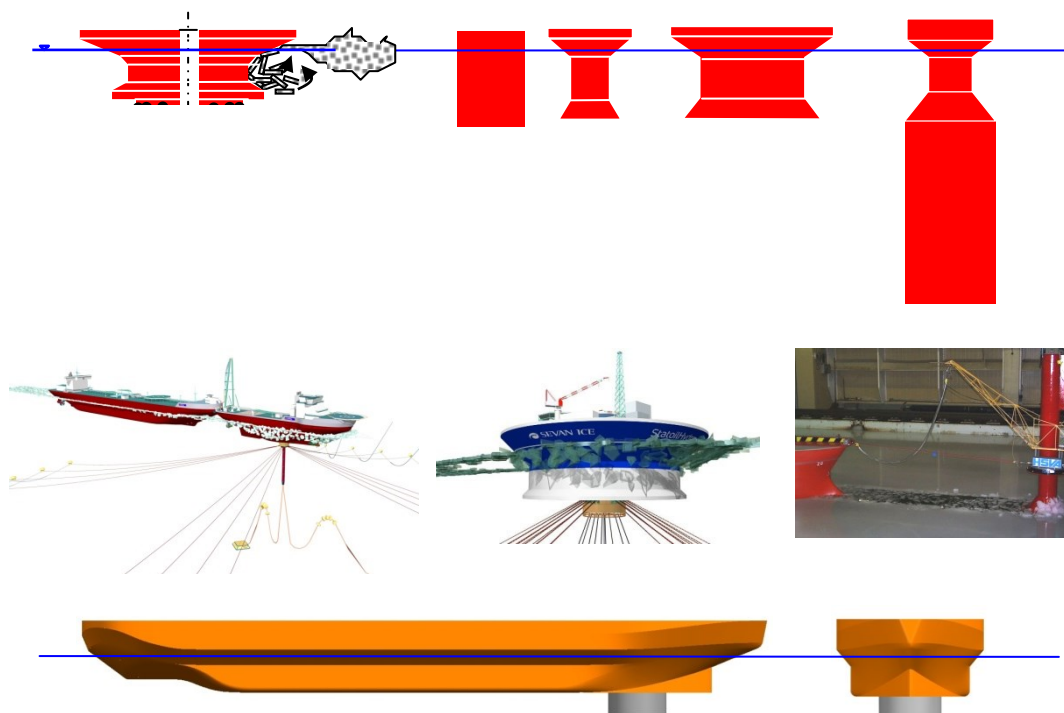


Figure 2.15 Selected different concepts of moored floating structures and vessels tested in ice at HSVA



In general the moored floating structure should be capable of breaking level ice sheets associated with ridges and ice rubble fields and should also be able to disconnect from the mooring system in the case of iceberg collision risk. A reconnection at a later date should be possible. Ice management by means of purpose built ice breaking supply and standby vessels may be necessary to ensure maximum operability in case of extreme ice conditions.

The hull at the waterline should be designed to allow the level ice and the consolidated layer of the ridge to fail by bending. Even more important is the hull design with respect to ice clearing, i.e. the transportation of broken ice floes and ridge fragments around the floating structures. In particular for buoys the hull diameter below the waterline should be reduced as much as possible to avoid serious accumulation of broken ice pieces around the structure, which consequently increases the effective diameter and generates higher ice loads.

#### **2.4.2 Mooring systems in ice**

In general shallow water mooring systems are designed to fulfill the strength and fatigue requirements. But in deepwater the mooring systems experience higher pretensions and the taut nature of the mooring system results in dynamic tensions which can be significant higher under wave and ice conditions. Thus in modern mooring designs a mooring system usually consists of several mooring lines providing a robust design for operational and survival design criteria. The pre-tension of the mooring lines (stiff or soft) has significant influence on the dynamic response offset due to waves and ice (Allen et. al. 2009).

Spread mooring systems for FSPOs typically have mooring lines in groups at each of the four quadrants, while turret moored vessels have three groups of mooring lines.

In the described example, the anchoring system consists of 20 identical legs arranged in four bundles of five legs each. The angle between two bundles is 90 degrees. The separation angle between two adjacent legs of the same bundle is 3 degrees (see Figure 2.13). The mud-line radius is about 1100 meters (full scale) from turret center. Since the geometry of the mooring system cannot be modelled due to its large dimensions, a substituted mechanical spring system of the mooring system has to be fabricated. In general a truncated system is chosen. Tension springs of various stiffness are connected parallel or in series with PE-fibres (e.g. Dyneema cords). It is challenging to assemble tension springs and cord that they fit the target restoring force curve. The substituted mechanical spring system does not reproduce exactly the vertical angles of the mooring lines. Depending on our experience the stiffness of the individual mooring lines should be slightly softer than the target stiffness in order to get a line of best fit with the target restoring force curve. Figure 2.12 shows the curve of an individual mooring line, while Figure 2.13 shows catenary mooring line arrangements and Figure 2.14 and Figure 2.15 present the corresponding restoring moment and restoring force curves obtained from pull-out tests in open water conditions.

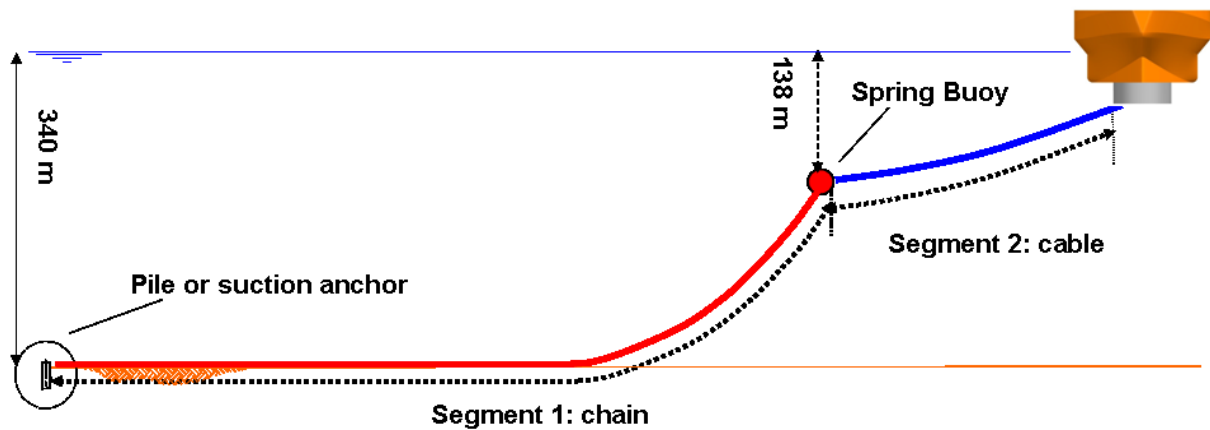


Figure 2.16 Catenary mooring line arrangement (example)

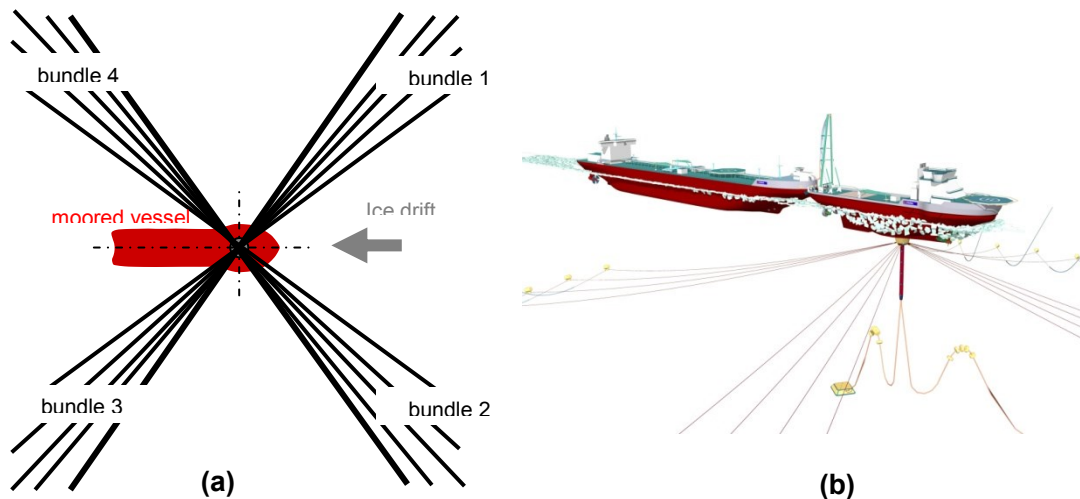


Figure 2.17 Mooring lines arrangement (a) & components of catenary mooring system (b)

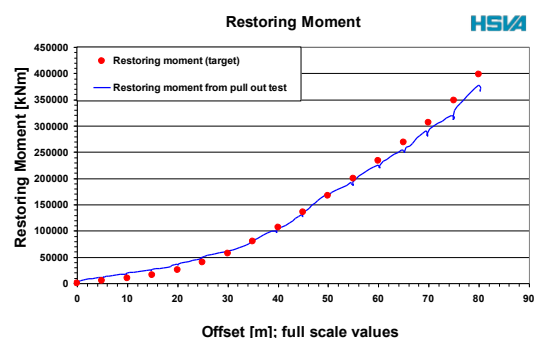
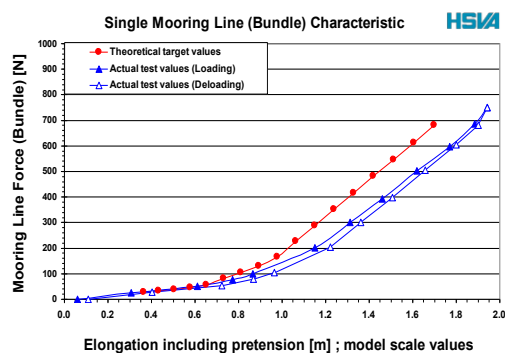


Figure 2.18 Single mooring line characteristic (left) and restoring moment (right)

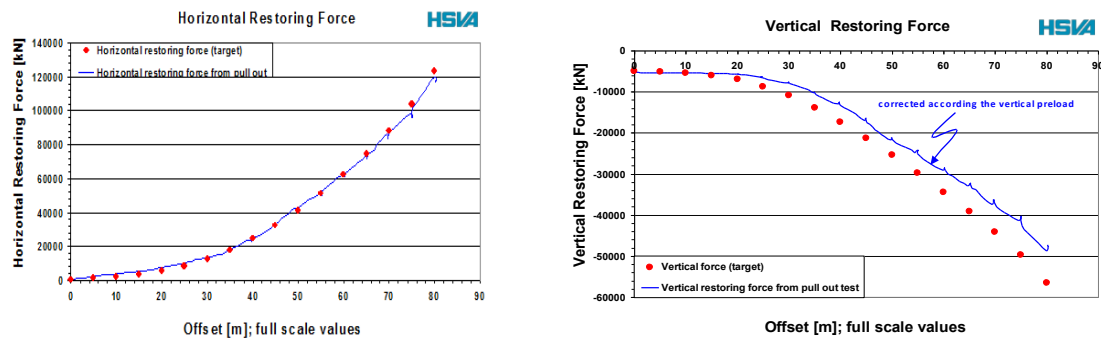


Figure 2.19 Horizontal restoring force curve (left) and vertical restoring force curve (right) [full scale values]

#### 2.4.2.1 Set-up of a moored FPU model tested at HSVA

Due to the limited dimensions of the ice test basin an equivalent truncated mooring system is designed. The model mooring system is simplified by modelling only one mooring line for a bundle consisting of five individual model lines. The mooring lines, Dyneema cord, are running from the buoy to the underwater carriage where they are turned into the horizontal by using roller bearings. After another 2 m of Dyneema cord the set of springs is connected running in half pipes in order to reduce friction. The spring set is connected to a worm gear which permits the adjustment of the pretension even underwater. The worm gear is rigidly attached to the underwater framework.

The mooring system is installed on the underwater carriage, a movable false floor at a water depth of 2.0 m. This configuration is called “wet mooring”, i.e. the mooring system and the turret are below waterline. The underwater carriage is a framework, combined from two rectangular shaped frames 10 m x 2.5 m and two single pushing frames, aligned by several cylindrical and rectangular shaped pipes of different length and size. This framework is suspended from U-shape rails mounted along the side-walls of the ice basin approx. 30 cm below the water level. The underwater-carriage is completed by main wheels and guiding rollers and is pushed by the main carriage by rigid pusher bars, which can be installed at different places on the main carriage.

The elasticity of the full scale mooring system is modelled as accurately as possible with a sequence of coil springs with different spring stiffness combined with a Dyneema cord of 5 mm diameter. The Dyneema cord is much stiffer than the stiffest spring in the individual mooring line set-up. The weaker springs of the system were blocked by a parallel cord, stopper line, at the inclination points of the target load-extension curve. A spread sheet was used to determine the individual stiffness of each single coil spring, the length of the stopper lines as well as the characteristics of a single mooring line and of the total mooring system. Not only the mooring line forces but also the horizontal and vertical restoring forces as well as the restoring moments of the model is calculated. As it is not possible to model the three above mentioned parameters correctly over the total offset range, the client demand was to reach the given target values for the horizontal restoring force and the fairlead angle within a deviation of  $\pm 5\%$  for the horizontal restoring force. Figure 2.16 shows a moored FPU during ice vaning tests.



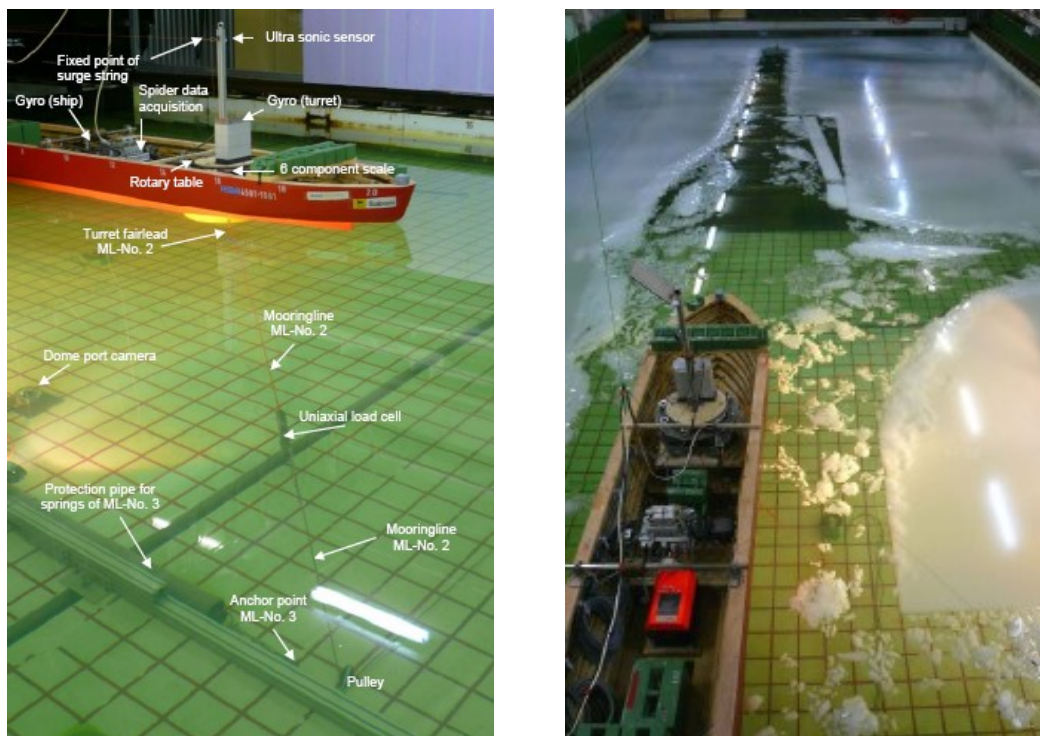


Figure 2.20 Moored FPU during ice vaning model tests (Evers, 2008)

#### 2.4.2.2 Set-up of a moored SPAR model tested at HSVA

The model of a moored SPAR buoy is divided into three segments, whereby the cylindrical segment and the lower conical segment are firmly connected when the model is assembled for the tests. The lower conical segment is equipped with a column from which the upper segment is suspended by three 3-axial load cells. This configuration makes it possible to measure the ice loads directly acting on this part of the hull. There is a small horizontal gap between the lower and upper conical segment and positioned immediately above the fairleads of the mooring lines. Another gap is between the supporting column and the duct inside the upper conical segment. Both gaps are filled with water, which is heated inside during the freezing period, in order to avoid icing. The mooring lines are tightened from the SPAR fairlead to a guide pulley at the bottom of a post and then vertically guided to the coil springs connected in series. The coil spring arrangement is close to the water surface which allows easy access for adjustment of pretension in the springs. In order to measure the mooring line load a uniaxial load cell is shackled between the fairlead and the guided pulley close at the bottom. Figure 2.21 shows the assembly steps of the three segments and Figure 2.22 presents the principle design of the SPAR buoy and the complete SPAR model including mooring system in the 5 m deep section of the ice tank. The performed ice model test shows that the concept is feasible to operate in the tested ice conditions (Bruun *et al.* 2009).



Figure 2.21 Different segments of the SPAR model (Evers & Jochmann, 2011)

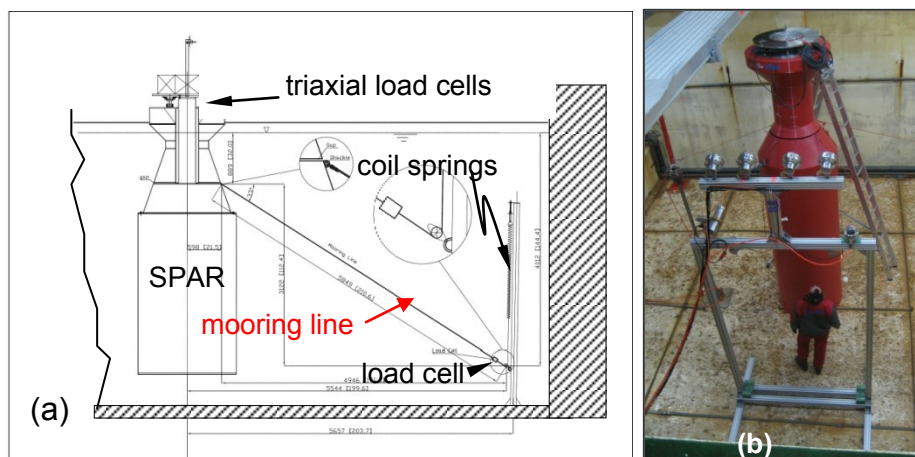


Figure 2.22 (a) Schematic diagram of moored SPAR model; (b) SPAR model in the 5 m deep ice tank section (model scale 1:45), (Evers & Jochmann, 2011)

#### 2.4.2.3 Extended test capabilities for modelling ice drift change scenarios with a moored or fixed floating structure

A removable transverse carriage is permanently installed as a sub-carriage at the rear side of the main carriage. Both carriages together make it possible to run offshore structures or floating vessels in a combined and computer-controlled x-y-motion (planar motion) through the ice sheet. The device gives us the opportunity to simulate, for instance, ice drift scenarios with slow or rapid ice drift direction changes or manoeuvring tests, whereby the model is guided by the main carriage and transverse carriage simultaneously while the ice sheet is kept stationary.

The transverse carriage has a maximum static load capacity of 5 kN in any horizontal direction and a load capacity of nearly 10 kN in vertical direction. The horizontal load can be applied on a vertical lever of up to 1.2 m length. A maximum driving force of about 3 kN is applied to the transverse carriage at speeds of up to 0.5 m/s by a geared electric motor.

This transverse carriage facilitates the execution of manoeuvring or dynamic positioning tests in the ice tank with free sailing icebreaking vessels in level ice, ridges and ice rubble fields. To a certain extent this device can also be used for moored floating vessels or offshore structures, and is very suitable for the execution of tests regarding slow or rapid ice drift change scenarios. In this case the turning radius of the vessel and the ice drift speed can be varied, when the model is guided through the ice by the towing carriages and the ice sheet is kept stationary (see Figure 2.23).

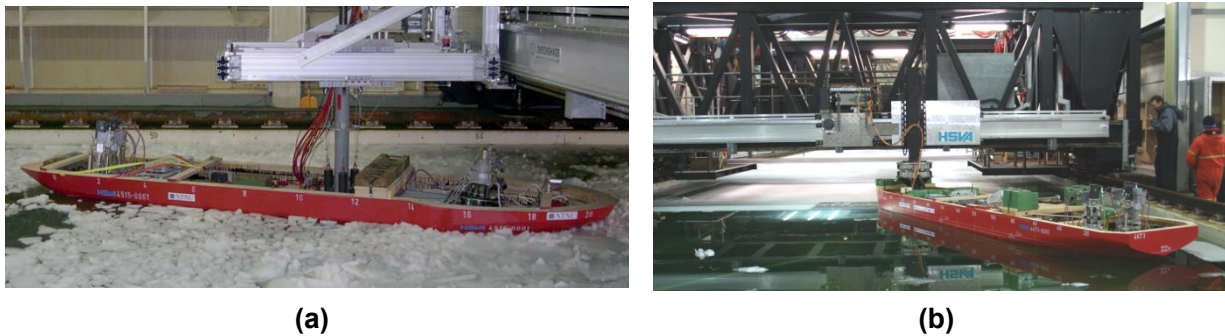


Figure 2.23 OIB model with “dry” mooring system (a) ; FPU model in fixed mode connected to the transverse carriage (b)

### “Dry” mooring system

Manoeuvring tests are conducted with an offloading icebreaking vessel (OIB) in level ice and first year ice ridges. The tests performed included various aspects and are related to the concept development. The study points focused on:

- increasing the general knowledge about mooring in ice.
- mooring forces in different ice conditions and ice drift events
- OIB ability to cope alone with severe ice and ice drift conditions
- ice management by the OIB using its own propellers
- subsurface ice transport under the OIB
- load reduction on the turret mooring from the azimuth thrusters
- manoeuvring of the moored vessel and stability in yaw.

The test matrix was elaborated on the background of previous studies (Bonnemaire *et al.* 2008, 2009 and 2010) and ice model tests during ATOT Phase 1 and the improved reamer design of the OIB. Figure 2.24 presents the scenarios carried out in three level ice sheets. For practical reasons, a “dry” mooring system mounted “upside down” above the model is more convenient to handle, i.e. easy access to the mooring system without discharge of tank water. A new system giving mooring characteristics independent of the vessel excursion was developed by HSVA and Barlindhaug Consult AS for test series, where the model manoeuvres in different ice conditions (level ice, ridges, ice rubble and managed ice).

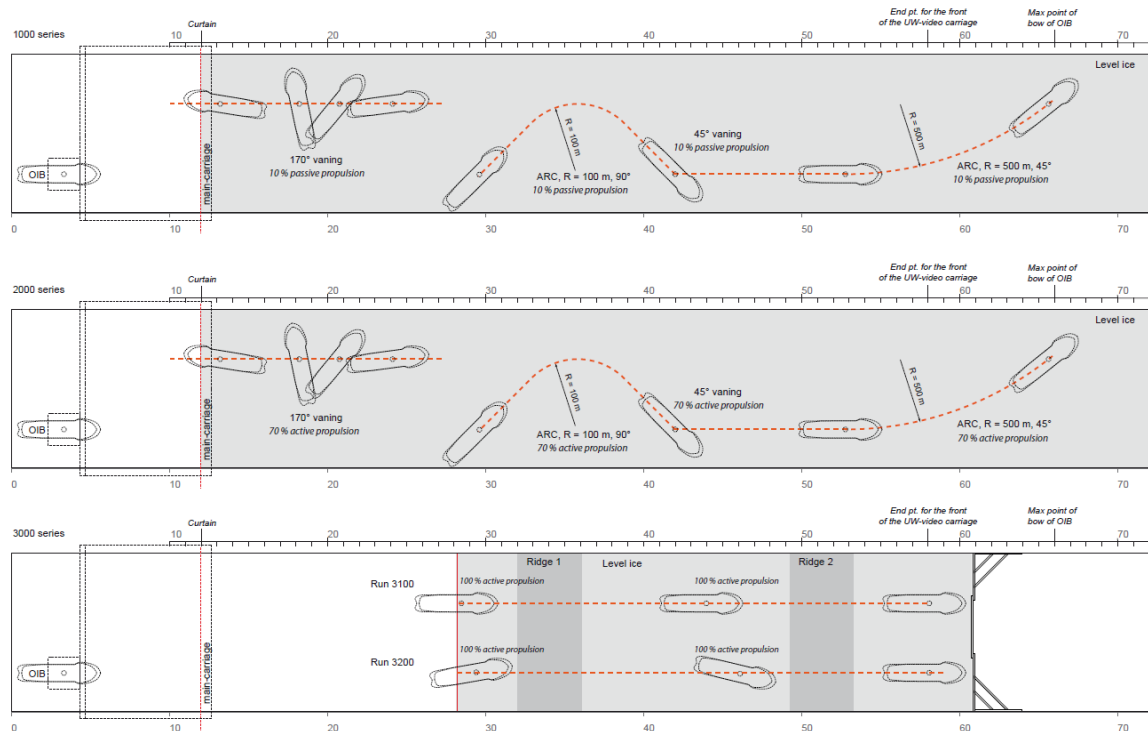


Figure 2.24 Outline of ice-icing scenarios carried out in level ice and manoeuvring in ridges (Evers, 2011)

Figure 2.25 presents a schematic diagram of the dry mooring device. A vertical column is fixed to the bottom of the vessel via a universal joint and a triaxial load cell. The column is thus fixed in surge, sway and heave to the vessel. However the column is free to heave in the mooring frame. The column is mounted on the transverse carriage that can move simultaneously with the main carriage in x and y-directions. On each beam a coil spring - mooring line and load cell system is mounted, that controls the force in surge and sway between the vessel and the towing carriage (see Figure 2.25).



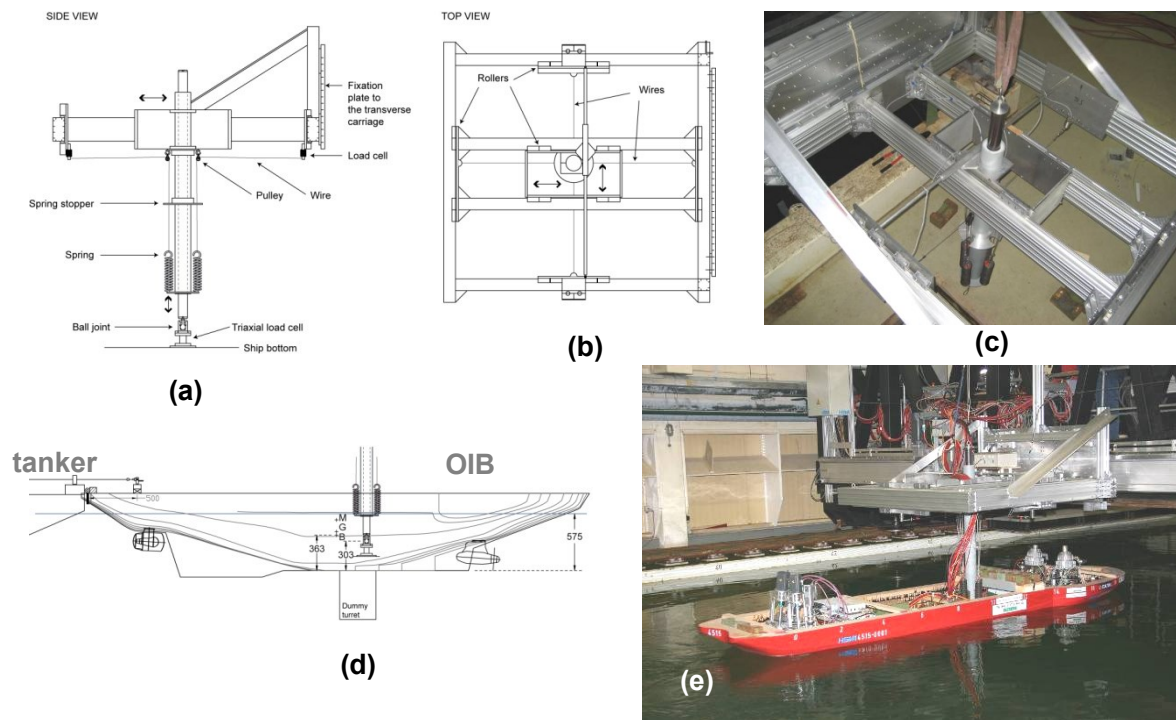


Figure 2.25 Schematic diagrams and photographs of a “dry” mooring system

#### 2.4.2.4 Set-up of a fixed FPU model

In the fixed mode the FPU model is connected to the main carriage by a post, which is rigidly connected to the transverse axes. Tests in fixed mode are carried out in order to measure the effective icebreaking forces excluding response forces caused by a mooring system. The model is equipped with a universal joint, a rotary table and a heave guidance allowing the model to freely turn around all three axes and heave. Both components are located inside the attached buoy as close as possible to the area of the fairlead points. A special arrangement allows to block the yaw-motion individually while roll and pitch motion can be blocked together only. The heave guidance could be replaced by a rigid beam in order to block the heave motion. To determine the loads acting on the FPU model during ice interaction a 6-component scale is attached to the flange plate of the post. A cylindrical pipe is connecting the lower part of the six component scale with the heave guidance which is located on top of the rotary table inside the rigid and watertight attached buoy. The 6-component scale enables the measurement of the three force components and the three moments around the axes during structure-ice interaction. Figure 2.26 presents a drawing and a photo of the “fixed mode” test set-up.



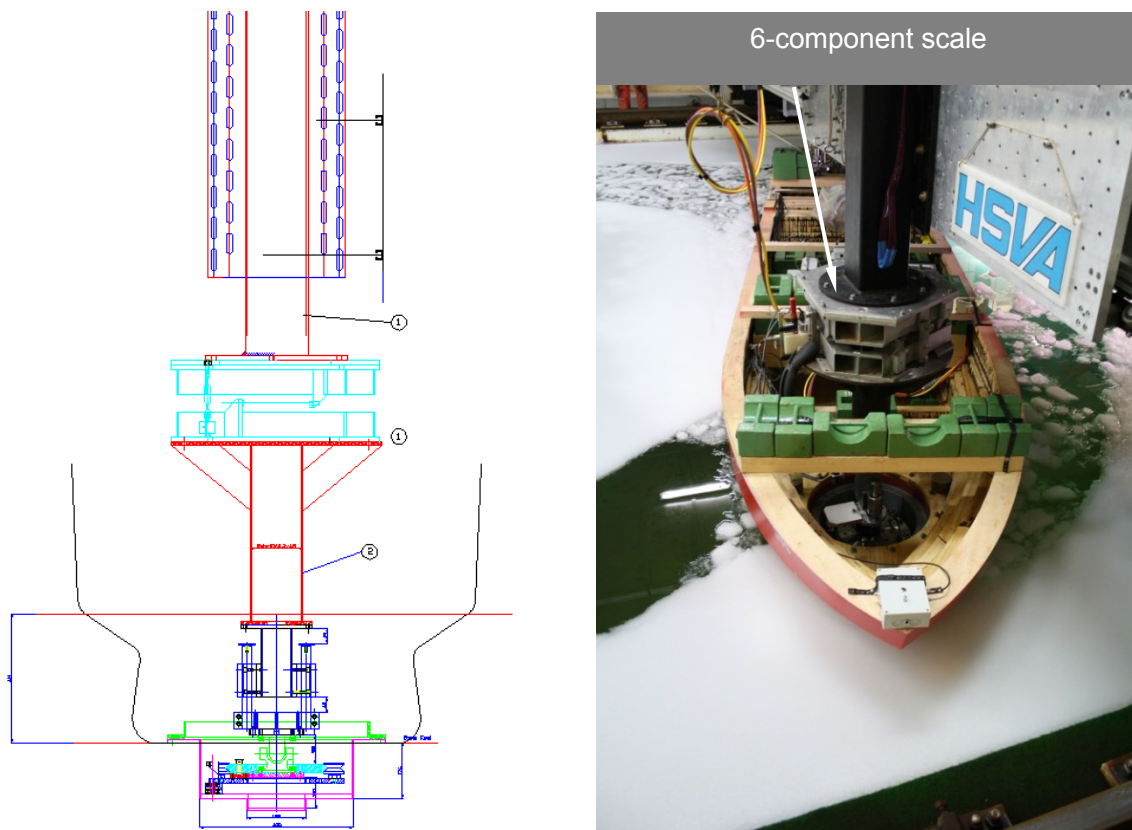


Figure 2.26 Fixed mode test setup of a floating production unit (FPU)

## 2.5 Changes in the use of laboratories

The use of hydraulic laboratories is changing. This section contains some thoughts about recent trends in their use.

### 2.5.1 From tides to turbulence

A number of large physical models were constructed from the 1950's to the 1990's, including large physical models of tidal estuaries, river systems and dams. For example, Delft Hydraulics opened a second laboratory at de Voorst in 1951 to house large, open air models. From about 1970 to 1995 some 45,000m<sup>2</sup> of premises and offices were available (van Os, 2010). However, the end of the Delta Works and the increase in computing power in the mid-1990s caused Delft Hydraulics to reduce the available space for large models. The tidal model of the Rhine-Meuse had already closed in 1988. Similarly, the largest single model in the USA, the Mississippi Basin model, occupied an area of 3.3 km<sup>2</sup> and was in operation from 1946 to 1990, while the 100 m by 70 m Maplin Building at HR Wallingford (UK) was constructed in 1972 to house a single physical model of the Thames Estuary, which ran for about two years (and recorded water levels and current speeds onto paper tape).

These very large models of shallow water flows are rare today, due the increases in computer power and improvements in shallow water flow modeling. Shallow water flow modeling over large areas is done routinely today using a range of validated and accepted numerical models. Physical modeling today concentrates on the smaller-scale non-linear phenomena, such as the effects of turbulent, rapidly changing flows on structures, rock armour and scour protection.

Physical modeling is concentrating more and more on high frequency, fine resolution phenomena, and the experimental techniques have evolved over the years to capture data at the required frequency, accuracy and spatial resolution.

### **2.5.2 The rise of marine renewable energy**

The ever-increasing data and modelling results that support the theory of anthropogenic climate change are forcing governments to consider low-carbon forms of energy. Marine renewable energy (including wind turbines situated at sea) is an attractive resource in Europe, thanks to the supplies of wind, wave and tidal energy. The development of practical, efficient and durable devices for extracting energy from the marine environment is still at an early stage. The most mature technology is the use of wind turbines on a marine foundation: there are now hundreds of wind turbines installed in European waters, although each new deployment still requires a thorough analysis and the move to deeper water (such as for Round 3 wind farms in UK waters) is presenting a new set of difficulties as the limits monopole foundations are reached. Wave energy converters (WECs) and tidal energy converters (TECs) are at a much lower stage in their commercial development. This situation calls for a lot of physical model testing on these devices, while CFD is also used in a number of areas, including the modelling of non-linear free surface dynamics of oscillating water columns and flow round WEC or TEC blades.

Important issues to be considered include:

1. Performance of novel foundation types, including jackets, multiple piles, gravity bases and floating foundations (including seabed scour)
2. Combined effects of turbulence, waves and currents on marine renewable energy devices. Areas of concern include the flows round blades and other components, the forces on these components and the power take-off (PTO) in different conditions.
3. Multiple resource simulations, such as wind & waves for wind turbines, waves & current for marine current turbines and the effect of arrays of turbines on these resources.

Although the third item will be addressed by numerical modelling, the first two will be addressed using a combination of physical modelling and CFD. The measurement of global forces and local pressure distributions will make an important contribution to the development of WEC and TEC devices into practical marine renewable energy sources.

### **2.5.3 Impact of climate change on hydrodynamic load testing**

Changes in climate are expected to result in two main problems related to the hydrodynamic loads on structures:

- Increased water levels;
- Changed (potentially increased) storm intensity and possible changed directions of wave impact; and

It is not likely that these changes will present new and unexplored phenomena with regard to wave/structure interaction. The direct effect will be a changed level of impact, and hence priority, but the fundamental processes will be as known in the past. Nevertheless the inherent statistical uncertainties in design basis may very well lead to a different practice among designers who must design for flexibility and adaptation to new conditions to a larger extent than in the past.

The fact that the exposure to hydrodynamic processes will change and potentially create larger risks to people and to existing man-made structures will change the attitude among the population and require stronger attention to the conditions for exploitation of the coastal and marine zones as the locations for people and critical infrastructure. Not only will new structures

have to be planned and designed for increased exposure, but existing structures and infrastructure will also need to be adapted to the new conditions.

For economic reasons adaptation of existing structures – dikes, port infrastructure, protection of urban areas, bridges, pipelines – to more exposed conditions will be a key issue. It is likely that cost benefit considerations related to risk assessment will lead to higher demands regarding precision of the tools we use to assess water-structure interaction. Safeguarding existing infrastructure will be weighed against complete replacement and new-built facilities. The assessment of alternatives will thus be a challenge to the accuracy of our methods.

Exploitation of renewable energy sources is of great importance to our future. The focus will be on marine areas and thus require improved understanding of the behaviour of complex structures at sea. The joint exposure to natural forces is scientifically challenging and will lead to new design codes that will have to be based on experimental back-up and verification as well as on systematic feedback from prototypes.

It is evident that increased attention to the hydrodynamic impact on facilities in urban and recreational areas on the coasts and for new energy sources offshore will require increased capacity among specialists and institutions to cope with the decision processes.

Thus, although the climate change considerations will not as such change the fundamental scientific challenges, it is important that our scientific community prepare for new and more exposed environmental conditions. The following elements are vital for the future developments of our methodologies:

- Increased attention to flexibility of design solutions.
- Enhanced focus on methods to cope with service life design versus limit state design.
- Improved methods for analysis of joint exposure to aerodynamic and hydrodynamic impact on structures.
- Improved and cost effective methods for analysis of multi-body structures (offshore and shore/structure connected floating structures).
- Development of cost-effective coastal protection methods.
- Development of rapid deployment methods for mitigating effects of unexpected extreme events.
- Feed-back monitoring of structures and adaptation solutions.

#### **2.5.4 Impact of climate change on ice load testing**

The average temperature in the Arctic has increased due to the increase of the greenhouse gas concentration in the atmosphere. This has led to a rapid reduction in sea ice extent, the melting of glaciers and the thawing of permafrost (see box below). This climatic evolution is going to have strong impacts on both marine ecosystems and human activities in the Arctic. It also opens up business opportunities regarding new shipping routes with higher volume of traffic and extensive oil and gas explorations in the Arctic.

## Summary of facts (Ref.: SWIPA 2011 Executive Summary Report)

- The extent and duration of snow cover and sea ice have decreased across the Arctic. Temperatures in the permafrost have risen by up to 2 °C. The southern limit of permafrost has moved northward in Russia and Canada.
- The largest and most permanent bodies of ice in the Arctic – multiyear sea ice, mountain glaciers, ice caps and the Greenland Ice Sheet – have all been declining faster since 2000 than they did in the previous decade.
- The Arctic Ocean is projected to become nearly ice-free in summer within this century, likely within the next thirty to forty years. In this context it would be possible to navigate on new transportation routes from Europe to Asia and vice-versa.
- Transport options and access to resources are radically changed by differences in the distribution and seasonal occurrence of snow, water, ice and permafrost in the Arctic. This affects both daily living and commercial activities.
- Changes in the cryosphere cause fundamental changes to the characteristics of Arctic ecosystems and in some cases loss of entire habitats. This has consequences for people who receive benefits from Arctic ecosystems (e.g. indigenous people).
- Arctic infrastructure faces increased risks of damage (buildings, pipelines etc.) due to changes in the cryosphere, particularly the loss of permafrost and land-fast sea ice.
- Loss of ice and snow in the Arctic enhances climate warming by increasing absorption of the sun's energy at the surface of the planet. It could also dramatically increase emissions of carbon dioxide and methane and change large-scale ocean currents. The combined outcome of these effects is not yet known.
- Arctic glaciers, ice caps and the Greenland Ice Sheet contributed over 40% of the global sea level rise of around 3 mm per year observed between 2003 and 2008. In the future, global sea level is projected to rise by 0.9–1.6 m by 2100 and Arctic ice loss will make a substantial contribution to this. The rise of sea level will definitely affect the shore protection measures even in European countries.
- Socio-economic effects - people who live and work in Arctic regions will need to adapt to changes in the cryosphere. Adaptation also requires an increased investment in infrastructure.
- There is a great uncertainty about how fast the Arctic cryosphere will change in the future and what the ultimate impacts of the changes will be. Interactions between elements of the cryosphere and climate system are particularly uncertain, thus concerted monitoring and further research is needed to reduce this uncertainty.

The decline of ice extent in the Arctic shows that longer navigation seasons and greater access will occur around the entire periphery of the Arctic Ocean basin in the future. Maritime transport in the Arctic has become a widely discussed issue since the Northern Sea Route (NSR) was almost free of ice in months September-October and even ships without ice class were able to sail along the route (see Figure 2.27).



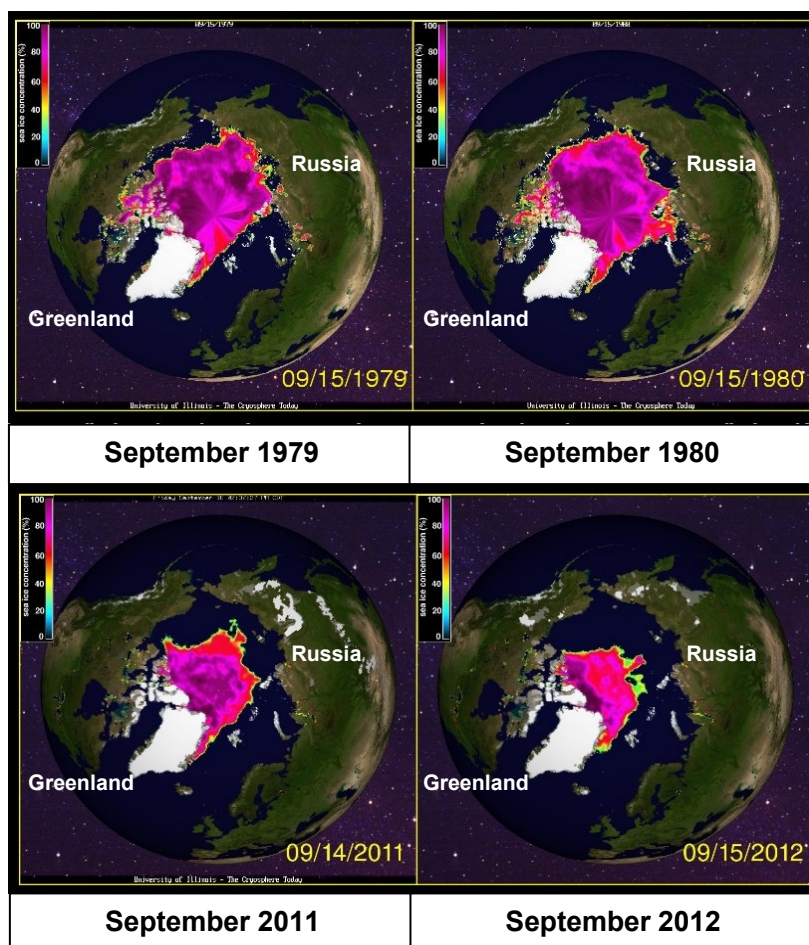


Figure 2.27 Changes in sea ice extent

Cargo and passenger vessels in the Arctic are confronted with safety issues in terms of bad or dangerous practices. These include navigating in unmapped waters, near approach to icebergs and other hazards or not coordinating voyages with other vessels in Arctic areas with particularly limited Search and Rescue (SAR) availability. Also a safe ship design regarding ice strength and ice class is of great importance to be able to navigate in severe ice conditions. Shipping activities pose greater risk for accidents in the Arctic than further south in ice free waters, because of the extreme conditions with ice, darkness and fog. The potential for the increased use of Arctic waters for shipping and mineral/fuel extraction is expected to lead to the following developments in hydraulic laboratory testing.

#### 2.5.4.1 Oil spill countermeasures

The installation of fixed or floating offshore structures for resource exploration, extraction, and transportation in ice-covered waters increases environmental risks, and contingency planning for mitigation of risk is necessary. Oil spill contingency and response strategies vary considerably between open water and areas covered with sea ice. An oil spill in ice-covered waters would be much more serious than in open waters because no suitable oil recovery equipment is available to combat a larger oil spill in ice-covered waters. Significant environmental impacts are likely to result from large, concentrated accidental releases of oil. However, chronic oil discharges and the dumping of waste at sea also have a negative impact on sensitive wildlife habitat or hunting areas used by indigenous communities. The same climatic conditions also complicate the rescue and clean-up work (e.g. recovery of spilled oil) and thus increase risks of environmental impacts as a consequence of shipping accidents.



Thus methodologies and procedures must be developed to prevent larger oil spills in cold regions and further action is needed to ensure that best practises is available. The technology and procedures should be developed and tested in hydraulic and hydrodynamics laboratories in order to achieve high safety standards for oil spill combating, response techniques and countermeasures associated with the transportation of hydrocarbons.

#### **2.5.4.2 Ice route optimisation along the Northern Sea Route (NSR)**

The decreasing volume and extent of sea ice in the northern hemisphere favours ship navigation from Europe to East Asia along the Northern Sea Route, with the logistic support of harbours in Russia. This route shortens the oceanic route from Europe to Asia via Suez Canal about 30 per cent and has potential for significant cost savings and reduction in shipping days needed. . In addition to potential financial savings from slow steaming (less fuel consumption) emissions are reduced which is positive from the environmental perspective. These developments have drawn interest from the shipping community and from exporting and importing countries as an opportunity to increase their global competitiveness. However these developments affect shipping and navigation along the NSR as well as for the North-West Passage (NWP). Numerical models have to be developed to optimise the transport chain and in this context physical ice model tests representing actual ice conditions have to be carried out.

As the average transit speed in ice is very sensitive to the change of certain ice properties like ice thickness, strength and density, but also on the type of ice accumulation and concentration, methods need to be developed which provide correlations between the speed and these ice parameters in order to be used for travel time prediction and evaluation of ice covered routes. Different routes may be compared within an optimizing process for navigation assistance.

Reliable theoretic methods have not been developed yet for deformed ice conditions and, therefore, model tests represent an essential basis to complete analytic calculations which themselves take into account the main dimensions of ships, relevant hull shape parameters and certain ice properties.

#### **2.5.4.3 Dynamic positioning (DP) in ice**

As oil and gas resources exploration continues to grow in northern latitudes, increasing demand is placed on arctic technology to ensure safety and efficiency operations. For the oil and gas industry it is of great interest to extend offshore drilling and production activities in ice-covered waters. For station keeping especially for operations in ice specific DP modules are required. Controlled movement is vital for the safety of personnel and the environment. DP systems on the market today are not optimised to fully account for the forces and movements that exist in ice environments. Physical model tests (Figure 2.24) are required as input variables that need to be understood for effective and reliable DP operations in the Arctic (<http://www.dypic.eu/>).



Icebreaking supply vessel Vidar Viking



Model test: dynamic positioning in ice

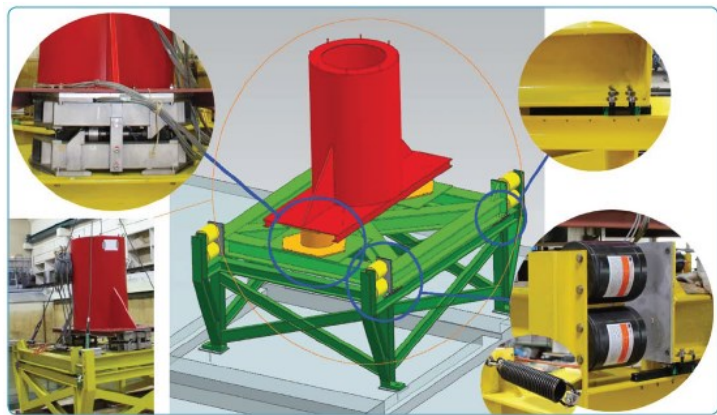
Figure 2.28 Dynamic positioning in ice

#### 2.5.4.4 Ice induced vibrations on offshore structures

There is still a poor understanding of the physical parameters that control ice induced vibrations, which may occur when level ice crushes against a compliant structure (Figure 2.24). In particular, the onset and offset of frequency lock-in and spatial synchronization of ice failure along the ice-structure interface has to be considered in detail. Physical modelling should be conducted with fixed and elastically supported structures, set in harmonic motion using displacement control. In each case the structural motion and the ice load should be measured simultaneously and the energy flow into the structure can be identified. The effect of spatial synchronization of ice loads along the ice-structure interface should be investigated in more detail, because the synchronization plays a key role in understanding of ice crushing loads in general and with respect to ice-induced vibration. This is of particular interest for the design of wind-turbine foundation structures located in ice-covered waters like the Baltic Sea.



Ice crushing failure at Lighthouse  
Norströmsgrund, Sweden  
(Photo: K. Kolari, VTT)



Test set-up of the simplified lighthouse model at  
HSVA

Figure 2.29 Ice failure at a lighthouse and a physical model of the lighthouse

### 3 Establishing the correct environment

The experiments listed in Section Two require the correct hydrodynamic or ice conditions to be generated successful. This section describes the methods used to create the correct environment for the tests and is split into two parts:

- Establishing the correct hydrodynamic environment (covering waves, currents and wind)
- Establishing the correct ice environment

#### 3.1 Establishing the correct hydrodynamic environment

##### 3.1.1 Wave generation and absorption

###### 3.1.1.1 Wavemaker theory

Physical modelling of wave loads on structures is done in wave tanks (flumes and basins), which are equipped with wavemakers capable of reproducing wave fields. The theoretical basis for reproduction of waves has developed over the years since the first analysis of small amplitude surface waves was made (Havelock 1929). A comprehensive review of wavemaker principles was published by Biesel & Suquet in 1954. A review of the developments were presented by Svendsen (1985) and Dean and Dalrymple (1991). Essentially wavemaker theory describes the motion of a paddle at the boundary of the wave tank required to create a wave field of a specified form. The paddle can take many forms but essentially two forms are used today – a piston type of paddle that moves backwards and forwards in the direction of wave propagation and an articulated type where the paddle rotates around a hinge at or above the bottom of the tank (see Figure 3.1).

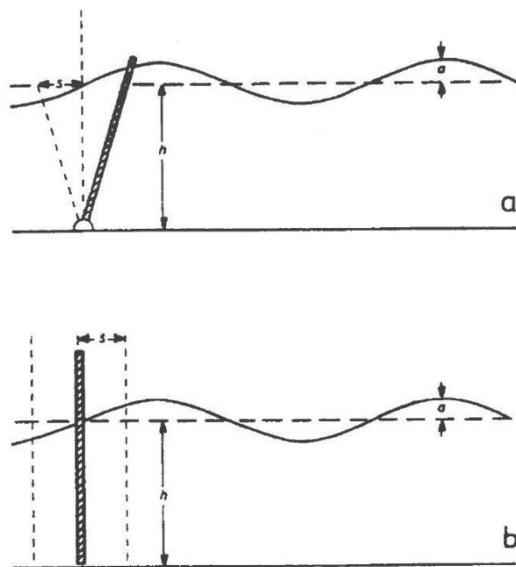


Figure 3.1 Wave paddles. (a) Articulated type. (b) Piston type.

The function of the paddle is to approximate the velocity profile in a progressive wave. This motion of the paddle is linked to surface wave amplitudes by a theoretical expression – the transfer function.

The differences between the paddle velocity profile and the theoretically correct velocity profile give rise to deviations between the intended surface wave profile and the actually created

profile. Both of the paddles described above produce a linearly varying velocity profile over the water depth whereas in reality the profile deviates from a linear distribution. The deviations – or disturbances – are least when using a piston type in shallow water cases and an articulated type for reproducing waves in deep water.

The fundamental theoretical transfer functions for regular waves are based on sinusoidal waves and are valid for waves of small amplitude. With increasing amplitudes the waves change form and the sinusoidal wavemaker will create a wave motion with irregularities such as secondary crests. The secondary wave will propagate at a different speed to the primary wave. These waves interact and give rise to an inhomogeneous wave field, which also incorporates second-order components. To cope with these problems wave researchers have developed second order schemes for control of wavemakers (Fontanet 1961, Hudspeth and Sulisz 1991, Moubayed and Williams 1994, Spinneken and Swan 2009a,b).

For practical design problems (tests of port layouts, floating systems and breakwater stability) tests must be conducted in irregular waves and at times even in multi-directional seas. This is due to the fact that natural sea states are complex and can generally be described by decomposition in spectral components. Consequently modelling of irregular waves is traditionally done by superposition of a number of sine components or by direct reproduction of a wave time series (measured in nature or artificially generated from a wave spectrum) (Lundgren and Sand 1978). An important characteristic of irregular waves is the wave groups which give rise to a set-down (lowering) of the mean water level under a wave group that propagates with the wave group as a long wave (Longuet-Higgins & Stewart 1964). These wave groups may generate harbour resonance and resonance of moored ships (Bowers 1977, Ottesen Hansen 1978, Schäffer 1996, 2000). When the set-down is not properly included by the wavemaker a compensation propagating as a separate long wave will be generated which may lead to unrealistic low-frequency disturbance in the model. The challenge is that the set-down can only be reproduced when the wavemaker has an extremely large stroke compared to the stroke needed for creating the primary wave (Sand 1982).

Second-order wavemaker theory has been extended to irregular and multi-directional waves (Zhang and Schäffer 2007, Sulisz and Paprota 2008).

#### **3.1.1.1 Absorbing paddles and boundaries**

A wave tank represents a limited volume of a water body. The boundaries of the tank represent unnatural limits for wave propagation and they may give rise to unwanted reflections that interact with the generated primary wave field. Also the test object (the model) may give rise to reflections that are trapped inside the wave tank. In addition to interference with the objective of the model experiment the reflections from boundaries and the model affects the wave measurements.

Boundaries that are not part of the test object should be shaped as absorbing slopes and beaches in order to avoid unrealistic reflections. This requires careful planning of the test layout.

Part of the reflections will reach the wave paddle and will lead to re-reflection from the wave paddle, if not counteracted. To solve this problem laboratories develop wavemakers with so-called active absorption. This means that the control signals to the paddle(s) are modified to adapt to the reflected wave (Milgram 1970, Schäffer and Klopman 2000). Active absorption needs a hydrodynamic feedback in order to detect the waves to be absorbed. One method is to integrate wave gauges in the paddle front whereby the surface elevation can be measured continuously. A difference between the measured elevation and the intended wave profile is then a proof that reflected energy reaches the wave paddle and the difference is minimised by a servo loop of the wavemaker control (Schäffer 2001) see Figure 3.2.





Figure 3.2 Oblique waves generated by the wave generator to the right. (a) 3D wavemaker at rest. (b) 3D wavemaker in absorbing mode.

Interestingly, the same problems are now being faced by the developers of computational fluid dynamics (CFD) wave flumes (Maguire and Ingram, 2011) who also have to create and absorb waves at the offshore boundaries of their models. It is quite possible that we may see more of the development and testing of new techniques in CFD models before they are applied in physical models.

### 3.1.1.2 Deterministic generation of extreme wave groups

Existence of rogue waves and associated damages to offshore structures and ships in the past (eg. Draupner wave) led to the investigation of wave-structure interaction in extreme seas. For the design of safe and economic offshore structures and ships, the knowledge of the extreme wave environment and related wave structure interactions is required (Clauss 2002). Deterministic investigation of extreme events such as freak waves, breaking wave impacts and associated structural responses in the laboratory environment thus requires methods of generating deterministic wave sequences at prescribed locations.

Traditionally the investigations of structural response to waves are carried out in hydraulic laboratories using regular waves or irregular spectra. Both methods are time consuming as with regular waves a great number of individual runs is necessary and with irregular waves testing for large number of waves is required in order to obtain statistically valid results (Grigoropoulos *et al.* 1994). For these reasons, a new type of testing was investigated by several authors using transient waves, which are of short duration that may represent a broad banded energy spectrum. The essential advantage of testing ship or floating structure models in transient waves is the drastic reduction of the required time and hence the cost of the experiments, when compared to regular or random wave testing (Grigoropoulos *et al.* 1994). Additional advantages of transient wave testing are avoidance of wave maker reflected waves, reduction of tank wall interference and repeatability of test conditions.

Transient wave technique was first introduced by Davis and Zarnick (1964) for the determination of seaworthiness characteristics of a ship design. They used a linear sweep technique to generate a wave train of increasing wave length (Clauss and Bergmann 1986). Due to the frequency dispersion, the wave train concentrates and converges to its highest amplitude at a predefined location in the flume. However, it was difficult to control the shape of the wave train and the spectrum as the transfer function of the wave generator influences the results. Later,



this technique was significantly improved by Takezawa and Hirayama (1976, cited in Clauss and Bergmann, 1986) by deriving the input signal of the wave maker starting from the desired wave spectrum using inverse Fourier transform. Although the improved method allows excellent control of the spectral characteristics, the control of the shape of the wave train is still rather poor. Clauss and Bergmann (1986) implemented a special type of transient waves, i.e. Gaussian wave packets, which allows both shape of the wave train and its spectrum. Gaussian wave packet is composed of infinite number of superimposed harmonic components. The wave profile is defined by:

$$\eta(x, t) = \int_{-\infty}^{\infty} a(k) \cdot e^{-i(kx - \omega t)} dk$$

Where  $x$  and  $t$  are space and time respectively,  $k$  is the wave number and  $\omega$  is the wave frequency. The amplitude spectrum is given by:

$$a(k) = \frac{a_0}{s\sqrt{2\pi}} e^{-\frac{(k-k_0)^2}{2s^2}}$$

Where  $a_0$  is the maximum wave amplitude,  $k_0$  is the corresponding wave number and  $s$  is the standard deviation of the amplitude spectrum.

Gaussian wave packets have the advantage that their propagation behaviour can be predicted analytically. This technique yields accurate and highly resolved results in seakeeping tests. The required duration of the experiment is reduced drastically (Clauss and Bergmann 1986).

With increasing efficiency and capacity of computer, the restriction to a Gaussian distribution of wave amplitudes has been abandoned, and the entire process is performed numerically (Clauss and Kühnlein 1995). The shape and width of the wave spectrum can be selected individually for providing sufficient energy in the relevant frequency range. Assuming linear wave theory a synthesis and upstream transformation of wave packets is developed from its so called concentration point where all component waves are superimposed without phase-shift. This wave train is linearly transformed back to the wave maker and by introducing the electro-hydraulic transfer function of the of the wave generator, the associated control signal is calculated (Clauss 2000). Based on this technique, the seakeeping behaviour of ships or offshore structure is efficiently determined with just a single model test. Figure 3.3 shows a linear wave packets at different positions, which are converging at the concentration point at 107 m, and the instantaneous wave profiles.

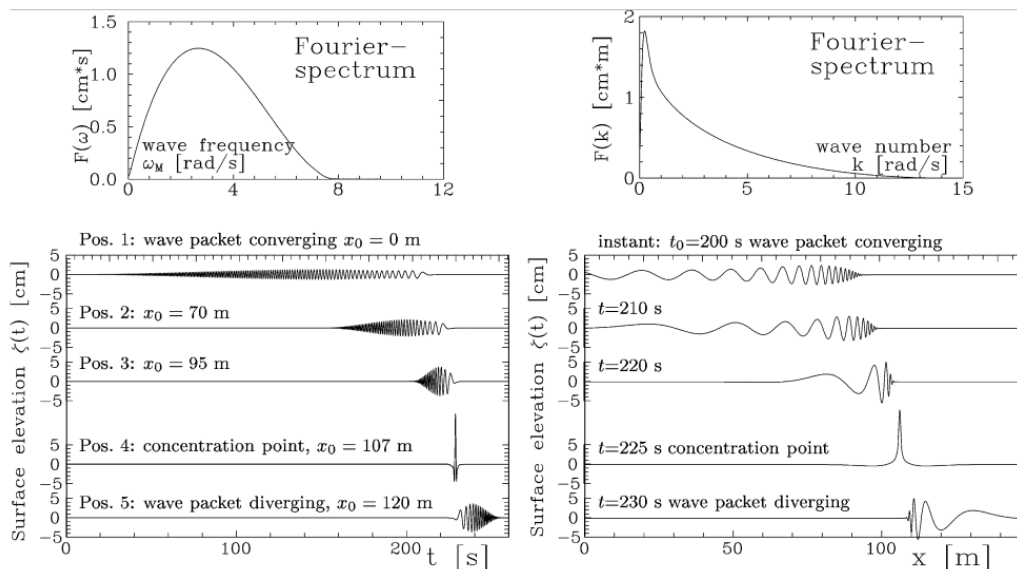


Figure 3.3 Wave packet registration at different positions (left), instantaneous wave profiles at selected instants (right) (Clauss 2000)

The generation of higher and steep waves requires a more sophisticated approach as propagation velocity increases with the wave height. Kühnlein (1997 cited in Clauss, 2002) developed a semi-empirical procedure based on linear wave theory for the determination of the control signal of extremely high wave groups. With this technique ‘freak’ waves up to 3.2 m heights have been generated in the large wave flume (GWK) with a water depth of 4 m. However, substantial differences between the measured and the target wave train at the target location have been generally observed, particularly closed to the concentration point, when a linearly synthesized control signal is used for the generation of higher and steeper waves (Clauss, 2002). Thus it becomes essential to incorporate the non-linear characteristics of the flow field in the wave generation processes. A detailed knowledge of the non-linear characteristics of the flow field is required in many applications such as wave elevation, pressure field as well as velocity and acceleration fields.

Clauss and Schmittner (2007) presented a method to generate a target wave train based on given parameters such as wave height, wave length, period, and crest elevation. A first control signal is created by linear transformation of the target wave train from upstream to the position of the wave maker by phase shift in frequency domain. Using the Subplex optimization, this wave train is improved in a small wave tank until the measured wave train satisfies all predefined target parameters. The advantage of this experimental optimization process is the inherent inclusion of all nonlinear wave effects by using a physical wave tank. The basic idea of the wave generation method is to optimize wave sequences in a small wave basin and transfer the final signal to a large wave basin where tests with appropriate scaled models are conducted. Figure 3.4 shows the fully automated optimization scheme, steering the wave maker, analyzing waves and modifying the control signal until convergence is achieved. Although this method provide accurate results, a large number of iteration processes is required to achieve the target wave train.

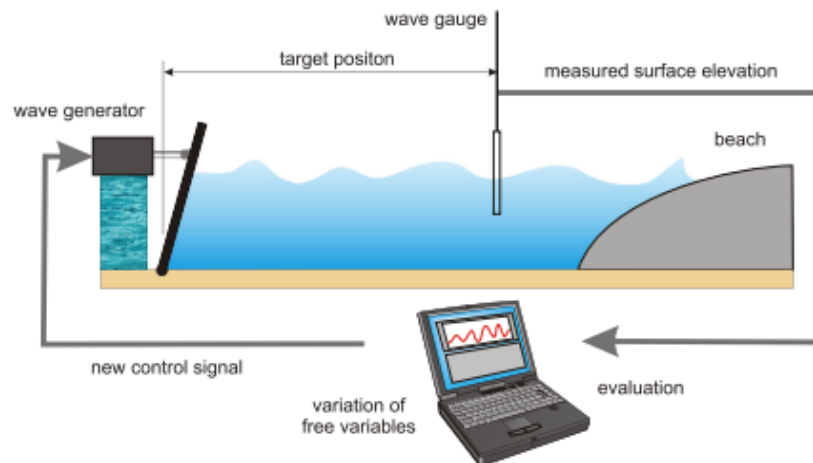


Figure 3.4 Schematic view of the computer controlled optimization of waves (Clauss, Schmittner 2007)

Schmittner *et al* (2009) presented an alternative ‘phase-amplitude iteration scheme’ for synthesizing deterministic wave sequences, based on the method proposed by (Chaplin 1996) who improved the accuracy of a focused wave train. Based on a first wave sequence generated with linear wave theory and measured in the wave tank, the phases and amplitudes are modified in frequency domain. The iteration scheme modifies both the amplitudes and phases, resulting in an improved deterministic wave train at the target location. This method is relatively fast and accurate. The number of iterations required to obtain a final solution depends on the quality of the starting control signal.

Shemer *et al* (2005) studied a nonlinear focussing process both experimentally and theoretically. The unidirectional spatial version of the Zakharov equation is applied in the numerical simulations. Good agreement is obtained between the experimental and corresponding numerical results. However, for very steep waves, the reproduction in the experiments of the desired waveform at the wavemaker becomes more complicated due to the effects of bound waves. Hence the agreement between the model predictions and the experiments is only qualitative.

Recently, an algorithm is made by Hofland *et al* (2010) for the generation of steering signal based on the work by Van den Boomgaard (2003), with some features added. The focussing signal is developed in the time domain, where the signal is the composition of very small wave groups with their own group speed and phase speed, both of which are focused at the focal point. The focused wave is used to study the wave impact loads at a vertical wall in the large delta flume of Deltares. By changing the focal point, different types of impacts are created at the vertical wall. The major advantage of this approach is that an explicit empirical non-linear dispersion relation (Kirby, Dalrymple 1986) for a regular wave can be used to determine the wave number and phase celerity from the group velocity.

Although the recent methods explained above, such as experimental optimization and time domain method, take into account non-linear effects in the process of wave focussing, they are developed for applications with constant water depth. The summary of strengths and weaknesses of some key methods used currently for wave focusing is shown in Table 3.1. None of the present techniques can be applied for the studies in the case of varying topography (such as a beach). Therefore, an extension of the present techniques towards a model for propagation

over an uneven bottom can be the first step, which is considered in Hydralab WP9 (see Section 5).

Table 3.1 Wave focusing methods as currently used in physical wave modelling

Method	Mechanism	Strengths	Weaknesses	Remarks
Gaussian wave packets (Clauss & Kühnlein 1995)	Short wave trains with an energy spectrum covering the entire frequency range	Excellent control of both shape of the wave train and its spectrum	Necessity to have a constant water depth; Reflections on the focusing process is not considered	The wave train is linearly transformed back to the wave maker
Frequency dispersion (van den Boomgaard 2003)	(Non)linear superposition and phasing of different wave components (wave-wave interaction)	Effect of amplitude dispersion is mimicked by the use of non-linear dispersion relation $\omega(k,h,a)$	Only applicable for constant water depth; Reflection is not considered	Application of 2 <sup>nd</sup> order wave maker theory is more efficient
Experimental optimization (Clauss & Schmittner 2007)	The control signal from the linear optimization approach is iteratively improved by a fully automated experimental optimization process	Use of small wave tank to optimize the signals whereas the larger flume is used for specific seakeeping tests Satisfactory target parameters can be achieved; Non-linear free surface effects are included	Requires many iteration processes; No consideration is given for the effects due to wave reflection on the structures	Phase-amplitude iteration scheme is efficient for the large wave flume
Time domain method (Hofland <i>et al.</i> 2010)	Focusing signal is developed in the time domain	Non-linear dispersion relation can be used to determine the celerity and wave number from the group velocity; Breaking point can be shifted explicitly without altering the setup/water level	Limited to constant water depth; The last wave is treated separately	Extension of the model for uneven bottom also possible
Non-linear wave focusing (Pelinovsky <i>et al.</i> 2000)	Focusing of non-linear wave field with phase modulation	Phase modulation leads to greater amplification of freak waves than amplitude modulation	Wave field structure is more complicated	Advanced mathematical knowledge is required
Steep transient wave (Shemer <i>et al.</i> 2005)	Spatial version of Zakharov equation is applied in numerical simulation	Includes non-linear effects; Higher number of wave harmonic is considered	Generation of extremely steep waves cannot be reproduced; Constant water depth	Corrections due to bound waves and dissipation along the tank has to be added

### 3.1.1.3 Tsunami wave generation

Tsunami waves differ markedly from wind or swell waves, generally being of durations of many minutes length. Example measurements from the Thai coast under the 2004 Indian Ocean tsunami, and from the Eastern Japanese coast under the 2011 Tohoku tsunami, are shown in

Figure 3.5. Each of these waves have a duration of order 20 minutes, so equivalent to 170s if modelled at 1:50 scale or 120s (model) at 1:100 scale.

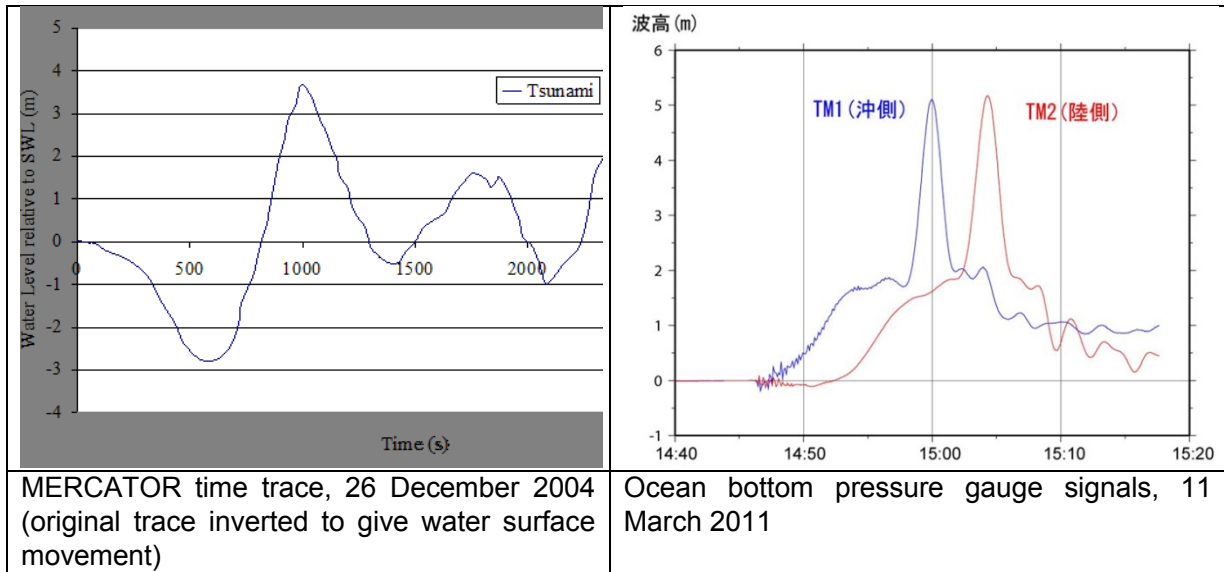


Figure 3.5 Tsunami time series

#### 3.1.1.4 Solitary waves, solitons and N-waves

Very few laboratories are able to reproduce these waves, but many have attempted to model solitary waves, or in a few instances trough-led N-waves. Many experiments using solitary waves to simulate a single displacement of water above the mean water level have been used. Hammack (1972) and Hammack & Segur (1974) showed how a positive initial surface disturbance will eventually decompose into solitons. A mathematical formulation of a solitary wave propagating over a constant water depth was given by Boussinesq (1872) and Rayleigh (1876) as a function of distance  $x$  and time  $t$

$$\eta(x, t) = H \operatorname{sech}^2(k(x - Ct))$$

Where

- $\eta$  is the water elevation above the mean water level,
- $H$  is the maximum wave height (which occurs at  $x=0$  when  $t=0$ )
- $k = \sqrt{\frac{3H}{4h^3}}$ ,
- $h$  is the water depth and
- $C$  is the wave celerity  $C = \sqrt{g(h + H)}$ .

Solitons can be created in the laboratory using a wave paddle (Goring, 1979, Hughes, 1993, Briggs *et al*, 1994, Schmidt-Kopenhagen *et al*, 2006), although the performance is restricted by its limited stroke. For trough-led waves, Tadepalli & Synolakis (1994) replace the solitary wave with N-shaped solitary-like waves, where the generalized N-wave is given by:

$$\eta(x, 0) = \alpha H (x - x_2) \operatorname{sech}^2(k(x - x_1))$$

where



- $k = \frac{1}{h} \sqrt{\frac{3H}{4h}}$  and
- $\alpha$  is a scaling parameter to allow comparison with solitary waves,
- $x_1$  and  $x_2$  define the locations of the trough and the crest.

Attempts to reproduce trough-led tsunamis, rather than simple positive waves, were supported by accounts of receding water before the arrival of the tsunami wave in Indonesia 1992, Nicaragua 1992, Philippines 1994, Mexico in 1995 and Thailand in 2004. Madsen *et al* (2008) have however argued strongly that the assumptions underlying the use of solitons and N-waves are not strictly applicable to many tsunamis.

### 3.1.1.5 Making tsunami-like waves in laboratories

Testing of tsunamis in hydraulics laboratories is relatively rare, so advances in tsunami generation at scale are similarly rare. Wiegel (1955) studied landslide-generated waves by using a wedge-shaped box sliding down a plane. The “moving block” method is still the most common way of modelling landslide waves (e.g. Panizzo, *et al*, 2005, Liu *et al*, 2005), or a granular slide (e.g. Yim, *et al* 2009, Heller *et al*, 2009).

Buoyant wedge paddles controlled by electric or hydraulic rams have been one of the common ways to generate wind or swell waves in laboratories, and similar wave paddles are used at Oregon State University to provide solitary waves in the Tsunami Basin under the US Network for Earthquake Engineering Simulation (NEES) programme. Each sliding wedge (29 no.) is driven by piston-type electric motors to give wave periods of 0.5 to 10 seconds, and maximum wave heights of 0.8 m in 1 m depth, Yim *et al* (2004).

A novel approach of moving the seabed was explored in the early 1970s in the WM Keck laboratory of California Institute of Technology where Hammack (1972) used a moving section (0.3m or 0.6m) of a test flume floor, raised or lowered suddenly by a hydraulic ram to reproduce sub-sea bed motion. Potentially the best way to simulate effects of sub-sea bed movement directly, this approach does not however appear to have been repeated since, probably due to the difficulty in reproducing appropriate depths, and artificial constraint of the up-ward moving 'piston' of water.

Thunsyanthan & Madabhushi (2008) generated some form of wave ( about 0.1m high, 1.5s period) by dropping a 100kg rectangular block (free-fall) into the water at the deeper end of a very short (4.5m) flume. Those waves, equivalent to  $H=2.5\text{m}$ ,  $T=7.5\text{s}$  at 1:25 scale, will have been relatively poorly controlled and bear very little similarity with realistic tsunami waves.

Some piston wave makers have been developed with long enough stroke to be able to model the near-shore transformation of solitary or N-waves and their related impacts, although these seldom have sufficient stroke to reproduce realistic time series for the larger tsunamis, see Figure 3.5. For those tsunamis that might be modelled by a long transient wave (train) with assumed constant celerity and constant shape, the paddle position as function of time might be described as:

$$X(t) = \int_{-\infty}^t \frac{c \cdot \eta(X, t')}{h + \eta(X, t')} dt',$$

where  $c$  is the celerity of the transient wave,  $\eta(x, t)$  the required water surface elevation at location  $X$  and time  $t$ , and  $h$  the water depth. Using this relation, the paddle motion can easily be

determined with an explicit numerical integration (see e.g. Goring & Raichlen 1980). As a transient wave is created, usually no reflections will be present at the wave paddle during generation of the primary wave, so that the full stroke can be used to create the waves (i.e. no active reflection control is needed during wave generation of the primary peak). As the entire tsunami has to be created, the tsunami bore will only be relatively small (order 1 - 10 cm) in a normal size wave flume with depths around 1 m. An example of such a small scale wave is shown in Figure 3.6.



Figure 3.6 Tsunami / bore wave created on shallow foreshore of GLOBEX Hydralab project (Deltares).

Similar solitary or N-waves have also been generated at larger scale in large flumes in Japan, Germany and the Netherlands. N-waves have been created in the original Delta flume with wave heights around 1-2 m, and wave lengths of 300 m to 100 m, examples shown in Figure 3.7. As expected, the maximum wave height decreases with reducing water depth. [Note: During 2013/14, the old Delta Flume is due to be replaced by a new Delta flume with depths up to 8m and similar / improved wave-making performance.]



Figure 3.7 N-wave generated in old Delta Flume and overtopping a dike slope (Hofland et al 2013)

### 3.1.1.6 Generating realistic Tsunami time series

Most piston paddles are severely limited by their stroke (often restricted to no more than about 1.6m) whereas generating realistic tsunami waves in the laboratory may require a stroke of order 10m. A very long stroke piston paddle is used in the large Hydro-Geo Flume at PARI described by Shimosako et al (2002). This flume used a piston paddle originally with a stroke of -4m to +4m giving a maximum (wind) wave height of  $H_{max} = 3.5\text{m}$  (6-8s),  $H_s = 1.4\text{m}$  at  $T=5.5\text{s}$ . The wave maker has since been up-graded to give a stroke of -7m to +7m (14m) and a maximum tsunami height of 2.5m, with periods of 30-60s.

Simulation of full tsunami time series in the hydraulics laboratory was substantially improved in 2008/2011 by development by HR Wallingford and UCL of a new Tsunami Generator to recreate scaled tsunami waves in the hydraulic laboratory. Allsop et al (2008), Rossetto et al

(2008, 2011) presenting the first controlled and stable simulation of extremely long waves led either by a crest or a trough (depressed wave).

The concept of the Tsunami Generator (Figure 3.8) is based on a Pneumatic Tide Generator developed by HR Wallingford (then Hydraulics Research Station) in the 1950's, see Wilkie & Young (1952). A sealed tank sits at one end of a test flume or basin with a submerged outlet facing into the open flume. An air pump or fan extracts air from the sealed top of the tank, drawing water from the test flume through the outlet. This water is then (later) released to generate a (crest) wave. An air valve in the top of the tank is controlled to give the desired wave shape. This form of wave generation is ideally suited to simulating tsunami as it allows the controlled movement of large volumes of water in a confined space using very few (and small) mechanical elements.

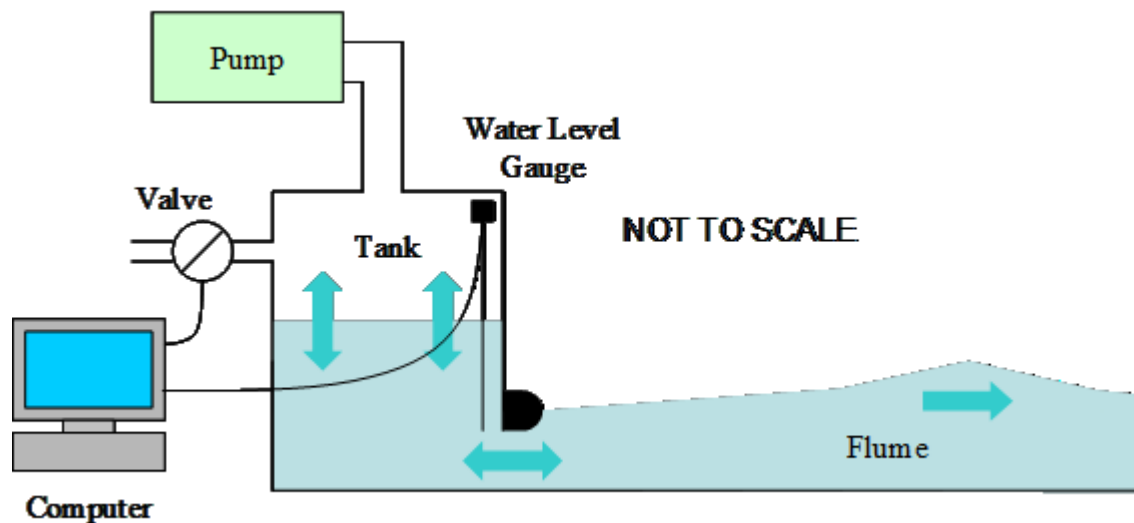


Figure 3.8 Schematic drawing of the HR Wallingford / UCL Tsunami Generator

The Tsunami Generator tank itself was made from steel panels bolted together in sections. The modular construction allowed easy fabrication and assembly. Bracing of the side panels was required to avoid distortion under the pressure differences between inside and outside of the tank, and those braces also acted as anti-sloshing baffles within the tank. The device was designed to be installed in either of the two main wave flumes (45m long and 1.2m wide) at HR Wallingford's modelling facilities in Oxfordshire, see Figure 3.9.

Control of the air valve in the Tsunami Generator might use either open or closed loop systems. In theory, the closed-loop method requires no individual wave calibrations, but requires substantial care in the choice of input parameters in order to work reliably. For the work described here, open-loop control was found to be simpler and most efficient.



Figure 3.9 Tsunami Generator mounted within the wave flume, the adjustable outlet is in the foreground under water

The original Tsunami Generator was tested and used by Charvet (2011) to measure tsunami run-up, and by Lloyd et al (2009) to measure wave forces on an example building model. Most of those experiments used solitary or N-waves. Initial attempts to reproduce the Mercator signal, Rossetto et al (2011), were partially successful. Improvements to the Tsunami generator in 2012 however gave a very good match with the Mercator time series at 1:50 scale, Figure 3.10. In considering the use of simplifying wave forms, it is useful to note the 20 minute (prototype) duration of the signal.

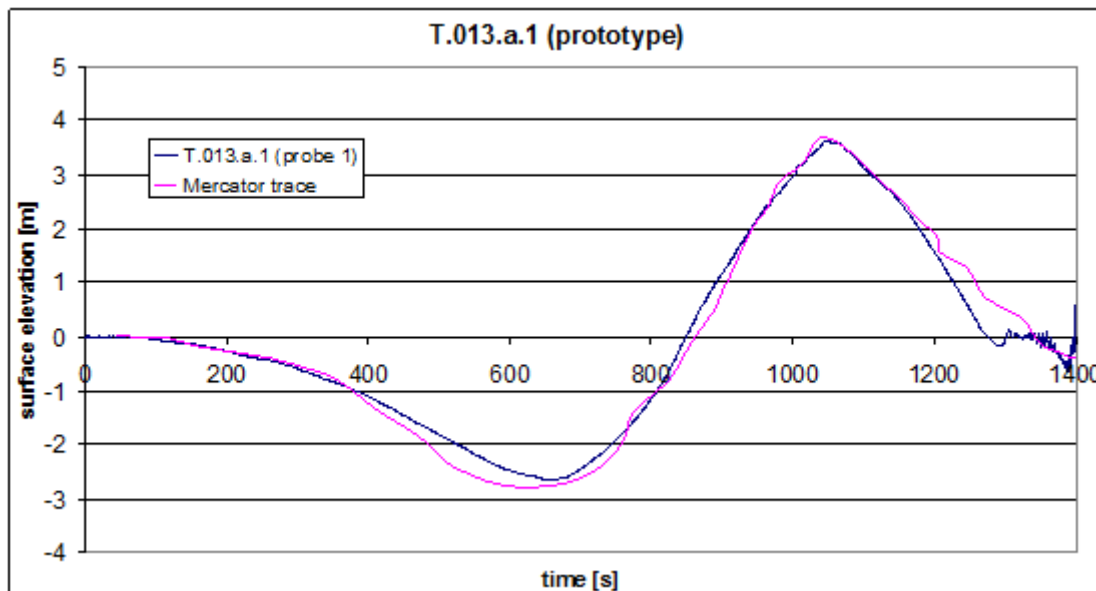


Figure 3.10 The Mercator time series at 1:50 scale using the HR Wallingford Tsunami Generator

### 3.1.1.7 How to represent a storm

Typically, incremental loading procedures are used for testing coastal structures. For the evaluation of structural stability, a test series of individual tests with increasing wave attack are



used, typically 3 to 7 tests, up to design wave conditions, usually followed by an overload test for testing reserve stability, typically 110% to 120% of the design wave height. This build up of tests simulates the storm profile of the rising storm. Moreover, each test can be linked to a probability of occurrence. Each test usually has a fixed mean water level, with (statistically constant) irregular wave conditions. The duration of each individual test is typically one to three thousand waves. A duration of a thousand waves is required to obtain a reasonably accurate representation of the wave spectrum. Tests on coastal structures often combine rubble mound stability testing, force measurements, and overtopping (e.g. a caisson that is placed on a rubble mound). Therefore, such a test series is also typically applied to force and overtopping measurements, though not strictly necessary.

If the extreme forces should be known accurately, then the maximum force should be sampled a few times, leading to a test duration of up to ten times the test duration under consideration. This is not often done for coastal structures. Usually a fit can be made through the exceedance curve of the measured peak forces, and hence a more reliable estimate of the extreme waves is obtained. When only a few events occur during a test series, this approach is not possible, however.

If time permits their execution, repeatability tests are always sensible. Repeatability tests demonstrate the capability of the model to produce similar results under similar forcing conditions. Some scatter can always be expected when repeating the same test conditions. However, time and budget constraints make repeatability tests seldom possible.

Verification tests at full scale are usually not possible. Most studies involve the testing and optimization of a design that has yet to be built, and very rare hydrodynamic conditions. Moreover field measurement data for proper validation is difficult to obtain. Most model tests rely on the scaling guidance that has been proven correct by several studies in which prototype damage has been re-created in a scale model (Hughes, 1993). As long as the model has been carefully scaled and constructed, and it has been determined that laboratory and scale effects are minimal, the engineer can have reasonable confidence that the model is correctly, or conservatively, reproducing the hydrodynamic phenomenon.

### 3.1.2 Wind Generation

The modelling of wind in wave basins is needed in order to establish a model of the complete metocean condition experienced by the system. However, a wave basin is not a wind tunnel, and limitations are encountered. Thus, accurate determination of wind coefficients are found from pure wind tunnel tests in advance. Usually, in wave basins one aims to model the correct wind *forces* rather than the wind *velocity field* itself. The Froude scaled velocity does not exactly reproduce the target wind force correctly when simulating mean wind forces, and therefore a calibration curve is needed to obtain the corresponding wind speed. Froude scaling is used to generate the wind speed at model scale, under the assumption that the above water shape of ships and offshore structures are insensitive to Reynolds number. However, it seems that there is no clear similitude law for the physical modelling of wind even though there are many unknown factors that have an effect at model scale, such as wind driven currents, the splash of waves due to strong winds and shielding effects, etc.

Wind forces are usually either modelled by arrays of wind fans, by wind fans directly attached to the model, and by spring-weight systems. The fan array concept is usually recommended and seems to be most frequently applied. More details are also given in ITTC (2005). An alternative approach to including the effect of wind on a physical model of a moored ship is to calculate the expected wind force on the ship using empirical approaches and to simulate that force on the



model ship by attaching a thin line to the ship and applying the same force (commonly using a weight over a pulley) in the expected direction of the wind force.

CFD models of the wind field can be a helpful tool in getting more knowledge about the laboratory wind field, although this is still an area of development.

### 3.1.3 Current generation and recirculation

There are a number of methods for generating a recirculating current in a wave flume or wave basin. They are discussed in turn below, with the final option being to reproduce the current-induced force on a structure without having to reproduce the force itself:

#### 3.1.3.1 Recirculation in pipes

Recirculation in pipes from outlet sump to inlet sump. Such a system may use several pumps to control the flow across facility. For example, the UK Coastal Research Facility (Simons et al, 1995, Whitehouse et al, 1995) has four axial flow pumps, each with a maximum discharge of  $0.3 \text{ m}^3\text{s}^{-1}$ . Each pump is continuously reversible through zero speed and is linked to sumps at each end of the facility. Each of the four sumps at each end has 10 undershot weirs to regulate cross-shore distribution of longshore current (Figure 3.11).



Figure 3.11 UK Coastal research facility (courtesy of HR Wallingford)

#### 3.1.3.2 Recirculation in a sump

Some current flumes use an outlet weir to control the water level and discharge into an open sump, with pickup at inlet end using relatively low head pumps (Figure 3.12). This sort of system may include a flow regulator.

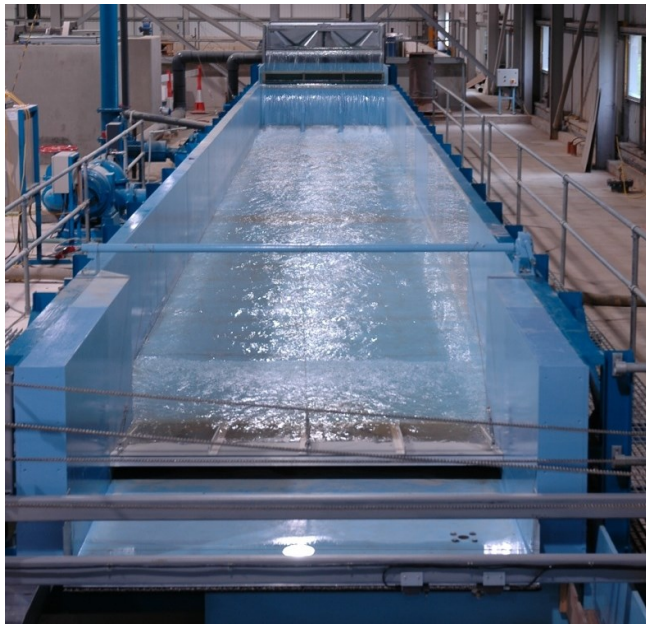


Figure 3.12 General purpose flume with variable height tail gate (courtesy of HR Wallingford)

#### 3.1.3.3 Recirculation using entrainment in a parallel channel

In some cases (particularly for a short-lived model) the current may be recirculated in an open channel, which is an extension of the test area (In a wave basin) or a parallel return flume (in a current flume). The flow is generated using entrainment, where water in return channel speeded up to form a high-speed jet, which acts to push the rest of the water along at a higher speed. The water can be accelerated using a propeller in the flow or by extracting some water from the channel, passing it through a pump and re-introducing it further along the channel.

#### 3.1.3.4 Vertical circulation around a false bottom

Several of the deeper wave basin have a false floor, which can be raised or lowered to change the water depth in the test area without altering the volume of water in the facility. The false floor can be used as the basis for a current re-circulation system (Stansberg, 2008) by having the current pass one way over the false floor and allowing it to return under it. Pumps are required at one end to drive the recirculation.

#### 3.1.3.5 Reproduction of current forces

An alternative approach to modelling a current is to calculate the force that would be caused by the current (if it were present) and to apply an equivalent force (typically using thin wires connected to weights via a pulley) without generating the current itself. Modelling current forces in this way will generally not be recommended as, for example, wave-current interactions will be missing.

### 3.1.4 Surface elevation measurement and analysis

#### 3.1.4.1 Surface elevation measurement

A number of conventional laboratory techniques for measuring surface elevation at a point are described in the following sections.

##### The resistive wave gauge

These gauges are made of two electrodes under a constant voltage (Figure 3.13). The current intensity between the electrodes is proportional to the electrode length under the surface and depends on the water conductivity.

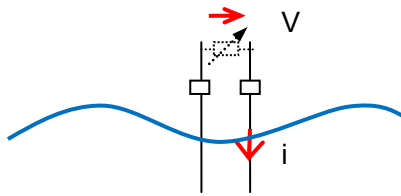


Figure 3.13 Resistive wave gauge functional diagram

### The capacitive wave gauge

It consists of one reference metallic electrode and one electrode made of a doubled thin isolated electric wire (Figure 3.14). These gauge are similar to a capacitor, the dielectric is the water for the underwater part of the electrode and the air for the upper part. The capacitance changes with the water elevation. These sensors are usually used to measure water elevation along the model's hull.

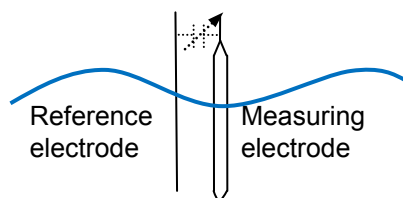


Figure 3.14 Capacitive wave gauge functional diagram and example of set up on a model at Ifremer

### The servo wave gauge

The current intensity between the two electrodes depends on the platinum needle length under the water surface. The Platinum electrode is set up on a stick which vertical position is servo controlled to have a constant current between the two electrodes. The platinum electrode follows the surface elevation (Figure 3.15).

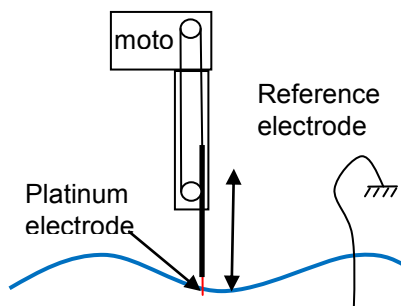


Figure 3.15 Servo wave gauge functional diagram and example at Ifremer

### Ultrasonic wave gauge

The sensor sends an ultrasonic signal which is reflected on the surface and flies back to the sensor. With the flight duration measurement, the distance between the sensor and the surface is deduced (Figure 3.16). These sensors generally have a large footprint and cannot handle steep or breaking waves.



Figure 3.16 Ultrasonic wave gauge functional diagram and example at Ifremer

### Laser wave gauge

Surface elevation measurements based on laser techniques are being developed (Richou, 2009, Hydrotesting Alliance conference). A vertical laser beam create a light spot on the water surface, which position is recorded by camera (Figure 3.17). After a calibration the water height can be deduced from the camera pictures.

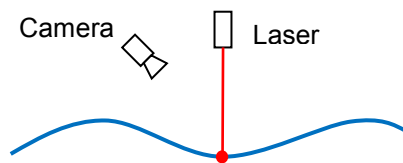


Figure 3.17 Laser wave gauge functional diagram and example at Ifremer

All the previous techniques measure water elevation at single point on the surface. Multiple examples can be deployed in any model setup. Eventually, the number of frames or tripods and wires becomes difficult to manage, and there are cases where it would be desirable to obtain data at an array of points over the water surface. The earliest attempt to capture the water elevation field was the "starry sky" technique of Valembois (1951) which consists of a fixed grid of lamps and cameras above the tank. The camera's shutter is opened for a duration longer than a wave period. The reflected lights appear as dots in the camera image in still water, but become ovals under waves, with an orientation and length depending on the wave's direction and steepness. An example is shown in Figure 3.18.

Some full water surface elevation techniques are being developed (see Section 6.8) but they are not yet available as standard instrumentation for hydrodynamics facilities.

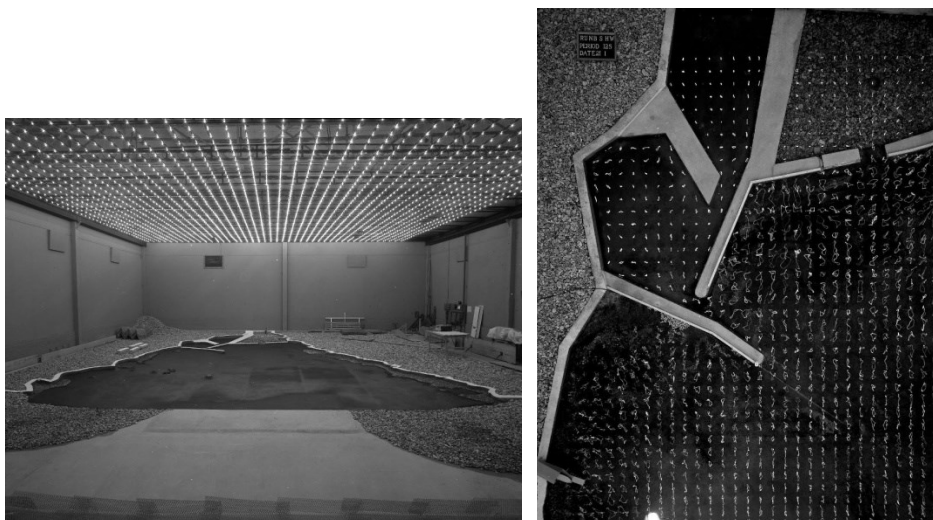


Figure 3.18 Starry sky basin at HR Wallingford in 1974



#### 3.1.4.2 Surface elevation analysis

Surface elevation analysis can be carried out as a time series analysis or as a spectral analysis (Goda 1985, IAHR 1986, IAHR 1989, Hughes 1993, Chakrabarti, 1994). The first stage of analysis is often to check for any trends in the data and subtract the mean signal. Note that the mean water level recorded may be due to drift in the measurement equipment or by a natural phenomenon, such as set-down or set-up. This can be detected by taking an additional short recording of the still water surface before the experiment begins, which will identify any drift in the instrumentation.

##### Time series analysis

A de-trended time series of surface elevation will often be analysed to give the following values:

- Mean value
- Root-mean-square value and variance
- Skewness and kurtosis may also be calculated.

A time series of waves is normally also analysed on wave-by-wave basis, by first identifying each wave in the record, based on the zero up-crossing or the zero down-crossing methods:

- In a zero up-crossing analysis each wave begins when the surface elevation rises from below the mean water level to above it. To undertake the analysis each zero up-crossing time is identified and the period between successive up-crossings defines the duration of the wave.
- In a zero down-crossing analysis each wave begins when the surface elevation falls from above the mean water level to below it. To undertake the analysis each zero down-crossing time is identified and the period between successive down-crossings defines the duration of the wave.

A zero down-crossing analysis is more common as it includes the trough before a wave crest, which helps to determine the interaction between a wave and a structure. A zero up-crossing analysis can be used for the analysis of asymmetric (or saw-tooth) shallow-water waves, as the surface elevation gradient is much higher for the up-crossing than the down-crossing, so the moment of crossing is more accurately determined.

A wave-by-wave analysis of heights and periods typically gives at least:

- Mean wave height
- Mean wave period
- Significant wave height,  $H_{1/3}$  which is the average of the highest one third of all wave heights.
- Maximum wave height,  $H_{max}$
- The average period of the highest one third of the waves,  $T_{1/3}$ .

In addition, rarer conditions are sometimes given to represent extreme conditions in a sea state such as  $H_{1/250}$ , the average height of the highest 1/250 of the waves. The accuracy of wave statistics depends on the sampling rate at which the record is digitised. Tayfun (1993) provides recommendations on sampling rates to maintain errors to less than 1%.

A similar analysis can be undertaken on velocity measurements.



### Fourier series analysis

Fourier analysis is based on the premise that any piece-wise continuous signal can be represented by the linear sum of a large number of sine waves, which are equally-spaced in the frequency domain. As the energy in each wave is proportional to the square of the wave height, we can represent the energy in a time series of waves as an energy-density spectrum ( $\text{m}^2/\text{Hz}$  versus frequency) with the variance in the time series given by integrating the area under the spectrum.

Typical outputs from a Fourier analysis are:

- $H_{m0} = 4 \times \sqrt{m_0}$ , the spectral significant wave height, where  $m_0$  = the zeroth order spectral moment;
- $T_p = 1/f_p$  = spectral peak period, where  $f_p$  = frequency at peak of spectrum;
- $T_{0,1} = m_0 / m_1$  = average wave period;
- $T_{0,2} = \sqrt{(m_0 / m_2)}$  = average wave period.

### Spectral analysis of unimodal, multi-directional sea states

There are a number of methods for estimating directional wave spectra (Hughes, 1993). The paper by Benoit (1993) reviews all the methods listed below. Teisson and Benoit (1994) compare the performance of many of these methods in dealing with an extensive set of experiments on the reflection of irregular oblique waves off a rubble mound breakwater. The methods include:

- Direct Fourier Transforms, where the cross-spectra from 2 or more pairs of gauges is used. This method is reviewed by Goda (1985) and includes truncated and weighted fourier decomposition (Borgman, 1969).
- Maximum Likelihood Method (MLM) which seeks to minimise the variance of the difference between the estimated and true spectra (Lundgren and Klinting 1987, Isobe 1990). MLM gives better directional resolution than DFT.
- Extended Maximum Likelihood Method, EMLM
- Iterated Maximum Likelihood Method, IMLM (Pawka 1983)
- Maximum Entropy Method (MEM), which is an iterative method that maximises the entropy at each frequency. It is reviewed by Nwogu *et al.* (1987) and is supposed to give even better directional resolution than the MLM.
- Extended Maximum Entropy Method, EMEM (Hashimoto *et al.*, 1993. Hashimoto, 1997).
- Bayesian Directional Method, as derived by Hashimoto and Kobune (1988) and reviewed by Hashimoto (1997). This takes into consideration errors in the cross-spectra, so can be slow, but is increasingly being used in preference to the methods above.

These techniques can be used to separate incident and reflected wave spectra far from a structure. Close to a structure, the incident and reflected waves become phase locked – when the phase of the incident and reflected waves can no longer be considered independent. The following techniques have been developed for wave reflection close to a structure.

Isobe and Kondo (1984) developed the Modified Maximum Likelihood Method (MMLM), which was the first method to evaluate the directional wave spectrum accurately in the presence of phase-locked reflections (i.e. close to the structure). However, this method requires the reflection line to be input, and that is not necessarily at the shoreline. Moreover, the method is sensitive to the position of the reflection line, so it is easy to generate spurious results. Davidson *et al.* (1998) developed an extension to the MMLM that calculated the position of the reflection line using a process of iteration. Both these methods break down and start to produce spurious

peaks in the spectra when the measurement array is further away from the reflecting structure. The spurious peaks are caused by uncorrelated noise at frequency / direction pairs that have partial nodes at the location of the measurement gauges.

Hashimoto and Kobune (1987, 1988) developed the modified Bayesian method that is capable of evaluating the directional spectra of waves close to reflective structures, by optimising a hyper-parameter.

Huntley and Davidson (1998) recognised that the effect of phase locking depends on the position of the gauge array relative to the reflection line. Increasing the bandwidth (i.e. increasing the number of degrees of freedom) effectively smoothes over the effect of phase locking and allows non-phase-locked techniques to be used. However, too much smoothing limits the frequency resolution and reduces the accuracy of the directional analysis technique. Davidson *et al* (2000) and Chadwick *et al* (2000) have also published in this area. If the incident waves are uni-directional and the angle of incidence is known, or is small, the wave reflection can be treated as a quasi-2D problem and be analysed using the techniques in the section below.

### **Separation of incident and reflected waves in a flume**

The most common methods for resolving two-dimensional spectra into incident and reflected components include:

- the two probe, one phase angle method of Goda and Suzuki (1976);
- the three probe, two phase angle method of Mansard and Funke (1980);
- the three probe method of Isaacson (1991);
- the vertical array of probe plus velocity method (Hughes, 1993);
- the co-located velocities method (Hughes, 1993).

All the methods rely on the linear superposition of many sinusoidal wave components; no non-linear interactions are represented. Isaacson (1991) provides a good review of the 2 and 3 probe methods, outlines the circumstances in which they fail and favours the Mansard & Funke (1980) 3 probe method. Isaacson shows that all 3 methods can be extended to the case of oblique reflection of regular waves over a flat bed, with his method being the easiest to extend. Zelt and Skjelbreia (1992) extended the method to an arbitrary number of wave gauges and introduced weighting functions to try to minimise the effect of having probe spacings close to a multiple of half a wavelength.

Hughes (1993) also provides a thorough review of the 3 methods above as well as the vertical array and co-located gauge methods. The vertical array can be a pressure gauge plus a horizontal velocity or a wave gauge plus a horizontal velocity.

### **Wavelet Transform**

In recent years, the Fourier Transform (FT) and Wavelet Transform (WT) have been applied to analyse fluctuation signals in various scientific fields. The FT is strictly restricted to linear systems and stationary data series. The conventional FT uses linear superposition of trigonometric functions to approach the original signal (Huang *et al.* 1998). Although the FT is valid under general conditions, there are some critical restrictions. As the FT is used to analyse a signal, many additional components are introduced, giving rise to misleading results. In order to overcome this shortcoming, a windowed FT is often calculated, in which a time–frequency distribution is obtained by sliding the window along the time axis. Since this method depends on the conventional FT, the analysis data are assumed to be piecewise-stationary. However, there are practical difficulties in applying the method: in order to localize an event in the time domain, the window width must be narrow enough; on the other hand, the frequency resolution requires

longer time series (Mallat, 1989). These contradictory requirements have posed significant limitations on the applicability of the FT.

Unlike the FT, WT is a time–frequency analysis tool suitable for non-stationary signal analysis. WT can be interpreted as a decomposition of a signal into a set of frequency bands with the same bandwidth on a logarithmic scale. WT can be viewed as an extended version of Fourier analysis but with an adjustable window using short windows at high frequency and long windows at low frequency (Mallat, 1989, Schlurmann, 2002). Since WT is fundamentally still based on Fourier analysis, all the possible complications associated with the FT still exist. WT satisfies the Heisenberg inequality, thus the resolutions in the time and frequency domains cannot have the same accuracy simultaneously. For practical applications, the elementary wavelet function can be adaptively modified by changing the dilation factor and the translation factor. However, the elementary wavelet function has to be given beforehand and is difficult to change during analysis. The main drawback of WT is that the fixed elementary wavelet function does not necessarily match the varying nature of a signal. In practice, it is difficult for WT to obtain a quantitative definition of the energy–frequency–time distribution by the limited size of the elementary wavelet function (Huang *et al.* 1996, Huang *et al.* 1998).

The Hilbert–Huang Transform (HHT) is a new time–frequency analysis method (Huang *et al.* 1998, Huang 2005a, Huang 2005b). The main difference between the HHT and all other methods is that the elementary wavelet function is derived from the signal itself and is adaptive. The main feature of the HHT is the Empirical Mode Decomposition (EMD), which is capable of extracting all the oscillatory modes present in a signal. Each extracted mode is referred to as an Intrinsic Mode Function (IMF), which has a unique local characteristic. After the Hilbert transform on each IMF has been performed, the time–frequency distribution of the signal energy is obtained, which is referred to as the Hilbert spectrum. The primary advantages of the HHT over other methods are that it can deal with the nonlinear problem objectively and the resolutions of the Hilbert spectrum are satisfactory in both time and frequency domains. The HHT is therefore suited to the exploration of the local properties of a signal (Veltcheva 2002).

The HHT process comprises two main steps. Firstly, IMFs are extracted from the signal itself based on EMD. Secondly, the Hilbert transform is applied to each IMF component. Consequently, the instantaneous frequency can be calculated and the energy distribution of the signal is obtained in the time–frequency plane (Huang *et al.* 1999).

EMD is an adaptive technique that decomposes the original signal into a family of IMF components. Each component emphasizes the local embedded characteristics of the signal. An IMF must satisfy two constraints: (i) the number of extrema and the number of zero crossings must either equal each other or differ at most by one; and (ii) at any time, the mean value of the envelope defined by the local maxima and the envelope defined by the local minima is zero. The first constraint is similar to the traditional narrow-band requirements for a stationary Gaussian process. The second constraint modifies the global requirement to a local one and is necessary so that the instantaneous frequency will not include unwanted fluctuations.

The HHT has been widely applied in recent years in the fields of meteorology, ocean engineering, earthquake studies, etc. As waves are nonlinear, Fourier analysis needs harmonics to simulate the distorted wave profiles. However, harmonics are mathematical artifacts generated by imposing the linear Fourier representation on a fully nonlinear wave system. As a result, in the wave spectral representation we could not separate the true energy content from the fictitious harmonic components. Most field studies such as those of Hwang *et al.* (2003), Schlurmann (2002), Datig and Schlurmann (2004), Veltcheva (2002), Veltcheva *et al.* (2003), and Veltcheva and Soares (2004) confirmed this observation. Additionally, Hwang *et al.*

(2006) also observed the drastic change of wavefield energy density across the Gulf Stream fronts, a nonlinear interaction yet to be fully explored.

HHT has been used by several authors for the analysis of wave records under different situations. Water waves are nonlinear, but the effects of nonlinearity are shown most clearly only near the point of wave breaking. HHT has been used to study such phenomena from freak waves (Wu and Yao, 2004) to breaking, bubble generation, and turbulence energy dissipation (Banner *et al.*, 2002, Gemmrich and Farmer, 2004, Vagle *et al.*, 2005). Veltcheva and Guedes Soares (2004) analyzed wave data collected at the Portuguese coast while Veltcheva (2005) considered data coming from the Japanese coast. Schlurmann (2000, 2002) considered waves produced in a laboratory wave flume and waves from the Sea of Japan. Dätig and Schlurmann (2004) give a detailed analysis of the positive and negative characteristics of HHT and consider both numerically simulated nonlinear waves and waves produced in a laboratory wave flume.

Ortega and Smith (2009) presented a spectral analysis of a North Sea storm that lasted over five days using the HHT and provided a comparison with the classical Fourier analysis.

### **3.1.5 Flow velocity measurement**

Flow velocities are sometimes measured in conjunction with forces in order to gain a better understanding of the incident and/or reflected flow conditions. As the focus is on wave forces, we only describe flow measurement devices. Hughes (1993) Chakrabarti (1994) and Smits and Lim (2012) for example, describes several types of measurements, including those defined in the following sections.

#### **3.1.5.1 Pitot tube**

A pitot tube is a thin tube, one end of which faces the dominant flow direction, while the other is connected to a manometer tube, which gives a measure of the total head. Flow velocity is determined from the dynamic component of the total head. They are sensitive to small changes in direction and are best suited to quasi-steady flows.

#### **3.1.5.2 Propellor meter**

A propellor meter, or impeller current meter (Hughes, 1993) consists of a small rotating propellor that is driven by the fluid flow. It is mounted on an axle that is oriented to face the flow. A sensor logs the number of rotations in a given time-span (typically about one second) which can be related to current speed using a calibration curve. Propellor meters only record fluid speed, so the direction of flow must be determined by other means. Performance decreases as the direction of flow varies from the direction of the impeller's axis.

#### **3.1.5.3 Hydrodynamic force probes**

Chakrabarti (1994) describes the use of relatively simple, robust flow and wave probes that are based on the principles of wave force measurements. In these probes a ball is mounted on a slim rod, which acts as a cantilever shaft. The flow or wave induced force on the ball is measured and the flow speed is back-calculated using Morison's equation with assumed drag and inertia coefficients. Such probes are considered old-fashioned today.

#### **3.1.5.4 Electromagnetic current meter**

Electromagnetic current meters (EMCMs) have been widely used in the field and in the laboratory. Each probe generates a magnetic field and the movement of water induces a voltage that is proportional to its speed. Chakrabarti (1994) describes the principles of EMCMs, which are less common today than they were, due to the increased use of acoustic and optical measurement devices.

#### **3.1.5.5 Acoustic Doppler Velocimeter**

An Acoustic Doppler Velocimeter (ADV) measures flow kinematics by detecting the Doppler-shifted reflections from a short acoustic pulse of sound generated in the water.

#### **3.1.5.6 Particle Image Velocimetry**

Particle Image Velocimetry (PIV) is a non-intrusive optical flow measurement technique that began in the 1980's as variation of speckle interferometry to low seeding densities. A light source (normally a lasers) is used to illuminate a plane through the flow and a camera (perpendicular to the plane) captures multiple images of seeding particles and analyses the distances travelled in the known time interval between images to determine speed and direction. Variations on standard PIV include stereo PIV, which uses two cameras to capture the third velocity component within the plane and 3D PIV, which uses two, three or four cameras to measure three components of velocity in a small volume of water. Analysis is typically carried out in a measuring volume of few millimetres across. The frequency with which successive images can be captured has increased in recent years, but typical sampling rates are still lower than Laser Doppler Anemometry.

#### **3.1.5.7 Laser-induced fluorescence**

Laser-induced fluorescence (LIF) or Planar LIF (PLIF) is a non-intrusive optical technique used to measure instant concentration or temperature maps. In mixing studies one of the fluids is marked with a tracer compound. A laser is used to illuminate a plane through the flow, as in PIV. The laser light excites the tracer, which fluoresces (releases light at a longer wavelength). A digital filter is used to separate the fluorescence from the laser wavelengths and the concentration (or temperature) can be determined from the level of fluorescence. LIF can be combined with PIV to give simultaneous maps of velocity and temperature/concentration. Further details of flow visualisation techniques can be found in Smits and Lim (2012).

#### **3.1.5.8 Laser Doppler Anemometry**

Laser Doppler Anemometry (LDA) is another non-intrusive optical technique where a laser beam is split into two parallel beams, which are then focussed on a point using a lens. As the beams cross they interfere with one another, creating an alternating patten of light and dark areas over a volume that is typically about 1 mm in width and a few millimetres in length. As small seeding particles cross though this volume they scatter light, which contains a small Doppler shift, which is related to the particle's speed. Some of this scattered light is captured by a photo-detector, which converts it into an electrical Doppler burst, which can be analysed to give the Doppler frequency and hence speed of the seeding particles. A two-beam system measures one component of velocity. Two and three dimensional systems can be created by adding additional beams and different wavelengths. LDA is used to measure high frequency time series in a relatively small measuring volume.

### **3.1.6 Air content**

Entrainment of air by breaking waves has been shown to influence a number of physical processes, including air–sea transfer of gases (Melville 1996), generation of sea-surface sound (Deane 1997) and the production of the sea-salt aerosol (Cipriano & Blanchard 1981). The dominant factor for all of these processes is the spectrum of bubble sizes, and numerous authors have attempted to make measurements of this distribution (Deane and Stokes (2002), Leifer and De Leeuw (2006) among others). However, it was suggested by Melville (1996) that for accurate estimates of gas transfer it is also important to know the total volume of air entrained in the water column and the subsequent evolution of this air volume. In addition, it has been shown by Lamarre and Melville (1991, 1994) and Hoque (2002) that the entrainment of large numbers of air bubbles during breaking contributes significantly to the total energy dissipation. Consequently, a detailed knowledge of the distribution of entrained air and the



behaviour of the entrained bubble plumes would contribute to a better understanding of wave breaking in general as well as the influence of air entrainment on these processes. However, largely due to the practical difficulties of making measurements in a violent two-phase flow, the existing information is limited.

Many previous authors have made estimates of void fraction in the bubbly flow beneath breaking waves in either the laboratory or the field (Loewen *et al.* 1996; Deane 1997; Vagle and Farmer 1998; Kalvoda *et al.* 2003). However, these measurements have generally been taken at a single often undefined location in the flow, using instruments that average void fractions over regions and intervals that are not small in comparison with the wave's characteristic length and time scales.

Papanicolau and Raichlen (1988), Bonmarin (1989) and Kalvoda *et al.* (2003) examined the large-scale geometric properties of bubble plumes generated by breaking waves using photographic and video techniques and provided information about the variation in size, shape and position of typical bubble plumes with time. However, they provided no quantitative data about the concentration of air within the plumes.

Several researchers including Hoque (2002), Cox and Shin (2003) and Hoque and Aoki (2005) have carried out more detailed laboratory investigations of the void fraction field in breaking waves, providing useful information about the vertical and horizontal distributions of void fraction. But by far the most comprehensive set of measurements was completed by Lamarre (1993) and is also reported by Lamarre and Melville (1992, 1994). Lamarre (1993) used a conductivity probe to produce contour plots of the time-varying void fraction field beneath both two- and three-dimensional focused laboratory breakers as well as making some further measurements in deep water ocean waves. The results showed that the bubble plumes generated by breaking waves undergo rapid transformations and lose 95% of their initially entrained air volume during the first wave period. Lamarre and Melville (1994) also concluded that the entrainment and subsequent submergence of large quantities of air can account for between 30 and 50% of the total energy dissipated at breaking. Measured void fraction results were used to calculate various integral properties of the void fraction field and it was shown that these evolved as simple functions of time and scaled reasonably well from small two-dimensional laboratory waves to larger three-dimensional breaking waves.

These previous studies have made use of a variety of techniques including various types of conductivity probe (Lamarre and Melville 1994, Hoque and Aoki 2005), acoustic techniques (Loewen *et al.* 1996) and laser methods (Hwung *et al.* 1992). Optical fibre probes are commonly used for the investigation of two-phase flows, predominantly in the chemical industry, and have been previously used to study a variety of flow conditions including air-bubble columns (Chabot *et al.* 1992), hydraulic jumps (Murzyn *et al.* 2004) and even liquid sprays (Hong *et al.* 2004). Optical fibre phase detection probes are highly sensitive, low-profile instruments which rely on the change in refractive index to detect the presence of air or water at the probe tip in a two-phase flow. Serdula & Loewen (1998) suggested that optical probes represent the most promising technique for the examination of the high void fraction bubble plumes entrained by breaking waves, but no such measurements seem to have been published previously. Blenkinsopp and Chaplin (2007) used optical probes to measure the void fraction distribution in three breakers in deep water. Figure 3.19 presents photographs and corresponding void fraction maps from one of their waves.

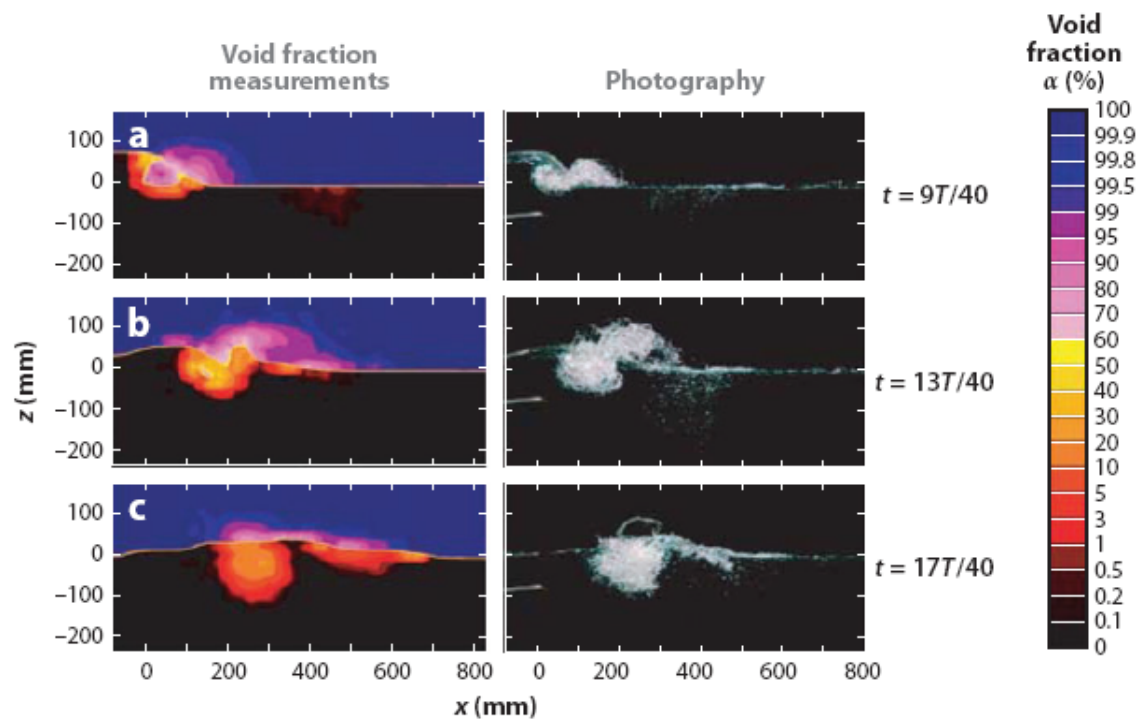


Figure 3.19 Void fraction measurements and photographs of air entrained in a plunging breaker: (a)  $t = 9T/40$ , (b)  $t = 13T/40$ , and (c)  $t = 17T/40$ , where  $T$  is the wave period. (Blenkinsopp and Chaplin 2007).

A dual-tip conductivity probe was used by Murzyn and Chanson (2009) to record the air–water flow properties of a hydraulic jump. It is a phase detection intrusive probe designed to pierce the bubbles and its principle is based on the difference between electrical resistance of air and water. The streamwise distance between probe sensors was  $\Delta x = 7\text{mm}$  (Figure 3.20). The response time of this sensor is  $<10\mu\text{s}$ . The signal output is scanned for 45 s at 20,000Hz per sensor. The data accuracy was on the void fraction  $\Delta C=2\%$ , on the bubble frequency  $\Delta F/F = 0.5\%$ , on the mean bubble chord length  $\Delta d_{\text{mbcl}} = 0.2\text{ mm}$  and on the interfacial velocity  $\Delta V/V=5\%$  (if  $0.05 < C < 0.95$ ) or 10% (if  $C < 0.05$  or  $C > 0.95$ ). Depending on the upstream Froude number, three to four vertical profiles were recorded at different cross-sections downstream of the jump toe. Each profile contained at least 30 points. The step between 2 points ranges from 3mm (closed to the bottom) to 10mm in the upper part of the flow. Figure 3.15 presents a typical voltage output of the conductivity probe leading sensor. The high voltage level corresponds to water whereas the lower level is relative to air. The distinction between both phases was performed using a single threshold technique.

The main properties of the air–water flow (void fraction ( $C$ ), bubble count rate ( $F$ ), mean bubble chord length ( $d_{\text{mbcl}}$ ), interfacial velocity ( $V$ ), turbulence levels ( $T_u$ ) and turbulence time scales ( $T_{xx}$ )) were calculated.

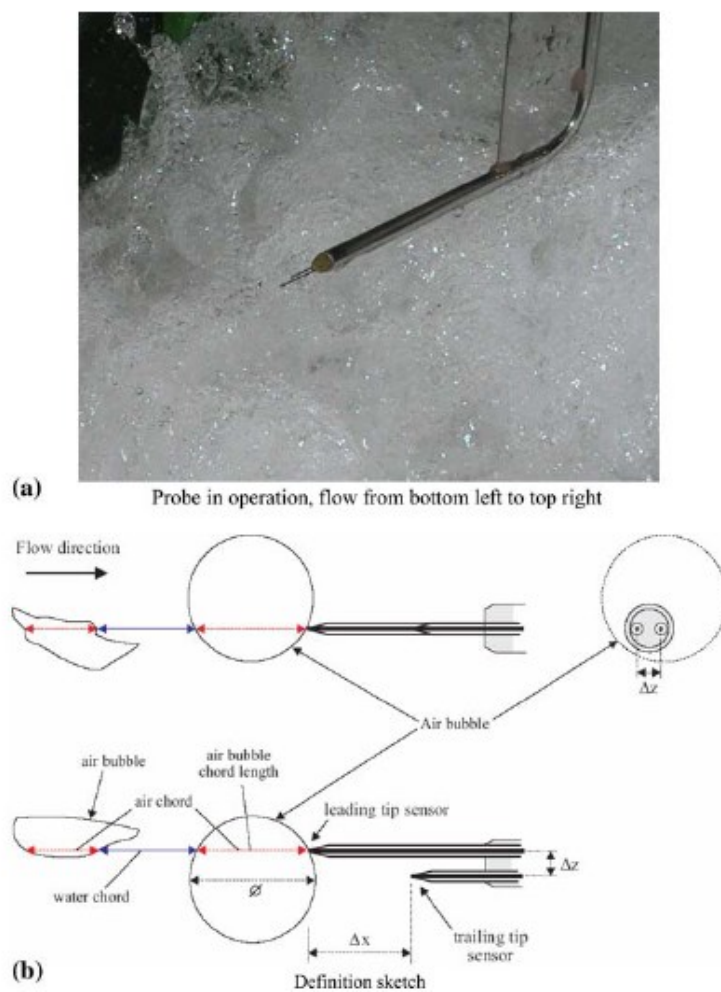


Figure 3.20 Dual-tip conductivity probe (a) Probe in operation, flow from bottom left to top right (b) Definition sketch (Murzyn and Chanson 2009)

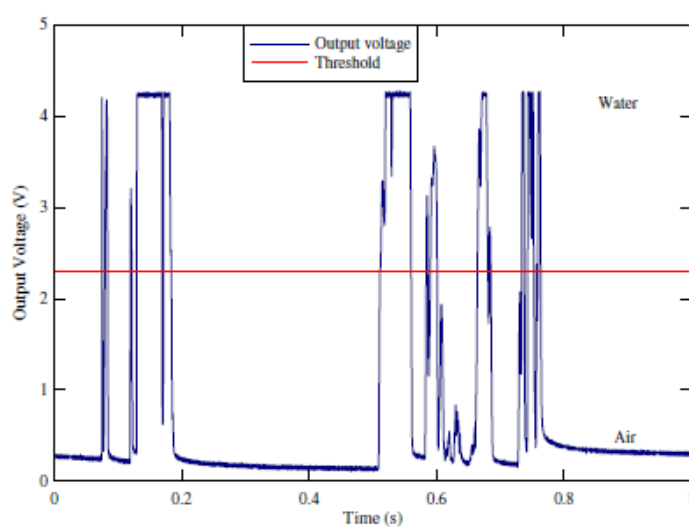


Figure 3.21 Voltage output of conductivity probe (Murzyn and Chanson 2009)

## 3.2 Establishing the correct ice conditions

### 3.2.1 Production of model ice sheet

Physical modelling of an ice-structure interaction has become an important technique in determining the ice loads and optimizing the design of ice breaking vessels, Arctic offshore structures, etc. Today hydrodynamic facilities in Canada, U.S.A., Germany, Russia, Finland, Japan and Korea are operating ice tanks and refrigerated laboratories. Model ice is an integral part of the physical modelling process of ice-structure interaction. The model ice must be represent accurately the full scale mechanical sea ice properties (Sinha, 1987). Froude and Cauchy scaling laws are used for the majority of ice model tests so that the prototype structure is reduced in its linear dimensions by a constant scale factor  $\lambda$ .

The properties of the model ice must be adjusted such that its strength (compressive, flexural, shear and tensile), stiffness and thickness must be reduced from the full scale or prototype value by  $\lambda$ , however its density and frictional characteristics must be the same as the full scale values. It is important that the model ice is an accurate representation of the prototype ice - either freshwater ice or sea ice. (Timco, 1986).

For example: if a 1 to 25 scale is chosen, then the ship or structure model is 1/25th the size. The ice used must also be 1/25th the thickness and 1/25th the strength. If only pure-water ice is used, the problem exists that pure-water ice does not soften.

For this reason many ice tanks simulate model ice using a mixture consisting mostly of water and chemical additives called dopants. Dopants are chemicals which reduce the melting temperature of pure water ice. Common dopants used are sodium chloride, salt, ethanol, ethylene glycol or urea.

In the first modelling tests with ice in St. Petersburg, Russia in 1957 (Shvayshteyn, 1957), the model ice was produced by freezing an aqueous solution containing a relatively high (~3%) concentration of sodium chloride salt. The salt was trapped within the ice and by internal melting, reduced the strength of the ice. This type of ice however, was not satisfactory because its stiffness (or strain modulus) was far too low and the ice exhibited unrealistic plastic deformation (Timco, 1986).

In Canada a synthetic model ice was developed by Michel in 1969, which was patented and used by a private company in Canada and the US. However this type of model ice has not endured.

Schwarz (1975) developed a tempering technique whereby sheets of ice were frozen from solutions containing a lower concentration of sodium chloride (0.6%) and by warming up the ice after the freezing process. The improvement due to this technique is a more accurately scaled stiffness of the ice sheet compared to ice sheets containing higher concentrations of sodium chloride (salt).

In 1979 Timco developed a refrigerated model ice grown from an aqueous solution containing urea as a chemical dopant, in order to achieve lower model ice strength compared to pure freshwater model ice. This type of ice has a thin upper granular congelation layer which can be minimized by seeding and growing the ice sheet at the lowest temperature that can be achieved (Zufelt and Ettema, 1996).

Furthermore experiments with different chemical dopants were made and in 1986 Timco introduced a new type of model ice – termed EG/AD/S ice – containing ethylene glycol, aliphatic

detergent and sugar. This type of model ice is single-layered without a congelation layer and has a fine grained and strictly columnar crystal structure. This EG/AD/S ice produces flexural strength and elastic modulus to flexural strength ratio values that are very close to those of urea-doped ice, but it has more realistic fracture-toughness performance, and thus cracking replication, because it is nearly single-layered (Zufelt and Ettema, 1996; Timco, 1986).

A new type of fine-grained model ice called WARC FG-ice was developed in Finland (Enkvist and Mäkinen, 1984) The ice sheet is grown by continuously spraying tank water (at 2% saline concentration) above an initially seeded sheet at air temperatures of  $-16$  to  $-22^{\circ}\text{C}$ . It is reported that similar results have been obtained using a 3% urea solution with the same growing technique, but that the urea provides no inherent advantage over the less costly NaCl (Zufelt and Ettema, 1996). The FG-ice is a fine-grained granular structured model ice which has several promising features. However, the granular structure limits the use of the ice since it does not accurately represent the structure of sea ice which is mostly columnar. The fine-grained model ice does not allow the ice to be scaled correctly in either uni-axial compressive strength or confined compressive strength (Timco, 1986). This may lead to a premature ice failure and a corresponding under-prediction of the loads on the full scale structure (Timco, 1984b; Wang, 1984).

The WARC-FG has been modified by spraying a 2% saline solution, spraying is conducted with water of saline concentration varying between 0.1 and 1.6%. It is reported that WARC FGX-ice has better strength simulation characteristics than WARC-FG ice (Nortala-Hoikkanen, 1990).

At the NKK Ice Model Basin (nowadays Universal Shipbuilding Corporation (USC)) in Japan the ice sheet production is similar to that of the FG- or FGX-ice. The tank water urea concentration is held at 2.5% and the spray water concentration at 0.5 to 1.3%. This allows the tank water temperature to be brought down to  $-0.4^{\circ}\text{C}$  (the approximate freezing point of the spray water yet still above the tank water freezing point) prior to seeding. The difference in concentrations of the tank and spray water prevent the growth of columnar ice at the bottom of the initial ice sheet during consolidation and tempering (Narita *et al.*, 1988).

In 1989 the Helsinki University of Technology (HUT) rebuilt their ice model basin and sought an ice material that was fine-grained and brittle to properly model icebreaker testing. Investigations on different model ice types like FG-ice, EG/AD/S-ice, EG/AD-ice (without the sugar), and EG-ice (only the ethylene glycol), were carried out at HUT (nowadays Aalto University). Their decision to use only 0.5% ethanol as a dopant was based on a desire for a noncorrosive, nonhealth-hazardous material. Today 0.3 ethanol is used as dopant. The resulting GE (granular ethanol) ice is produced by continuous spraying over the basin at air temperatures of approximately  $-10^{\circ}\text{C}$  (Jalonen and Ilves, 1990).

Until late 1980's The Hamburg Ship Model Basin (HSVA) produced a refrigerated model ice grown from an aqueous solution containing urea as a chemical dopant by application of a seeding technique. This type of model ice is strictly columnar structured but has a thin upper granular layer. The brine is entrapped along the boundaries of columnar ice crystals. Some time before the target ice thickness is achieved the ice growing process is stopped and the ice is warmed up at a constant air temperature to achieve the desired strength in the model regime. Consequently the ice strength decreases.

Investigations with respect to the improvement of ice properties were made by using various dopants like EG/AD/S and glycerol instead of urea. However on one hand these chemical dopants reduce the translucence in the water and glycerol is rather costly. The aspect of excellent water translucence is important, because it is very important to observe ice failure



processes, propeller-ice interaction and ice clearing by means of underwater video recording. On the other hand the content of sugar in the EG/AD/S dopant may cause bacterial pollution and the chemical components cannot easily be kept stable.

Thus, today an aqueous solution containing sodium chloride (~0.7% concentration) is used as dopant at HSVA in combination with air bubble entrapment, in order to get a stable chemical condition in the tank water and to improve the mechanical properties.

By using a single dopant system the grown model ice sheet consists of a three layer system:

- thin hard upper granular layer;
- transition layer with higher dopant concentration;
- weak columnar crystal layer.

Since the model ice is denser than in full scale, the criteria for buoyancy similitude may not be met. Thus methods were developed at NRC Canada for EG/AD/S CD-ice (Spencer and Timco, 1990) and HSVA, Germany, for NaCl doped model ice to incorporate air bubbles (see Figure 3.22) into a growing ice sheet in order to control its overall density (Evers and Jochmann, 1993). For this purpose a patented technique (Patent No. PCT/EP1992/000305; DE 4106930 A1) was developed at HSVA and is applied by pressing air saturated water under high pressure through perforated tubes fixed at the bottom of the ice tank during ice growth process at  $-22^{\circ}\text{C}$  air temperature. When the water leaves the tubes the pressure drops tiny air bubbles of 200-500  $\mu\text{m}$  diameter rise upwards and are embedded in the growing ice sheet. The content of micro bubbles affects also the elastic modulus to flexural strength ratio which increases significantly and the ice is more brittle when it fails. A secondary effect of air inclusions is the opaque colour of the ice giving a better contrast between model and ice in images taken from underwater (Evers and Jochmann, 1993).

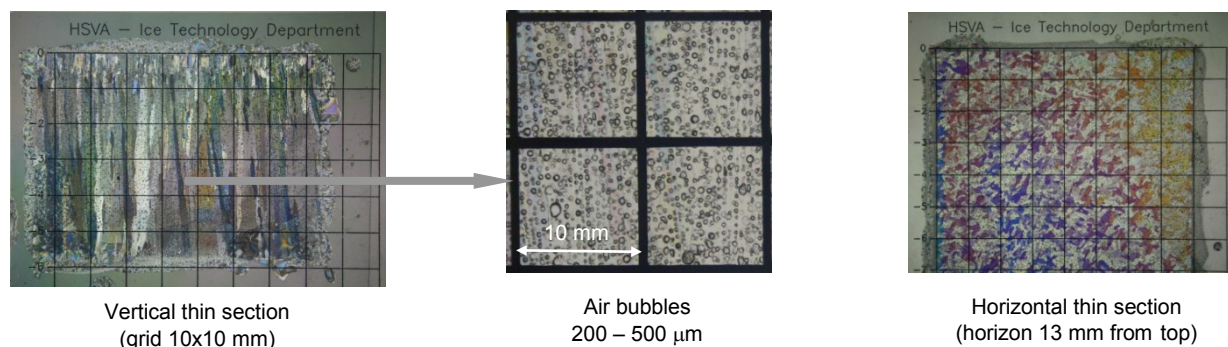


Figure 3.22 Vertical and horizontal thin sections with microbubble inclusions of HSVA's model ice

In 2009 the first Korean ice model basin facilities were completed at the Maritime and Ocean Engineering Research Institute (MOERI). MOERI started with EG/AD/S-CD type model ice, but due to problems with organic bacteria, they abstain from sugar and chose the EG/AD model ice without sugar.

Today different methods and procedures are used in the various ice tank facilities to produce model ice. At HSVA (Germany), NRCC-IOT and NRCC-CHC (Canada) and MOERI (Korea) the "seeding method" is the standard procedure to obtain columnar model ice. At KSRI (Russia), USC (Japan), Aker Arctic and Aalto University (Finland) the "spraying method" is applied and each facility has their own customized recipe of the dopants in the water summarized in Table 2.2.

Table 2.2 Method of model ice production and use of dopants at different ice facilities

Ice tank facility	Method	Chemical composition
Hamburg Ship Model Basin (HSVA), Germany	seeding + air bubbling (controllable ice density)	0.7 % sodium chloride
Institute of Ocean Technology (NRCC-IOT), Canada	seeding + air bubbling (controllable ice density)	EG/AD/S <sup>*)</sup>
National Research Council of Canada (NRCC-CHC), Canada	seeding + air bubbling (controllable ice density)	EG/AD/S <sup>*)</sup>
Maritime Ocean Engineering Research Institute (MOERI), Korea	seeding	EG/AD <sup>*)</sup>
National Maritime Research Institute of Japan (NMRI), Japan	seeding + air bubbling (controllable ice density)	propylene glycol
Aalto University, Finland	spraying	0.3 % ethanol
Universal Shipbuilding Corporation (former NKK), Japan	spraying	0.5 –1.3% urea
Aker Arctic, Finland	spraying	2 % sodium chloride
Krylov Shipbuilding Research Institute (KSRI), Russia	spraying	sodium chloride

<sup>\*)</sup> EG = ethylene glycol, AD = adhesive detergent, S = sugar

### 3.2.2 Ice sheet production methods

#### 3.2.2.1 Seeding Method

HSVA's current model ice is frozen from a 0.7% sodium chloride solution in the natural way, i.e., the ice surface is exposed to cooled air. The preparation of the ice sheet is started by a seeding procedure (Figure 3.23). For this purpose water is sprayed into the cold air of the ice tank. The droplets freeze in the air forming small ice crystals which settle on the water surface. By this method the growth of a fine-grained ice of primarily columnar crystal structure is initiated.



Figure 3.23 Water is sprayed under high pressure into the air of the pre-cooled ice tank at HSVA forming crystal nuclids which settle down on the water surface

By using a sufficiently cold temperature, both water and dopant are frozen in solution together forming an ice sheet. This impure ice sheet is inherently softer than pure-water ice but may be harder than the scale strength desired. Once a desired thickness is achieved, the air temperature is raised to a tempering temperature. As the temperature of the ice rises the dopants come out of frozen solution and form liquid brine pockets. These brine pockets slowly drain out of the ice sheet thus weakening it. Provided the ice-sheet isn't allowed to refreeze, the strength of the ice continues to decrease approaching an asymptotic value. Choosing a correct ice scale then becomes a question of when to conduct the test. This softening is often referred to as warming-up.

Before reaching the target ice thickness the cooling system is switched off and the air temperature is raised slightly above the freezing point. This temperature is kept until the properly scaled strength is reached. Then, the heat transfer into the tank is reduced to a minimum in order to keep the strength nearly constant for the duration of the test.

Figure 3.24 shows the history of a typical freeze-warming-cycle.

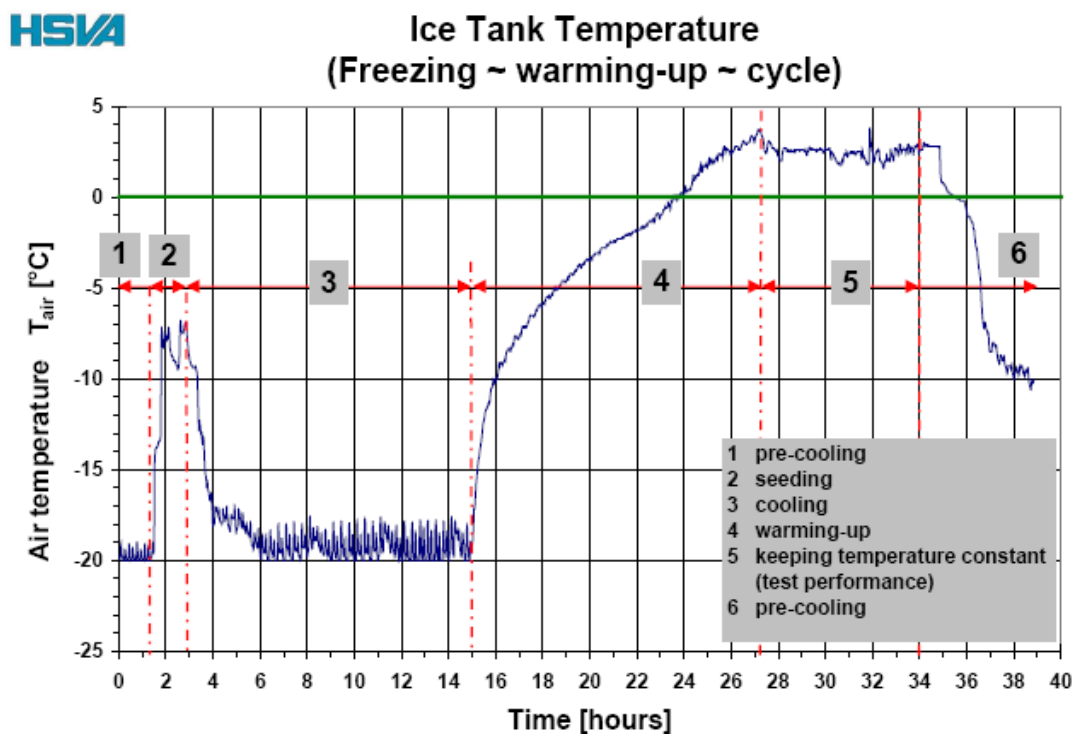


Figure 3.24 History of temperature during a freezing-warming-cycle in the ice tank at HSVA

### 3.2.2.2 Spraying Method

At Aalto University, Aker Arctic and KSRI the model ice is produced by the spraying method, where a dense water fog is sprayed onto the ice. Unlike natural ice the model ice produced in these ice facilities is growing upwards and not downwards. Compared to the seeding method the ice texture is fine granular (FG-ice; FGX-ice) instead of columnar (Nortala-Hoikkanen, 1990).

The spray water is taken from the tank, which contains 0.3% of ethanol. The small water droplets are sprayed at a temperature lower than  $-10^{\circ}\text{C}$  and nucleate to ice crystals before hitting the surface of the tank water. The spraying process is started before natural grown ice is

formed on the surface. Depending on the target thickness of the model ice compound the spraying process is repeated several times. Figure 3.25 illustrates the spraying process.



Figure 3.25 The spraying process at Aalto University

Once the spraying process is concluded the ice strength is adjusted during the freezing and warming-up period. The ice strength is adjusted immediately after the spraying process. A stronger ice is achieved by an extension of the cooling time in the strength adjustment period. Once the target strength is reached the temperature is raised in order to conserve the strength and thickness properties until the model tests start.

Prior to model testing with an ice breaking vessel or offshore structure the ice properties (e.g. ice strength, ice density and ice thickness) are measured along the ice tank at locations in accordance with the test run sections.

### 3.2.3 Ice properties

The most important ice properties of interest for model testing of icebreaking vessels and Arctic offshore structures are:

- ice thickness;
- flexural strength;
- modulus of elasticity (strain modulus);
- uni-axial compressive strength ;
- shear strength;
- fracture toughness;
- freeze-bond;
- dynamic ice friction;
- ice density; and
- ice salinity.

#### 3.2.3.1 Ice thickness

The thickness of model ice is measured after each test by a caliper gauge. The accuracy of the ice thickness measurement is 0.2 mm.



### 3.2.3.2 Flexural strength

The flexural strength of ice is not a basic material property. Any flexural test creates a nonuniform stress distribution in the ice and failure is usually caused by the maximum tensile stress in the top layer. Therefore,, assumptions are required about the ice properties in order to interpret the test results. The flexural strength, therefore, is generally considered to be an index test (Timco, 1986).

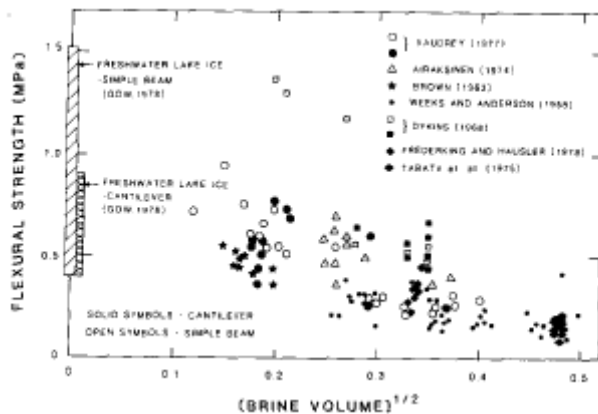


Figure 3.26 Flexural strength versus brine volume fraction for sea ice as measured with large beams in field testing (Timco, 1986)

Figure 3.26 shows a compilation of test results obtained in field testing for both sea ice and freshwater lake ice using large beam samples in both cantilever and simple beam loading arrangements. Although the scatter is considerable, the trend shows flexural strength values which decrease from ~1.2 MPa down to 0.2 MPa as the brine volume in the ice increases.

For sea ice, there is no significant difference in strength as measured using either the cantilever or simple beam approach. However for freshwater ice, there is an apparent difference such that the simple beam approach gives higher values. The reason for this is not known, although this difference has been attributed to a stress concentration at the root of the beam (see Schwarz and Weeks, 1977; Gow *et al.*, 1978; Timco, 1985).

With respect to the loading rate Tabata *et al.* (1967) and Määtänen (1975) report that the flexural strength increases with increasing stress rate, although Määtänen (1975) shows that if a correction factor is included to compensate for the inertial forces of the beam mass and the hydrodynamic water forces, this rate-dependence disappears (Timco, 1986).

Other tests carried out by Kayo *et al.* (1983) and Timco and Frederking (1982, 1983a) indicate no strong loading rate effects. For both sea ice and freshwater ice, when loaded to failure, the load-time curve exhibits an abrupt drop at yield, indicating brittle-type failure.

Regarding loading direction, tests by Weeks and Anderson (1958), Tabata *et al.* (1967) and Kayo *et al.* (1983) have indicated that the flexural strength of sea ice does not depend upon whether the top or bottom of the ice sheet is placed in tension. Tests on freshwater ice, on the other hand, indicate that the flexural strength is significantly higher when the top is loaded in tension (Gow *et al.*, 1978).

It appears that the flexural strength of sea ice is relatively insensitive to test technique, loading rate and loading direction. It is, however, a function of brine volume which itself is a function of temperature and salinity. Because of this, it is necessary to generalize the results into two different cases (1) very cold sea ice and (2) warmer sea ice which are of interest to model tank



operators in order to achieve representative values of flexural strength for scaling purposes (Timco, 1986). To obtain appropriate values of flexural strength for these two cases, it is necessary to know the brine volume in the ice for both cases. The brine volume can be calculated by using the relationships derived by Cox and Weeks (1982) if the salinity, temperature and density of the ice are known.

The flexural strength of model ice is usually determined before each test run at all of the model basins by measuring the strength using *in situ* cantilever beams. This method is preferred over the simple beam since the ice can be tested *in situ* and there is minimal handling of the ice (Timco, 1981).

The relative size and geometry of the beam is also important since it is known for both sea ice (Frederking and Häusler, 1978) and freshwater ice (Svec and Frederking 1981) that the apparent flexural strength depends upon the length to thickness ratio of the beam and the transition between root and beam, where notch related stress concentrations occur; the same is true for model ice. This type of test is therefore best regarded as a strength index of the ice. It is important that a standard size and geometry be adopted in order to have a meaningful comparison of the flexural strength from one tank to another. If the beam is short in relation to its thickness, the failure mode involves shearing as well as bending. If the beam is very long in relation to its thickness, the buoyancy of the beam affects the apparent strength. The IAHR guidelines recommend a beam length to thickness ratio of 7-10 (Schwarz *et al*, 1981), however tests carried out by Timco indicate that, for model ice, the length to thickness ratio should be less than this in order that the strength is not a function of this ratio. Preliminary tests on the influence of the width to thickness ratio on the apparent flexural strength of the ice indicates that strength is not a strong function of this ratio (Timco, 1981). It would thus seem that for tests on model ice, the length to thickness ratio of the cantilever beams should be of the order of 5-7, and the width to thickness ratio should be 1-2.

To load the beams a screw-driven load cell can be used to determine the breaking load of the beam. The load cell gives information on the loading rate and time. A loading time of 1-2 s to failure is considered to be realistic to represent the time in which a model icebreaker would ride up and break the model ice. For most tests, the beams should be loaded downwards. In the cases where ice fails against an inclined structure the strength should be determined by pull-up tests (Timco, 1981).

In model tests, the flexural strength can be measured using both the cantilever beam and simple beam loading arrangement (see Figure 3.27 to Figure 3.29). The beam is loaded downward to failure at load  $P$  and the flexural strength  $\sigma_f$  is determined using linear elastic beam theory from  $\sigma_f = 6 PL/bh^2$  for the cantilever beams, and  $\sigma_f = 3 PL/2bh^2$  for the 3-point beam (upward failure) or simple beam (downward failure).  $L$  is the spacing between outer supports. However, it must be acknowledged that *in situ* and *ex situ* tests can differ significantly due to fluid drains and / or mechanical and thermal damages during the extraction process.

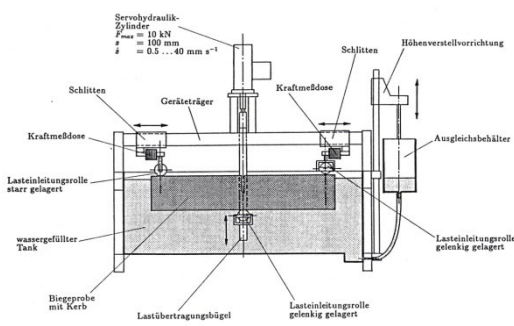
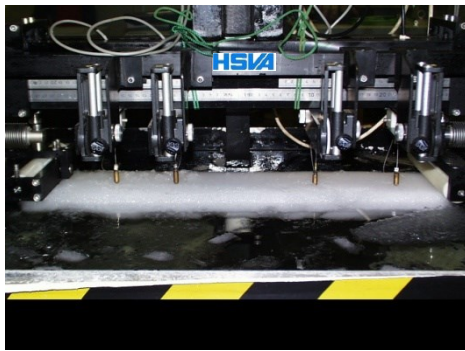


Figure 3.27 Point loading beam with LVDT designed by HSWA (upward loading)

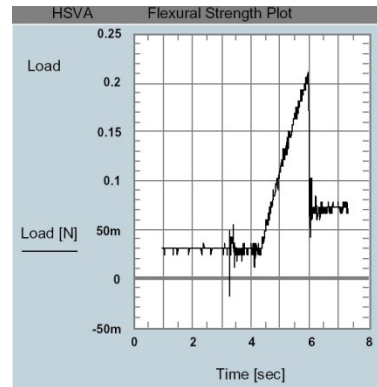
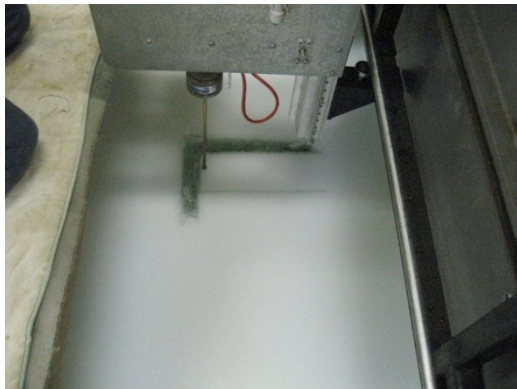


Figure 3.28 In-situ cantilever beam loading (downward loading); load vs. time plot



Figure 3.29 3-point loading beam (downward loading)

### 3.2.3.3 Modulus of elasticity (strain modulus)

Similar to the ice strength, the strain (apparent elastic) modulus  $E$  must be scaled by the geometric scaling factor of the tests. Since the proper scaling of this parameter in model tests is important, an acceptable test must be defined to measure this property. Basically, it can be measured using either static or dynamic techniques (Timco, 1981). In the static method, the strain modulus can be determined using either a beam or plate approach.

In the former, the modulus is determined by measuring both the load and deflection characteristics of a cantilever beam during loading to failure, whereas in the latter the modulus is determined by monitoring the deflection of the ice sheet as it is loaded with a known increasing load. In ice tanks which measure the strain modulus, the latter technique is usually preferred since it integrates over a large area of the ice sheet and is both simpler and quicker to perform.

In this test, the ice can be loaded with either dead weights in discrete increments (see Figure 3.30), or with a screwdriven apparatus in series with a load cell. During loading, the deflection can be measured either adjacent to or slightly away from the load (within one characteristic length) by either dial indicator, LVDT or LASER-sensor which gives a continuous recording. On the other hand, the dead weights and dial indicator are much simpler and faster to use and may serve as a method of quickly determining the modulus immediately prior to a model test.

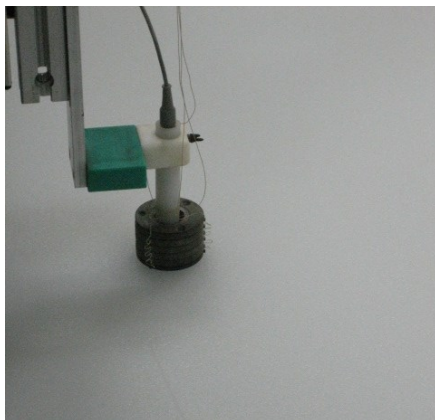


Figure 3.30 Determination of strain modulus (plate approach)

Knowing both the load and deflection characteristics of the ice sheet, the strain modulus can be determined from the consideration of an elastic plate on an elastic foundation (Wyman 1950, Frederking 1975). The theory is based on plain stress theory and refers to thin plates. In this case, for a point load  $P$ , the deflection  $\delta$  is given by

$$\delta = P \operatorname{kei}(r/l) / 2\pi k l^2$$

where  $\operatorname{kei}(r/l)$  is a modified Bessel function,

$k = \rho g$  is the subgrade reaction,  $\rho$  is the density of water,

$g$  is the gravitational acceleration,

and  $l$  is the characteristic length defined by  $l = [Eh^3/12k(1 - \nu^2)]^{0.25}$ , where  $\nu$  is Poisson's ratio.

If the deflection is measured at the point of load application,  $\operatorname{kei}(0) = -\pi/4$  and the equations can be solved for  $E$ . If the deflection is measured away from the point of load application, an iterative procedure must be used to determine the modulus  $E$ .

At HSVA the modulus of elasticity of the model ice is determined by applying the **plate method**. Hereby the ice cover is loaded at some locations along the centerline of the ice tank with defined weights, e.g. 50 g or 200 g depending of the sheet ice thickness. The deflection of the ice cover is measured at the center of the load by means of a LVDT.

The measurements are carried out contemporary to the flexural strength tests. Both, load and deflection are recorded. The modulus of elasticity can be calculated according to:

$$E = 0.1875 * 10^9 * (F/w)^2 * (1-\nu^2) / (\rho_w * g * h^3)$$

where

$E$	=	elastic modulus [MPa]
$\rho_w$	=	water density 1006 [kg/m <sup>3</sup> ]
$g$	=	acceleration due to gravity 9.814 [m/s <sup>2</sup> ]
$\rho_w g$	=	foundation factor $k$ for elastic foundation $k$
$\nu$	=	Poisson's Ratio = 0.3
$h$	=	ice thickness [mm]
$w$	=	plate deflection [mm]

#### 3.2.3.4 Shear Strength

Since there are no IAHR recommendations for testing the shear strength of natural ice, there are no guidelines to assist in the design of a suitable test for model ice. However, in the testing of the shear strength of model ice, it would seem that a test is required which will simulate the action of a model icebreaker shearing the ice. For this, a single shear test in which a block of ice of known dimensions is sheared at a loading rate of 1-2 s would give a reasonable estimate of the shear strength of the ice. In order to eliminate any sample size effects when comparing the shear strength determined for both vertical and horizontal loading directions, the width of the sample should be the same as the thickness (Timco, 1981).

#### 3.2.3.5 Uniaxial compressive strength

Measurement of the compressive strength of model ice is important, especially for the horizontal loading direction, when ice impacts rigid vertical structures it often fails in a crushing mode.

#### 3.2.3.6 Conventional method

After the ice sample has been collected from the field or grown under laboratory conditions, rough cutting of prismatic ice blocks or of cylindrical cores is advisable in order to obtain manageable sample size.

Three different shapes are in use:

- (i) cylinders,
- (ii) prisms,
- (iii) cubes.

Tests on cubes may introduce significant errors, thus it is suggested that such specimens should not be used in the conventional method of testing.

Cylindrical specimens are usually prepared by a coring drill. Specimen diameter should be within a range of 7 to 10 cm. Specimen ends must be plane and parallel within close tolerances; this can be achieved by a rotary cut-off machine, by a milling machine, or by a lathe. The specimen length should be approximately 2.5 times the diameter. It is recommended that

prismatic specimens for laboratory tests should be prepared by the use of a milling machine or surface grinder.

The compressive strength of ice may depend on the ratio of sample size to crystal size. In order to be independent of this ratio, it is desirable to have the sample width,  $d$ , some 15 to 20 times the crystal diameter,  $d_{cr}$ .

In the conventional uni-axial compression test, axial force is applied to the ends of a right circular cylinder through steel platens that make direct contact with the test specimen. Friction between platen and specimen produces radial restraint, so that there is a triaxial state of stress near the end planes; the triaxial field is significant over an axial distance from the end planes of about one specimen radius. Placing a highly compliant sheet (elastic or plastic) between platen and specimen often changes the sign of radial end forces, but does not eliminate the triaxial stress state.

The usual procedure for testing ice in uni-axial compression is to accept positive frictional restraint at the specimen end planes and to use a specimen that is long enough to provide a mid-section that is reasonably free from end-effect stress perturbations (length/diameter ratio of 2 to 3) (Schwarz *et al*, 1981).

At HSVA uni-axial compression tests are carried out on a rigid closed loop controlled testing machine by a hydraulic piston, having 10 kN capacity, for load application. The specimen for compression tests are sampled from the same location in the ice tank, where in situ flexural strength tests are being carried out at the same time. This allows the ratio between flexural strength and compressive strength of the model ice to be determined.

For HSVA's model ice regression calculations reveal that the ratio compressive versus flexural strength can be well approximated with a power function:

$$\sigma_c = A * \sigma_f^\alpha$$

where

$\sigma_c$  = uni-axial compressive strength

$\sigma_f$  = flexural strength

$A$  = factor of the best fit power function ( $A=0.4$ )

$\alpha$  = exponent of the best fit power function ( $\alpha = 1.4$ )

Prismatic ice samples having a size of  $1h \times 2h \times 4h$ , with  $h$ = ice thickness, are cut and placed in between the two loading plates of the test frame. Compliant platens or thin sheet of compressible material (e.g. paper) is used in order to avoid sliding of the specimen and to apply uniform axial load to the specimen. The applied load and crosshead movement will be recorded and the results presented as load deflection curve. Figure 3.31 shows the testing machine and the hydraulic aggregate in the refrigerated laboratory.





Figure 3.31 10 kN uni-axial compression testing machine as used at HSVA

The required strain rate respectively crosshead speed of the hydraulic piston is adjusted according to the ice drift velocity and the structure width according to the formula:

$$V_c = (V_{ice} \times L_s) / (4 \times w)$$

where

$V_c$  = crosshead speed

$V_{ice}$  = ice drift velocity

$L_s$  = sample length (=  $4 \times h_{ice}$ ), where  $h_{ice}$  = ice thickness

$w$  = structure width

### 3.2.3.7 Ice density

The determination of the density of model ice using the standard technique - cutting a sample block, measuring its dimensions (i.e. volume) and weighing it - has several inaccuracies, the primary one being that a large number of the liquid impurity pockets in the ice drain out when it is removed from model ice sheet. Nevertheless, the technique can be used to obtain semi-quantitative density values, although measurements of the freeboard of model ice may prove to be a better method of density determination (Timco, 1981).

At HSVA a different method to determine ice strength is applied. Ice samples ( $120 \text{ mm} \times 120 \text{ mm} \times \text{ice thickness}$ ) are sampled from the model ice sheet at locations where cantilever beam tests are carried out and stored in a plastic bowl filled with tank water in order to avoid any drainage.

The specimen is submerged and the displaced water volume is collected and weighed. The buoyancy force is measured.

The ice density is calculated by:

$$\rho_{ice} = \rho_{water} - F_b / (V_d \text{ g})$$

where

$\rho_{ice}$  = ice density [kg/m<sup>3</sup>]  
 $\rho_{water}$  = water density = 1006 [kg/m<sup>3</sup>]  
 $F_b$  = buoyancy force [N]  
 $V_d$  = displaced water volume [m<sup>3</sup>]  
 $g$  = acceleration due to gravity 9.814 [m/s<sup>2</sup>]

Figure 3.32 shows the entire ice density test setup.



Figure 3.32 Test setup for ice density tests at HSVA

### 3.2.4 Modeling of different ice conditions

#### 3.2.4.1 Level ice

Level ice is a homogeneous ice sheet unaffected by deformation with consistent ice thickness. Level ice sheets are produced according to the procedure described above.

#### 3.2.4.2 Broken ice (ice floes)

For ship navigation in broken ice conditions (ice floes) it is essential to consider the floe size and the coverage (or concentration) of ice floes (Figure 3.33). Also broken ice conditions around fixed or floating structures have to be taken into account for ice management. Therefore many test programmes include tests in broken ice.

When modeling broken ice conditions a predefined parental level ice sheet is prepared first and then cut into pieces corresponding to the required size and shape. Ice floes are defined as a flat piece of ice 20m or more across. The floes are subdivided according to size and horizontal extent as summarized in Table 3.3.

Table 3.3 Types of ice floes

Type of ice floe	Ice floe size
• small	20 - 100 m across
• medium	100 - 500 m across
• big	500 - 2000 m across
• vast	2 km – 10 km across
• giant	> 10 km across



Ice floes in full scale



Ice floes in model scale

*Figure 3.33 Modeling of ice floes*

The preparation of ice floes in the ice tank is done manually by cutting the parental level ice sheet into pieces of required size and shape and distributing them to achieve the required different ice concentration (e.g. 60% to 90%). Figure 3.34 shows the ice preparation of ice floes with different sizes and the ice floe arrangement at the end of the ice tank (90% ice concentration).

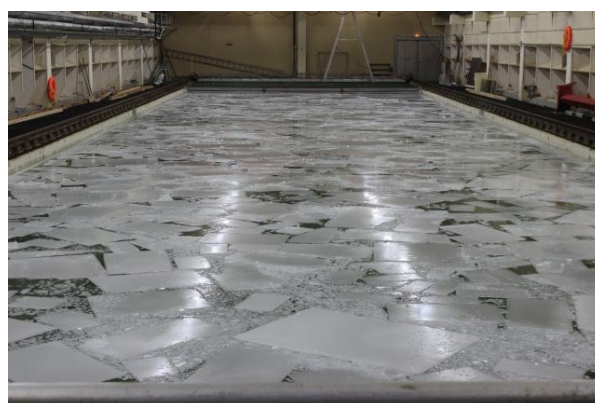
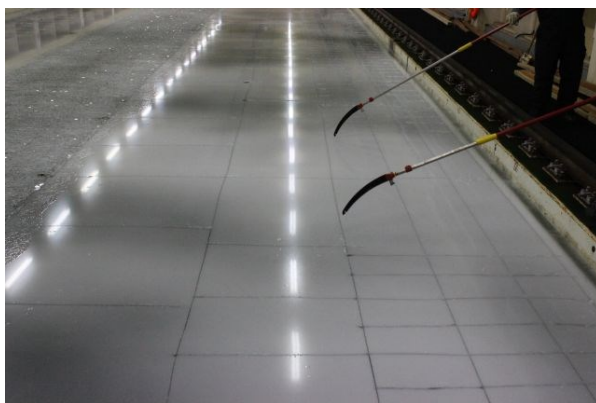


*Figure 3.34 Ice floe production (left) and ice floe distribution prior to testing (right)*

The processing of images is done with the main focus on the static ice concentration in advance of the model tests over the total ice tank length. Before each test in broken ice, 28 pictures are taken by a digital camera from about 4.4 m above water surface. Since the camera lens does not capture the entire width (10 m) of the ice tank, 2 images are taken and 14 images in length direction (60 m) of the ice tank. All of those pictures are stitched together using the overlap that is among them. The resulting images such as presented in Figure 3.35 and Figure 3.36 are evaluated to obtain the ice concentration.

The results of ice concentration are based on a technique using a pixel analysis. To evaluate the image pixel by pixel it has first to be converted to grey scale. Then each pixel has a value between 0 (pure black) and 255 (pure white). A set threshold value divides the pixels into two



groups; grey scale values below the threshold become black and those above become white. In this way a black and white (or binary) image is created. An example is given in Figure 3.36. With the ratio between the black and white pixels the coverage of ice on the water surface can be determined. The results of the pixel analysis from the overall pictures from top of the ice tank are given as global ice concentrations. A more detailed description of the method is given by van der Werff (2012), van der Werff *et al.* (2012), Haase *et al.* (2012), Zhang *et al.* (2012) and Benne (2012).

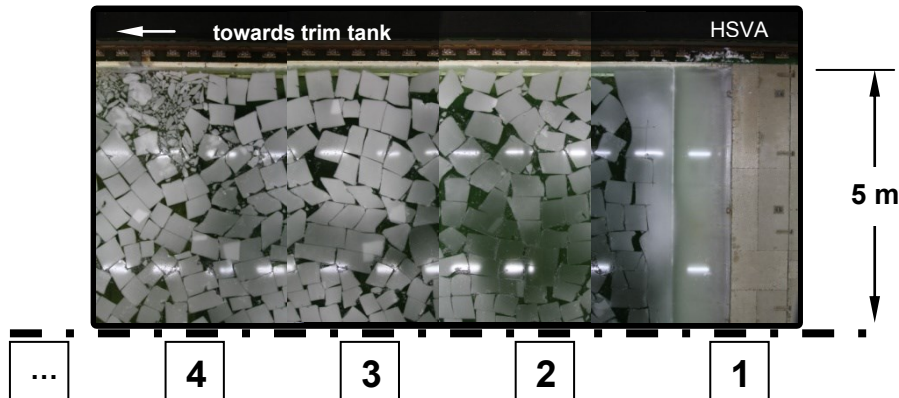


Figure 3.35 Picture sequence along the ice tank (example)

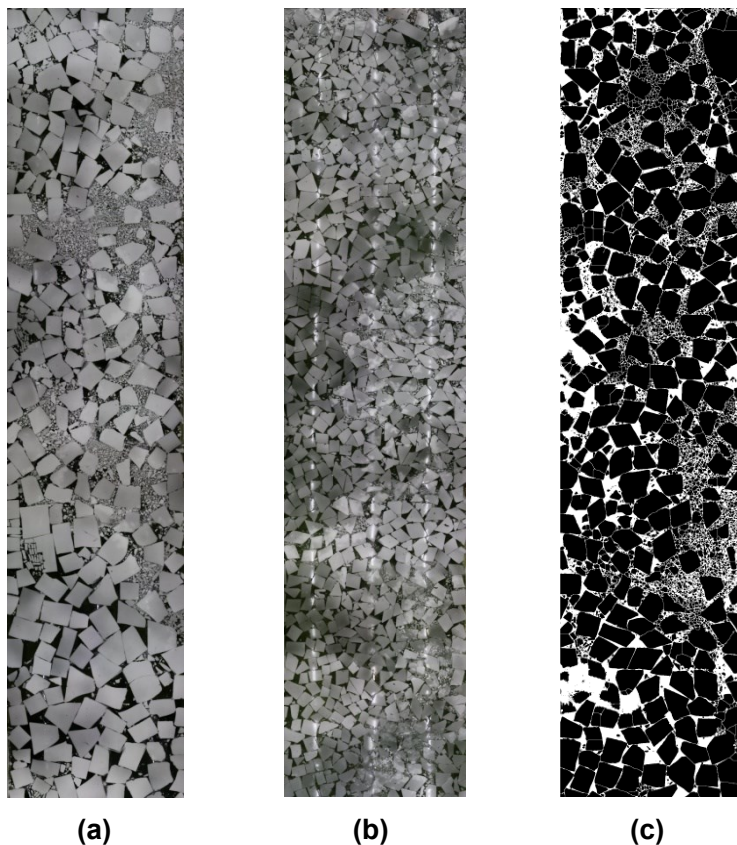


Figure 3.36 Examples of stitched pictures (a-b), (c) example of binary image

Image editing software ImageJ<sup>™</sup> is used to analyse the images and gives information about number of ice floes, average ice floe size [ $L^2$ ], ice concentration [%] which is equivalent to the total ice floe area [ $L^2$ ].

### 3.2.4.3 Brash ice tests at HSVA

A parental level ice sheet of adequate thickness is prepared according to the standard model ice preparation procedure. After a predefined level ice thickness has been reached, the air temperature in the ice tank is raised. When the air temperature is close to  $-3^{\circ}\text{C}$ , an ice channel with straight edges is cut into the ice sheet. This is done by means of two ice knives being pushed by the auxiliary carriage. Thereafter, the ice stripe between the two cuts is manually broken up into relatively small ice pieces using special ice chisels (see Figure 3.37 and Figure 3.38).



Figure 3.37 Preparation of brash ice channel at HSVA

Those channel sections, where the ice pieces remain in a regular pattern, are cautiously stirred in order to achieve a most realistic appearance of the brash ice channel. In order to obtain a brash ice channel of the desired brash ice thickness (one thickness below and one above the ice thickness stipulated for the designated Ice Class in the guidelines (e.g. Finish-Swedish Ice Class Rules) the ice material in the channel has to be compacted. The compacting is done in sections by means of a channel-wide grid, starting from the rear end of the channel.

For the second test run the ice pieces are rearranged in the channel and further compacted. Since the channel filled with brash ice becomes shorter due to the compacting procedure, some of the level ice from beside the forward part of the channel is additionally broken up and refilled into the remaining part ice-free section of the channel.

Typically, the brash ice thickness is measured before the tests at 7 positions across and in 1m distances over the whole length of the brash ice channel. A special device is used for the measurements, which consists of a slide gauge with a perforated plate mounted under a right angle at the lower end of the gauge. With the slide gauge the thickness of the brash ice is measured whereby the ice is floating in the water. This is done by slightly pressing the lower plate up against the bottom of the ice, raising it about 1 cm. The top plate is lowered in such way that it just get in contact with the top of the brash ice. The brash ice thickness determined in



this manner is measured over the peak values of the sample. The thickness of the brash ice is measured as accurately as possible.

#### 3.2.4.4 Brash ice tests at Aalto University

The initial level ice thickness depends on the scale of the model, since the ice thickness also determines the piece size of the broken bits in the channel. With the application of geometric Froude-scaling the target full-scale piece size is a diameter of  $D = 0.5$  m.



Figure 3.38 Production of a brash ice channel at Aalto University

The level ice is broken with a shoe (see Figure 3.38) and then the level ice field behind is pushed together. After the ice is pushed together the ice is manually redistributed to obtain an evenly distributed channel thickness. Figure 3.39 shows a made brash ice channel with 100% coverage.



Figure 3.39 Brash ice channel (Aalto University)

### 3.2.4.5 Preparation of first year (FY) ice ridges at HSVA

Pressure ice ridges are prepared in a way that a section of the a level ice sheet is cut free from the side walls of the tank, cut into strips of a defined width and pushed against the resting ice sheet by means of the carriage's pushing board. The ridging process is supported by a beam with inclined face put across the tank (Figure 3.40). During the ridge formation the beam is successively moved forward. At the end of the ridge building procedure a part of the unbroken surrounded level ice cover is pushed over the ridge forming the consolidated layer. By this way an ice ridge of defined ice mass is generated. The ridge has a typical natural underwater profile (triangular or trapezoidal shape) and is embedded in surrounded level ice. The geometric ridge characteristics are illustrated in Figure 3.41. Examples of ad-frozen ridge fragments in the consolidated part of the ridge are shown in Figure 3.42.



Figure 3.40 Ice sheet cut into stripes (left) and steel beam submerging ice when pushed by towing carriage (right)

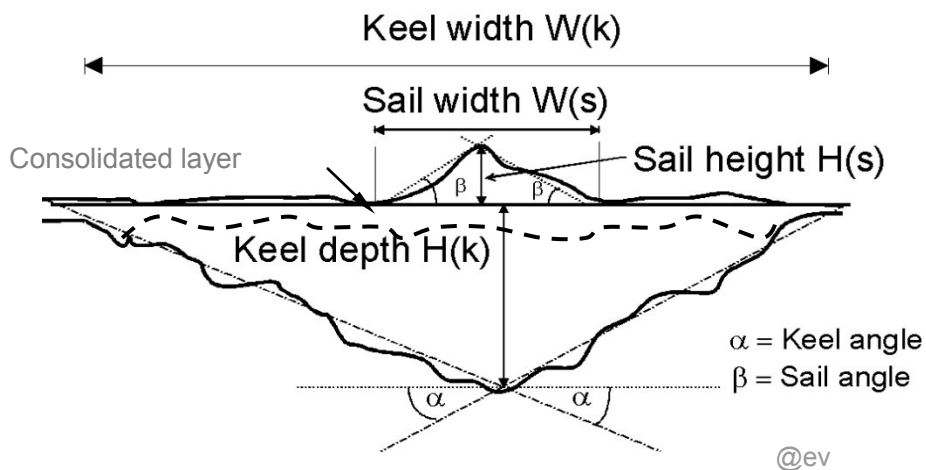


Figure 3.41 Geometric characteristics of a pressure ice ridge

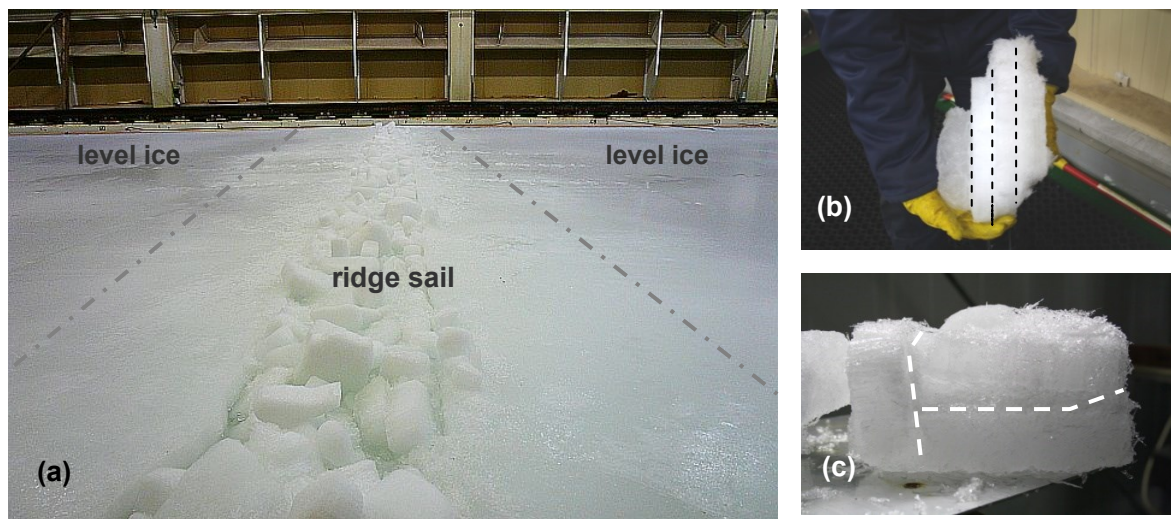


Figure 3.42 First-year ice ridge modelled at HSVA: (a) ridge embedded in level ice sheet, (b-c) adfrozen ridge fragments from consolidated part of ridge

Prior to the ridge building process several temperatures and the ice thickness are measured along the mid-line of the tank in order to find the right starting time for the ridge building process. This starting time is very important in controlling the thickness and strength of the consolidated layer, which is strongly dependent on the temperature and strength of the initial ice sheet used to build the ridge. The ice temperature will be taken 2 cm below the ice surface, while the air-temperature is measured 2 cm and 1 m above the ice surface.

The required volume of ridge fragments, taking into account the ridge porosity, is calculated based on the required ridge geometry parameters (e.g. length, width, sail height and keel depth). If the volume and porosity are known the length for cutting the ice into strips is calculated. An layout example is shown in Figure 3.43, where the cut length for each ridge is about 7.5 m. Figure 3.44 shows the layout of ice free water, locations of ridges and areas of level ice.

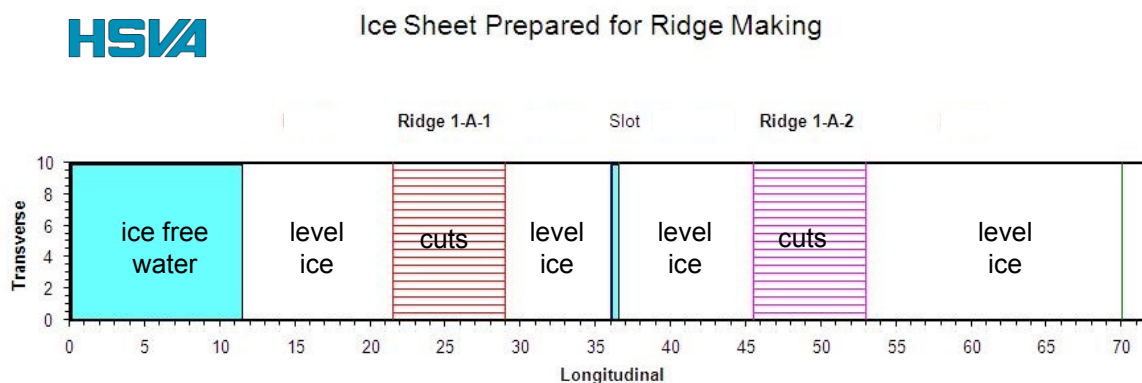


Figure 3.43 Schematic diagram of required cut length and layout for cuts to be prepared





Ridges Completed

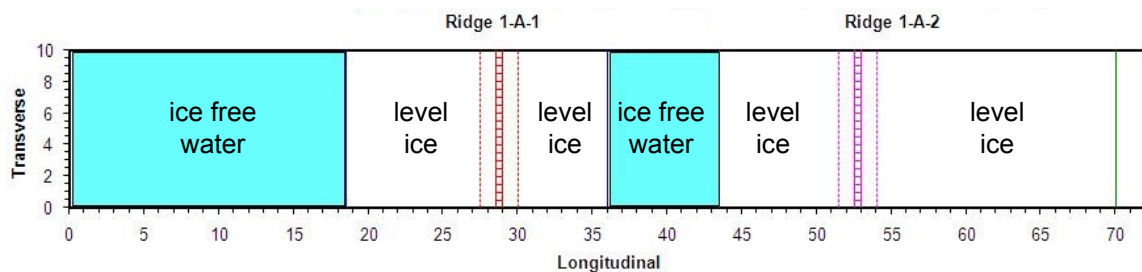


Figure 3.44 Location of ridges, level ice and open water in the ice tank (example)

After the ridges have been built the keel depths and sail heights are determined by profiling. In general three profiles are taken preferably in the area of the model trace (portside – center – starboard). This is done by pressing a stick in equidistant intervals through the ridge. At the lower end of the stick a cross-bar is activated and the stick can be lifted upwards until a certain resistance indicates the bottom of the ridge. The keel depth is indicated at the reading line (yellow circle) by a marker in the upper part of the stick (see Figure 3.45). From the measured data a profile of the ridge sail and keel can be plotted (see Figure 3.46).

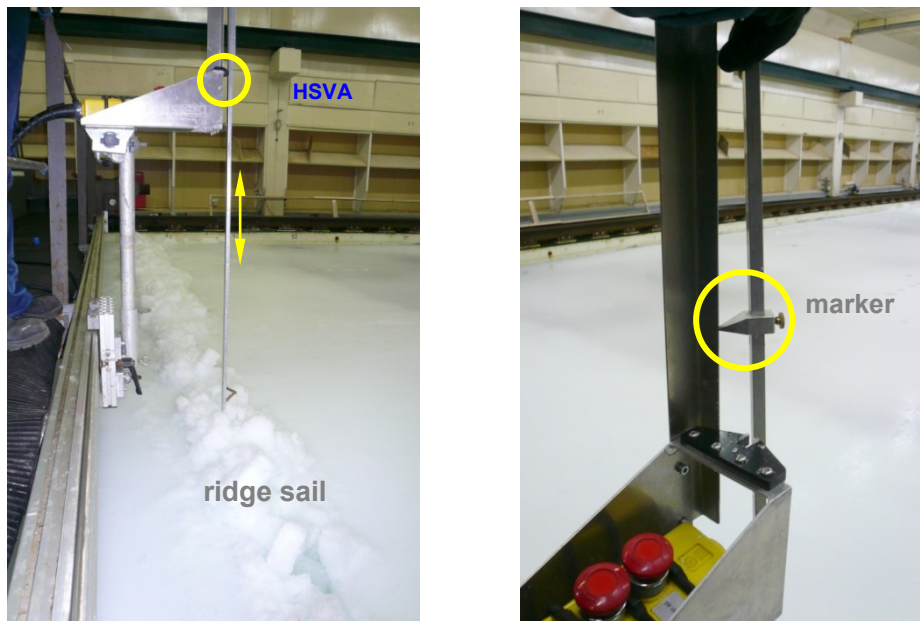


Figure 3.45 Ridge profiling device to determine keel depth and sail height

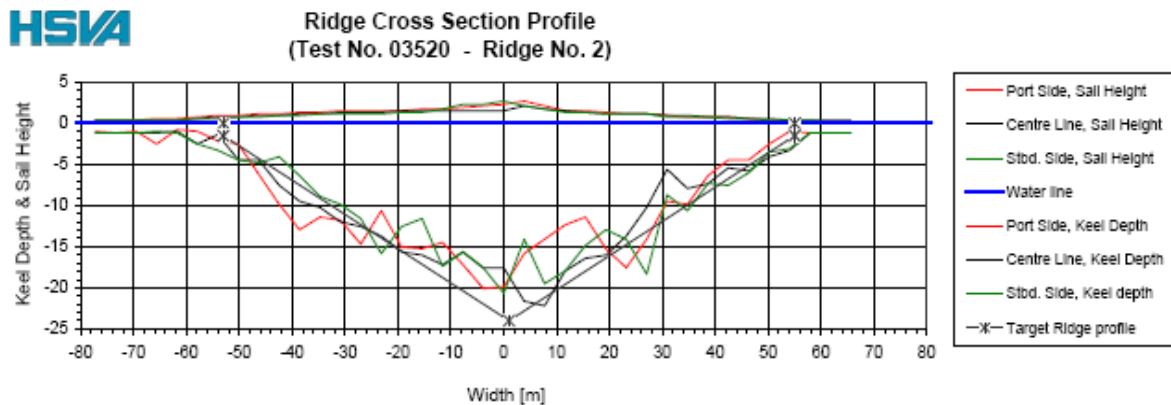


Figure 3.46 Cross section profiles of a FY- ice ridge

#### 3.2.4.6 Ridge punch tests

Punch tests may be carried out to determine the internal shear strength of the unconsolidated ice rubble being accumulated in the ridge keel. To prevent adverse effects on the model tests the punch tests are performed subsequent to the tests with the model. A ridge area beside the sail and with sufficient distance to the wake of model and to the tank walls is chosen.

The device for punch tests consists of a polished stainless steel barrel of 0.5 m diameter with a total mass of about 310 kg (including ballast weights). The cylinder is suspended from and lowered by the service crane above the ice basin. A constant crane speed of about 7 mm/s is used to lower the barrel into the ridge. A load cell mounted below the crane hook is used for the force measurement. The testing device is shown in Figure 3.47.



Figure 3.47 Test set-up of the punch tests

Where the keel ice rubble is covered by a 'consolidated layer', a circular trench is cut through this layer about 1cm beyond the punching plate. Effort is taken to cut only through the consolidated layer but not into the rubble ice pieces below.



The ridge depth is measured 8 times on a circle approximately 5 cm beyond the edge of punching plate. The punching procedure is affected also by the buoyancy of the submerging plate and ballast weights. Thus, open water tests are performed where the punching plate including the ballast weights is lowered into the ice-free water with the same lowering speed as in the ridge punch tests. For the low speed ( $v \sim 7$  mm/s) it can be assumed that the change in the measured force is mainly related to the buoyancy of the plate and ballast weights being submerged.

### Analysis of punch tests

In order to derive the pure shear force generated by the ice rubble, the forces measured in the open water test are subtracted from the forces measured in the ridge punch tests. In a second step the buoyancy force of the ice rubble below the plate is determined (after the plate had been stopped at the lowest position) and also subtracted. This procedure leads to three curves, such as those shown in Figure 3.48. Assuming that the shear force is acting along a cylindrical surface (instead of a slightly conical surface) which linearly decreases with the immersion depth of the plate, the stress in the shear plane can be calculated. The momentary shear stress calculated is plotted in Figure 3.49.

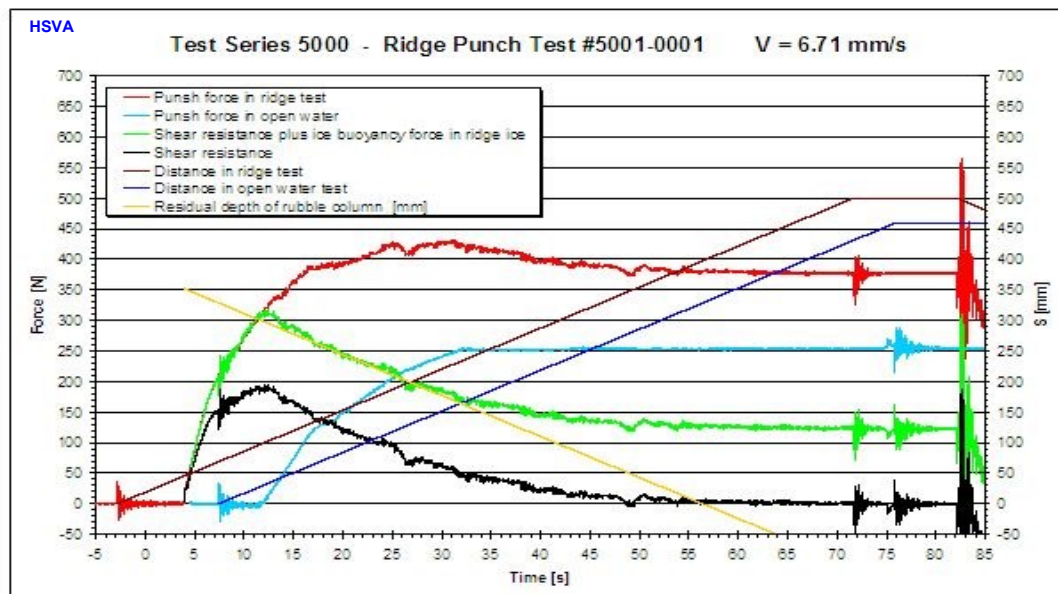


Figure 3.48 Example of ridge punch tests analysis

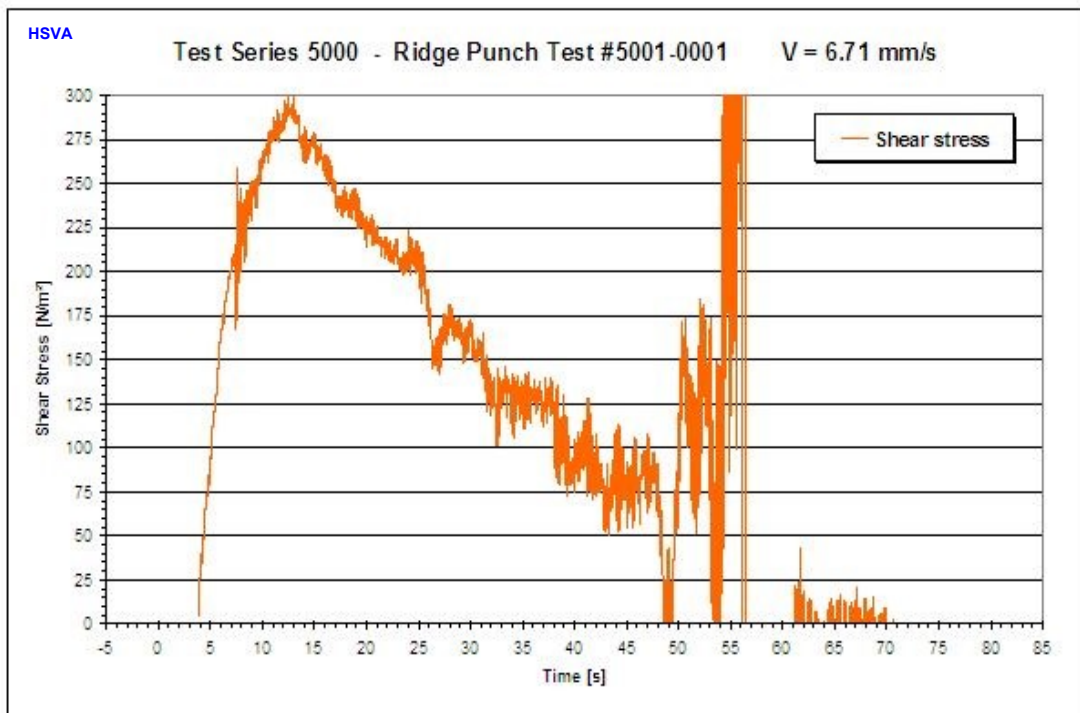


Figure 3.49 Calculated shear stress in a ridge (example)

#### 3.2.4.7 Preparation of ice ridges at Aalto University

First, the level ice sheet is broken along the y-axis (along the carriage) for a determined width. After breaking the level ice, the broken field is compressed together by the carriage. The amount of compressed broken level ice is determined by the required ridge height. When the required ridge height is obtained, the carriage is left in a resting position for a 1 to 1.5 hour consolidation period. The test runs are carried out after the consolidation period. If the time is not limited, spraying can be performed in order to obtain more consolidated ridged field. The shape of ridges produced as described above do not necessarily correspond with natural ridges, because the geometry of the ridge built by this method is more uniform than of ridges in nature.

Due to the width of the ice tank it is possible to conduct three different test runs in one ridge, but the properties of the ridge cannot be varied. In order to carry out tests with different ridge parameters, a new ice sheet with ridge needs to be produced. A principal picture from measurements in the ridged ice field is presented in Figure 3.50. Once the manufacturing process of the ridge is concluded the ridge is profiled by thickness measurements in approximately 20cm distance.

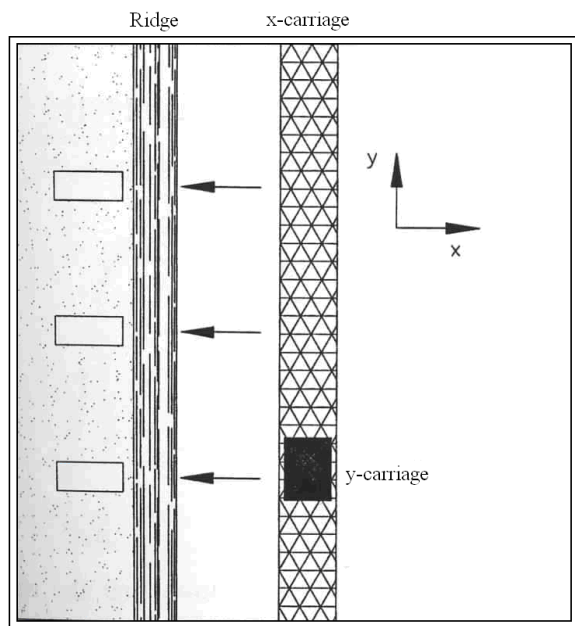


Figure 3.50 The Aalto University ice basin, the carriage and the ridge. Measuring places are marked with arrows (Leiviskä, 1999)

The modelling of ridges still lacks comparison to full scale data. Additional important parameters (after height and depth) are the porosity and the strength of the ridge. The porosity describes the amount of air voids and water pockets that do not contribute much to the resistance. The strength of the ridge depends on the consolidated bounds between the ice blocks due to refreezing. The strength and porosity are governing parameters for the resistance in ridges and require data from full scale measurements to assess the comparability of the model ridge. Furthermore, the modelling of ridges with high porosity is very challenging and often not feasible.

#### 3.2.4.8 Preparation of Ice rubble fields at Aalto University

Ice rubble fields are prepared in a similar manner like first-year ice ridges. A section of a level ice sheet is cut free from the side walls of the tank, cut into strips of a defined width and pushed against the resting ice sheet by means of the carriage's pushing board. The rubbing process is supported by a beam with inclined face put across the tank. During the rubble formation the beam is successively moved forward. The rubble field building procedure is started at an air temperature of about  $-2^{\circ}\text{C}$  when the ice is still cold in temperature  $-1^{\circ}$  to  $-1.5^{\circ}\text{C}$  and has enough cooling energy to perform freeze bonding between the floes in the rubble. After finishing of the rubble building process, the cooling is started again to deliver a room temperature of  $-6^{\circ}\text{C}$  for two hours. During this period a consolidation of the top layer of the rubble field is created (Figure 3.51).



*Figure 3.51 Ice rubble field at HSVA's ice tank (left), moored FPU model entering the ice rubble astern (right)*

## 4 State of the art in modelling techniques

The experiments listed in Section Two require specialist facilities, equipment and procedures in order to be successful. This section is split into two parts:

- Model construction; and
- Measurement and analysis techniques.

### 4.1 Model construction

#### 4.1.1 Stiffness / rigidity

Each physical model has a natural frequency (or frequencies) of resonance, as does the structure it represents. The natural frequency of a model or structure can be measured by subjecting it to an impulsive point load (for example, by hitting it with a hammer) and measuring the resulting ringing (for example by monitoring a force transducer used to mount the model or an accelerometer mounted on the model). The natural frequencies are then determined by a spectral analysis, normally using a fast Fourier transform (fft). The spectral peaks give the natural frequency and its harmonics.

It is important that the natural frequency of the model is higher than the highest frequency of interest in the model tests. If this is not the case it will not be at all easy, and may be impossible, to separate out the ringing of the model structure from the hydraulic response of interest. For example, when undertaking a Fourier analysis of the drag and inertia forces on a piggyback pipeline (Branković *et al*, 2010) the analysis went up to eight times the incident wave peak frequency, so it was necessary to make the model pipelines sufficiently rigid that their natural frequency was higher than this.

#### 4.1.2 Mooring lines, catenary moorings and fenders

##### 4.1.2.1 Mooring lines

Mooring lines are often replicated by inserting springs into zero or low stretch lines (steel cable or Kevlar for instance) these lines will incorporate either an in-line load-cell or a cantilever load cell for measurement of the force. Alternatively, or in combination, mooring lines may be modelled as geometrically downscaled realistic lines (see Catenary lines below).

The springs that are inserted are matched to ensure that the overall line elasticity is as close as possible to the desired characteristic. For more accurate models this involves building a series of extension-limited springs and coupling them together to approximate a non-linear characteristic. The limitation of this technique is that it can only model increasing stiffness curves.

In general, single stage linear approximations are used as these are the simplest, however in situations that require more accurate matching, two and very occasionally three stage approximations are used. These multiple extension-limiting springs are individually hand built and documented and are exceptionally time consuming to produce.

Some of the effects that cannot easily be modelled include:

- Highly non-linear line characteristics. (“Sandow” type cord have non linear behaviour but the characteristics are not easy to assess);
- Over-working of a line near its MBL (the effect of a line irreversibly stretching);
- Effects of single lines breaking; and



- Effects of multiple lines breaking (unzipping) due to an overload caused by a single line failure.

An alternative to using multiple extension-limiting springs is a 'craw foot' arrangement of two or more linear springs, shown in Figure 4.1. However, this method is time consuming to produce.

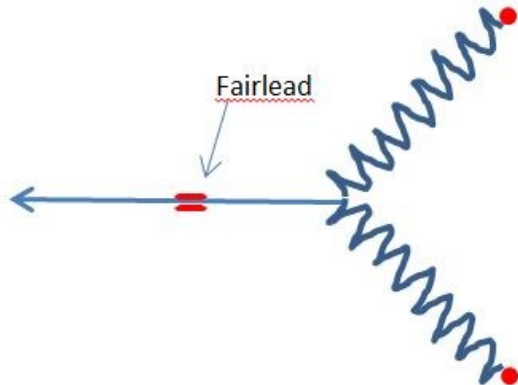


Figure 4.1 Model mooring line in a craw foot arrangement

#### 4.1.2.2 Catenary moorings

For catenary mooring, it can be quite important to model the lines with the correct geometry as downscaled but realistic line models, including all individual lines in the model with the right diameters (slightly adjusted / reduced to account for scaling effects). An additional, small spring is usually needed in addition to ensure the correct axial line stiffness. This gives a reasonably proper modelling of the hydrodynamic drag forces and resulting line dynamics on the mooring. It can be quite important to represent the proper system low-frequency damping from the lines (and risers), and proper anchor line loads can also be extracted (Stansberg *et al.*, 2000). It also ensures a good reproduction of the time-varying horizontal and vertical system stiffness experienced by the floater. The same philosophy is also often used for taut mooring, especially if the (instantaneous) vertical stiffness is important. The equations describing a catenary mooring of a homogeneous line are given in Appendix A.

For very deep waters, a realistic line (and riser) modelling is impossible due to limitations in depth (and area, sometimes) and hybrid techniques with truncation are needed (Stansberg *et al.* 2000, 2004). Model tests at a reduced depth are then used to calibrate a numerical model, which is often a coupled analysis model based on FEM, and full-depth results are numerically extrapolated from the calibrated numerical model.

Catenary mooring lines can be easily described in static configuration, the evaluation of their shapes and internal forces can be computed from a semi-analytical approach (catenary shapes). When bending stiffness is accounted for, finite difference or finite element methods are used.

Loads related to the incoming flow (current and waves) and to the proper motion of the lines are generally computed by Morison's formula. The accuracy of the results depends on the accuracy of the drag and added mass coefficients.

Depending on the water depth (from shallow to deep), the type of mooring (taut mooring, semi-taut, catenary) and the lines material (chain, steel cable, textile rope), the resulting mooring stiffness may depend mainly on the shape and weight of the lines, on the (visco-)elasticity of the materials, or both. Software based on the same theoretical formulation and algorithm (such as Deepline, OrcaFlex) is used for modelling mooring lines and risers (flowlines).

Vortex Induced Vibrations (VIV) may occur with current and Vibration Induced by Motions are originated by the floating body.

At model scale, linear mass, linear weight in water, drag forces should be extrapolated with the same ratio. Because of the variation of the hydrodynamic coefficients, the ratio of diameters could be different from the main geometrical ratio based on lengths and global shape. Bending stiffness and axial stiffness must be taken into account with the appropriate ratios.

A false bottom can be used to simulate the right water depth.

Table 4.1 Froude scaling for catenary mooring lines

	Full scale	Model scale
Length (reference)	$L$	$\lambda$
Diameter	$D$	$\lambda$
Linear mass (in air)	$\mu$	$\lambda^2$
Linear weight (in air)	$\varpi = \mu g$	$\lambda^2$
Linear buoyancy (in water)	$\varpi_b$	$\lambda^2$
Linear weight (in water)	$\varpi_w = \varpi - \varpi_b$	$\lambda^2$
Linear added mass (in water)	$\mu_a$	$\lambda^2$
Young Modulus	$E$	$\lambda^0$ or other material
Axial force	$T$	$\lambda^3$
Bending moment	$M$	$\lambda^4$
Section area	$A$	$\lambda^2$
Elongation	$\Delta X$	$\lambda^2$
Axial stiffness modulus	$EA$	$\lambda^3$
Axial stiffness	$\Delta T / \Delta X = EA / L$	$\lambda^2$
Bending stiffness	$\partial M / \partial \theta$	$\lambda^4$

The above table gives the scaling parameters that must be fulfilled in the case of dynamics in waves. An obvious question arises when considering the material stiffness. For a given line material, the axial stiffness modulus  $EA$  cannot be obtained by a simple reduction of the diameter  $D$  with scale  $\lambda$  which induces a  $\lambda^2$  scale on the section. The equivalent section area must be scaled by  $\lambda^3$  instead of  $\lambda^2$ . Then a reduced scale model of an elastic line could be made with a different material or a reduced section of the same material. In this last case, the overall diameter must be obtained with some additional components : for instance a smaller portion of the original material included in a tube with very low axial stiffness or not connected to the inner material. In addition the weight in water must be carefully adjusted by distributed additional buoyancy or weight included in the domain limited by the external diameter.

The bending stiffness can be an issue in the case of risers and flow lines built with steel. The reduced scale thickness of the steel tube could be too small to find an equivalent on the shelf tube. A different material can then be used, for instance composite tube (fibreglass and epoxy) with additional mass inside (Chatjigeorgiou 2007, 2008).

#### 4.1.2.3 Fenders

Fenders are flexible elements between ships and quay walls or between ships moored alongside, which usually behave as non-linear springs in compression. When testing floating objects resting against fenders the location and the stiffness characteristics of the fenders must be carefully represented in the model.

Two main types of fenders are currently used:

- Cylindrical Fenders with radial loading. This type has increasing reaction forces with compression and are generally soft for low loads as they react by ‘flexing of the rubber’ or by the compression of air for pneumatic fenders.
- Buckling fenders which can be axially loaded cylinders/cones or similar. These fenders are initially stiff as the reaction is created by compression of the material. When a certain load is exceeded the fender will start to buckle and the fender will react with a gradually reducing force until the buckling process stops and a sharp rise of the reaction force again appears.

Examples of the different fenders and their generic load compression characteristics are shown in Figure 4.2.

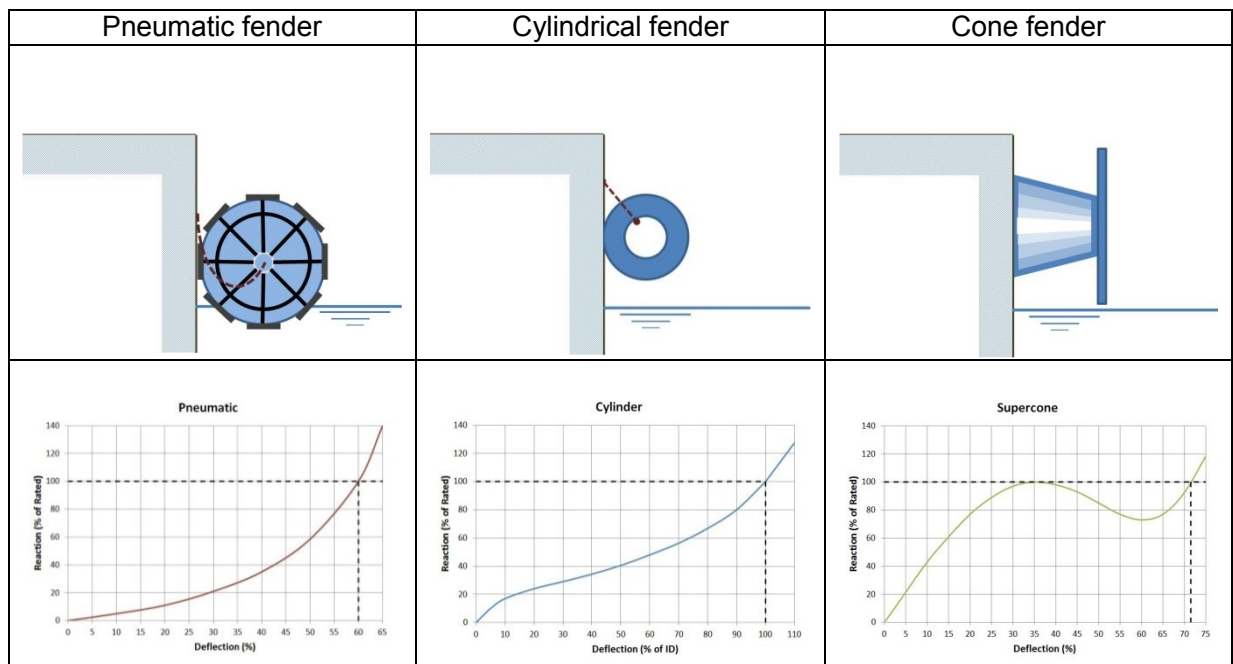


Figure 4.2 Typical performance curves for fenders (Ref. Fentek)

Fenders are frequently model by a linear spring, which is acceptable for small values of compression around a mean position. When the total capacity of the fenders is used the non-linearities must be represented. This can be done mechanically in various ways. An example of the approximation of a buckling fender is shown in Figure 4.3. Here the fender element is mounted on a linear spring. The lever arm will lift the counterweight at a constant force until stopped at a certain compression. The fender model is mounted on a two component force gauge.

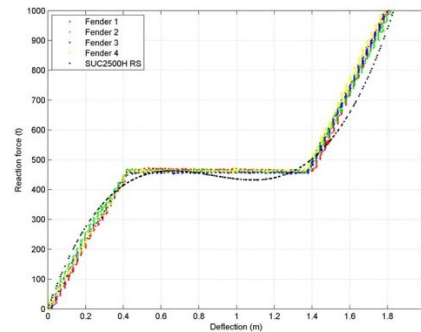
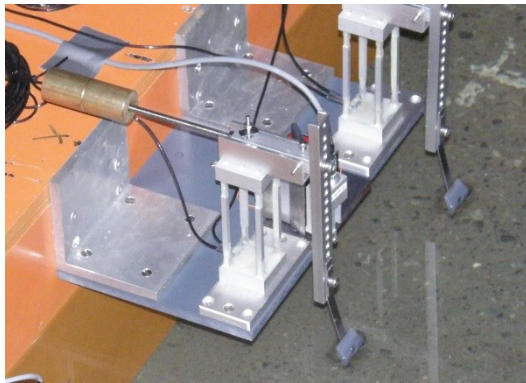


Figure 4.3 Model of buckling type fender. The graphs show model characteristics compared to prototype.

Friction between the fender and the hull is important for correct reproduction of vessel behaviour in models. This aspect is generally solved by proper selection of model materials. The stiffness and damping characteristics of berthing lines and fenders are prominent parameters in the dynamics of side by side arrangement of floating bodies (Lécuyer 2012). An example showing mooring lines and fenders is shown in Figure 4.4.

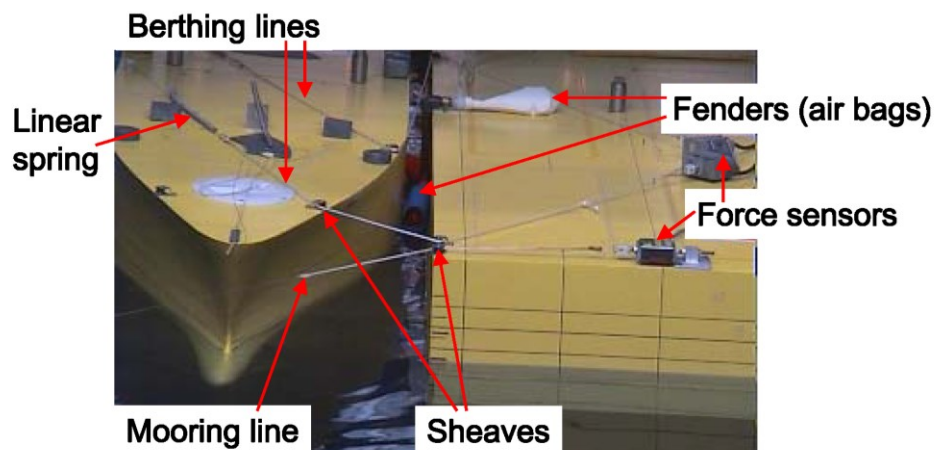


Figure 4.4 Side by side tankers with mooring lines, berthing lines and fenders

#### 4.1.3 Ballasting and mass distribution in floating bodies

Floating models need to be checked with respect to (DNV 2010):

- geometry, mass, mass distribution, metacentric heights, waterline;
- restoring force stiffness from moorings and risers;
- heeling stiffness, when applicable; and
- checking the natural periods in actual degrees of freedom.

#### 4.1.4 Permeability of rock structures

Flow within rubble mound structures will influence stability and hydraulic responses. The influence of structure permeability on the stability of rock armour is well-established by the use of the P factor in Van der Meer's armour stability prediction methods. The influence of mound and armour layer permeabilities on other responses is often less-clearly described, particularly

wave overtopping and/or transmission; upward pressures on caissons or crown walls; and geotechnical stability including liquefaction.

In the prototype structures (1:1 scale), these flows in a rock structure are generally turbulent. In an un-distorted small scale model, however, some of these flows may be laminar, and therefore offer too much resistance. If these layers become less permeable, wave-driven flows in the inner layers are limited and the flow effects in the armour are increased (Oumeraci 1984). Simple geometric scaling of underlayers and core material may thus be regarded as providing conservative estimates for certain responses like armour stability, forces and overtopping, as larger damage and overtopping are likely to occur in the model.

There are two alternative approaches. To obtain the same type of flow in a scale model may require use of a rather larger-scale model, so that pore-velocities are turbulent. Alternatively, in small scale models, scaling of material modeling the underlayers and core may be adjusted to ensure turbulent flows and thus to correct viscous scale effects.

Various methods are available to scale the permeability of core and underlayer materials in a better way (e.g. Jensen & Klinting (1983), Van Gent (1995), Burcharth et al (1998, 1999), Troch et al (2002), Vanneste & Troch (2010). The scaling of permeability is thereby usually achieved by equating a characteristic hydraulic gradient at the interface between rock layers in prototype and model. The hydraulic gradient that has to be scaled however changes as a function of both time and location, and it is not known a priori, such that it remains difficult to estimate. A conservative estimate of the permeability may be made. In some models, the corrected scale may be varied through the model to ensure the maintenance of appropriately adjusted hydraulic gradients in both outer and inner layers.

#### **4.1.5 Dynamic ice friction**

Since friction is of great importance in various cases of ice action, for example in the resistance of icebreaking ships and in ice forces on structures, the establishment of the friction coefficient between ice and structural materials and coatings is mandatory in any full scale or model tests.

The friction coefficient of ice does not obey classical Amontons-Coulomb laws of dry friction; instead it is a lubricant phenomenon which varies with temperature, contact pressure, and slightly also with the relative velocity between the ice and substrate material.

In order to avoid conditioning of the material surface by sheared off ice crystals clogging cavities, frictional heating, orientation of surface molecules and stripping off of surface coatings, friction tests should not be carried out by rotating a disc or slider on the ice surface or by towing a plate of the material over the ice surface.

Instead it is recommended that friction coefficient be established by towing a block of ice over the material surface (wet or dry depending on the test conditions). It is important that this surface is perfectly horizontal (Schwarz *et al.*, 1981).

The following parameters should be measured:

1. Horizontal towing forces;
2. Total normal force;
3. Dimensions of the ice sample;
4. Velocity; and
5. Temperature.



The ice and material surface should be described. The initial peak resistance divided by the normal force represents the static friction coefficient (Schwarz *et al.*, 1981).

At HSVA investigations on the effect of dynamic friction between ice and model surface are performed according to the recommendations of Working Group on Standardizing Testing Methods in Ice, IAHR Section on Ice Problems (see Schwarz *et al.*, 1981). A testing apparatus developed and designed at HSVA is used to determine the dynamic ice friction coefficient. During the varnishing process of the model a plate of same material as the model is painted at the same time to ensure same surface characteristics. The plate is fixed on the carriage of the friction apparatus (see Figure 4.6 and Figure 4.6) which can be moved back and forth. The ice specimen is loaded into a frame. Two slightly pre-stressed load cells are mounted between this frame and the support, which remains stationary, while the carriage moves back and forth.



Figure 4.5 (a) Friction testing device; (b) ice sample loaded between load cells

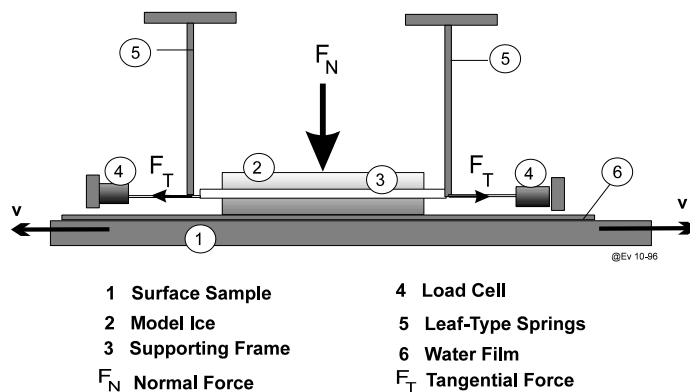


Figure 4.6 Schematic diagram of the friction testing apparatus

The tangential force is measured by two load cells. Two different normal loads, 50 and 100 N, are applied by adding ballast weights to the weight of the ice specimen. For each normal load 10 test runs are carried out. An average value is calculated, giving the dynamic friction coefficient between the ice and the tested surface.

The dynamic friction coefficient is calculated according Coulomb's friction law:

$$C_{if} = F_t / F_n$$

where

$C_{if}$	=	dynamic friction coefficient
$F_t$	=	mean value of measured tangential force [N]
$F_n$	=	normal load [N]

#### 4.1.6 Sliding of caissons, blockwork and crown-walls

A rapid-assessment method for the stability of caissons, blockwork walls, and crown wall elements in seawall or breakwater testing may be to test the movement of reduced-density model elements. The reduction of density is calculated to match the intended Factor of Safety so that the element being tested will move in the model (usually sliding) at the load condition at which the prototype has reached its intended Factor of Safety. This does require however that the model element will slide at the same coefficient of friction ( $\mu$ ) as the prototype, or the stability equation used to derive the reduced density is adjusted for any difference in friction.

Measurements of sliding friction of concrete caissons / blocks in the laboratory may be conducted using essentially similar equipment as discussed in Section 4.1.5 above. The wall or block will be towed across the model underlayer, taking account of any fine bedding layer that might be used in the prototype. [NB – In-situ concrete crown walls will nearly always be cast onto a fine blinding layer over the core / underlayer to avoid loss of concrete.]

## 4.2 Measurement and analysis techniques

### 4.2.1 Load cells (Force Measurements)

Most of the force sensors used in hydrodynamics experiments use strain gauge technology. The force to be measured acts on a sensing element and the resulting strain is converted into an electrical signal by strain gauges set up on this sensing element. Depending on the number and positions of strain gauges, on the sensing element shape, up to the three components ( $F_x$ ,  $F_y$  and  $F_z$ ) of the force and the three components of torque ( $M_x$ ,  $M_y$ , and  $M_z$ ) can be measured. S shaped beam, or ring, or cantilever load cells are typical single axis force sensors.

Multi-axis force measurements can be carried out by linking mono axis measurement units or setting up several strain gauges with defined orientation on a specific sensing element (a cylinder for instance). Another available option is to use piezoelectric load cells. They can measure up to three components of the applied force. By setting up four of these three axis sensors, six components force measurements can be performed. They have an excellent resolution, even for large measuring range sensors. They are appropriate for dynamic measurements, but attention must be paid to signal drifting when measuring static forces.

The technique of oversampling and then filtering is highly recommended for all analogue force acquisition systems.

#### 4.2.1.1 Whole body forces

For detailed and accurate whole body forces the caisson (or similar rigid body) may be suspended from a number, usually 4, of 3 axis rigid force measurement devices. This requires a small gap left around the unit to allow for the small movement required to record the applied force accurately. The 3-axis rigid force measurement devices used at HR Wallingford are shown in Figure 4.7. These comprise three single s-beam load cells coupled together around a common axis giving  $x$ ,  $y$  and  $z$  components. Each of these gauges is rated up to 50kg, although many other ranges are available. The combination shown in Figure 4.7 is quite adaptable, although the rigidity is increased by combining four 3-axis devices together. An example application is shown in Figure 4.8. It is important to check that there is no cross-talk in such a

setup, for example where the application of a load in the x-direction causes a signal in the transducers measuring y and z forces.

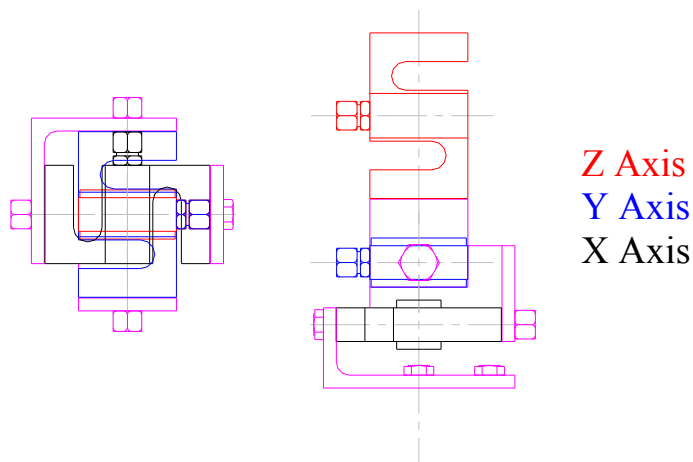


Figure 4.7 Current HR Wallingford three axis rigid force measurement device



Figure 4.8 Caisson with rigid force measurement rig (left) and pressure sensors (right)

Alternatively 6-axis units are available that have an exceptionally high rigidity and accuracy. For more rigidity a dynamometer or strain gauge table may be used. These are of necessity weighty and usually massive and have to be placed flush with, or under the seabed, with the structure fixed atop. Their advantage though, is usually that they have a very high natural frequency (Figure 4.9).

A particular difficulty in using any bottom-mounted dynamometer or load table in determining loads on breakwater caissons or similar GBS structures on rubble foundations is that the measurement device interferes with the up-lift forces acting on the structure underside. Even with appropriate spacer rods between the force table and the structure, the clearance holes needed will distort flows / pressures within the rubble mound. Alderson & Allsop (2007) have compared methods to deduce global forces using caisson units suspended by load gauges from above (see Figure 4.8), or from multiple pressure transducers.

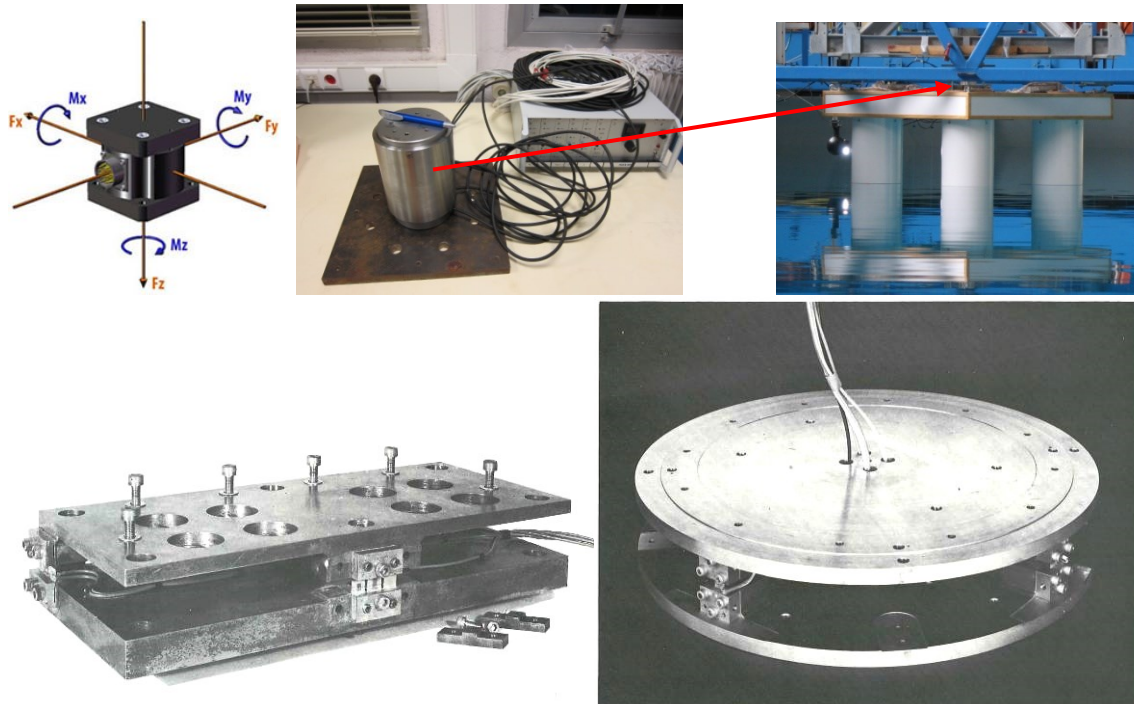


Figure 4.9 Sensors (top row) and large scale force-plates (bottom row) used for measuring overall structure loads

A 6-component scale, designed and fabricated at Hamburg Ship Model Basin (HSVA), is used to determine the forces acting on moored FPU models. The scale is mounted on top of the turret pipe (see Figure 4.10). The 6-component scale consists of two parts connected by Lorenz K-1427 strain gauge load cells. The capacity of the 6 component scale is 4 kN in horizontal and 10kN in vertical direction while it is able to handle overturning moments up to 2 kNm. The scale was calibrated using a special calibration table and it was found that the deviation from the target was smaller than 1% over the full range of the scale, while the cross-talk is smaller than 1.5%. The assembly of the 6-component scale is shown in Figure 4.11.



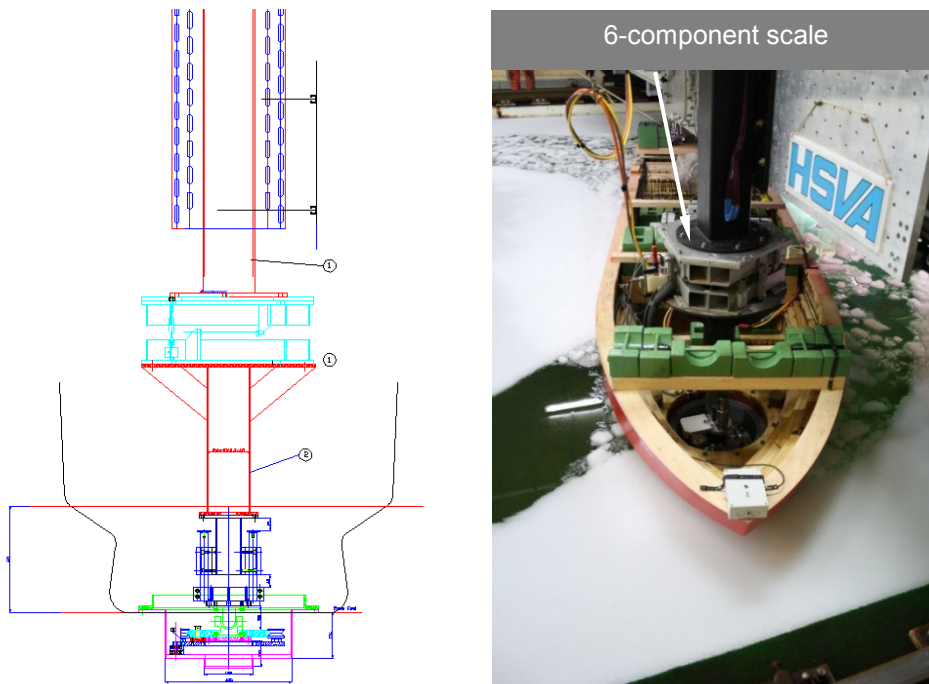


Figure 4.10 Fixed mode test setup of a floating production unit (FPU)

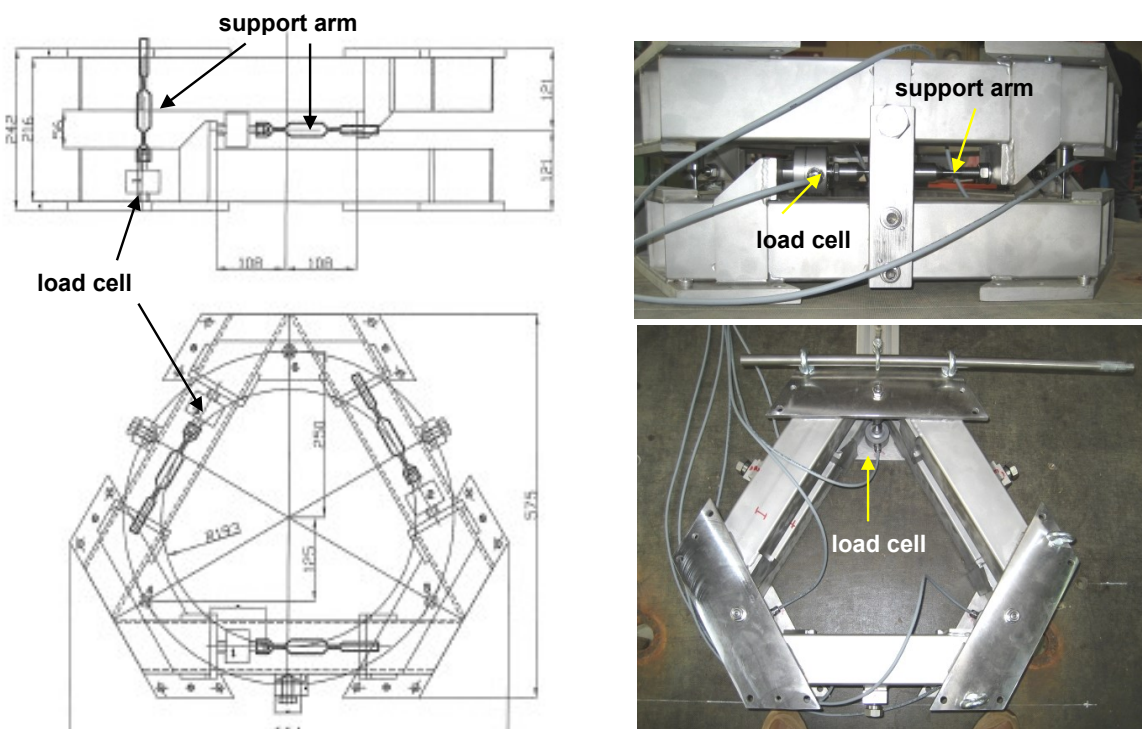


Figure 4.11 Schematic diagram and photographs of the six component scale

Ultimately, the use of rigid force measurement devices can produce true forces acting in a full 6 degrees of freedom on the structure. However, very careful attention must be paid to ensuring maximum rigidity when installing any instrumentation and the influence the system will have around its boundaries.



In order to allow linear movement the caisson needs to be isolated from any interference and above the sea bed, however in order to reduce pressures acting on the underneath of the structure it may be sat on a foam sheet. While this flexes reasonably easily, it will affect the calibration and as the foam restricts the movement, the resulting measurement will be underestimated. This can be accounted for if a way can be devised to calibrate the unit in-situ, and hence a non-linear calibration can be found. At the least check calibrations must be performed to identify the variation from calibration. In addition the movement will be reduced due to added mass and damping effects that will be manifest between the instrumented structure and the adjacent structures. This cannot be adjusted for (easily) and will be an inherent under-estimation error.

An additional item which needs to be considered when selecting the foam to be placed under the base of the caisson is the permeability and behaviour of pressures around the prototype material and how this differs from the behaviour around the foam.

Obviously in order to reduce the error and problems in this method the amount of movement in the caisson needs to be minimised. This can be achieved either by

- increasing the spacing between multi-axis force measurement devices (normally at each corner of the model) so that the same deflection in the units gives a lower deflection at the base of the model, or :
- using force transducers with low deflections.

Modern multi-axis devices are available with exceptionally low deflections that can allow the separation around the unit to be very small. Of course, it follows that more attention must be paid to the mounting the transducers in this case as the rigidity of the mounting itself must be accordingly more rigid.

Rigid force measurement units should be chosen that will keep the movement of the caisson small under the maximum loads so that hydrodynamic effects are minimised and any compression of underlayer foam is minimised. It is not unreasonable to set an upper limit for this movement at 1-2mm (model). The effect this will have on objects surrounding the caisson needs also to be considered carefully. For example, in the situation where armour units are placed against the structure as scour protection, any unrealistic movement of the structure will cause unrealistic movement of the armour units.

It should also be noted that when selecting a rigid force measurement unit, evaluation and extraction of high magnitude / short duration impulsive loading will be complex and may not give the resolution required for detailed design of panelling, beams etc. When there is a requirement to measure short duration impulsive loads it is advisable to deploy pressure transducers (see Section 3.3.6) as impulsive loading may be spatially limited.

The reproduction of mooring lines and fenders in physical models are examples of elastic force measurements, where the deformation of the transducer is a requirement for the correct reproduction of forces in the model. For tensile applications, such as mooring lines, this is commonly done by adding elastic elements in-line with a rigid measurement device. For compressive applications, such as fenders, the transducer itself is designed to have a specific (elastic) deformation.

## 4.2.2 Torque measurements

### 4.2.2.1 Propeller shaft stresses

Propeller shaft stresses can be measured during free model tests. A typical solution is to set up strain gauges on the shaft. For example, the shaft on the picture has been modified to set up the gauges on four bending elements (Figure 4.12). Electric signals from the gauges or amplifiers have to be recorded on a memory in the shaft or measured through a rotating connector.

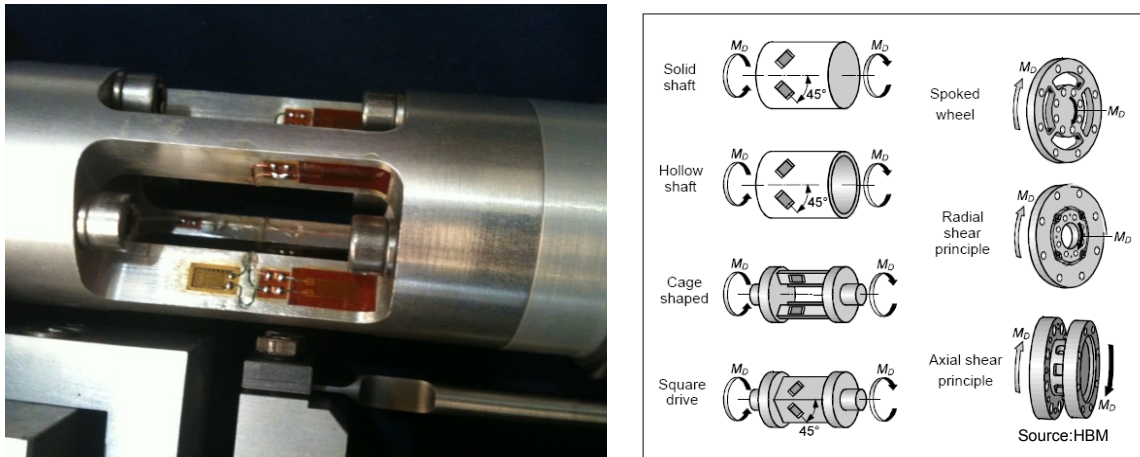


Figure 4.12 Instrumented propeller shaft (left) and different HBM torque transducer types (right)

### 4.2.2.2 Thrust and torque measurements on ship model propellers

For torque and thrust measurements on ship model propellers dynamometer are commonly used. There are different types of torque transducers and corresponding components, e.g. torque flanges, as well as non-rotational torque transducers for measuring reactions, couplings etc. commercially available. Torque transducer should possess high rigidity which causes high eigenfrequency enabling the smallest dynamic changes to be measured. More detailed information is given in the HBM manual "Measuring torque correctly" written by Schicker and Wegener, which provides an overview of all the essential aspects of using torque transducers.

According to ITTC recommendation the thrust should be measured in the line of the propeller shaft. If the propeller is working in a nozzle, the additional thrust or the resistance of the nozzle has to be measured.

If the propeller is fitted on a pod (see Figure 4.13) or on a Z-drive, the resistance of the pod or Z-drive behind or in front of the working propeller has to be considered as well. The indicated propeller thrust is measured by means of a dynamometer usually fitted in the model between the motor and the propeller. When a pod or a Z-drive is fitted on the model the propeller thrust is measured in the line of the propeller shaft in the pod housing. The total thrust of the propulsive device is measured in the model.

The required ship power can be calculated from torque and thrust measurements.

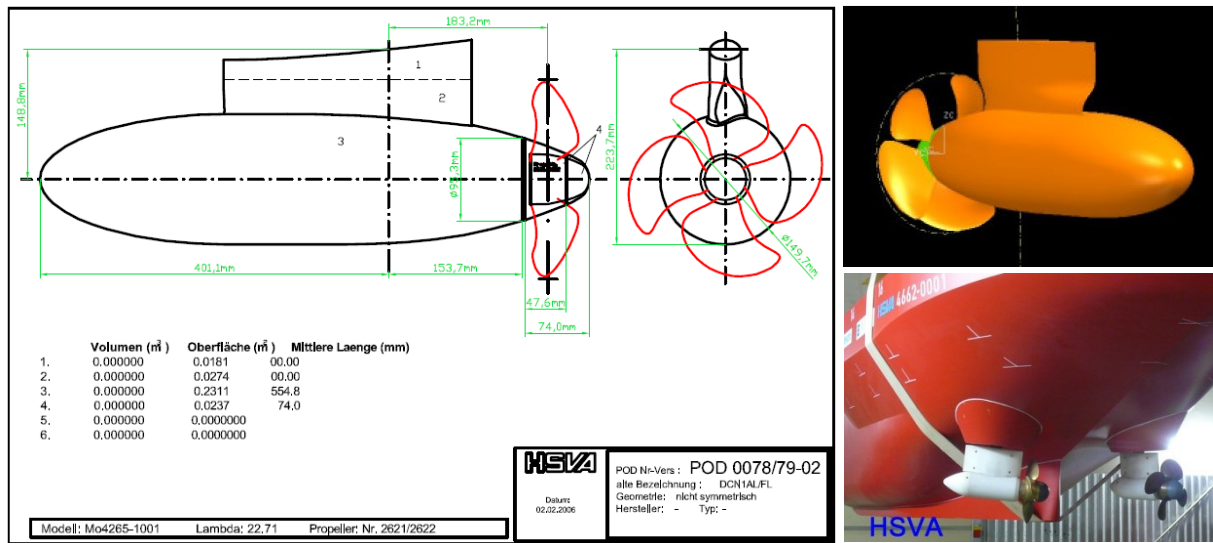


Figure 4.13 Icebreaking vessel with POD-drive

#### 4.2.3 Pressure measurements

Pressure Measurement whereby force per unit area is measured by the deformation of a membrane substrate of a known area. This method measures pressures only over the area of the transducer therefore forces over larger areas, or for whole bodies must be calculated based upon multiple small (point) measurements and an assumed pressure distribution.

Forces can be measured through the use of pressure transducers fitted at the external boundaries of the caisson unit (as shown in Figure 4.8, right). Assumptions are made about the distribution of pressures across the exposed surface and then the pressure measurements are integrated to give an overall estimate of the force acting upon the structure.

Pressure transducers provide an excellent means to indirectly measure the forces upon a structure when it is impractical to mount the structure with a rigid force measurement device. The sensors themselves are mounted into a realistically and rigidly positioned structure relatively easily and may be used submerged without any trouble. However there is the requirement to assume a lateral and horizontal pressure distribution across the structure where there are no transducers present and this requires careful attention and understanding of the interaction with the wave climate around structure.

As a pressure transducer can provide only magnitude information, for 2D or simple oblique long crested 3D studies where the pressure distribution can be well predicted and wave envelopes suggested, the loading upon the structure can be measured quite accurately using this method.

For more complex studies, such as where multi-directional incident waves or spatially varied short duration impulsive loads are considered, the pressure distribution will be significantly less well known, as a result the direction and magnitude of the resultant calculated force may vary quite considerably from the actual force and therefore give conservative or under predicted loads.

In recent years, a number of researchers have explored the use of piezo-film transducers to measure the spatial disposition of pressures around complex bodies. These have shown some potential success, but they require significant effort to encapsulate and waterproof, and can only

be deployed for relatively short exposure. To date their cost versus projected operating life has been regarded as prohibitive unless the experiments are short and the data have particularly high value.

#### **4.2.4 Motion detectors**

Motions of floating bodies may be measured using different technologies, such as gyroscopes, accelerometers, potentiometers, laser, optical systems or mechanical systems. Mechanical measurement of motion (with magnetostrictive sensors for instance or weights and pulleys) induces mass, stiffness and damping effects that corrupt the original phenomenon. Therefore, measurements should be performed by robust and non-contacting systems, to avoid any interference with the physical model response.

Six Degree of Freedom (6-DOF) motions (i.e. surge, sway, yaw, heave, roll and pitch) of free floating or moored vessels or structures can be determined by laser displacement sensors or a real-time optical tracking system (Figure 2.2). The core components of an optical tracking system are:

- Two or more high-resolution and high-speed infrared video cameras;
- a number of small, lightweight reflective marks rigidly fixed to the model;
- a high speed network; and
- a data acquisition and processing unit.

The principle of operation consists of exposing the reflective marks to the infrared light emitted by the cameras and to detect the light reflected, although it is also possible to use active marks, able to emit infrared light. Each camera measures a 2D position of the reflective marks. The system combines processed data from two or more calibrated cameras to calculate 3D position of the markers. If several markers are attached to the model (ship or floating structure) its six degrees of freedom motions may be calculated in real-time. Measurements may be influenced by sunlight.

A number of institutions, including HSVA, IFREMER and HR Wallingford use the QUALISYSTM system in ice tanks and wave basins, although other brands are available. The cameras are connected daisy chained via Ethernet 100 Mbps cable to a desktop computer, which additionally hosts a 16 channel D/A converter. This provides the capability for outputting data as an analogue voltage signal. A schematic layout of the system is shown in Figure 4.14. Such systems are considered to be standard equipment in this field of research.

The QUALISYS<sup>TM</sup> Tracking Manager QTM software provides among others the following features:

- Hardware setup, camera control and calibration
- 2D and 3D tracking & 6-DOF position determination of a defined rigid body
- Data acquisition and video capture

The accuracy of the system within a measuring area of  $L=10\text{m} \times B=10\text{m}$  is better than  $\pm 1\text{mm}$  for translational motions and  $\pm 0.1^\circ$  for rotational movements.

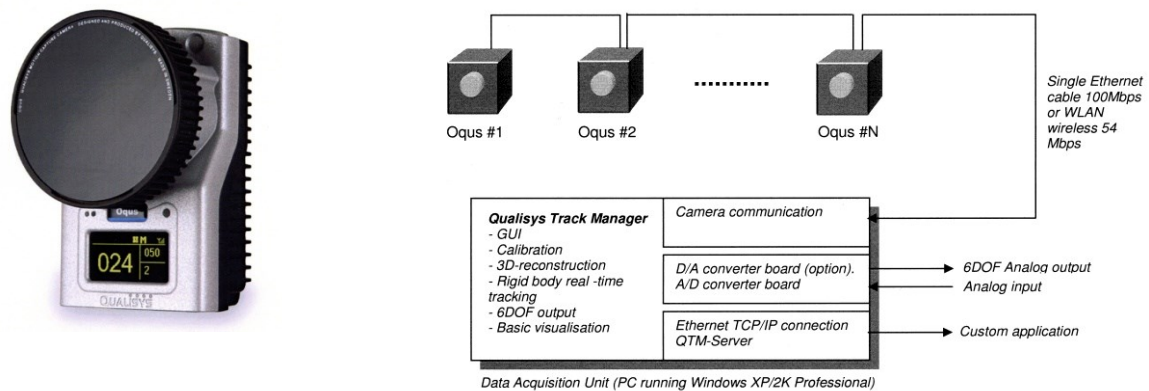


Figure 4.14 Oqus 300 camera and schematic layout of optical tracking system

Qualisys also provides underwater cameras to track underwater objects (Figure 4.15).



Figure 4.15 Underwater camera for motion tracking

## 4.2.5 Photography

### 4.2.5.1 Still photographs

Still photographs are taken of most experiments in hydraulics laboratories. They are good for publicity, normally included in reports and other publications and provide a visual record of how the model was set up. They can also be used in a quantitative way to assist in the analysis of experiments (e.g. digital image processing). Examples of the use of still photographs include:

- To determine the concentration of ice flows and the movement of elements (see also Section 3.2.4.2 and Figure 4.16)
- To document the ice failure on a structure (buckling-, bending- or crushing failure) (see Figure 4.17).
- To establish how many armour units have moved during a test. Digital still photographs are often taken of breakwater armour units (whether stone or concrete) both before and after an experimental test. Subtracting one from the other provides a quick way of viewing how many armour units have moved.





Figure 4.16 Digital photographs used to determine ice flow concentration and movement of elements



buckling



bending



crushing

Figure 4.17 Digital photographs used to document the mode of failure of an ice sheet

#### 4.2.5.2 Video recordings

Digital video recordings above and underwater are taken to monitor continuously the sequence of test runs (wave runup and overtopping, underwater motion, ice floes around (and under) structures).

Examples of the use of video records include to monitor the movement of ice floes underneath the structure or vessel (Figure 4.18)

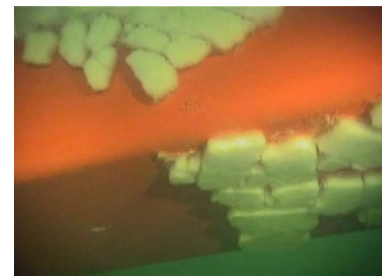
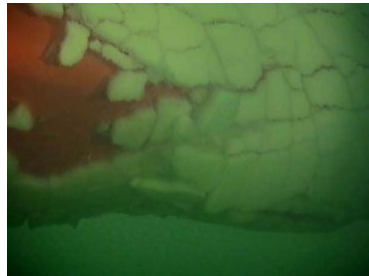
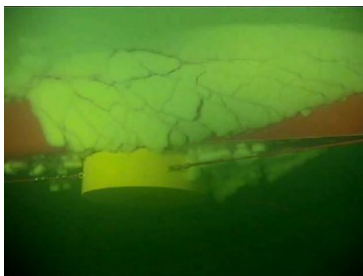


Figure 4.18 Submerged ice floes under the hull of a moored structure (snapshot from video records)

Moreover, video sequences can be implemented and synchronized in corresponding time histories of the test run (Figure 4.19)

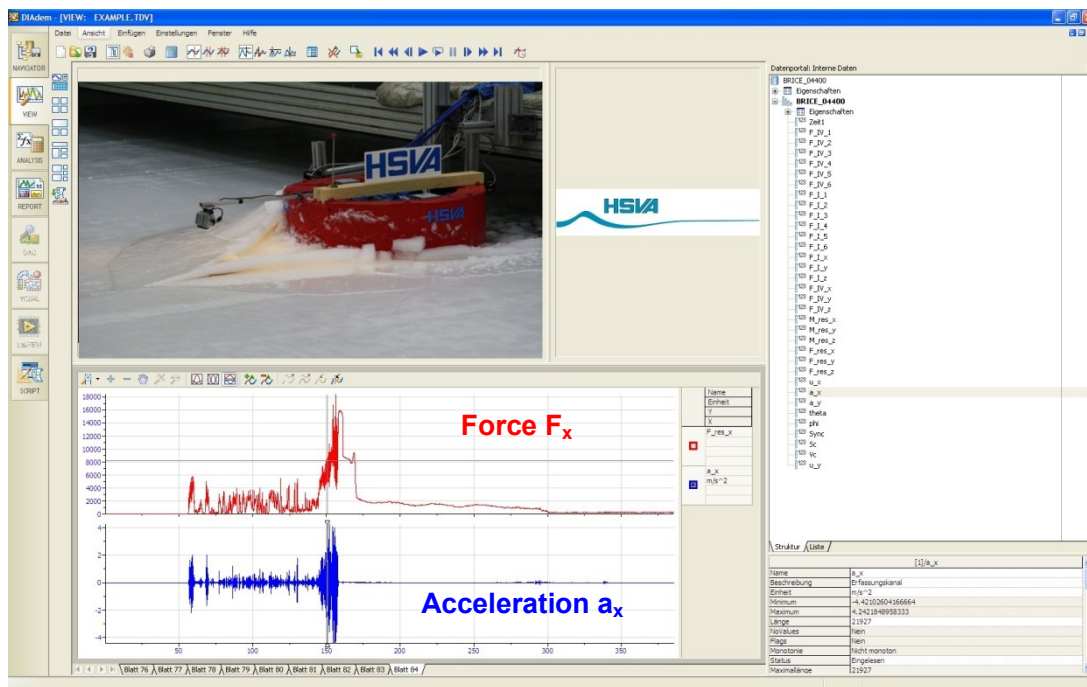


Figure 4.19 Force and acceleration time history synchronized with video record

The use of (high-speed) video can also be used to get more quantitative information. For example, in the total load measurement of wave impact on a jetty structure in Figure 4.20, the point of action of the force can be estimated by determining the impact location at the simultaneous high-speed measurement.

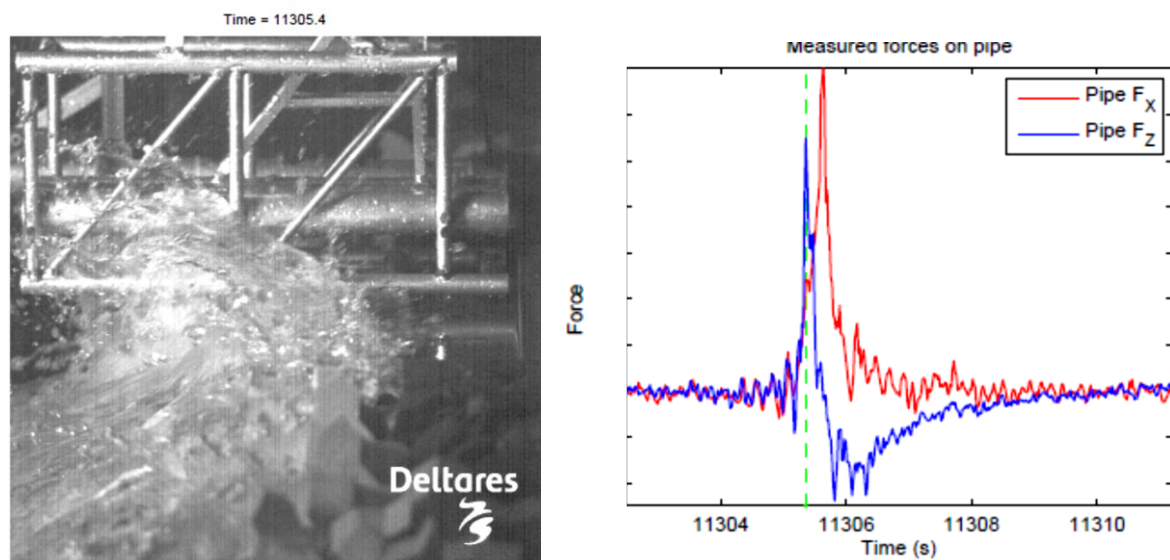


Figure 4.20 Synchronized high-speed recording of wave impact on jetty, and force measurements on the structure.

## 5 Shortcomings

This section outlines the areas where experimentalists consider there to be shortcomings in the way we undertake studies at present, based on the statistical nature of the phenomena measured, limitations in sensors, limitations in facilities and limitations in the way we handle our data. It concludes by considering whether climate change or changes in demand will lead to new requirements in the future.

### 5.1 Statistical nature of response

#### 5.1.1 Long duration tests for extreme response

As described in Section 3.1.1.5 for an accurate measurement of extreme responses, a long test duration (or several repetitions of tests) are necessary, but for practical reasons (time, money) this is not often done. This would lead to a large modelling effort to obtain measurements of only few extreme events caused by a few extreme waves. Therefore it seems more sensible to only regard the extreme waves.

Single extreme waves are usually not addressed in typical physical model studies for coastal structures. In the offshore field some examples do exist. In these cases extreme events can be modelled by wave focusing, that is the superposition of a wave modes with varying velocities which produces an extreme event at a defined point in the wave channel. However, the following reliability aspects need to be addressed during modelling:

- On which part of the wave field is the extreme event to be based?
- What is the associated probability of occurrence?
- Difficulty of correct response: the largest waves do not necessarily produce the maximum response.

Some knowledge on these matters is present, especially for offshore applications, this is described below.

#### 5.1.2 Sampling extreme waves from field measurements

To determine rare extreme events that can occur sometimes an extreme event can be taken from nature, like a recording of a tsunami close to the shore, or a measurement of an extremely large ‘freak’ wave at an offshore platform. For instance, on 1 January 1995 a single very large wave was measured at the Draupner platform. This measured wave profile was later sampled in various papers to represent an extreme wave, and this wave was used as the design wave signal to be created by wave focusing techniques (see sections 3.1.1.2 and 6.5). As the conditions are known around the time of occurrence of the wave, this approach can give an extreme wave in the sense that it was the ‘highest’ and/or ‘steepest’ ever measured. This does not directly say something about the response that the wave will create, or its probability of occurrence.

#### 5.1.3 Design wave

The “NewWave” wave group as described by Tromans *et al.* (1991) produces a probabilistic description of the extreme wave (defined as the maximum crest elevation) for a particular wave spectrum. The NewWave wave group describes the average shape surrounding the extreme crest as obtained from an infinite number of random seas – at least according to linear theory. This shape is equal to the autocorrelation function of the wave elevation, which can be derived directly from the spectrum. The theory suggests that we can describe the extreme wave crest directly without having to model many thousands of waves. Also extensions of the model have

been made where the wave period can also be chosen for this deterministic wave (e.g. Hansen and Nilse, 1995).

However, several drawbacks are present. First of all the wave still has to be made in the model by a wave-focussing technique. This is further described in Section 3.1.1.2. For an offshore case the wavemaker signal has to be determined only once, as no bathymetry is present that influences the wave propagation, but for coastal applications this is much harder. Secondly, it is not clear whether the largest wave gives the largest response. Though usually a large response is linked to a large wave, many large waves do not give a large response. Therefore this approach needs further development and validation to be readily applicable.

At present the principles of the NewWave method have not been applied to the field of coastal engineering. While coastal structures do not, in general, exhibit a dynamic response, a possible influence of wave grouping on the measured response remains. An example is the influence of setup at structures, where waves preceding the overtopping wave cause a rise in the local mean water level, influencing the runup and overtopping response. A deterministic wave group may offer some insight into these behaviours. It would need to be proven, however, that the deterministic group described the wave shape (i.e. deterministic wave) that is associated with the extreme response (i.e. the design wave).

#### **5.1.4 Sampled waves**

Stansberg *et al.* (2004) use a sampling scheme for impacts on a deck of an offshore platform for very low probabilities of occurrence ( $10^{-4}$  per year). Waves were obtained from the design storm around the design conditions. In order to increase the occurrence of the rare deck impacts, tests with slightly increased wave heights were used (with equal wave period) which led to more wave crests in the range of interest and a larger number of samples. Later a set of ten waves was pasted together and the sea state could be repeated quickly for different water levels, wave directions and structures. The signals were pasted together by taking a period of rest in between the single events, and a long rest period of 5 minutes around the extreme wave. It was not reported or determined what the minimum required rest time was to still obtain an exact replication of the extreme event. It must be noted that for coastal applications it is usually not possible to use the same wave signals for different water levels and directions, as the wave transformation over the foreshore will alter.

#### **5.1.5 Importance sampling**

Davey *et al* (2008, 2010) investigated an approach to decrease the duration of a test run for a coastal engineering problem (overtopping over a vertical breakwater). They applied the importance sampling technique. Based on a measured distribution of wave parameters during a design sea state (DSS) with few extreme events, extreme waves are sampled from a more extreme sea state (ESS), to increase the accuracy of the measured response in the DSS. This approach includes the following steps:

- preselect wave parameters that should be linked to the response;
- measure extreme response events during a design sea state and determine bivariate distributions of these wave parameters;
- measure extreme response events during an extreme sea state (ESS) with more events;
- filter the results such that the selected wave parameters of the waves from the ESS fall within the range of possible events of design sea state; and
- Obtain a more reliable estimate of extreme response now more events are known.



Using this approach (only) a “speed-up” in testing of a factor 2 to 5 can be obtained. Also, the original test run still has to be performed. Moreover, the wave parameters required to filter the ESS have to be preselected, such that a good physical understanding of the wave process still is required. However, in a test programme, often a sequence of tests with an increasing wave height are executed, see section 3.1.1.4. This technique could therefore be applied to the results of a standard test series, and increase the confidence in the results of a first test series by using the knowledge from the more severe conditions. The technique needs further validation for other structures and responses, and it should be made clear which parameters are of importance for a certain response.

#### **5.1.6 Scatter and repeatability in impulsive wave events**

A test of a thousand waves is sufficient to make an accurate representation of the (averaged) spectrum. However, when determining the magnitude of rare extreme events a multiple of this duration could be required, in order to obtain good statistics of the wave (field) that leads to the extreme response.

Additional to this variability, the response itself could also lead to extra variability. Since the early measurement campaigns on impulsive wave impact loads, (e.g. Bagnold 1939), it is known that these loads are very variable, even when using exactly the same test conditions (wave signal) and test setup. The pressures can have a variation of a few hundred percent, but also the peak forces can still be very variable, even if the same wave steering is applied in a very controlled wave flume. This means that besides the variability of the wave field (that is treated in Sections 5.1.6 and 3.1.1.4) the single wave can also give rise to a source of large variability.

A last source of variability is the exact shape of the structure, which will always be slightly different in reality, compared to the model. The shape can also alter during the lifetime of a structure.

### **5.2 Limitations in sensor technology**

#### **5.2.1 Limited spatial resolution of sensors**

Many instruments today collect point time series of measurements, whereas in many cases it may be more beneficial to collect time series at a grid of points over the area of interest. Examples of where the collection of grid time series would be beneficial are listed below.

Time series of 2D (line) and 3D (surface) free surface elevation measurements are needed for the many applications. However, adding more and more physical measuring devices creates a greater disturbance to the flow or waves, indicating a need for the development or implementation of less intrusive, remote sensing devices. Examples include:

- identification of wave breaking and setup, which requires several closely-spaced measurements of surface elevation;
- characterisation of wave disturbance within a harbour. Although this can be carried out with wave gauges at every dock and in each channel, the results would be improved by having a larger array of sampled points within the harbour; and
- assessment of diffraction and radiation of waves from floating bodies. These data are particularly important for the energy capture assessment of wave energy converters.



The integration of pressures over a surface area to get the resulting force requires there to be an adequate number and distribution of pressure cells to characterise the spatial distribution of pressure. Generally a limited number of pressure cells are available and there would be less error in the integration if the number of sensors was increased, particularly where there are waves breaking on the structure or ice cracking, where there may be very short-lived, local spikes in the pressure time series.

Instruments which operate over an area and not just a point, may still be limited by the area they cover. For example, optical motion tracking systems operate in a limited volume. Tracking objects over large areas, above, under or across the water surface requires many cameras. Such set ups are possible with the present techniques but are extremely costly.

### **5.2.2 Sensor range (Sensor resolution over a large measuring range)**

There is always a relation between the ultimate strength of a sensor and its measuring range, which can have implications for our ability to extract the signal of interest from the total signal recorded. For example it is difficult to extract a small drag force from a large total load, which includes a heavy structure weight.

A typical experiment in testing tank is to measure the six components of the hydrodynamics forces on a model exposed to current, waves, or forced motions. It is usual to have a large ratio between the model's mass, its buoyancy, its inertia and the expected hydrodynamics forces to measure. Most of the six-components force sensors have an accuracy between 0.1% and 1% of the measuring range. One option is to choose a large range sensor able to handle the model in the water and in the air (where it is often easier to prepare the experimental set up), but in this case it can be difficult to distinguish weak hydrodynamics forces from sensor uncertainties. The other option is to choose a sensor with a smaller range, but a lots of attention must be paid during mounting, un-mounting, towing acceleration, towing deceleration and motion generation to avoid an overload, which would destroy the sensor.

Some solutions can be mechanical stops allowing overloading without damaging the sensor, silicon gauges with a high signal to noise ratio, or the use of piezoelectric load cells. Such measuring systems, with waterproof quality, are not "on the shelf" products, and not easy to find.

### **5.2.3 Sensor resolution and signal on noise ratio.**

A better resolution, and signal on noise ratio would be also very useful when the data needs to be processed very finely. For instance, when the second order forces on a structures are investigated, these second order components are often weak compared to first order components. It is sometimes difficult to extract them from the signal noise.

### **5.2.4 Whole body movement**

Whole body force measurements using load cells require the structure to be able to move. Flow can get under and / or around the body being moved. This can be minimised by careful design of the experiment – by careful fitting of end caps, sealing the edges using a flexible seal or reducing flow by inserting a flexible, permeable material (such as a sponge) between the instrumented section and the rest of the structure. Flows around the instrumented section and materials used to reduce these flows both have an effect on the measurements, which can be minimised by careful experimental design, but not removed completely.

### **5.2.5 Mooring lines**

Representation of nonlinear mooring is difficult (see Section 4.1.2.1). Mooring lines are commonly represented by two linear springs, which is a reasonable approximation of many common mooring lines, but cannot handle many cases near to breaking. An ideal mooring line unit would in effect be a programmable spring that would be able to represent any elastic characteristic simply by supplying the appropriate force-displacement curve. This would enable much more accurate modelling and would save much of the work when setting up a model vessel mooring. This programmability would also allow the line to switch to a 'no resistance' setting if a predetermined value is exceeded and hence replicate a line-break condition.

### **5.2.6 Two phase flows**

It is still difficult to take measurements in two-phase flows – essentially air / water mixtures – as there is not an abrupt change from one phase to the other. Instrumentation for the measurement of air content in two-phase flows is relatively rare and specialised.

### **5.2.7 Optical techniques in turbid water**

Turbid water making optical observations / measurements difficult. Indicates a potential move towards the use of acoustic instruments.

### **5.2.8 Wave-structure interactions**

Our knowledge of wave-structure interactions would be improved by having detailed measurements of wave kinematics around a structure. In two-dimensional flumes, optical techniques such as PIV can be used to measure array time series of velocities as a wave breaks against a seawall (for example) but techniques to measure the spatial and temporal variations in velocities around three-dimensional structures is more difficult – particularly in cases where the wave overtops a structure.

## **5.3 Limitations in facilities**

### **5.3.1 Wave generation in deep water**

Waves are typically generated in relatively deep water and then propagate up an artificially steep slope to an area where the bathymetry is realistic and can produce realistic wave characteristics at the structure. A smaller geometric length scale could be used in the same facility (or a smaller facility could be used at the same scale) if waves with the correct non-linear characteristics could be generated in intermediate to shallow water depths.

### **5.3.2 Current generation**

It is difficult to reproduce current distributions, either spatial variations or time variations. (See Section 3.1.3 for details.)

## **5.4 Using model results**

### **5.4.1 Linking to numerical models**

Hybrid modelling and composite modelling – integration of physical and numerical models. Putting the results in broader context.

#### **5.4.2 Data management**

Increases in computer power and the available peripherals have led to great increases in the speed of computation and communication and the sheer volume of data that can be collected. Twenty-five years ago it was not uncommon to find desktop computers with 40MB hard drives. Today it is possible to collect single files of that size in a few minutes.

This community does not have a tradition of appending strong meta-data records to data files. Nor are there established data or meta-data standards. This makes it difficult for data to be re-used, particularly by scientists and engineers who have not been involved in collecting this data. This is a problem as public money will be more efficiently spent if data is collected once and used often. This will only occur if data records can be read, understood and trusted by third parties. This is often not the case. This problem will be exacerbated by the trend towards open access to data and publications. Open access to data will only be a productive step for this community if data can easily be read, understood and trusted.

The increased volumes of data collected may lead to data driven methods for analysing and interpreting data. The era of 'big data' is upon us in many areas and the machine-learning or data-driven techniques used in this world may change the way we construct 'models' from our data. A data-driven model is a means of deriving a functional relationship between input and output data, where the parameters and coefficients have been fitted to the data, so are not based on physical laws (Cunge 2003). Data driven model types include: correlations, ARMA methods, Artificial Neural Networks, Genetic Algorithms and Genetic Programming. These models are rapid to run, but depend on the number, range and accuracy of the input data. Cunge (2003) warns against possible misuse of these models, but they have become increasingly popular in the last decade and commonly feature in almost any recent issue of popular journals such as the Journal of Hydroinformatics.

## 6 Short-term developments

This section described technological developments that will most probably be made as step-by-step improvements of present technologies such as more refined instrumentation and/or facilities, e.g. depending on development of supporting technologies. These developments are expected within a few years and several are developments that have already begun.

### 6.1 Sampling Schemes

In offshore engineering techniques to sample extreme events, or to generate designer waves with pre-described characteristics, are sometimes used already (Section 5.1).

However, several drawbacks are present. First of all the sampled waves still have to be made. An iterative technique, and/or non-linear wave model are required to determine the exact wave-paddle motion required to generate the wave in the flume or basin (see Section 5.1.3). For an offshore case this has to be done only once, as no bathymetry is present that influences the wave propagation, but for coastal applications this often is much harder.

Secondly, it is not clear which wave leads to the largest response. Though usually a large response is linked to a large wave, by far not all large waves give a large response. Therefore further development and validation is necessary for the existing sampling approaches to be readily applicable.

### 6.2 Quadratic transfer functions

Quadratic transfer functions are used to describe second order effects related to the free surface dynamics and associated loads on floating structures (see chapter 2.2). The basic approach for waves QTF modelling is to consider bi-chromatic waves. Considering two elementary first order waves with two different frequencies (Airy waves), the second order development of the free surface boundary condition gives rise to the combinations at twice the frequencies (second order Stokes waves) and at the difference and sum frequencies. These components can be analytically calculated in constant water depth from standard formulae (Schaffer 1996, Chen 2006) and can be compared to the values extracted from analysis of free surface elevation measurements or from numerical simulation of the same conditions. For irregular waves, second order developments consider cross interactions between each pair of first order Fourier components.

Second order wavemaker theory (Schaffer 1996) should be used in wave tank testing to generate correct waves trains without parasitic components.

Low frequency components related to the difference components are particularly important in shallow water where the set-down component may be important (Chen 2006). Ongoing improvements of bi-chromatic waves in shallow water and associated loads deal with variable bathymetry effects including three dimensional aspects of a sloped bottom on the incident waves. The influence of the seabed variation can be accounted for by semi-analytical methods (Liu 2011) and assessed by Boussinesq type simulations (Bingham 2009, Liu 2011). Further improvements will take account of waves and current interaction effects.

### 6.3 Coupling of Boussinesq model to wave paddle

Numerical models and physical models are two approaches to study water wave problems in coastal areas. The former can be applied to large areas but are unable to accurately capture the most non-linear effects such as wave breaking. The latter is generally good at describing complex non-linear features but the scale and size of the model is restricted by physical facilities which often implies that wave generation boundaries cannot be positioned in sufficiently deep waters to justify linear wave generation.

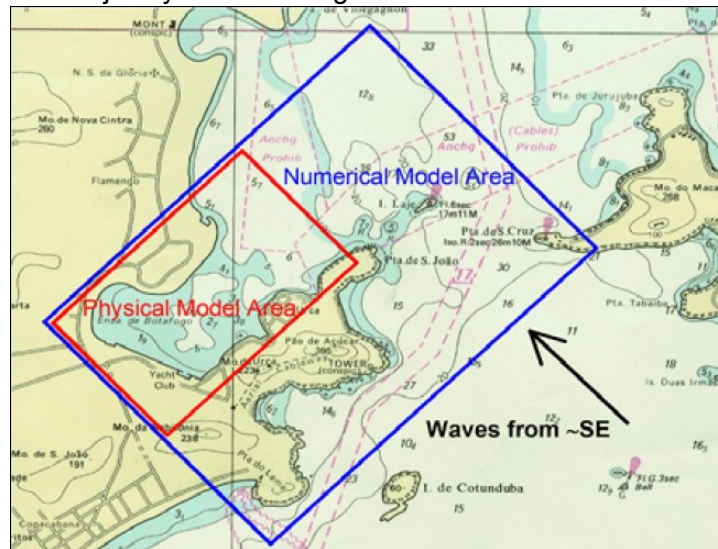


*Figure 6.1 Example of combination of numerical and physical wave model*

Combination of numerical and physical wave models are desirable in order to combine strengths of the two approaches. Typically, this combination has been done by determining statistical wave conditions at the wave generation boundary. Much information is lost, however, by only allowing data transfer between the numerical and physical model at a stochastic level with bulk parameters such as significant wave height and peak period.

It is suggested that the data transfer instead is carried out on a deterministic level. In the coupling procedure originally developed by Zhang and Schäffer (2005) results from Boussinesq model is used in a coupling equation that accounts for linear dispersion and shallow water nonlinearities - solving this equation gives the wave paddle position. Local wave phenomena – evanescent modes – are also taken into account which allows for determination of the elevation at the moving paddle. This makes it possible to run the wave generation in so-called dual mode with active wave absorption (DHI AWACS).

## 6.4 Tsunami generation

The development of the pneumatic tsunami generator will be improved by the use of computational fluid dynamics (CFD) tools to test potential improvements with only the best improvements being constructed and tested in the laboratory.

One of the ways to deal with the small scale at which tsunamis can be created is to just build a very large flume. In 2013 a new Delta Flume will be built. To obtain an idea of the capabilities of the large new Delta Flume (Hofland et al 2013), some possible N-waves that can be created at a water depth of 8 m, and the solitons with maximum wave height for different water depths, were calculated, see Figure 6.2. The solitons have wave heights around 1 m. Note that the



maximum wave height is decreasing with water depth, as the wave period (and hence wave stroke) of a soliton of constant steepness grows with water depth. The N-waves have wave heights of 1.0 m to 2.4 m and corresponding wavelengths of 300 m to 100 m. The shape of the latter waves is not constant (see Figure 6.3) when travelling through the flume, just as is the case with a real tsunami. The receding water level that is often observed before a tsunami crest arrives, can be created.

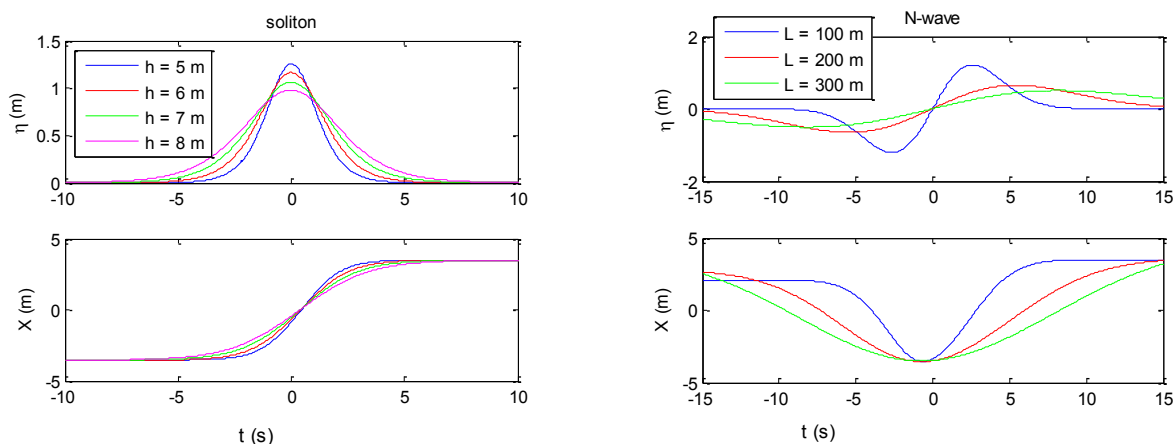


Figure 6.2 Water level variation and wave paddle position of tsunami models that can be created in Deltares' new Delta Flume. Left: solitons for water depths of 5 to 8 m. Right: leading-depression N-waves at 8 m water depth with lengths of 100-300 m



Figure 6.3 N-wave generated in old Delta Flume travelling through flume and overtopping a dike slope (Holland et al 2013)

## 6.5 Focused wave generation

In order to design safe and economic floating and non-floating structures along the coast and offshore, it is essential to model freak waves and other extreme wave patterns (e.g. Three Sisters). Physical modelling of such waves requires a deterministic approach to accurately specify the location of occurrence in the flume or basin and to make tests reproducible.

Various approaches have been developed to generate freak waves which are based on the wave focusing technique as explained in Section 3.1.1.2. This method takes advantage of the fact that waves of different frequencies travel at different speeds and can therefore superimpose at one location, if they have been generated as a succession of waves by the wave maker. To achieve maximum wave height through superposition, wave phases during generation and the distance between wave maker and focus point need to be taken into account (Testa 2006). Most methods achieve this by applying linear wave theory to transform the wave train from the focus point back to the wave maker in time and space. The transformed signal is then translated

into a wave maker signal. Running this signal should result in the desired wave form at the focus point. While linear theory is an efficient and robust transformation (Clauss, Kühnlein 1995), it neglects possible nonlinear wave-wave interactions. Resulting errors may lead to not fully focused waves or deviation from the focus point (Clauss, Kühnlein 1995). Several methods therefore exist that modify the linear approach by either iteration (Clauss, Schmittner 2007) or numerical simulation (Shemer *et al.* 2005). Alternatively, higher order wave theories have been used (Van den Boomgaard 2003; Pelinovsky *et al.* 2000).

Currently, all existing techniques are limited to constant water depth and neglect effects caused by wave reflection. The latter is a phenomenon that is more prominent in laboratories than in nature, where freak waves often occur offshore where reflection off structures is negligible. A limitation to constant water depth, however, is an aspect that reduces the applicability of laboratory tests to natural environments.

Gaussian wave packets (Clauss, Kühnlein 1995) and iterative optimisation (Clauss, Schmittner 2007) have been identified as suitable methods to generate focused waves in large laboratory facilities (e.g. GWK in Hannover). It is therefore planned to extend these methods to applications over sloping beds with the aim to eventually implement arbitrary bathymetries. A similar expansion will be explored for the time domain method by Hofland *et al.* (2010) with the aim to compare its application potential to frequency domain methods.

## **6.6 Tactile sensors**

Traditionally, pressure measurements are conducted using an array of pressure transducers placed in the middle of the structure where the maximum pressures are commonly assumed to occur. Total forces are calculated by integrating the point measurements by assuming uniform pressure distribution between the sensors. For more complex studies, such as breaking wave impacts on coastal structures producing impulsive loads with short duration, the pressure distribution is significantly less well known. As a result, the calculated resultant force may vary quite considerably from the actual force and therefore give conservative or under predicted loads (Alderson, Allsop 2007). Hence, there is a requirement to have a pressure measurement system with very high spatial and temporal resolution.

### **6.6.1 Tekscan sensors**

Tekscan provides matrix based tactile sensors, which are attractive when there is a need to measure the pressure distribution with very high spatial resolution. Their FlexiForce Sensors, are ideal for designers, researchers, or anyone who needs to measure forces without disturbing the dynamics of their tests. The tactile sensors are capable of functioning in both static and dynamic environments, ultra-thin and flexible and can easily be integrated into most of the applications. These sensors are capable of measuring pressures ranging from 0-15 KPa to 0-175 MPa with the maximum sampling rate up to 20 kHz in a 44 load cell configuration ([www.tekscan.com](http://www.tekscan.com)). However, each application requires an optimal match between the measurement area, spatial resolution and the pressure range provided by Tekscan.

FlexiForce sensors are available in both grid-based and single load cell configurations, and are also available in range of shapes, sizes and spatial resolution (sensor spacing). A sensor consists of two thin sheets, which have electrically conductive electrodes deposited in varying patterns (Tekscan 2003). The inner surface of one sheet forms a row pattern while the inner surface of the other sheet employs a column pattern (Figure 6.4 left). The intersection of these rows and columns creates a sensing cell called a 'sensel'.

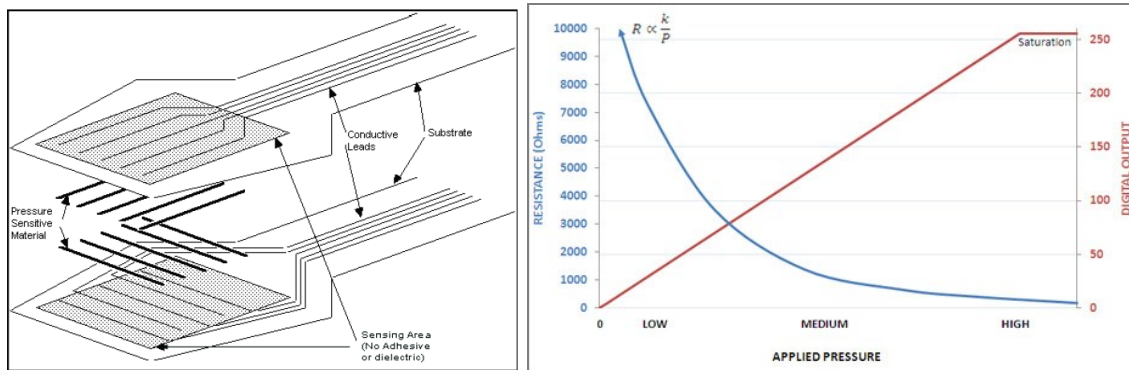


Figure 6.4 The layout of the tactile sensor (left), typical sensor performance (right)

The FlexiForce sensels act as a variable resistor in an electric circuit, i.e the resistance of the active sensing area varies inversely with applied load. Typical sensor performance is shown in Figure 6.4 (right). The system linearizes the sensor output into digital counts on a scale from 0-255 ([www.tekscan.com](http://www.tekscan.com)).

This technique has been majorly applied in the medical and automobile researches. As the first time, Stagonas et.al (2011) achieved simultaneous mapping of the horizontal and vertical distribution of wave impact pressures at the face of a vertical seawall in a small scale model. As further step, application of tactile sensor in a large scale model has been explored within HYDRALAB work package 9, 'Hydraulic Response of Structures'. The sensor model used for the experiments consists of 2016 sensor locations or sensels with 1 sensel/cm<sup>2</sup>, whilst the measuring area is 42cm x 48cm, and capable of recording pressures up to 5 PSI (34.5 kN/m<sup>2</sup>) at a maximum rate of 680 Hz.

Calibration of the I-Scan tactile sensor has been a challenging task due to various limitations of the sensor (eg. Lower sampling frequency), which requires a lot of effort to find out an appropriate procedure. A simple calibration method is finally developed with the use of a pendulum (Figure 6.5 left), which produces dynamic impact loads at the sensor surface. The applied force during the impact is measured simultaneously by means of a force transducer connected with the pendulum mass. Required load ranges can be achieved by changing the drop height and the weight. The peak force recorded by the transducer is compared with the peak, un-calibrated digital outputs delivered by the Tekscan system to achieve a calibration (Figure 6.5 right).

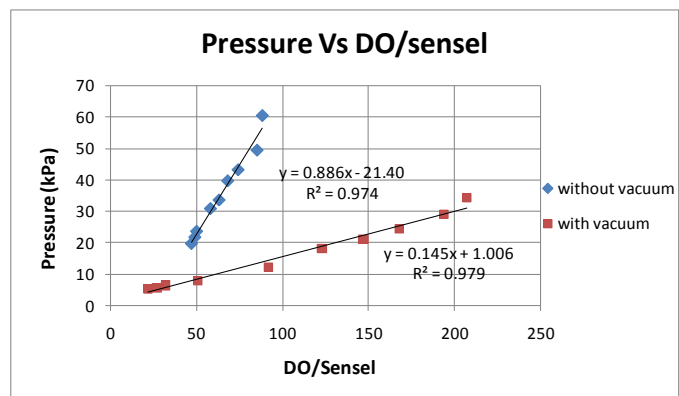


Figure 6.5 Experimental setup (left), calibration curves (right)

The effect of trapped air inside the pressure sensor has been explored during the calibration. A vacuum pump is used to remove the trapped air inside the pressure pad, which significantly improved the outputs (Figure 6.5 right). In the case of without vacuum, the tactile sensor delivers lower output than in the case of with vacuum under the same impact loads. This is due to the trapped air inside the sensor forms a ‘cushioning effect’, which subsequently reduces the sensor output. This confirms that producing vacuum is extremely important when measuring impact loads. However, the vacuum does not play any significant role when measuring static load as it acts for relatively longer duration; the trapped air has enough time to escape through the vents.

A comparison between the results obtained from static and dynamic calibration is shown in Figure 6.6. The static calibration curve significantly deviate from the one obtained from dynamic calibration, further the comparison also indicates that static calibration underestimates the impact loads. The experiment results confirmed that the static calibration cannot be applied for the dynamic loads and vice versa. This is mainly due the differences in associated duration of the applied load, which is much shorter in the case of impact load than the static load.

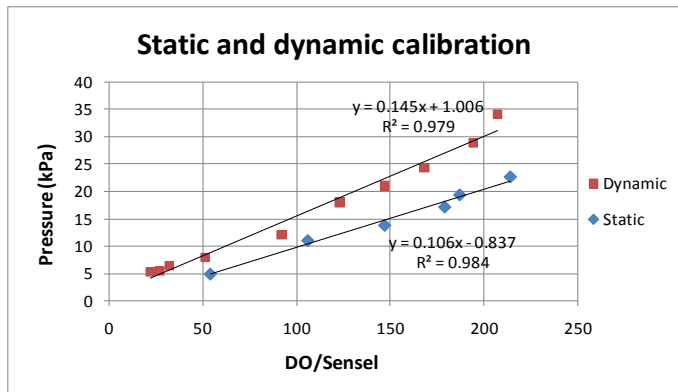


Figure 6.6 Comparison of static and dynamic calibration results

### 6.6.2 Application in wave flume

Preliminary experiments were carried out at Large Scale Wave Flume (Großer Wellenkanal, GWK) in Hannover by collaborating with University of Southampton. Prior to the experiments the pressure sensor including the handle were prepared to be waterproof. Then the sensor including the handle is placed on a dike slope (1:3) and the breaking wave loads are recorded with I-Scan system (Figure 6.7 left). Series of tests were conducted with regular waves with wave heights ranging from 0.6 m to 1.0 m; periods of 3 s to 6 s were tested. Pressure distribution recorded by the I-Scan sensor on the dike during a plunging breaking ( $H_s=0.9\text{m}$ ,  $T_p=3\text{s}$ ) at the time of peak is shown in Figure 6.7 (right).

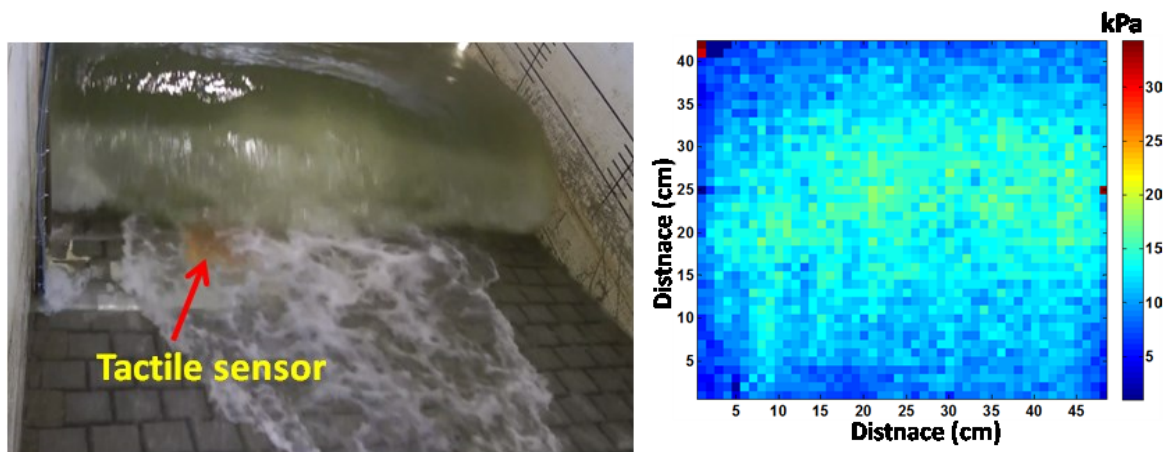


Figure 6.7 Plunging breaking on the dike (left), spatial distribution of the impact pressure recorded by I-Scan (right)

There is a clear impact caused by the plunging breaker on the middle of the pressure pad, well captured by the I-Scan system. The maximum pressure recorded is about 20 kPa in the middle. The pressure time history of the impact is shown in Figure 6.8, indicates the average pressure over the entire matrix, where the peak is about 13 kPa, considerably lower than the maximum pressure. The shape of the loading history resembles the traditional trend explained in the literature (eg. Grüne 1992).

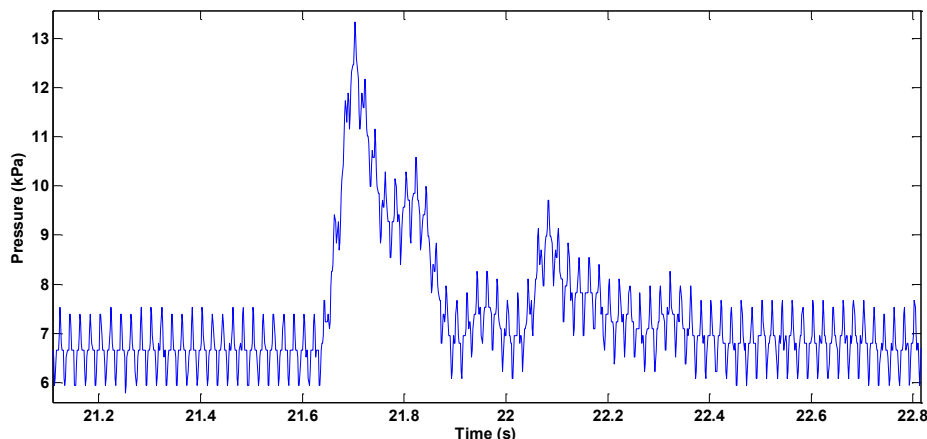


Figure 6.8 Pressure-time history of a breaking wave recorded by I-Scan pressure sensor

It should be kept in mind that the tactile sensor has certain limitations such as lower sampling frequency and 8 bits digital output system (0-255 scale) may lead to uncertainties in the results. For example, scanning rate of 680 Hz may not be sufficient to entirely capture the peak impact pressures resulting from breaking waves. Further, simultaneous measurements of lower hydrostatic and impulsive peak pressures become quite challenging due to the lower output resolution (8 bits system). Overcoming these issues with the tactile sensors will be the future challenge. Thus, I-Scan tactile sensors currently provide qualitatively good results, but not quantitatively.

Despite of above drawbacks, the use of tactile sensors with such a high spatial resolution provides a new insight into the complex phenomenon of the wave impact processes which has never seen before by the coastal community. The experiments conducted in GWK provide



better insight into the application of the I-scan pressure sensor in measuring wave impact pressures on coastal structures. There are certain aspects such as producing a vacuum and making the whole system as waterproof should be further improved in the future. An appropriate analysis method should be developed with Matlab in order to work with Tekscan movies more effectively.

### 6.6.3 Application in ice model testing

To measure local ice pressure on structures and vessels, in particular when non simultaneous ice failure occurs tactile sensors could be an alternative. This sensor type was recently used in two Hydralab IV Transnational Access projects (DIIV and RITAS) at the Hamburg Ship Model Basin (HSVA).

In the Hydralab IV TA project “Deciphering of ice induced vibrations (DIIV)” project tactile sensor was installed now for the first time on a cylindrical structure to study the crushing pressure distribution at different phases of an ice-structure dynamic interaction cycle. The objectives were to find out both the vertical and circumferential pressure distributions, and crushing pressure synchronization. The used sensor sensing area  $416 \times 156 \text{ mm}^2$  is divided into a grid of 52 columns and 44 lines, a total of 2288 individual sensing elements. It covered 216 degrees frontal sector around the 220 mm cylinder, e.g. wider than the active circumferential contact area. The sensor was protected from direct ice abrasion by a 0.5 mm thick aluminium foil, and it was waterproofed by silicon. Figure 6.9 gives an example of recorded line like contact during crushing, colour code in kPa. Note that only a sector about 180 degrees is loaded from the total sensor width of 220 degrees (Määttänen *et al.*, 2012).

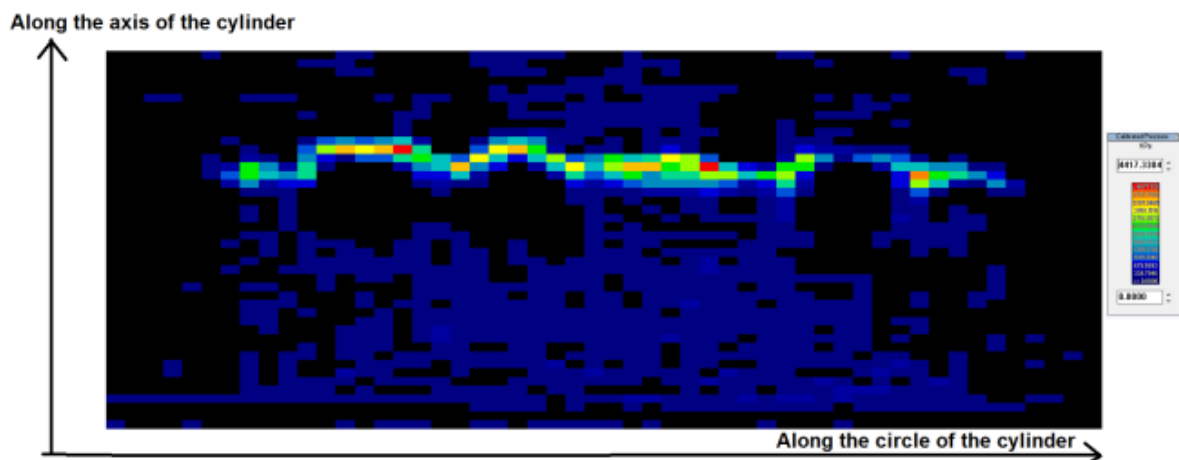


Figure 6.9 Line-like ice contact pressure distribution on the model cylinder

Lessons learned during the DIIV project with respect to the tactile sensors (Metrikin, 2011) are:

#### *Bending the tactile sensor*

Sensors are flat by nature. Yet they are flexible, and so can be wrapped around a curved surface. When the sensor is placed on a curved surface (such as a cylinder), the sensor will read an output, though the output is a result of the curvature acting on the sensor, and not a result of any bad applied (there is no physical load on the sensor). The Tare feature in the Tekscan software can remove this unwanted load and provide a “Net Force” as opposed to the “Gross Force”. When Tare is invoked, it operates on a sensel-by-sensel basis, and removes the force by raising the threshold from which Digital Output (DO) is converted to engineering units.

The sensor's DO range is 0-255. If one sensel reads 20 from unwanted influences, then 20 is subtracted from the range of the sensor, and that sensel's net range will be 0-235 (255-20 235 pressure levels). In this way we removed the unwanted readings from the tactile sensor output.

#### *Temperature variations*

The output of an I-Scan sensor varies with temperature. To account for this thermal coefficient of the sensors, we calibrated the sensor inside the ice tank, i.e. at the temperature at which it was used in the application. However, after the cylinder was placed into the water, we had to wait for ~10 minutes before the thermodynamic equilibrium between the cylinder and the water could be reached. After this we made another Tare operation in order to remove the thermal offset in the pressure readings.

#### *Use of tactile sensor during the ice tests*

During the testing it was important to observe the 3 green lights on the tactile sensor handle, which indicated that it had been functioning properly (Figure 6.10 (a)).

#### *Water isolation*

In order to isolate the tactile sensor from water during the test runs, we used several layers of silicone gel sealing. The process of sealing the tactile sensor is presented in Figure 6.10 (b-d).

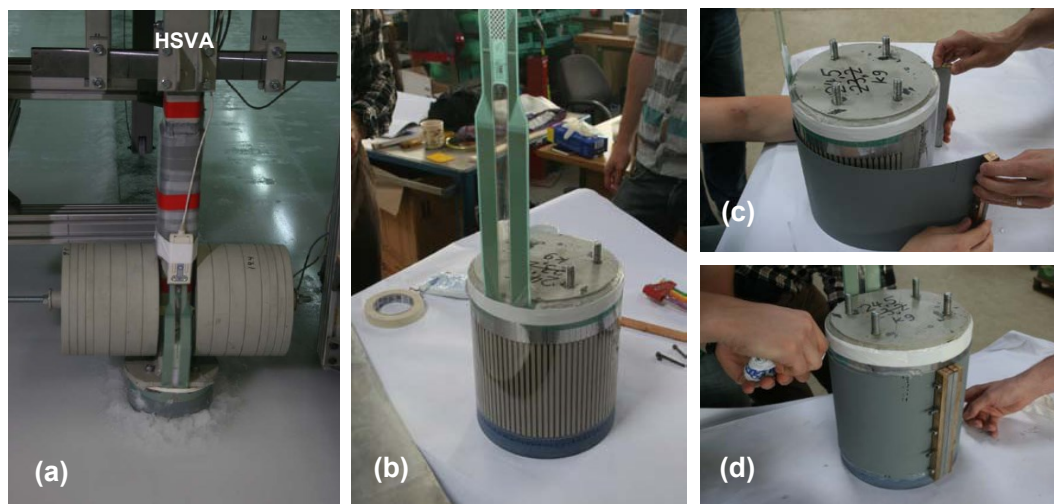


Figure 6.10 (a) Line-like ice contact pressure distribution on the model cylinder, (b-d) process of sealing the tactile sensor (source: HSVA)

#### *Test results*

The results of the DIIV tests have not been thoroughly analyzed yet, so only sample readings from the tactile sensor are presented in this section. Line-like ice contact pressure distribution is presented in Figure 6.9.

The project 'Hydralab-IV TA project "Rubble ice transport on Arctic offshore structures (RITAS)"' was designed to understand the governing principles of rubble transport and structure clearing capabilities. The utilization of tactile sensor together with the buoyancy box enable us to measure how the ice load acts on the structure locally, how much load originates from the already broken ice.

There is one big advantage of the tactile sensor compared to conventional load cells. The tactile sensor is able to measure the variation of local ice pressure on a defined instrumented area, while the load cell usually gives the global ice load.

Lu (2012) reported about experiences made by usage of tactile sensors applied on an inclined plate which are summarized:

#### *Installation of tactile sensors*

When mounting the sensor, two important protections have to be carefully treated. It has been stated in the manual that the sensor can be exposed to wet environment for limited time. For extended period of time, it is recommended to insert the sensor in a barrier material to prevent wet intrusion. In the current study, two plastic films were utilized to cover the sensor (Figure 6.11). The edges of these two plastic films were adhered together with silicone gel.



Figure 6.11 Waterproof protection by plastic films

However, during the experiment, it turned out that these two plastic films were not 100% waterproof. Certain amount of water eventually entered into the plastic film bag and had contact with the sensor. It is not sure if the water has ever entered the electronic units through the tiny vents in the sensor. However, before and after each test, the sensor was re-examined so as to make sure that it is still properly working. In the current practice, the waterproof purpose was not achieved. However, due to the sensor's durability, the sensor works properly in all the experiments. In the future, better plastic (softer, more durable and easier to be adhered) film should be chosen for such purpose.

#### *Protection against abrasion*

To protect the sensor against ice abrasion, and in the meantime, the ice pressure has to be truthfully transferred to the sensor, special protections has to be chosen. In previous experiments, the 0.5 mm aluminium foil has been utilized in (Metrikin, 2011), and a sailing cloth has been utilized in experiments with tactile sensors at Aalto University.

However, the 0.5 mm aluminium foil itself is quite strong. It is expected that the aluminium foil will first take some pressure away before the ice pressure can be transferred to the sensor. This draws a large question mark to the measured ice pressure (i.e. if only part of the ice pressure is measured).

Regarding the sailing cloth, according to experience at Aalto University, this material is very durable and of course, soft enough to transfer all the ice pressure to the sensor. This might be a very good practice.

Kujala (2012) used tactile sensors to analyze the crushing pressure distributions and compared the results to full scale measurements. However, Kujala (2012) does not describe the calibration procedure of the tactile sensors, which is referring to model testing results in the SAFEICE project (Kujala P. *et al.*, 2007). Izumiyama (2007) indicated that the contact conditions during the calibration can have a significant impact on the analysis of the test results. Therefore the contact conditions in the calibration process should be as equal as possible to the test condition. Izumiyama (2007) used an indenter equipped with a load cell and pushed it through model ice. In this case the load on the load cell could be correlated to the signals obtained from the tactile sensor. The achieved correlation is stated as 15%.

In the EU FP7 project called SAFEWIN, tactile sensor sheets are used to determine the pressure distribution due to compressive ice forces on a ship model. The ice model tests are conducted at Aalto University. The tactile sensors are mounted over sections that are equipped with load cells in order to correlate results.

Tactile sensors were calibrated for SAFEWIN tests as instructed in the Tekscan manual. The manual instructs that static calibrations is to be done at the same temperature as the tests itself and the loading time in the calibration should be in line with the actual test length in time, the loaded area should be at least 25% of the total area of the sensor sheet and the calibration pressure should be 80% and 20% of the maximum expected pressure on the sheet. In addition, it is recommended that similar materials are used in the actual tests would be used in the calibration. These requirements were followed in the calibration.

As the materials used in the calibrations should be the same as in the actual test, a plate of divynycell (the material used in the ship model hull at Aalto University) was prepared and painted with the same procedure as the ship models used at Aalto University. However, using model ice in the calibration tests is not possible due to its consistency. Therefore an unpainted divynycell plate was used in the calibrations. First, the sensor sheet was placed on top of the painted plate. Secondly, the unpainted plate was placed on top of the sheet and the dead weights were placed on top of this plate (see Figure 6.12).

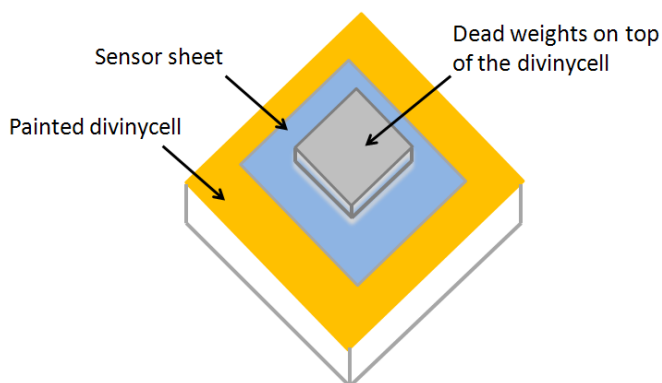


Figure 6.12 Schematic presentation of the calibration set up at Aalto University

As mentioned above, pressures acting on the ship model hull are measured simultaneously at the same locations with the load cells and the tactile sensor sheets. The correlation of the load cell loads and sensor sheets is studied by comparing the measured one (1.0 s) and half (0.5 s)

second average loads and maximum loads. Table 6.1 summarizes the results of the correlation and it can be seen that the correlation is rather good at midship area and fairly good at bow shoulder area.

The minimum correlations at the midship occurred in open channel test. The reason for this low quality correlation could be that there is only small ice contact at midship during the tests, which was measured by the tactile sheet when it was in direct contact with the ice. The difference in correlation between bow shoulder and midship area most probably results from the different curvatures of the frames at these areas. The midship area is perpendicular with respect to the ice sheet, but the bow shoulder area curves at the location of the load cell and sensor sheet.

Table 6.1 Correlation between load cell and tactile sensor sheet

		Bow shoulder				Midship			
		Average load		Maximum load		Average load		Maximum load	
		1 s	0.5 s	1 s	0.5s	1 s	0.5 s	1 s	0.5s
Correlation coefficient	Average	0,73	0,67	0,75	0,70	0,87	0,85	0,89	0,88
	St.dev.	0,08	0,08	0,08	0,08	0,09	0,09	0,06	0,05
	Min	0,50	0,49	0,54	0,51	0,51	0,52	0,74	0,73
	Max	0,85	0,80	0,85	0,83	0,97	0,95	0,97	0,96

#### Test setup 1

During testing the tactile sensors must be protected to avoid damaging. In Määttänen (2011) it is described that the sensors are protected with a 0.5mm thick steel sheet. The stiffness of the protective sheet is 4 orders of magnitude lower than the stiffness of the impacted structure where the reaction pressure is measured. The concern here was that the protective material is spreading the applied load.

#### Test setup 2

In measurements for the EU projects SAFEWIN and HYDRALAB IV the used protective material is adhesive sail repair material, which is commonly used to fix the sails of sailboats. The material is very flexible and strong. Compared to setup 1 it is assumed the sail patches spread the applied load negligibly if they spread the load at all. It must be taken into account that in setup 1 the tested ice has not been classical model ice that is used to scale structure / ship ice interaction, but ice which has strength properties closer to natural ice.

For setup 1 the sail patches might not be able to withstand the loads. The protection with adhesive sail-repair might lead to air voids between the protective material and the sensor sheet, which can affect the results. During the pressure measurements with strong granular model ice the forces have been up to several kN and the sharp corners of the ice specimens have damaged the tactile foil. However, it was observed that the correlation between load cell and tactile sensor improves, which might be related to trapped air in the foil prior to the damage.

## 6.7 Active transducers for nonlinear loads

### 6.7.1 Traditional representation of non-linear loads

Physical modelling studies are regularly undertaken in order to understand the complex interactions between waves and floating structures. Advances in wave generation, motion capture and the computing power available to physical modellers have allowed increasingly



more detailed realistic models to be set up and studied. A field of floating structure physical modelling which has seen little change in decades is the representation of model elements with nonlinear responses to applied loads. For such elements it is common practice to include an item of known stiffness e.g. a coil spring or length of metal. Individually these will give a linear response to the applied load which can be representative of the system to a critical point- such as the buckle load of a fender. However through the introduction of stops for example limiting the extension of the first element in a series, the modeller can combine linear responses to better replicate the real non-linear system.

This approach gives a fair approximation of relatively simple full scale load responses but becomes increasingly complex to implement and time consuming to setup and tune in cases where the load response is highly non-linear. Good examples of this are the buckling and recovery of a fender at high loads or the rapid irreversible extension of mooring lines prior to breaking. Figure 6.12Figure 6.13 highlights how even using a two stage coil spring arrangement there are still instances in which the physical model will give a poor representation of what would happen at full scale, as this technique can only model increasing stiffness curves. Where this is not the case the analysis of a physical models moves towards judgments of likely outcomes rather than the desired measurable metrics of a structure's response.

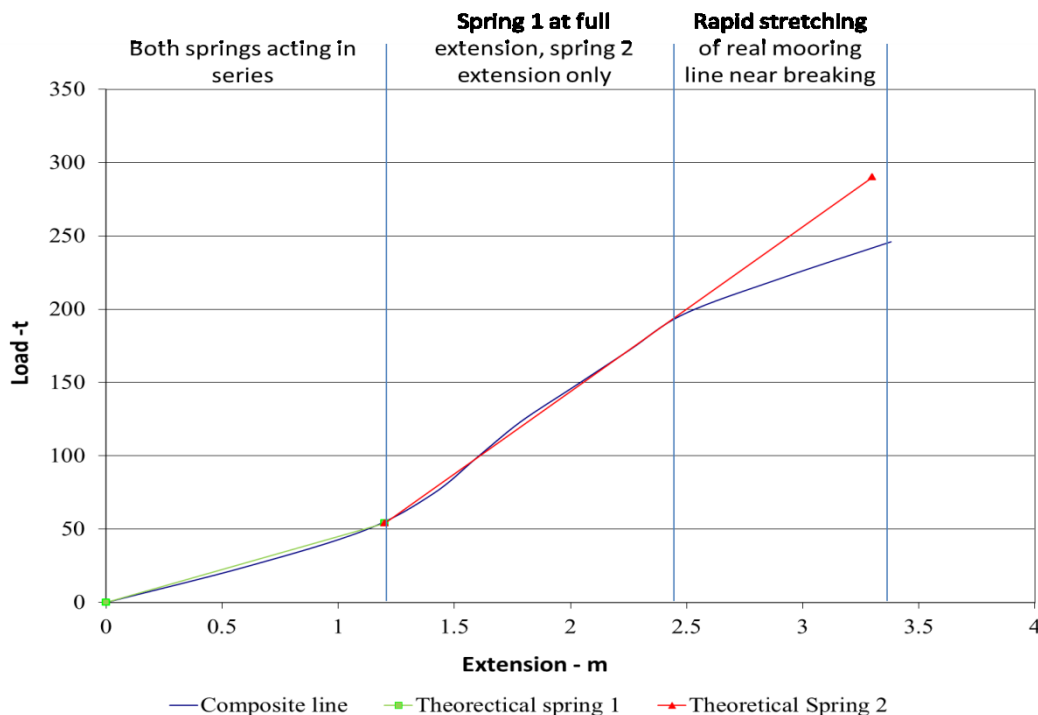


Figure 6.13 Traditional two-stage coil spring representation of mooring lines in physical model

### 6.7.2 Application of servo-motor

HR Wallingford is currently developing an active transducer in the form of a servomotor which will be capable of reproducing any elasticity curve on a physical model. With changes in the hardware attached to the servomotor this system should be capable of modelling any part of a model for which precise deflection or extension under load is important. The technique is illustrated using mooring lines.

The control capabilities of modern servomotors connected to programmable logic controllers allows for the accurate monitoring and control of both the torque being developed by the servomotor and the position of the servomotors shaft. Assuming a linear relationship between the requested and delivered load, it is possible to adjust the torque of the servomotor dependent upon the shaft's position which essentially allows the replication of any elasticity characteristic likely to be required on a physical model. Figure 6.14 shows this, with the example of a mooring line being modelled on a servomotor. In this example the increase in torque would be calculated via a look-up table representing the stiffness curve of the mooring line.

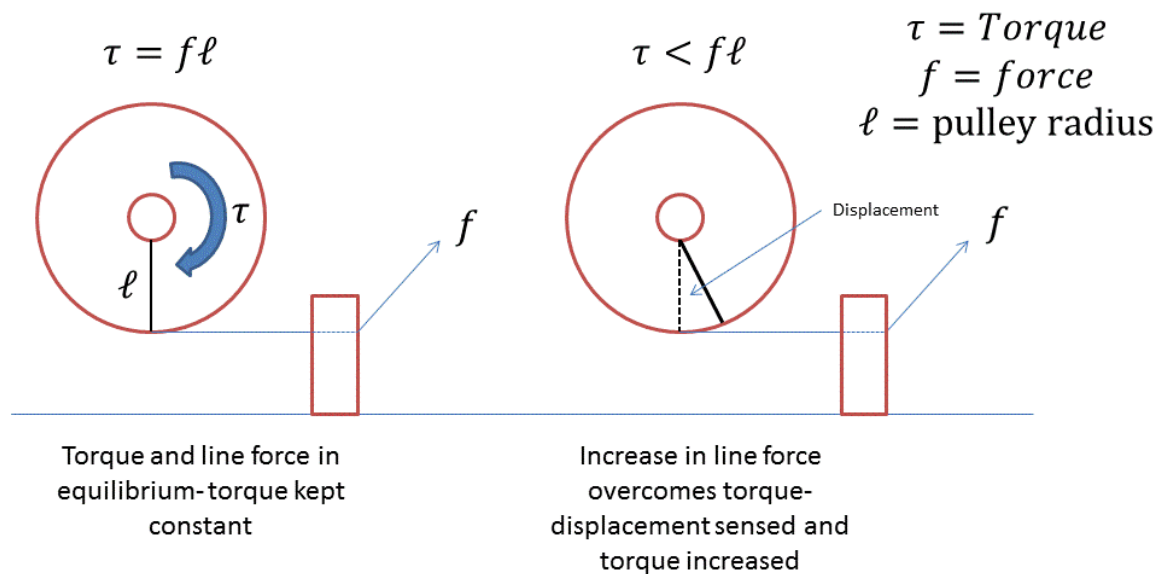


Figure 6.14 the response of servomotor to changes in line load when modeling a mooring line

Figure 6.15 shows a schematic illustration of the control and monitoring processes which would be required in order to model a mooring line using this system. Using this logic the system operates with no direct measurement of the load in the line, rather it is calculated through knowledge of the relationship between the current applied to the servomotor and the torque developed. If implementing such a system two key sources of error must be addressed:

- The accuracy and reliability of the relationship between the applied current and the developed torque.
- The amount that the load changes between measuring the stator's position and applying the current.

The first point can primarily be seen as a hardware issue, with hysteresis and torque ripple from the servomotor leading to increased error. Point two is a control logic issue with the cycle time of the closed loop control logic leading to increased error.

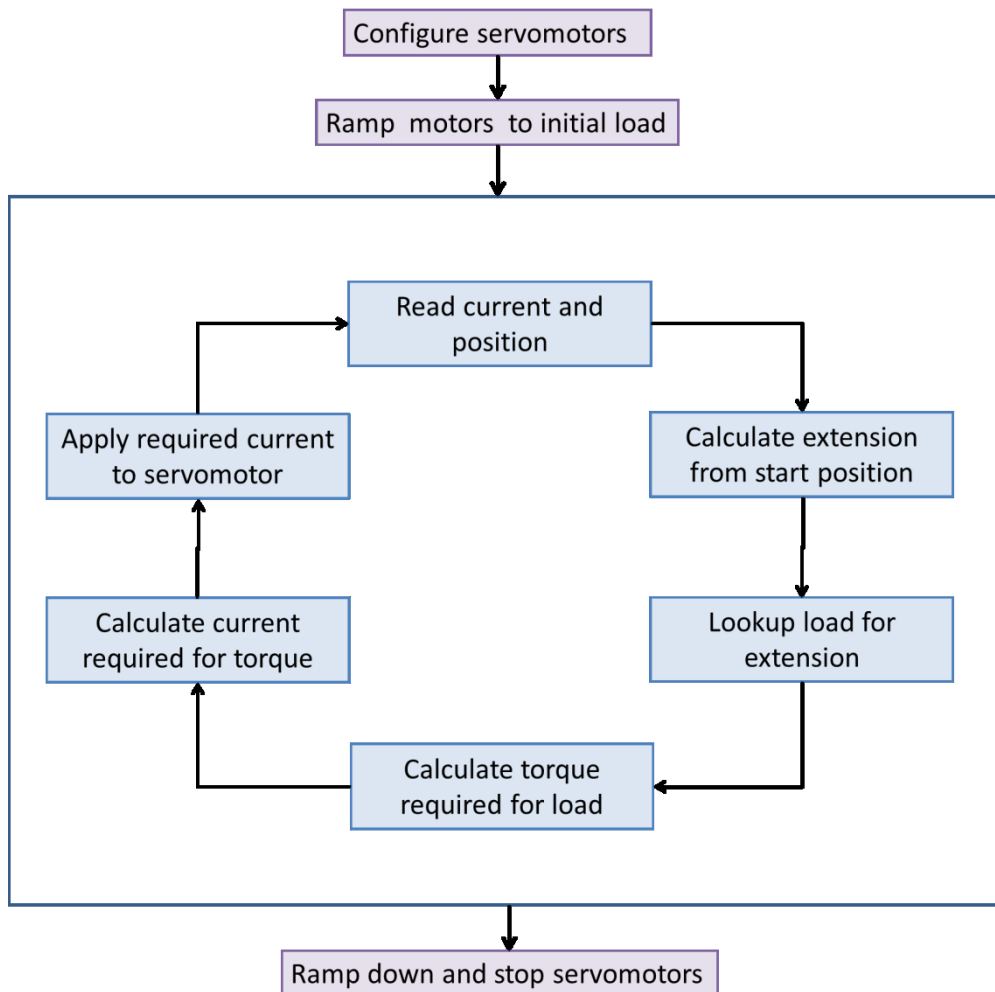


Figure 6.15 Control logic for servomotor only system

The addition of a force transducer in the system, which directly measures the line load, mitigates against errors inherent in converting from current to load through giving a measured benchmark against which the torque can be adjusted. It is common in such control systems to use a Proportional Integral Differential (PID) control loop which, using a target “setpoint” load, will iteratively adjust the current to the motor to correct for any line load error. Real time measurement of line loads gives the added advantage that statistics on the performance of the system will be available for every test in which it is used, allowing users to be quickly alerted if there is a system failure. Figure 4 shows a modified control logic loop which includes both the measurement of the line loads and the error correction using the PID control calculations.

Despite the advantages gained through the inclusion of a force transducer the system will still give poor results if the cycle time of the control loop is not sufficiently fast to prevent significant changes in the loads acting upon the line in the time between load measurement and torque correction. Modern high performance embedded PC's are capable of running control logic for multiple servomotors with a cycle frequency measured in kHz. As such these units provide an ideal platform from which to control a system such as this and should be capable of responding to very high frequency dynamic loads such as might be expected with wave slam on a structure. These systems have the added bonus of providing a degree of automation in the control of servomotors, for example setting the required current to deliver a demand torque. This automation makes the programming of the control logic less onerous and provides standardised performance across many servomotor units.

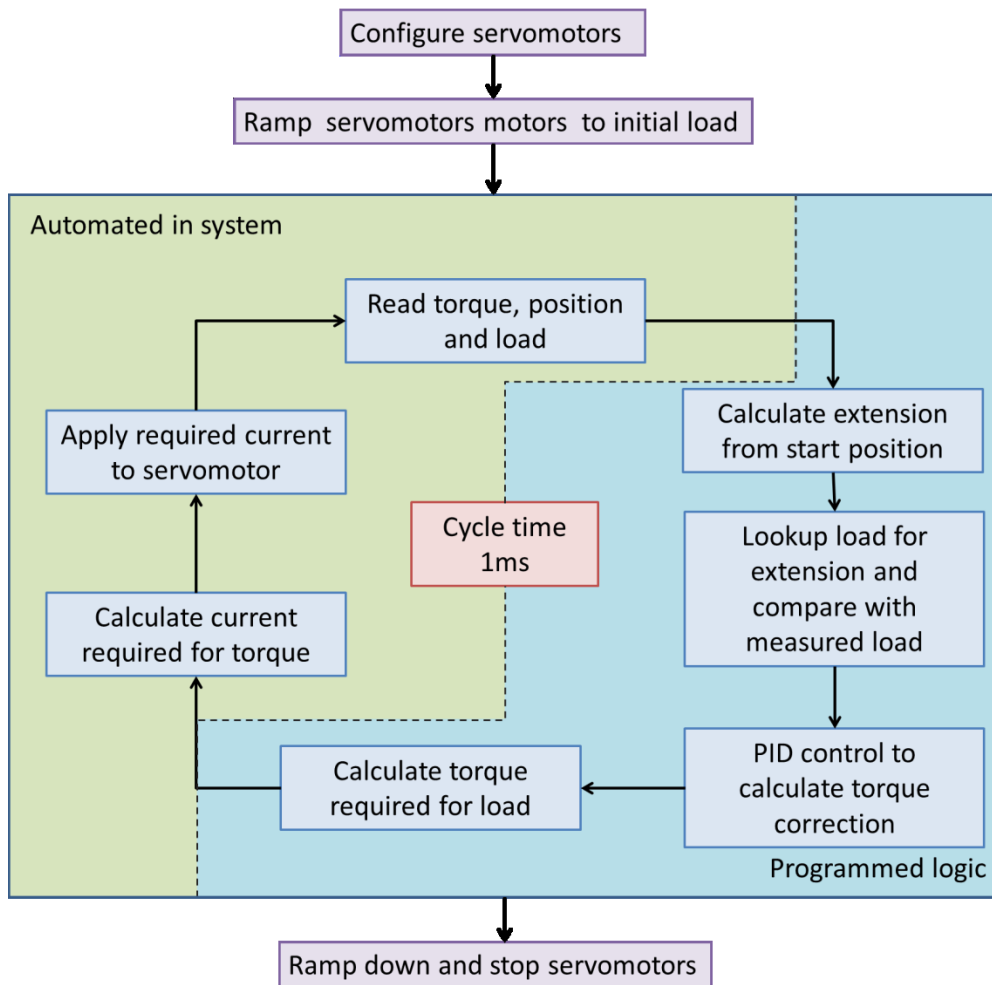


Figure 6.16 Control logic for servomotor and force transducer system

### 6.7.3 Non-passive effects

The application of active transducers in physical models holds many potential benefits and should be another step in the production of more realistic and reliable models. There is a potential that in the application of an active transducer to model a passive system, unwanted non-passive effects such as load oscillations or high dynamic loading might be introduced. Since it is important that any instrumentation system used on a physical model has well defined limitations, the next stage of testing is aimed at better understanding any non-passive effects and defining the conditions in which they are likely to occur.

## 6.8 Wave measurements (area)

Physical models usually give superior description of non-linear wave processes, but this information cannot presently be obtained from the basins and flumes at the same spatial resolution as numerical models.

However, in the last decades a number of techniques have been developed whereby a surfaces can be measured fast and accurately. Stereo photography using digital CCD cameras can give a digital representation of a surface area after some post-processing. Laser scanners are used to scan 3D topographic data with more than 100'000 points per second. Range cameras (for instance used in the XBox game computer) can directly measure distances at about 10'000

points using a CCD chip that measures the phase of reflected infrared light. All these techniques have been developed recently, mainly for measuring solid objects or surfaces.

A number of papers have derived with which waves are measured using these techniques. However, making these techniques ready for the hydraulic laboratory (robust) will require some work. The data processing must become fast and reliable (comparable to the development of numerical techniques), and the water surface must be visualized in an easy, not-too-intrusive, way. If these obstacles are overcome, it seems well possible to measure the water surface at relatively short notice. The next question will be to determine what to do with all the extra information that is obtained. First of all, the classical wave parameters are obtained at high resolution. This is a step forward, for example when regarding the wave agitation in a harbour, or the wave attack at a long breakwater trunk. But also new parameters might be thought of which describe processes in a completely different manner.

The following photogrammetric techniques have been validated for in fields measurements but need to be adapted to indoor conditions. One of the potential problem is the water surface identification which is different in a tank than on the open sea. The tank bottom is visible through the surface and may induce errors in the calculation.

- Photogrammetry was used to assess three dimensional waves surfaces (Santel *et al.*, 2006).
- Three dimensional surface wave measurements were performed with trinocular stereo imaging system (Wanek and Wu, 2006).

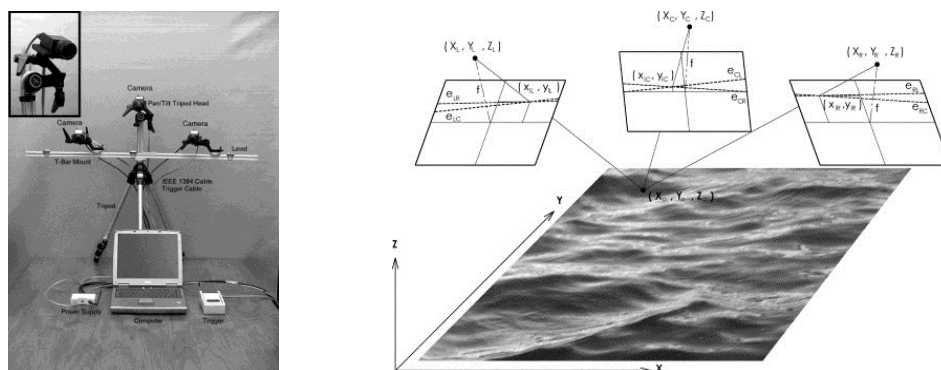


Figure 6.17 The automated trinocular stereo imaging system (ATSIS) and the schematic of a trinocular stereo-imaging mode

The following work uses PIV technique, and have the same problem of identification of the water surface. It has been resolved by seeding the surface but this is not always feasible.

- Particle image velocimetry techniques have been used to obtain a three dimensions water elevation field (Stagonas and Müller, 2007).

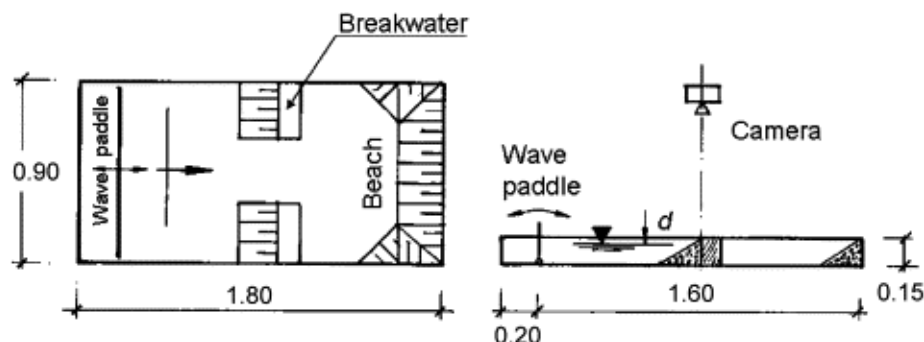


Figure 6.18 Particle image velocimetry used to obtain wave elevation field



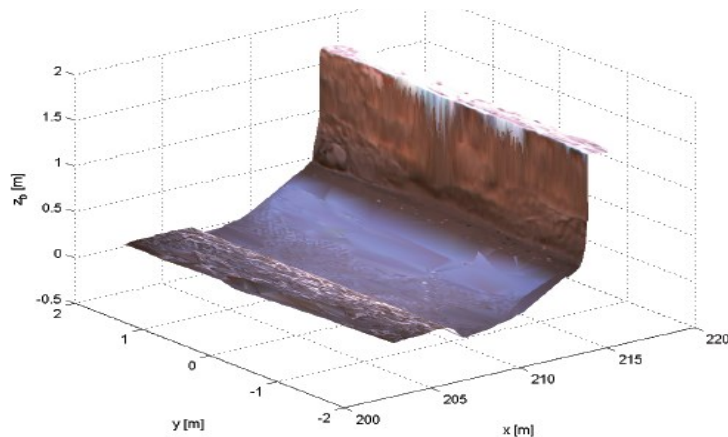


Figure 6.19 Wave surface near dune face measured by stereo photography (Van Thiel de Vries, 2009)

Terrestrial laser scanners (TLS) have been used for wave measurement in the field and in the laboratory a number of times recently, with promising results (e.g. Blenkinsopp et al, 2010; Allis et al 2011). In the envisaged set-up a laser beam is scanning the water surface over a line parallel to the flume axis, see Figure 6.20. The distance to the water surface is measured by determining the travel time of the reflected light to a receiver. The laser beam is moved by a rotating mirror. Hereby a wave measurement over a line along the flume axis is obtained with high spatial and temporal resolution. As the water itself cannot be measured, the water (surface) needs to be turbid to create diffuse reflection. The typical frequency of many laser scanners is in the order of 50 Hz. The accuracy of the scanners is less than for the classical point measurements, but the large spatial resolution could make this acceptable.

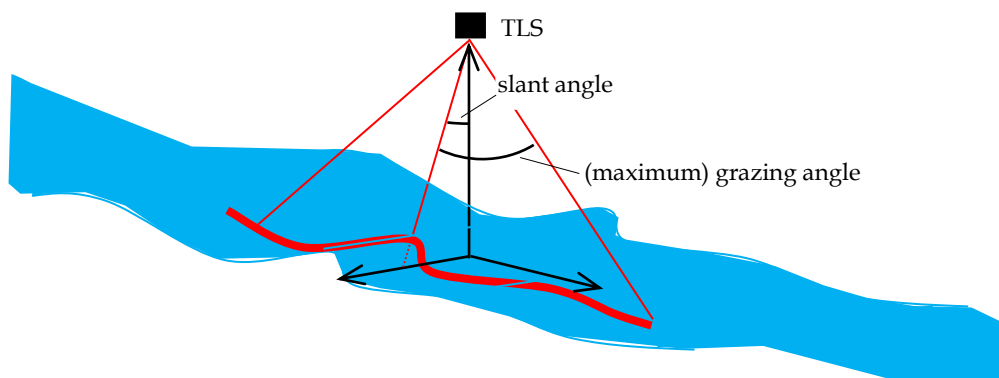


Figure 6.20 Terrestrial laser scanner wave measurement set-up

Allis et al (2011) use TLS to measure waves in a laboratory flume. The results of Allis could be reproduced in a small scale flume (Hofland, 2012). However, many unresolved questions remain to be tackled. These include the surface ambiguity (the measurement is made somewhat below the water surface), the required filtering operation, the exact setup, the amount of seeding, etc.

## 6.9 Extension of acoustic and optical measurements to 3D

Kinematic measurements:

- Extension of PIV to 3D volume - extension of multiple scans

- ADV – extension of dimension

## 6.10 Data access

There are two main stages to ensuring that data can be re-used:

- Ensuring that the data can be found and identified as useful and trustworthy by scientists and engineers who were not involved in collecting the data.
- Transferring data. File-based data transfer is sometimes inefficient but offers a well utilised and simple structure for sharing data from a variety of sources targeted at applications for accessing, reading, writing and analysing.

Within HYDRALAB ([www.hydralab-eu](http://www.hydralab-eu)) methods are being developed to share the meta-data collected on Transnational Access projects over the world wide web. In Transnational Access projects teams of scientists and engineers from a variety of countries travel to one of the unique facilities at a HYDRALAB partner and participate in a set of experiments devised by the team. The data is shared by the team and a copy is held by the host institution. The data collected becomes public two years after the experiment has taken place. HYDRALAB is using standards developed for the semantic web to make meta-data from these projects findable over the world wide web. This meta-data is designed to inform interested participants about:

- Which team undertook the experiments;
- Which facility and institution the experiments were undertaken in;
- Details of the facility, structures and instrumentation used;
- Positions of instruments;
- Hydrodynamic conditions generated for each model run.

This information should be easy to find using a search engine and should be sufficiently detailed to enable scientists and engineers to work out if the tests will be useful for their needs and to assure them that the data was collected with care and proper attention to detail.

A second development within the same HYDRALAB joint research activity is to allow participants in selected Transnational Access experiments to view the tests in real time from their own institutions. This may prove a useful basis for longer-term developments in data sharing both in real-time and for subsequent access to data (in addition to meta-data) over the web.

## 7 Longer time-scale changes in capabilities

The short-term developments in Section 6 are generally based on research projects and interests that are currently under way – many of them within [HYDRALAB-IV](#). They indicate a trend towards specialisation in more complex, nonlinear phenomena, resolved at smaller scales. In this section, we propose changes that are likely to occur over a longer timeframe. These technological developments will require innovation to bring us to a higher level of knowledge, which will allow physical modelling of wave and ice interactions with coastal and marine structures to remain a central part of the design and verification of these structures for many years to come. These advances will keep European laboratories at the forefront of technical advances, allowing them to offer new and improved services to academics and various relevant commercial sectors.

### 7.1 Development of composite models

Composite modelling involves the combined use of more than one modelling tool (commonly a physical model and a numerical model) to address a complex problem (Gerritsen et al. 2011, Gerritsen and Sutherland 2011, Sutherland et al. 2012). One type of composite model is a hybrid model - where a physical model and a numerical model are run simultaneously and pass information between themselves in real time. True hybrid models (with two-way exchange of information) are rare and most test set-ups allow the sequential running of models and the one-way flow of information. The reasons for this include the difficulties in (i) running a numerical model in real time, synchronously with the physical model, (ii) passing information from the physical model to the numerical model and (iii) getting the physical model to respond to the input from the numerical model. These difficulties are gradually being overcome, opening the realistic possibility that within a few years the full two-way coupling of numerical and physical models in real time will be achieved.

The starting point may be to use active transducers (Section 6.7) in a physical model, where the non-linear characteristics of the mooring line (for example) may be determined in advance. To advance from there, new technologies must be employed. For example, the reproduction of part of a mooring line may require an active transducer that varies its position, as well as its force/extension characteristics. That may require the use of a numerical model to calculate far field effects outside the physical model, with an active mooring line mounted on actuators at the interface between the physical and numerical models. Another potential development would be of a hexapode (6 dof motion mechanism) to enable the study of multi-parametric loads in relation to motions, eg full added mass or damping matrix. Two plates and 6 actuators could be used to simulate the motion of a sea state.

### 7.2 Learning from CFD

The development of Computational Fluid Dynamics (CFD) model code has put us in a position where CFD wave flumes and wave basins are being developed. This will draw the physical and CFD modelling communities together as both communities will be addressing similar problems, such as nonlinear wave generation and the absorption of reflected wave energy at the wave maker. The physical modelling community must be prepared to monitor developments in CFD and look for ways to implement the most promising approaches.

### 7.3 Sensor developments

Sensors will reduce in size, increase in resolution and increase in sampling rates. This will, for example, make tactile sensors (see Section 6.6) more useful as a means of detecting pressure

distributions as their present sampling rates and resolutions are much lower than those of a conventional pressure gauge and so may miss the short-duration peak of a wave impact event.

The use of non-intrusive optical and acoustic methods will become more common and will cover larger areas. For example we may expect to see the use of optical techniques to measure surface elevations over a high-density spatial array of points at sampling rates of tens of Hertz. New materials, such as ferrofluids and other coatings, will be developed to measure shear stress, so that maps of shear stress distributions that vary in time over a surface will be produced.

## 7.4 Facility developments

The development of physical modelling facilities has benefited tremendously from the increases in computer speeds, which has allowed more devices, such as wave paddles, to be controlled at higher speeds than before. The recent development of Ethernet technology (which can communicate over 1,000 channels at 1,000 Hz) has meant that communication speeds around the laboratory are substantially higher than could be achieved using RS232 or other cables.

Advances in wave generation and data collection are likely to continue in incremental steps. The mechanical designs of common wavemaker types (piston and flaps) are likely to remain substantially the same as they are today, with the development of new generation techniques for tsunamis (Sections 3.1.1 and 6.4) adding diversity to the portfolio of options. Wave generation software will improve, including developments for focussed waves (Section 6.5).

Both wind generation and current generation methods are relatively simplistic, with little control over changes in the spatial distribution or time-variation of wind or currents in many facilities. Developments in electronic control systems mean that it is now relatively easy to generate a time-varying control signal to a pump or fan. The cost of control systems has also dropped significantly. The development of spatial variations in wind or current fields may therefore come from the installation of many, smaller capacity pumps or fans, rather than through the manipulation of the output from a single unit. This may allow the natural gustiness in the wind hitting a floating structure to be reproduced, as well as a more realistic horizontal and vertical profiles. It would also allow the control of current in large scale coastal wave basins to be refined. Two areas where we may see developments that differ from the accepted norm are in the development of hybrid facilities (that allow laboratory control and reproducibility in a field setting) and improved links to geotechnical models, as discussed below.

### 7.4.1 Hybrid facilities: process simulators

Whether or not the strength of a coastal structure can be modelled at small scale depends on the structure considered. Materials like grass on clay cannot be modelled easily on a smaller scale. Thus one can only perform tests of the materials on real dikes, or on parts moved to a large (or prototype) scale facility like the Delta Flume (Netherlands) or the GWK (Germany). Recently, simulators of a single process, such as wave overtopping, have been constructed in order to undertake controlled tests in the field (Steendam et al, 2013), as shown in Figure 7.1 **Error! Reference source not found.** Different types of simulator are needed for different processes. In order to simulate a wave processes at a real dike, a good description of the process that should be simulated is needed. Description of the wave structure interaction process is, however, much more difficult than just the determination of a design value for a flume test (see sampling schemes). Recently experience was gained with simulating overtopping in countries like The Netherlands, USA, Belgium, and Vietnam. A similar approach has also been developed to simulate wave run-up on the front face of an embankment (van der

Meer et al, 2012). Both wave run-up and overtopping simulators could be used to generate forces on a structure.

For complicated processes, like wave impacts, the description of the process is not complete. Therefore, the results of tests with a wave impact generator will not have an absolute value. However, they can be used to compare different structures to each other. In a later phase, results obtained with a wave impact generator can then be compared with results obtained with large-scale physical model tests, which enables a translation of the results obtained with the wave impact generator to reality. It should be noted, however, that such a translation becomes more difficult if the impact testing is further from reality. Thus, the primary goal of the tests with a wave impact generator is to be able to compare the erosion rate at various locations with different clay and grass quality and the influence of several types of non-water-retaining (i.e. hard) structures and transitional structures. This can be used for further analysis in later phases.



Figure 7.1 Pictures of process simulators. Top left: wave impact generator with erosion generated (top right). Bottom left: wave impact generator at sand dike with erosion generated (bottom right)

#### 7.4.2 Link to geotechnics: modelling clay

Also attempts are made to model clay at small scale. With special mixtures of clay, sand and water the strength of clay can be adjusted, such that erosion will occur at small scale. First attempts were made to create the same erosion at small scale as at large scale, see Figure 7.2. The amount of erosion could be mimicked. However, the shape of the erosion was different. No terrace and cliff appeared as is the case with real clay erosion. The crucial aspect here is probably that clay in reality is structured with cracks and in-homogeneities. These aspects



should be modelled as well. This is still a challenge for the future. Detailed geotechnical knowledge is required for this.

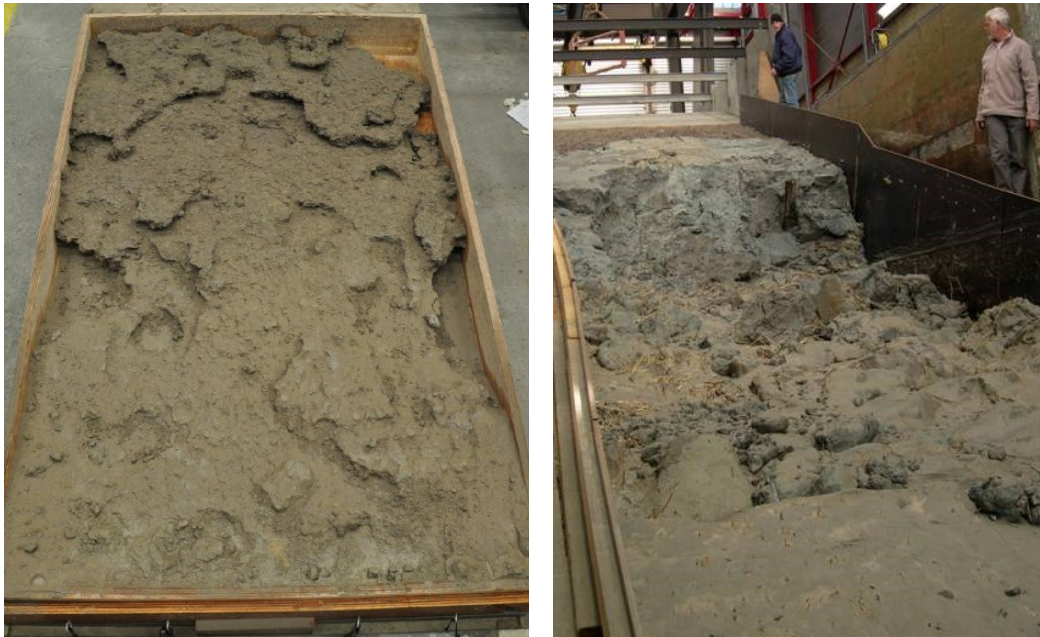


Figure 7.2 Left erosion of weak clay at small scale. Right erosion of (boulder) clay at full scale (courtesy Deltares)

This is one example of combining geotechnical expertise and hydraulic expertise. Many other combinations of geotechnical and hydraulic modelling could be considered. One such a challenge is to create wave loading in a geo-centrifuge in order to simulate dynamic loading on coastal structures and related processes like liquefaction.

## 7.5 The active laboratory

The development of active transducers for mooring lines has been described in Section 6.7, while the active absorption of reflected waves (Schaffer and Klopman, 2000) is included in many modern wavemaker systems. Other potential applications of the same technology to the modelling of floating structures include:

- Breakaway tests. The snapping of a mooring line can be represented by letting a servo-motor unwind after a threshold is crossed.
- Render recover and constant tension winches
- Fenders (see Section 4.1.2.3 for details of types of fender)
- Static and dynamic wind and current loading. In situations where it is difficult to include wind or current loading on a vessel, this could be applied using an active transducer.

Modern high performance embedded PC's are capable of running control logic for multiple servomotors with a cycle frequency measured in kHz, so several devices can be operated simultaneously alongside traditional wave gauges and other instruments. In the future we are likely to see laboratory set-ups featuring many more active systems (each with its own control loop)

## 7.6 Treatment of uncertainty

The increases in the volumes of data being collected and an improved awareness of risk (and hence uncertainty) are likely to lead to improvements in methods to define the uncertainty in measurements. Techniques will be developed to put uncertainty limits on measurements and to use measurements with uncertainty. It is common practice to compare predictions to measurements by assuming that the measurement is error-free. We will move towards analysis procedures that take into account the error in measurements.

Increases in spatial and temporal resolution, plus the increasing ability to measure over profiles or within volumes will lead to an increased capacity to measure the properties of turbulent flow fields. This is likely to lead to a better understanding of the role of turbulence and we will start to address more thoroughly questions such as:

- when is turbulence important?
- how do we characterise it?
- what is its role in creating uncertainty?

## 7.7 Open Science

An era of more open science is emerging, comprising:

- open source software;
- open software architecture;
- open data;
- open access publication; and
- open collaboration (or networked science).

There has been a rise in the use of open source numerical model codes, which has been boosted by the recent switch of existing closed source codes into open source codes by major players in the hydraulic modelling community such as TELEMAC (<http://www.opentelemac.org>) and elements of Delft3D (<http://www.deltaresystems.com>). The benefits of open source software have also been discussed by Harvey and Han (2002) Khatibi *et al.* (2004) and others. We have also seen the development of more open software architecture, which can incorporate component models from different code bases (often from different organisations) using an interface standard such as OpenMI (<http://www.openmi.org/>) or an integrated environmental modelling framework (Laniak *et al.*, 2012, Sutherland *et al.*, 2013). The concept of integrated environmental modelling benefits from open architecture and is commonly associated with open source software (Khatibi *et al.*, 2004).

Meanwhile the importance of open access to public sector research has been recognised by the OECD (2004) the EC (2011) and the UK (HM Government 2012). The European Commission has launched an Open Data Strategy for Europe, which is expected to deliver a €40 billion boost to the EU's economy each year (EC 2011) and there is a commitment to increasing access to data and publications within the EC's Horizon2020 research programme. Open Access to research publications is becoming increasingly common and open access journals are proliferating. Technologies for allowing open access to data from experiments are also being developed (Section 6.10).

Moreover, we are in an era of increasingly open scientific collaboration. Nielsen (2011) presents a number of case studies of networked-science, from citizen science to mathematical problem solving, that have occurred by open collaboration over the web, and advocates this as

the future of science. Academics are using social networking sites to support their research by sharing papers and information, participating in discussions and collaborating with their colleagues. Analysis of Twitter feeds and citations from an on-line medical journal showed that 'top-cited' articles can be predicted from top-tweeted articles with 93% specificity and 75% sensitivity' (Eysenbach, 2011).

The move towards open science, comprising open architecture, open source, open data, open access publication and open collaboration (or networked science) is on-going but faces many difficulties. Nielsen (2011) predicts that it will only take place when we learn to value openness and the sharing of models and data as much as our publication and citation records. This will be assisted by the development of methods to assign a Digital Object Identifier, or DOI to datasets. DataCite (<http://datacite.org/>) for example, allocates DOIs that take you to a public web page with meta-data about the associated dataset and a direct link to the data itself. This allows a dataset to receive a citation in a paper or report. The allocation of DOIs to quality physical model datasets will support researchers by helping them to find, identify and cite these datasets with confidence. The inclusion of citations to data in the metrics produced by organisation such as the Web of Science, which are used to compare the performance of academics (in particular) would assist in changing the culture of science to recognise the importance of data and encourage its sharing.

It therefore seems highly likely that DOIs will start to be allocated to hydraulic datasets that are collected as part of research projects and that making data publically accessible will become a more common requirement of research organisations (such as the European Commission). This will lead to the development of shared datasets, which will help to create a free market in data, which every member of the community has equal access to. This is more manageable within an organisation than between organisations, but the concept is similar to a distributed database, where the data owner maintains the data, with the ability for this data to be integrated with other data held in the distributed system. This will require protocols and standards to be developed, published, accepted and used.

Harvesting data from external knowledge bases is a much bigger challenge, partly due to the technical problem of searching for information over the web, but also due to the need to establish ownership, licence conditions and the quality of data. There will therefore be benefits to enhancing the richness of information about shared data. This extra information will enable any interested party to judge the suitability and quality of the data. In order to do this we need to develop (and ideally consolidate) metadata standards and ontologies. A primary requirement will be to extend from an established standard set to reduce the likelihood of independent bespoke implementations of the same standard being developed. Scientists and engineers will have to get used to the routine generation and use of metadata. Tools which map between different standard ontologies are beginning to arrive in the market place and will become increasingly useful.

There is likely to be a move towards the standardisation of data, which is tending to occur at two levels: the structure of the data and its technical implementation. Definitions of data structure are independent of the file encoding. For example, ISO19115 outlines the data structure of spatial metadata with its XML encoding given in ISO19139. The supporting (use and discovery) metadata can be given in separate files to the values themselves. This is exhibited in formats such as CSML and XDMF, both of which offer a binary file type (such as HDF5) for high volumes. Also, directives such as INSPIRE provide a legal and technical framework for data interoperability. It includes specifications for the data, discovery, use and download services and is aimed at making the finding, using and sharing of data easier across the EU. However, for any practitioner wishing to offer a dataset to the wider community, the set of standards on offer is incomplete, overlapping and highly esoteric.

There is a role here for impartial, international organisations, such as International Association of Hydro-Environment Research and Development (IAHR) to provide repositories of (or links to) datasets that can become the de-facto standard for benchmarking tests.

## 8 Discussion and conclusions

Physical modelling has been the foundation of hydraulic and hydrodynamic studies for the past century and a half, particularly when it comes to the analysis of forces on structures and their interactions with waves, currents or ice. The complex, nonlinear phenomena involved in these interactions have been reproduced in the laboratory by increasingly sophisticated techniques for the reproduction of environmental conditions. The techniques used to measure the hydraulic, hydrodynamic and ice conditions and the resulting forces on structures have also improved immensely during this time. This has always meant that the most detailed studies of wave, flow and ice interactions with structures have been carried out in the laboratory, where conditions are controlled and experiments can be repeated. Field measurements, although more expensive and less controlled, have also played an important part in establishing knowledge about these interactions.

Improvements in numerical models, particularly computational fluid dynamics (CFD) codes, mean that these can now be used to determine forces on structures in relatively simple flow cases. CFD codes are being used at research organisations to model more and more complex structures and flow cases, such as waves breaking over structures. As the number of cases modelled increases, and more knowledge is gained in how to apply these models, they will be able to undertake more and more studies that previously could only be undertaken by a physical model. This does not, however, signal the end of physical modelling. Rather, it is likely to signal the start of a new era where numerical and physical modelling are used in collaboration to address complex problems. There is a range of ways in which physical and numerical models can be combined (Sutherland and Barfus, 2011) including:

- Traditional nesting where a physical model is a detailed representation of a system, which is modelled at a larger scale (and at a more general level) in a numerical model;
- Numerical modelling can assist in the design of physical models by helping to set the location and type of boundary conditions that are to be applied;
- Numerical pre-modelling also provides information about potential problems associated with the theoretical design or proposed design changes to the structure, thereby reducing the number of physical modelling configurations necessary during the physical modelling portion of the study. This pre-modelling effort saves time and money once the physical modelling has commenced.
- Modelling the model can allow a numerical model to be calibrated or corrected using the physical model results. The calibrated or corrected numerical model is then available to undertake additional model runs that would be too time consuming in a physical model or were only considered after the physical model has been decommissioned.

Clever combinations of physical and numerical modelling will be used in the design and testing of complex structures subject to extreme conditions for many years to come.

Laboratories have developed active feedback systems for absorbing re-reflected waves at wave paddles over the last twenty years (Schaffer and Klopman, 2000). The concept of the active transducer has now been extended to the reproduction of non-linear mooring lines. The same concepts and control systems could be applied to other phenomena, such as the snapping of a mooring line, constant tension winches, fenders or static and dynamic wind and current loading. Therefore we are likely to see the development of laboratories with many more active control systems.

The increases in computer power, the development of Ethernet technologies for transferring data and the shrinking of electronics mean that physical models have been able to make more and more detailed measurements at finer resolution and higher frequencies. This has allowed more detailed investigations of increasingly complex phenomena to be undertaken. This trend



will continue and new measuring techniques will be developed, allowing physical measurements at a greater spatial density. We anticipate the use of more remote sensing (optical and acoustic). The improved spatial and temporal resolution of measurements will

- allow more detailed analysis of complex, often turbulent phenomena;
- provide more data to validate numerical models and drive their development;
- allow the design of structures to be refined more than ever before; and
- generate unprecedented volumes of data.

The increased volume of data being generated will provide opportunities for this community and create additional obligations (especially when funding organisations begin to require open access to data as well as publications). Greater value will come from the sharing and re-use of data. This will require organisations to ensure that their data can be understood and read by others and comes with sufficient supporting information to indicate its quality. This is likely to drive moves towards common standards for meta-data and data and increased use of semantic web technologies for data discovery (although there is never likely to be a single standard for data). In an era when more data sets are public, we are likely to see a rise in data driven modelling and may gain benefits from the re-analysis of multiple data sets (as occurs in medicine, for example) which may reveal more information than any single data set. These developments will require this community to engage more with software developers

Physical modelling of the interactions between structures and waves, flows or ice will continue to develop and will remain a core component of studies in this field for decades to come. There will be an increased focus on non-linear phenomena, as numerical modelling takes over more of the modelling of shallow water flows and non-broken waves. There will therefore be an increasing emphasis on smaller spatial and temporal scales and on working with CFD models.

The increasing specialisation in testing equipment and facilities makes it likely that there will be a reduction in the number of facilities with the capability to undertake the most advanced testing. There will therefore be a continued, and potentially increasing, demand for access to these facilities from regions and countries that do not possess such facilities. There is therefore a clear potential role for international funding organisations, such as the European Commission, in coordinating the access to and development of the largest facilities, in order to meet these needs.

## 9 References

- Alderson J.S & Allsop N.W.H (2007) Comparisons of observed pressure integrated and directly measured global force measurements on caisson breakwater models In *Proc. Coastal Structures 2007*, Venice. World Scientific, ISBN-13 978-981-4290-99-0, pp. 249–258.
- Allan, R., Barr, A., Seamen, D. and Duggal, A. (2009). Station Keeping Solutions for A Mobile Drilling Unit in Arctic Environments. *Proceedings of the 20<sup>th</sup> International Conference on Port and Ocean Engineering under Arctic Conditions*, June 9-12, 2009, Luleå, Sweden, paper POAC09-82.
- Allis MJ, Peirson WL, Banner ML. Application of LiDAR as a Measurement Tool for Waves. Proceedings of the Twenty-first (2011) *International Offshore and Polar Engineering Conference*. Maui, Hawaii, USA, June 19-24, 2011
- Allsop N.W.H., McKenna J.E., Vicinanza D. & Whittaker T.J.T. (1996) *New design formulae for wave loadings on vertical breakwaters and seawalls*" 25<sup>th</sup> ICCE, September 1996, Orlando, publ. ASCE, New York.
- Allsop NWH, Vicinanza D, & McKenna JE (1996) *Wave forces on vertical and composite breakwaters* Strategic Research Report SR 443, pp 1-94, HR Wallingford, March 1996, Wallingford.
- Allsop N.W.H., Bruce T., Pearson J., Franco L., Burgon J. & Ecob C. (2004) *Safety under wave overtopping – how overtopping processes and hazards are viewed by the public* Proc. 29<sup>th</sup> ICCE, Lisbon, publ. World Scientific, pp 4263-4274, ISBN 981-256-298-2.
- Allsop N.W.H., Franco L., Bellotti G., Bruce T. & Geeraerts (2005) *Hazards to people and property from wave overtopping at coastal structures* Proc. conf. Coastlines, Structures and Breakwaters, 20-22 April 2005, ISBN 0 7277 3455 5, pp 153-165, Thomas Telford, London.
- Allsop W., Robinson D, Charvet I, Rossetto T. & Abernethy R (2008) A unique tsunami generator for physical modelling of violent flows and their impact, *Proc. 14th World Conference on Earthquake Engineering*, October, Beijing.
- Bagnold, R.A. (1939). Interim report on wave-pressure research. *J. Inst. Civil Eng.* 12, 202–226.
- Baldock, T.E. (2006). Long wave generation by the shoaling and breaking of transient wave groups on a beach. *Proc. of the Royal Society A: Mathematical, Physical and Engineering Science*, Vol.462, N°2070, pp.1853-1876, doi:10.1098/rspa.2005.1642.
- Banner, M.L., Gemmrich, J.R. and Farmer, D.M. (2002). Multiscale measurements of ocean wave breaking probability, *J. Phys. Oceanogr.*, 32, 3364 – 3375, doi:10.1175/1520-0485(2002)032<3364:MMOOWB>2.0.CO;2.
- Battjes, J.A. (1974). Computation of set-up, longshore currents, runup, and overtopping due to wind-generated waves. PhD thesis Delft University of Technology
- Battjes, J.A., Bakkenes, H.J., Janssen, T.T., Van Dongeren, A.R. (2004). Shoaling of subharmonic gravity waves. *Journal of Geophysical Research*, Vol.109, N°C02009, 15p, doi:10.1029/2003JC001863.

Benne, K. (2012). Measuring ice-size-distribution during ice-tank testing, TU Delft, Bachelor thesis, 19<sup>th</sup> June 2012.

Benoit, M. (1993). Practical comparative performance survey of methods used for estimating directional wave spectra from heave-pitch-roll data. *Proc.23rd ICCE Vol 1*. ASCE pp.62-75.

Berthelsen, P.A., Baarholm, R., Pakozdi, C., Stansberg, C.T., Hassan, A., Downie, M. and Incecik, A. (2009). Viscous Drift Forces and Responses on a Semisubmersible Platform in High waves, Paper OMAE2009-79483, *Proc., the 28th OMAE Conf.*, Honolulu, HI, USA.

Besley P. (1999) *Overtopping of seawalls – design and assessment manual* R & D Technical Report W 178, ISBN 1 85705 069 X, Environment Agency, Bristol, also from: [http://www.hrwallingford.co.uk/downloads/projects/overtopping/overtopping\\_manual.pdf](http://www.hrwallingford.co.uk/downloads/projects/overtopping/overtopping_manual.pdf)

Bingham, H.B. (2000). A hybrid Boussinesq-panel method for predicting the motion of a moored ship. *Coastal Engineering*, Volume 40, Issue 1, April 2000, Pages 21-38, doi:10.1016/S0378-3839(00)00002-8.

Bingham, H.B. Madsen, P.A. and Fuhrman. D.R. (2009). Velocity potential formulations of highly accurate boussinesq-type models. *Coastal Engineering*, 56:467–478.

Blenkinsopp C.E. and Chaplin J.R. (2007). Void fraction measurements in breaking waves. *Proc. of the Royal Society A: Mathematical, Physical and Engineering Science*, Vol. 463, 3151–3170.

Blenkinsopp C.E., M.A. Mole, I.L. Turner, W.L. Peirson. 2010. Measurements of the time-varying free-surface profile across the swash zone obtained using an industrial LIDAR. *Coastal Engineering* 57, 1059–1065.

Bonnemaire, B., Lundamo, T., Evers, K.-U., Løset, S., and Jensen, A. (2008). Model Testing of the Arctic Tandem Offloading Terminal Mooring Ice Ridge Loads. *Proc. 19<sup>th</sup> IAHR International Symposium on Ice “Using New Technology to Understand Water-Ice Interaction”*, Vancouver, British Columbia, Canada, July 6 to 11, 2008.

Bonnemaire, B., Shkhinek, K., Lundamo, T., Liferov, P. and Le Guennec, S. (2009). Dynamic Effects in the Response of Moored Structures to Ice Ridge Interactions. *Proceedings of the 20<sup>th</sup> International Conference on Port and Ocean Engineering under Arctic Conditions*, June 9-12, 2009, Luleå, Sweden.

Bonnemaire, B., Aksnes, V., Lundamo, T., Evers, K.-U., Løset, S. and Ravndal, O. (2010). Ice Basin Testing of a Moored Offloading Icebreaker in Variable Ice Drift: Innovations and New Findings. *Proceedings of the HYDRALAB III Joint User Meeting*, Hannover, February 2010.

Borgman, L.E. (1969). Directional spectra models for design use. *Proc Offshore Technology Conference (OTC)*, Houston, Texas.

Le Boulluec, M., Forest, B. and Mansuy, E. (2008). Steady drift of floating objects in waves, experimental and numerical investigation. *27<sup>th</sup> International Conference on Offshore Mechanics and Arctic Engineering (OMAE2008)*, June 15-20, 2008, Estoril, Portugal.

Boussinesq, J. (1872), *Theorie des ondes et des remous qui se propagent le long d'un canal rectangulaire horizontal, en communiquant au liquide contenu dans ce canal des vitesses*

sensiblement pareilles de la surface au fond. *Journal de Mathématique Pures et Appliquées*, Deuxième Série 17: 55–108.

Branković, M., Zeitoun, H., Sutherland, J., Pearce, A., Jacobsen, V., Sabavala, H., Tørnes, K., Cumming, G. and Willcocks, J. (2010). Physical modelling of hydrodynamic loads on piggyback pipelines in combined wave and current conditions. *Proc 29th Int Conf on Ocean, Offshore and Arctic Engineering*, Shanghai, China. ASME, paper OMAE2010-20913.

Briggs MJ, Synolakis CE, Harkins G, & Green DR. (1995) Laboratory experiments of tsunami run-up on a circular island. *Pure and Applied Geophysics*; 144:569-593.

Bruun, P.K., Husvik, J., Le Guennec, S. and Hellmann, J.-H. (2009). Ice Model Test of an Arctic SPAR. *Proceedings of the 20<sup>th</sup> International Conference on Port and Ocean Engineering under Arctic Conditions*, June 9-12, 2009, Luleå, Sweden, paper POAC09-136.

Burcharth H.F. (1994) *The design of breakwaters*, Chapter 29 in Coastal, Estuarial and Harbour Engineers' reference book, pp 381-424, Editors M.B. Abbott & W.A. Price, ISBN 0-419-15430-2, E & FN Spon, London.

Burcharth H.F., Christiansen M., Jensen T. & Frigaard P. (1998) Influence of core permeability on accropode armour layer stability, *Proc. Int. Conf. on Coastlines, Structures & Breakwaters '98*, pp34-45, Institution of Civil Engineers / Thomas Telford, London.

Burcharth, H.F., Liu, P. and Troch, P. (1999). Scaling of core material in rubble mound breakwater model tests. *Proceedings COPEDEC V*, Cape Town, South Africa.

CEDEX (2009). Master in Port and Coastal Engineering. Section IV: advanced techniques in studying port and coastal engineering, Volume 2, Module IV.3.- Physical Models. *Centro de Estudios y Experimentación de Obras Públicas* (CEDEX), February-June 2009. Madrid, Spain.

Chadwick, A., Ilic, S. and Helm-Petersen, J. (2000). An evaluation of directional analysis techniques for multidirectional, partially reflected waves, Part 1: application to field data. *J of Hydraulic Research*, 38(4): 253 - 258.

Chakrabarti, S.K. (1994). *Offshore structure modelling*. Advances Series on Ocean Engineering – Volume 9. World Scientific, pp470.

Chaplin, J.R. (1996). On frequency-focusing unidirectional waves. In *International Journal of Offshore and Polar Engineering* 6 (2).

Charvet I (2011) Experimental modelling of long elevated and depressed waves using a new pneumatic wave generator, PhD thesis, University College London,

Chatjigeorgiou, I.K., Damy, G., Le Boulluec, M. (2007). Experimental investigation for the dynamic behaviour of a catenary riser under top imposed excitations. *Seventh International Symposium on Cable Dynamics*. Vienna (Austria). December 10-13, 2007.

Chatjigeorgiou, I.K., Damy, G. and Le Boulluec, M. (2008). Numerical and experimental investigation of the dynamics of catenary risers and the risers-induced-damping phenomenon. *27th International Conference on Offshore Mechanics and Arctic Engineering* (OMAE2008) June 15-20, 2008, Estoril, Portugal

- Chen, X.B. (2006). Set-down in the second-order Stokes' waves, *Proc. Conf. on Hydrodynamics*, pp. 179-185.
- Cipriano, R.J. and Blanchard, D.C. (1981). Bubble and aerosol spectra produced by a laboratory breaking wave. *J. Geophys. Res.* 86, 8085–8092.
- Clauss, G.F. (2000). Generation of task-related freak waves and critical wave groups. In *Rogue waves 2000 workshop*.
- Clauss, G.F. (2002). Dramas of the sea: episodic waves and their impact on offshore structures. In *Applied Coastal Research* 24, pp. 147–161.
- Clauss, G.F. and Bergmann, J. (1986). Gaussian wave packets - a new approach to seakeeping tests of ocean structures. In *Applied Ocean Research*.
- Clauss, G.F. and Kühnlein, W.L. (1995). Transient wave packets - an efficient technique for seakeeping tests of self-propelled models in oblique waves. In *Third International Conference on fast sea transportation*, Lübeck-Travemünde, Germany.
- Clauss, G.F. and Schmittner, C.E. (2007). Experimental optimization of extreme wave sequences for the deterministic analysis of wave/structure interaction. In *Journal of Offshore Mechanics and Arctic Engineering-Transactions of the ASME* 129, pp. 61–67.
- Cohen de Lara M. (1955). Coefficient de perte de charge en milieu poreux base sur l'équilibre hydrodynamique d'un massif, *La Houille Blanche*, no.2.
- Cornett, A., Mattila, M., Tarbotton, M. and Gittens, G. (1999). Mooring Study of a Large Cruise Ship. *Proc. of the 1999 Canadian Coastal Conference*, Victoria BC, Canada, May 19-22, 15p.
- Cox, D.T. and Shin, S. (2003). Laboratory measurements of void fraction and turbulence in the bore region of surf zone waves. *J. Eng. Mech.* 129, 1197–1205.
- Cox, G. and Weeks, W.F. (1982). Equations for Determining the Gas and Brine Volumes in Sea Ice Samples. *U.S.A. CRREL Report No. 82-30*, Hanover, N.H., U.S.A.
- Cunge, J.A. 2003. On data and models. *Journal of Hydroinformatics* 5(2) 75-98.
- Cuomo G. & Allsop N.W.H. (2004) *Wave impacts at seawalls* Proc. 29th ICCE, Lisbon, publ. World Scientific, pp 4050-4062, ISBN 981-256-298-2.
- Cuomo G., Allsop N.W.H. & McConnell K.J. (2003) *Dynamic wave loads on coastal structures: analysis of impulsive and pulsating wave loads* Proc. Conf. Coastal Structures 2003, Portland, ASCE / COPRI, 356-368.
- Cuomo G., Allsop N.W.H. & Takahashi, S. (2010) Scaling wave impact pressures on vertical walls, *Coastal Engineering*, Volume 57, Issue 6, June 2010, pp604-609, Elsevier.
- Cuomo, G., Allsop, N.W.H., Bruce, T. & Pearson, J. (2010) Breaking wave loads at vertical sea walls & breakwaters. *Coastal Engineering*, Volume 57, Issue 4, April 2010, pp424-439.
- Cuomo G., Piscopia R., Allsop N.W.H. (2011) Evaluation of wave impact loads on caisson breakwaters based on joint probability of impact maxima and rise times, *Coastal Engineering*, Volume 58, Issue 1, January 2011, pp9-27.



Cuomo, G., Tirindelli, M. and Allsop, N.W.H. (2007). Wave-in-deck loads on exposed jetties. *Coastal Engineering* 54 (9), 657–679.

Cuomo G., Shimosako, K. and Takahashi S. (2009). Wave-in-deck loads on coastal bridges and the role of air. *Coastal Engineering* 56, 793–809.

Dalrymple, R.A. (Ed.) (1985). *Physical Modelling in Coastal Engineering*. A.A. Balkema, Rotterdam, NL.

Dätig, M. and Schlurmann, T. (2004). Performance and limitations of the Hilbert-Huang transformation (HHT) with an application to irregular water waves. *Ocean Eng.*, 31, pp. 1783–1834.

Davey, T., Bruce, T. and Allsop, N.W.H. (2008). Getting more from physical modelling – measuring extreme responses using importance sampling. *Proc 31st ICCE*, pp3058–3070.

Davey, T. (2010). Modelling of extreme individual overtopping events at vertical seawalls. PhD thesis. University of Edinburgh.

Davidson, M.A., Huntley, D.A. and Bird, P.A.D. (1998). A practical method for the estimation of directional wave spectra in reflective wave fields. *Coastal Engineering* 33: 91 – 116.

Davidson, M.A., Kingston, K.S. and Huntley, D.A. (2000). New solution for directional wave analysis in reflective wave fields. *J. Waterway, Port, Coastal & Ocean Engineering*, 126(4) 173 – 181.

Davies, M., MacDonald, N. and Cornett, A. (2001). Optimization of Port Design Using Physical Modeling. Proc. of the *Ports '01: America's Ports - Gateways to the Global Economy*, ASCE, Norfolk, Virginia, USA, April 29 - May 2, 16p.

Davis, M.C. and Zarnick, E.E. (1964). Testing ship models in transient waves. In *Fifth Symposium on Naval Hydrodynamics*.

Dean, R.G. and Dalrymple, R.A. (1991). *Water Wave Mechanics for Engineers and Scientists*, Advanced Series on Ocean Engineering, Vol. 2, World Scientific Press

Deane, G.B. (1997). Sound generation and air entrainment by breaking waves in the surf zone. *J. Acoust. Soc. Am.* 102, 2671–2689.

Deane, G.B. and Stokes, M.D. (2002). Scale dependence of bubble creation mechanisms in breaking waves. *Nature* 418, 839–844.

DNV (2010). Hydrodynamic Model Testing, Chapter 10 in *Environmental conditions and environmental loads*. DNVRP- C205, Det Norske Veritas, Høvik, Norway.

European Commission (2011). Open Data, an engine for innovation, growth and transparent governance. Communication from the Commission to the European Parliament, the Council, the European Economic and Social Committee and the Committee of the Regions, COM(2011) 882 final, Brussels.

Enkvist, E. and Mäkinen, S. (1984). A fine grain model ice. *Proc. IAHR Symposium on Ice*, Hamburg, Germany, Vol. II, pp. 217–227.

Evers, K.-U. and Jochmann, P. (1993). An Advanced Technique to Improve the Mechanical Properties of Model Ice Developed at the HSVA Ice Tank, *Proceedings of the 12th International Conference on Port and Ocean Engineering under Arctic Conditions* (POAC), 17- 20 Aug. 1993, Hamburg, Vol. 2, pp. 877 - 888

Evers, K.-U. (2008). Shtokman Icebreaker FPU Conceptual Study - Ice Model Tests. HSVA Report IO 426-08, internal report (unpublished).

Evers, K.-U. (2010). Model Ice Production and Ice Properties Determination Methods at HSVA, HSVA-Report (unpublished), April 2010.

Evers, K.-U. and Jochmann, P. (2011). Experiences at HSVA with model testing of moored structures in ice-covered waters. *Proceedings of the 21<sup>st</sup> Port and Ocean Engineering under Arctic Conditions* (POAC'11), July 10-14, 2011 Montréal, Canada.

Eysenbach, G. (2011). Can tweets predict citations? Metrics of social impact based on twitter and correlated with traditional metrics of scientific impact. *Journal of Medical Internet Research*, available at <http://www.jmir.org/2011/4/e123/>

Faltinsen, O.M., and Timokha, A.N. (2002). Asymptotic modal approximation of nonlinear resonant sloshing in a rectangular tank with small fluid depth, *J. Fluid Mechanics*, vol. 470, pp. 319–357.

FEMA (2008) *Guidelines for Design of Structures for Vertical Evacuation from Tsunamis* P646. Federal Emergency Management Agency.

Ferrant, P., Gentaz, L., Monroy, C., Luquet, R., Ducrozet, G., Alessandrini, B., Jacquin, E. and Drouet, A. (2008). Recent Advances Towards the Viscous Flow Simulation of Ships Maneuvering in Waves. *International Workshop on Water Waves and Floating Bodies* (IWWWFB), Korea.

Frederking, R. and Häusler, F.U. (1978). The flexural behaviour of ice from in situ cantilever beam tests, *Proc. IAHR Symp. on Ice Problems*, Part I, Lulea, Sweden, pp. 197-215.

Frostick, L.E., McLelland, S.J. and Mercer, T.G. (Eds) (2011). *Users guide to physical modelling and experimentation, experience of the HYDRALAB network*. CRC Press / Balkema, Leiden, NL. ISBN 978-0-415-60912-8 (pbk).

Fylling, I.J., Stansberg, C.T. and Mo, K. (1992), Extreme Motions and Anchor Line Loads in Turret Mooring Systems, *Proc., Vol. 1, the BOSS 92 Conf.*, London, U.K., July 1992, pp. 197 - 210.

Gemmrich, J.R., and D.M. Farmer (2004). Near-surface turbulence in the presence of breaking waves, *J. Phys. Oceanogr.*, 34, 1067– 1086, doi:10.1175/1520-0485(2004)034<1067:NTITPO>2.0.

Gerritsen, H., Sutherland, J., Deigaard, R., Mutlu Sumer, Fortes, J.E.M., Sierra, J.P. and U. Schmidtke, 2011. Composite modelling of the interactions between beaches and structures. *Journal of Hydraulic Research*. 49: sup1, 2-14.

Gerritsen, H. and Sutherland, J., 2011. *Composite Modelling*. Chapter 6 (pp. 171 – 219) of L.E. Frostick, S.J. McLelland and T.G. Mercer (Eds), *Users guide to physical modelling and*

experimentation: experience of the HYDRALAB Network. CRC Press/Balkema, Leiden, the Netherlands, ISBN: 978-0-415-60912-8 (Pbk), ISBN: 978-1-4398-7051-8 (e-Book).

Ghoneim, G.A. (2011). Assessing the state of arctic technology development, *Offshore Magazine*, vol. 71, issue 2.

Goda, Y. (1985). Random seas and design of maritime structures. University of Tokyo Press, Tokyo, Japan.

Goda, Y. and Suzuki, Y. (1976). Estimation of incident and reflected waves in Random Wave experiments. Proceedings of the 15<sup>th</sup> Coastal Engineering Conference, ASCE, V1, 828-845.

Goring, D.G. (1979). Tsunamis - The propagation of long waves onto a shelf, PhD thesis, California Institute of Technology, Pasadena CA.

Goring and Raichlen (1980). The generation of long waves in the laboratory. Proc. *International Conference on Coastal Engineering* (ICCE) 1980.

Gourlay, T. (2009). Sinkage and trim of two ships passing each other on parallel courses. *Ocean Engineering*, Volume 36, Issue 14, Pages 1119-1127.

Gow, A.J., Ueda, H.T. and Ricard, J.A. (1978). Flexural Strength of Ice on Temperate Lakes. U.S. Army CRREL. Rept. 78-9, Hanover, N.H., U.S.A.

Grassa, J.M. *et al.* (1999). "Ferrol Outer Port: experimental and *in situ* design studies". Journal of Maritime Engineering. Proc. of the Institution of Civil Engineers U.K., Volume 162, Issue MA2.

Grigoropoulos, G.J., Florios, N.S. and Loukakis, T.A. (1994). Transient waves for ship and floating structure testing. In *Applied Coastal Research* 16, pp. 71–85.

Grüne, J. (1988). Wave induced shock pressures under real sea state conditions. In *Coastal Engineering*, pp. 2340–2354.

Grüne, J. (1992). Loads on sloping seadikes and revetments from wave induced shock pressures. In *Coastal Engineering*, pp. 1175–1188.

Grüne, J. and Bergmann, H. (1994). Wave loads on seadykes with composite slopes and berms. In *Coastal Engineering*, pp. 1075–1089.

Haase, A., van der Werff, S. and Jochmann, P. (2012). DYPIC - Dynamic Positioning in Ice: First Phase of Model Testing, *Proceedings of the 31<sup>st</sup> International Conference on Ocean, Offshore and Arctic Engineering OMAE 2012*, July 1-6, 2012, Rio de Janeiro, Brazil, [OMAE2012-83455].

Hammack, J.L. (1972). Tsunamis - a model of their generation and propagation, Rep. Kh-R-28, W. M. Keck Lab. of Hydraulic and Water Resour., California Inst. of Technol., Calif.

Hammack J.L (1973) A note on tsunamis: their generation and propagation in an ocean of uniform depth, *J. Fluid Mech.* Vol 60, part 4, pp 769-799.

Hammack, J.L., and H. Segur (1974). The Korteweg– de Vries equation and water waves. part 2: Comparison with experiments, *J. Fluid Mech.*, 65(2), 289–314.

- Harvey, H. and Han, D. (2003). The relevance of Open Source to hydroinformatics. *Journal of Hydroinformatics*, 4(4) 219 – 234.
- Hashimoto, N., Nagai, T. and Asai, T. (1993). Modification of the extended maximum entropy principle for estimating directional spectrum in incident and reflected wave field. *Rept. Of P.H.R.I.* 32(4) 25-47
- Hashimoto, N. (1997). Analysis of the directional wave spectra from field data. *Advances in Coastal and Ocean Engineering* Vol.3. ed.Liu, P.L-F. World Scientific, Singapore. pp.103-143
- Hashimoto, N. and Kobune, K. (1987). Estimation of directional wave spectra from a Bayesian approach in incident and reflected wave field. Rep of the Port and Harbour Res Inst. 26(4) 3 – 33 [in Japanese].
- Hashimoto, N. and Kobune, K. (1988). Estimation of directional spectrum from a Bayesian approach. *Proc.21st ICCE* Vol 1. ASCE pp.62-72
- Heller, V., Hager, W.H. and Minor, H-E. (2008). Scale effects in subaerial landslide generated impulse waves. *Experiments in fluids*, 44(5): 691-703.
- Heller et al, 2009 – reference needed
- Henderson, R. (2006). Design, simulation, and testing of a novel hydraulic power take-off system for the Pelamis wave energy converter. *Renewable Energy*, 31(2): 271-283.
- HM Government (2012). Open Data White Paper, unleashing the potential. The Stationary Office, Norwich, UK. ISBN 9780101835329
- Hofland, B., Kaminski, M.L. and Wolters, G. (2010). Large scale wave impacts on a vertical wall. In ASCE (Ed.): *Proceedings of 32<sup>nd</sup> Int Conference on Coastal Engineering*. Shanghai, China.
- Hofland, B., Hoffmann, R., Lindenbergh, R. (2012). Wave measurement techniques for the new large-scale delta flume. *Proceedings Coastlab 2012*. Ghent, Belgium.
- Hofland, B., Wenneker, I., Van Gent, M.R.A. (2013) Description of the New Delta Flume. *Proceedings of Coasts, Marine Structures and Breakwaters 2013*. Institution of Civil Engineers. Edinburgh. (draft paper submitted)
- Hoque, A. (2002). Air bubble entrainment by breaking waves and associated energy dissipation. PhD thesis, Department of Architecture and Civil Engineering. Toyohashi University of Technology, Toyohashi, pp. 151.
- Hoque, A. and Aoki, S. (2005). Distributions of void fraction under breaking waves in the surf zone. *Ocean Eng.* 32, 1829–1840.
- Huang, N.E., Shen, Z., Long, S.R., Wu, M.C., Shih, H.H., Zheng, Q., *et al.* (1998). The empirical mode decomposition and the Hilbert spectrum for nonlinear and non-stationary time series analysis. *Proceedings of Royal Society London Series A*, 454, 903–95.
- Huang, N.E., Long, S.R. and Shen, Z. (1996). The mechanism for frequency downshift in nonlinear wave evolution. *Advances in Applied Mechanics*, 32, pp. 59–111.

Huang, N.E., Shen, Z. and Long, S.R. (1999). A new view of nonlinear water waves: The Hilbert spectrum. *Annual Review of Fluid Mechanics*, 31, pp. 417–57.

Huang, N.E., Wu, M.L., Long, S.R., Shen, S.P., Per, W.Q., Gloersen, P., *et al.* (2003). A confidence limit for the empirical mode decomposition and Hilbert spectral analysis. *Proc R Soc Lond*, 459, pp. 2317-45.

Huang, N.E. (2005a). Introduction to Hilbert-Huang transform and some recent developments. In: Huang N, Attoh-Okine NO, editors. *The Hilbert-Huang transform in engineering*. CRC Press, pp. 1-23.

Huang, N.E. (2005b). Introduction to Hilbert-Huang transform and its related mathematical problems. In: Huang NE, Shen SSP, editors. *Hilbert-Huang transform and its applications*. World Scientific, pp. 1-26.

Hudson, R.Y., Herrmann, F.A., Sager, R.A., Whalin, R.W., Keulegan, G.H., Chatham, C.E. and Hales, L.Z. (1979). Coastal Hydraulic Models, Special report No. 5, US Army Engineer Waterways Experiment Station, Vicksburg, Mississippi.

Hughes, S. (2004). Estimation of wave run-up on smooth, impermeable slopes using the wave momentum flux parameter. *Coastal Engineering* 51.

Hughes S.A. (1993). *Physical models and laboratory techniques in coastal engineering*, Advanced Series on Ocean Engineering, Vol. 7, World Scientific Publishing, Singapore

Hunt (1959). Design of seawalls and breakwaters. *Journal of the Waterway and Harbours Division, ASCE 85 WW3*. pp 123-152.

Hwung, H.H., Chyan, J.M. and Chung, Y.C. (1992). Energy dissipation and air bubbles mixing inside surf zone. In *23rd Int. Conf. on Coastal Engineering* (ASCE), Venice, Italy, vol. 1, pp. 308–321.

IAHR (1986). List of sea state parameters. Supplement to Bulletin No. 52, Permanent International Association of Navigation Congresses (PINC), Brussels, Belgium.

IAHR (1989). List of sea state parameters. *Journal of Waterway, Port, Coastal and Ocean Engineering*, ASCE, 115(6): 793-808.

Isobe, M., Kondo, K. and Horikawa, K. (1984). Extension of MLM for estimating directional wave spectrum. *Proc. Symp. on Description and Modeling of Directional Seas*, Paper No.A-6. 15pp.

ITTC (2005). Report from the Ocean Engineering Committee, *Proc., The 24<sup>th</sup> International Towing Tank Conference*, Edinburgh, Scotland, Sept. 2005.

ITTC (2008). Report from the Ocean Engineering Committee, *Proc., The 25<sup>th</sup> International Towing Tank Conference*, Fukuoka, Japan, Sept. 2008.

ITTC (2011). Report from the Ocean Engineering Committee, *Proc., The 26<sup>th</sup> International Towing Tank Conference*, Rio de Janeiro, Brazil, Sept. 2011.

Isaacson, M. (1991). *Measurement of regular wave reflection*. *J. Waterway, Port, Coastal and Ocean Engineering*. 117(6), 553-569.



Isobe, M. and Kondo, K. (1984). Methods for estimating directional wave spectrum in incident and reflected wave field. *Proc 19<sup>th</sup> ICCE*, ASCE, New York, NY. 467 – 483.

Ivicics, L. (1980). *Hydraulic Models*. Water Resources Publications, Fort Collins, Colorado.

Izumiyama, K. (2007a). Increasing the safety of icebound shipping, Vol 1, Ice model tests. Espoo: Helsinki University of Technology.

Izumiyama, K., Takimoto, T. and Uto, S. (2007b). Length of Ice Load Patch on a Ship Bow in Level Ice. *The 10th International Symposium on Practical Design of Ships and Other Floating Structures*, Houston October 1-5, 2007, American Bureau of Shipping.

Jalonen, R. and L. Ilves (1990). Experience with a chemically-doped fine-grained model ice. In *Proceedings of the IAHR 10th International Symposium on Ice*, Espoo, Finland. International Association for Hydraulic Research, vol. 2, p. 639–651.

Jensen, O.J. and Klinting, P. (1983). Evaluation of scale effects in hydraulic models by analysis of laminar and turbulent flows, *Coastal Engineering* 7.

Johnson, M.F., Rice, S.P., Thomas, R.E. and Frostick, L.E. (Editors) 2012. Critical review of ecohydraulic experiments. HYDRALAB-IV Deliverable D7.1. [www.hydralab.eu](http://www.hydralab.eu)

Kalvoda, P.M., Xu, L. and Wu, J. (2003). Macrobubble clouds produced by breaking wind waves: a laboratory study. *J. Geophys. Res.* 108, 3207.

Kayo, Y., Kawasaki, T., Minami, T., Tozama, S., Tanaka, A. and Abdeinour, R. (1983). Field study on mechanical strength of sea ice at east coast of Hokkaido. *Proc. POAC 83*, Helsinki, Finland, Vol. I, pp. 109-118.

Kendon, T., Pakozdi, C., Baarholm, R.J., Berthelsen, P.A., Stansberg, C.T., Enger, S. and Peric, M. (2010). Wave In-Deck Impact: Comparing CFD, Simple Methods, and Model Tests, *Proc., The 29<sup>th</sup> OMAE Conf.*, Shanghai, China, June 2010.

Khatibi, R., Jackson, D., Curtin, J., Whitlow, C., Verwey, A. and Samuels, P. (2004). Vision statement on open architecture for hydraulic modelling software tools. *Journal of Hydroinformatics*, 6(1), 57-74.

Kirby, J.T. and Dalrymple, R.A. (1986). An approximate model for nonlinear dispersion in monochromatic wave propagation models. In *Coastal Engineering*, 9, pp. 545–561.

Klein Breteler, M. and Coeveld, E.M. (2004). Onderzoeksprogramma kennisleemtes steenbekledingen. Kwantificering golfbelasting op steenbekledingen. WL | Delft Hydraulics, rapport nr. H4419. Delft (In Dutch).

Klopman, G. and van Leeuwen, P.J. (1990). An efficient method for the reproduction of non-linear random waves, ASCE, *Proc. Int Conf Coastal Eng*, Vol.1, pp. 478-488, Delft

Kuiper, C. and Doorn, N. (2005). Determination of wave pressures using Skylla. Delft Hydraulics Rept. H4424. In Dutch.

Kujala, P. *et al.* (2007). Increasing the safety of icebound shipping, Final scientific report ,Vol 1. Espoo: Helsinki University of Technology.

- Kujala, P. *et al.* (2012). Statistical analysis of ice crushing pressures on a ship's hull during hull-ice interaction. *Cold Regions Science and Technology*, 1-11.
- Lamarre, E. (1993). An experimental study of air entrainment by breaking waves. PhD thesis, Department of Civil & Oceanographic Engineering. Cambridge, MA: MIT Press.
- Lamarre, E. and Melville, W.K. (1992). Instrumentation for the measurement of void-fraction in breaking waves: laboratory and field results. *IEEE J. Oceanic Eng.* 17, 204–215.
- Lamarre, E. and Melville, W.K. (1994). Void-fraction measurements and sound-speed fields in bubble plumes generated by breaking waves. *J. Acoust. Soc. Am.* 95, 1317–1328.
- Laniak, G.F., Olchin, G., Goodall, J., Voinov, A., Hill, M., Glynn, P., Whelan, G., Geller, G., Quinn, N., Blind, M., Peckham, S., Reaney, S., Gaber, N., Kennedy, R. and Hughes, A. (2012). Integrated Environmental modelling: a vision and roadmap for the future. *Environmental Modeling & Software*. Doi : 10.1016/j.envsoft.2012.09.006.
- Le Boulluec, M., Maisondieu, Ch., Du Plessix, G. and Cordeau, C. (2005). Well Head Production Floater – Experimental and Numerical Investigation. *24th International Conference on Offshore Mechanics and Arctic Engineering (OMAE2005)*, Halkidiki, Greece. Paper OMAE2005-67586.
- Lécuyer, B., Ledoux, A., Molin, B., Le Boulluec, M. and Heguiapal, B. (2012). Hydro-Mechanical Issues of Offloading Operations Between a Floating LNG Terminal and a LNG Carrier in Side-by-Side Configuration. Proceedings of the 31<sup>st</sup> International Conference on Offshore Mechanics and Arctic Engineering. June 10-15, 2012, Rio de Janeiro, Brazil.
- Le Méhauté, B. (1957-58). Perméabilité des diques en enrochements aux ondes de gravité périodiques, *La Houille Blanche*, No. 6 (1957), no. 2 (1958), no 3 (1958).
- Leifer, I. and De Leeuw, G. (2006). Bubbles generated from wind-steepened breaking waves: 1. Bubble plume bubbles. *J. Geophys. Res.* 111, C06020.
- Lécuyer, B., Ledoux, A., Molin, B., Le Boulluec, M. and Heguiapal, B. (2012). Hydro-Mechanical Issues of Offloading Operations Between a Floating LNG Terminal and a LNG Carrier in Side-by-Side Configuration. *Proc 31st International Conference on Offshore Mechanics and Arctic Engineering (OMAE2012)*. June 10-15, 2012, Rio de Janeiro, Brazil.
- Leiviskä, T. (1999). Ship's Ridge Resistance in Model Ice. *POAC 99*, (pp. 600-611). Helsinki.
- Liu, P.L.-F., Wu, T.-R., Raichlen, F., Synolakis, C.E. and Borrero, J. (2005). Runup and rundown generated by three-dimensional sliding masses. *J. Fluid Mech.* 536, 107–144.
- Liu, Y.N., Molin, B., Kimmoun, O., Remy F. and Rouault M.-C. (2011). Experimental and numerical study of the effect of variable bathymetry on the slow-drift wave response of floating bodies. *Applied Ocean Research* 33 199–207.
- Lloyd T, Allsop W, Charvet I, Robinson D, Robinson T, Rossetto T (2009) Physical modelling of violent flows and their impact using a new tsunami generator, *Proc ICE Conf. on Coasts, Marine Structures & Breakwaters*, Edinburgh, September 2009, publn. Thomas Telford, London.
- Loewen, M.R., O'Dor, M.A. and Skafel, M.G. (1996) Bubbles entrained by mechanically generated breaking waves. *J. Geophys. Res.* 101, 20 759–20 770.

- Lu, W. (2012). Experience with the I-scan system. Project interim report, NTNU, 2012, (unpublished).
- Lundgren, H. and Klinting, P. (1987). Rigorous analysis of directional waves. Proceedings of wave analysis and generation in laboratory basins. Proc 22<sup>nd</sup> IAHR Congress, pp 351 – 362.
- Määttänen, M. (1975). On the flexural strength of brackish water ice by in-situ tests. Proc. POAC 75, Fairbanks, Al, U.S.A., pp. 349-359.
- Määttänen, M. *et al.* (2011). Ice crushing tests with variable structural flexibility. *Cold Regions Science and Technology*, 120-128.
- Määttänen, M., Løset, S., Metrikine, A., Evers, K.-U., Hendrikse, H., Lønøy, C., Metrikin, I., Nord, T. and Sukhorukov, S. (2012). Novel Ice Induced Vibration Testing in a Large-scale Facility: Deciphering Ice Induced Vibrations, Part 1, 21<sup>st</sup> IAHR International Symposium on Ice "Ice Research for a Sustainable Environment", Li and Lu (ed.) Dalian, China, June 11 to 15, 2012, ISBN 978-7-89437-020-4.
- Madsen, P.A. and Sørensen, O.R. (1992). A new form of the Boussinesq equations with improved linear dispersion characteristics: Part 2. A slowly-varying bathymetry. *Coastal Eng.* 18, 183–204.
- Madsen, P. A. & Fuhrman, D. R. (2008) Runup of tsunamis and long waves in terms of surf similarity, *Coastal Engineering* no. 55, pp. 209-223.
- Madsen PA, Fuhrman DR, & Schäffer HA. (2008) On the Solitary Wave paradigm for Tsunamis, *Journal of Geophysical Research*, 113:C12012.
- Maguire, E. and Ingram, D. (2011). On Geometric design considerations and control methodologies for absorbing wavemakers. *Coastal Eng* 58: 135-142.
- Maisondieu, Ch., Le Boulluec, M. (2001). Flow dynamics in a moon-pool. Experimental and numerical assessment. *Proceedings of 20th International Conference on Offshore Mechanics and Arctic Engineering*, Rio de Janeiro, Brazil. Paper OMAE2001/OFT-1151.
- Mallat, S. (1989). A theory for multiresolution signal decomposition: The wavelet representation. *IEEE Transactions on Pattern Analysis and Machine Intelligence*, 11(7), pp. 674–93.
- Mansard, E.P.D. and Funke, E.R. (1980). *The measurement of incident and reflected spectra using a least squares method*. Proc. 17<sup>th</sup> ICCE, Sydney. pp154-172.
- Martins, R. (1989). *Recent Advances in Hydraulic Physical Modelling*, Kluwer Academic Publishers, Dordrecht, NL.
- McConnell K.J. (1998) *Revetment systems against wave attack: a design manual* ISBN 0-7277-2706-0, Thomas Telford, London.
- McConnell K., Allsop W., Cuomo G. & Cruickshank I. (2003) *New guidance for wave forces on jetties in exposed locations* Proc. Conf. COPEDEC VI, Colombo, Sri Lanka

- McConnell K, Allsop W. & Cruickshank I (2004) *Piers, jetties and related structures exposed to waves – guidelines for hydraulic loadings*. Thomas Telford, London, ISBN 0 7277 3265 X.
- McIver, P. and Newman, J. N. (2003). Trapping structures in the three-dimensional water-wave problem. *J. Fluid Mechanics.*, vol. 484, pp. 283–301.
- Melville, W.K. (1996). The role of surface-wave breaking in air–sea interaction. *Annual. Rev. Fluid Mech.* 28, 279–321.
- Metrikin, I. (2011). Tekscan I-Scan Tactile Sensor. Project interim report, NTNU, 2011 (unpublished).
- Moes, H. (2004). Mooring Optimization in South African Ports. *Proc. of the Harbor Long Wave 2004*, Yokosuka, Japan, July 12, 9p.
- Molin B. (2001), On the piston and sloshing modes in moonpools, *Journal of Fluid Mechanics*, Vol. 430, pp.27-50.
- Moslet, P.O., Masurov, M. and Eide, L.I. (2010). Barents 2020 RN02 – Design of Stationary Offshore Units against Ice Loads in the Barents Sea, *Proceedings 20<sup>th</sup> IAHR International Symposium on Ice*, Lahti, Finland, June 14 to 18, 2010.
- Murzyn, F., Mouaze, D. and Chaplin, J.R. (2004). Optical measurements of bubbly flow in hydraulic jumps. *Int. J. Multiphase Flow* 31, 141–154.
- Murzyn, F. and Chanson, H. (2009). Experimental investigation of bubbly flow and turbulence in hydraulic jumps. *Environmental Fluid Mechanics* 9, 143–159.
- Newman (2010). Analysis of wave generators and absorbers in basins. *AOR* 32(1) 71-82.
- Newman, J. N. (2003). Low-frequency resonance of moonpools. *18th Workshop on Water Waves and Floating Bodies* – Le Croisic, France – 6-9 April 2003.
- Nicholls, R.J., Wong, P.P., Burkett, V.R., Codignotto, J.O., Hay, J.E., McLean, R.F., Ragoonaden, S. and Woodroffe, C.D. (2007). Coastal systems and low-lying areas. *Climate Change 2007: Impacts, Adaptation and Vulnerability. Contribution of Working Group II to the Fourth Assessment Report of the Intergovernmental Panel on Climate Change*, M.L. Parry, O.F. Canziani, J.P. Palutikof, P.J. van der Linden and C.E. Hanson, Eds., Cambridge University Press, Cambridge, UK, 315-356.
- Nielsen, M. (2011). *Reinventing discovery: the new era of networked science*. Princeton University Press. 280pp.
- Nortala-Hoikkanen, A. (1990). FGX Model Ice at the Masa-Yards Arctic Research Centre. In *Proceedings of the IAHR 10th International Symposium on Ice*, Espoo, Finland. International Association for Hydraulic Research, vol. 3, p. 247–259.
- Nwogu, O.U. (1989). Maximum entropy estimation of directional wave spectra from an array of wave probes. *Applied ocean Research* 11(4) 176 – 182.
- OCIMF (1992). Mooring equipment guidelines 1992. Oil Companies International Marine Forum.

OECD (2004). Science, Technology and Innovation for the 21st Century. Meeting of the OECD Committee for Scientific and Technological Policy at Ministerial Level, 29-30 January 2004 - Final Communiqué.

Ortega, J., Smith, G.H (2009). Hilbert–Huang transform analysis of storm waves, *Applied Ocean Research*, 31, pp. 212-219.

Oumeraci, H. (2003). Role of Large-Scale Model Testing in Coastal Engineering - Selected example studies performed in GWK Hannover. *Towards a Balanced Methodology in European Hydraulic Research*. HYDRALAB II, Budapest, May 22-23.

Oumeraci, H. (1984). Scale effects in coastal hydraulic models. In *Symposium on scale effects in modelling hydraulic structures*, ed. H. Kobus, International Association for Hydraulic Research, pp. 7.10.1-7.10.7

Panizzo, A., de Girolamo, P. and Petaccia, A. (2005). Formulating impulse waves generated by subaerial landslides. *J Geophysical Research* 110 C12025:1-23.

Pawka, S.S. (1983) Island shadows in wave directional spectra. *J. Geophys. Res.* 88(C4) 2579-2591.

Pelinovsky, E., Talipova, T. and Kharif, C. (2000). Nonlinear dispersive mechanism of the freak wave formation in shallow water. In *Physica D* 147 (1-2), pp. 83–94.

PIANC (1995). Criteria for movements of moored ships in harbours. A practical guide. Supplement Bulletin 88. Working Group 24.

Puertos del Estado (1999). ROM 3.1.99. - Recommendations for the Project and the construction of accesses and flotation areas. Madrid, Spain

Pullen T., Allsop, N.W.H., Bruce T., Kortenhaus A., Schüttrumpf H. & van der Meer, J. W. (2007) *EurOtop: Wave Overtopping of Sea Defences and Related Structures: Assessment Manual*, pdf download available from : [www.overtopping-manual.com](http://www.overtopping-manual.com)

Rayleigh, L. (1876). On waves, *Phil. Mag. J. Sci.*, 1, 257–279.

Rosa Santos, P., Veloso Gomes, F., Taveira Pinto, F. and Brògueira Dias, E. (2010). Influence of the friction forces at the ship-fenders' interface on the behaviour of a moored oil tanker, Proc. of the *3rd Int. Conf. on the Application of Physical Modelling to Port and Coastal Protection – CoastLab'10*, Barcelona, Spain, Sept. 28-30 and Oct. 1. ISBN: 978-84-694-8586-6.

Rossetto T., Allsop N.W.H., Robinson D, Charvet I, Bazin, P-H (2008) Analysis of tsunami hazards by modelling tsunami wave effects, Proc *FLOODrisk 2008* conference, Oxford, publn Balkema

Rossetto, T., Allsop, N.W.H., Charvet, I. and Robinson, D. (2011). Physical modelling of tsunami using a new pneumatic wave generator, *Coastal Engineering* Vol 58, pp517-527, Elsevier.

Santel, F., Heipke, C., Könnecke, S. and Wegmann, H. (2002). Image Sequence Matching for the Determination of three-dimensional Wave Surfaces, *Proceedings of the ISPRS Commission V Symposium*, Corfu, Greece, Volume XXXIV Part 5, pp 596-600



- Schäffer, H.A. (1996). Second-order wavemaker theory for irregular waves. *Ocean Engineering*, Vol. 23, No. 1, pp. 47-88.
- Schäffer, H.A. and Klopman, G. (2000). Review of multidirectional active wave absorption methods. *J Waterway, Port, Coastal and Ocean Engineering*, pp 88-97.
- Schicker, R. and Wegener, G. "Measuring torque correctly", HBM manual, <http://www.hbm.com/en/menu/tips-tricks/torque-measurement/reference-book/>
- Schlurmann, T. (2000). The empirical mode decomposition and the Hilbert spectra to analyze embedded characteristic oscillations of extreme waves. In: *Rogue Waves*. Editions Infremer. pp. 157-165.
- Schlurmann, T. (2002). Spectral analysis of nonlinear water waves based on the Hilbert–Huang transformation. *Journal of Offshore Mechanics and Artic Engineering*, 124, pp. 22–7.
- Schmidt-Koppenhagen, R., Grüne, J. and Oumeraci, H. (2006). Tsunami wave decay in near- and onshore areas. *Proc Int Conf Coastal Eng*, 1664 – 1676.
- Schmittner, C., Kosleck, S. and Hennig, S. (2009). A Phase-Amplitude Iteration Scheme for the Optimization of Deterministic Wave Sequences. *Proceedings of 28th International Conference on Ocean, Offshore and Arctic Engineering*. ASME.
- Schüttrumpf, H.F.R. 2001. Wellenüberlaufströmung bei See-deichen, Ph.D.-thesis, Technical University Braunschweig.
- Schwarz, J. (1975). On the flexural strength and elasticity of saline ice. *Proc. 3rd IAHR Int. Symp. on Ice Problems*, Hanover, N.H., U.S.A., pp. 373-386.
- Schwarz, J. and Weeks, W.F. (1977). Engineering properties of sea ice. *J. Glaciol.*, 19(81): 499-531.
- Schwarz, J. (1977). New developments in modelling ice problems. In POAC 77: *Proceedings, 4th International Conference on Port and Ocean Engineering under Arctic Conditions*, 26–30 September, St. Johns, Newfoundland. Memorial University of Newfoundland, pp. 45–61.
- Schwarz, J. *et al.* (1981). Standardized testing methods for measuring mechanical properties of ice, *Cold Regions Science and Technology*, 4 (1981) 245-253 245, Elsevier, Amsterdam - Printed in The Netherlands
- Schwarz, J. (1983). Sea-ice investigations in in the Weddell Sea during the German antarctic expedition, 1979-80. *Ann. Glaciol.*, 4: 246-252.
- Serdula, C.D. and Loewen, M.R. (1998). Experiments investigating the use of fibre-optic probes for measuring bubble-size distributions. *IEEE J. Oceanic Eng.* 23, 385–399
- Shemer, L., Goulitski, K., Kit, E., Grüne, J. and Schmidt-Koppenhagen, R. (2005). On generation of single steep waves in tanks. In ASCE (Ed.): *Proc. 5th Int. Symposium on Ocean Wave Measurement and Analysis (WAVES)*. Madrid.
- Shimosako K, Takahashi S, Suzuki K, & Kang YK. (2002) *Large hydro-geo flume and its use for coastal engineering research*. Technical Note of National Institute for Land and Infrastructure Management; 41:81-89.

Shiraishi, S., Nagai, T., Hiraishi, T. and Yoneyama, H. (2006). Evaluation of cargo handling efficiency in the port taking into account the effect of long-period waves and its application. *Proc. of the 31st PIANC Congress*, Estoril, Portugal, May 14-18.

Shvayshteyn (1957). Laboratory for studying ice and testing models of icebreakers. *Problemy Arktiki*, 2:171-178 (in Russian).

Siffer, T. (2005) Mercator" depth gauge recording of 26 December 2004 tsunami. Previously available at <http://www.knmi.nl/onderzk/seismo>

Simons, R.R., Whitehouse, R.J.S., MacIver, R.D., Pearson, J., Sayers, P.B., Zhao, Y. and Channell, A.R. (1995). Evaluation of the UK Coastal Research Facility. *Proceedings Coastal Dynamics '95*, Gdansk, Poland, September 4-8 1995, 161-172.

Smits, A.J. and Lim, T.T. (Eds) (2012). *Flow visualisation: techniques and examples*, Second edition. World Scientific, 444pp.

Spencer, D.S. and Timco, G.W. (1990). CD Model ice: A process to produce correct density (CD) model ice. In *Proceedings of the IAHR 10th International Symposium on Ice*, August, Espoo, Finland. International Association for Hydraulic Research, vol. 2, p. 745–755.

Spinneken and Swan (2009). Second-order wave maker theory using force-feedback control. Part 1: a new theory for regular wave generation. *Ocean Eng* 36(8) 539-548.

Spinneken and Swan (2009). Second-order wave maker theory using force-feedback control. Part 1I: An experimental verification of regular wave generation. *Ocean Eng* 36(8) 549-555.

Stagonas, D. and Müller, G. (2007). Wave field mapping with particle image velocimetry. *Ocean Engineering*, 34 (11-12) August 2007, pp 1781-1785.

Stagonas, D., Müller, G., Batten, W. and Magagna, D. (2011). Mapping the temporal and spatial distribution of experimental impact induced pressures at vertical seawalls: a novel method. *5th International Short Conference on Applied Coastal Research*. RWTH Aachen University, Germany.

Stansberg, C.T., Baarholm, R., Fokk, T., Gudmestad, O.T. and Haver, S., (2004). Wave Amplification and Possible Deck Impact on Gravity Based Structure in 10-4 Probability Extreme Crest Heights. Paper No. 51506, *Proc., the 23rd OMAE Conf.*, Vancouver, BC, Canada, June 2004.

Stansberg, C.T. (2008). A Wave Impact Parameter, Paper OMAE2008-57801, *Proc., the 27th OMAE Conf.*, Estoril, Portugal, June 2008.

Stansberg, C.T. (2008). Current Effects on a Moored Platform in a Sea State, Paper OMAE2008-57621, *Proc., the 27th OMAE Conf.*, Estoril, Portugal, June 2008.

Stansberg, C.T., Øritsland, O. and Kleiven, G. (2000). VERIDEEP: Reliable Methods for Laboratory Verification of Mooring and Stationkeeping in Deep Water, Paper 12087, *Proc., Offshore Technology Conference (OTC) 2000*, Houston, TX, USA, May 2000.

Stansberg, C.T., Karlsen, S.I., Ward, E.G., Wichers, J.E.W. and Irani, M. B. (2004). Model Testing for Ultradeep Waters, Paper No. 16587, *Proceedings, Offshore Technology Conference (OTC) 2004*, Houston, TX, USA, May 2004.

Stansberg, C.T., Baarholm, R., Kristiansen, T., Hansen, E.W.M. and Rørtveit, G. (2005). Extreme Wave Amplifications and Impact Loads on Offshore Structures, Paper 17487, in *Proc., OTC 2005*, Houston, TX, USA, May 2005.

Stansberg, C.T. and Kristiansen, T. (2006). Non-linear Scattering of Steep Surface Waves around Vertical Columns, *Applied Ocean Research*, Vol. 27(2), pp 65 – 80.

Stansberg, C.T. and Pakozdi, C. (2009). Slowly Varying Wave Drift Forces Analysed from Model Test Data on a Moored Ship in Shallow Water. Paper OMAE2009-79491, *Proc., the 29th International Conference on Ocean, Offshore and Arctic Engineering*, Honolulu, HI, USA, May-June 2009.

Stansberg, C.T., Baarholm, R., Berget, K., and Phadke, A.C. (2010). Prediction of Wave Impact in Extreme Weather, Paper OTC-20573, *Proc., OTC 2010 Conf.*, Houston, TX, USA.

Stansberg, C.T., Berget, K., Graczyk, M., Muthanna, M. and Pakozdi, C. (2012). Breaking Waves and Resulting Slamming Pressures on a Vertical Column, *Proc., The 31<sup>st</sup> OMAE Conf.*, Rio de Janeiro, Brazil, June 2012.

Steendam, GJ, J. Van der Meer, P. van Steeg, A. Van Hoven, G. Van der Meer. (2013) Simulators as hydraulic test facilities at dikes and other coastal structures. *Proceedings of Coasts, Marine Structures and Breakwaters 2013*. Institution of Civil Engineers. Edinburgh.

Suliz, W. and Paprota, M. (2008). Generation and propagation of transient nonlinear waves in a wave flume. *Coastal Engineering* 55: 277-287.

Sutherland, J. and Barfuss, S. (2011). Composite Modelling, combining physical and numerical models. *Proc 34<sup>th</sup> IAHR World Congress*, Brisbane, Australia, p 4505-4512. CD-ROM, ISBN 978-0-85825-868-6.

Sutherland, J. and Evers, K.-U., 2013. Foresight study on the physical modelling of wave and ice loads on marine structures. *Proceedings of the 35th IAHR World Congress*, Chengdu, China. ISBN 978-7-89414-588-8.

Sutherland, J., Gerritsen, H. and Taveira Pinto, F. (2012). Assessment of test cases on composite modelling. *Proceedings of 10<sup>th</sup> International Conference on Hydroinformatics*, HIC 2012, Hamburg, Germany. ISBN 978-3-941492-45-5.

Svec, O.J. and Frederking, R.M.W. (1981). Cantilever beam tests in an ice cover: Influence of plate effects at the root, *Cold Regions Science and Technology* 4(2): 93-101.

SWIPA 2011 Executive Summary Report, AMAP Secretariat, Strømsveien 96, N-0032 Oslo, Norway

Synolakis CE. (1987) The runup of solitary waves. *Journal of Fluid Mechanics*, 185:523-545.

Tabata, T. Frijino, K. and Aota, M. (1967). Studies of the mechanical properties of sea ice. XI. The flexural strength of sea ice in situ. In: *Physics of Snow and Ice*. Inst. of Low Temp. Sc., Hokkaido Univ., Japan, Vol, I, pp. 539-550

Tadepalli, S. and Synolakis, C.E. (1994). The runup of N-waves on sloping beaches. *Proc. Royal Society, London, Series A* 445, 99–112.

Taveira Pinto, F., Veloso Gomes, F., Rosa Santos, P., Guedes Soares, C., Fonseca, N., Alfredo Santos, J., Paulo Moreira, A., Costa, P. and Brògueira Dias, E. (2008). Analysis of the behaviour of moored tankers, *Proc. of the 27th International Conference on Offshore Mechanics and Arctic Engineering - OMAE2008* (ed. ASME), Estoril, Portugal, ISBN: 0-7918-3821-8.

TAW Technical Advisory Committee on Water Defences (1990) *Probabilistic design of flood defences*, CUR, Gouda, the Netherlands.

TAW Technical Advisory Committee on Water Defences (2001) *Wave run-up and overtopping at dikes*, Technical Report A-99-32, Directorate-General for Public Works and Water Management, The Hague.

Tayfun, M. (1993). Sampling-rate errors in statistics of wave heights and periods. *Journal of Waterway, Port, Coastal & Ocean Engineering*, ASCE, 119(2) 172-192.

Teisson, C. and Benoit, M. (1994). Laboratory measurement of oblique irregular wave reflection from rubble-mound breakwaters. *Proc., 24th Int. Conf. Coast. Engrg.*, ASCE, 1610-1624.

Tekscan (2003): I-Scan Equilibration and Calibration Practical Suggestions (Rev.A).

Tekscan, Inc. South Boston, USA. Available online at <http://www.tekscan.com/sensor-technology>, checked on 21/05/2012.

Testa, D. (2006). Vorhersage kritischer Wellengruppen aus Seegangsregistrierungen im Ortsbereich. Diplomarbeit. TU Berlin, Berlin. Fachgebiet Schiffs- und Meerestechnik.

Thomas, R.E., Bouma, T., Dijkstra, J., Eiff, O., Frostick, L.E., Gobert, S., Henry, P.-Y., Johnson, M.F., Kemp, P., McLelland, S.J., Moulin, F.Y., Myrhaug, D., Neyts, A., Parsons, D.R., Paul, M., Penning, W.E., Puijalon, S., Rice, S.P., Stanica, A., Tagliapietra, D., Tal, M., Tørum, A. and Voudoukas M.I. (2012). Physical modelling of water, fauna and flora: Knowledge gaps, avenues for future research and infrastructural needs. HYDRALAB Deliverable D2.1, Available from [www.hydralab.eu](http://www.hydralab.eu)

Thunsyanthan, N. I. & Madabhushi, S. P. G. (2008) Tsunami Loading on Coastal Houses: a Model Approach. *Proc. ICE* vol 161, pp77-86.

Timco, G.W. (1981). Invited commentary: on the test methods for model ice. *Cold Regions Sci. and Tech.*, 4: 269-274.

Timco, G.W. and Frederking, R.M.W. (1982). Comparative Strengths of Freshwater Ice, *Cold Reg. Sci. Tech.*, 6: 21-27.

Timco, G.W. and Frederking, R.M.W. (1983a). Flexural strength and fracture toughness of sea ice. *Cold Regions Sci. Tech.*, 8: 35-41.

Timco, G.W. (1984a). Ice forces on structures: physical modelling techniques. In: M. Määttänen (Ed.), *2nd IAHR State-of-the-Art Report on Ice Forces on Structures*. Proc. IAHR Symposium on Ice, Hamburg, Germany, Vol. IV, pp. 117-150.

Timco, G.W. (1984b). Discussion of a fine grain model ice. *Proc. IAHR Symposium on Ice*, Hamburg, Germany, Vol. III, pp. 553-554.

Timco, G.W. (1985). Flexural strength and fracture toughness of urea model ice. *Proc. 4th OMAE Symp.*, Dallas, TX, U.S.A., Vol. II, pp. 199-208.

Timco, G.W. and Burden, R.P. (1997). An analysis of the shapes of sea ice ridges, *Cold Regions Science and Technology* 25 (1997) 65-77.

Troch P., De Rouck.J., Burcharth H.F (2002) Experimental study and numerical modelling of pore pressure attenuation inside a rubble mound breakwater, *Proc.28th International Conference on Coastal on Coastal Engineering*, ASCE, pp1607-1619.

Vagle, S. and Farmer, D.M. (1998). A comparison of four methods for bubble size and void fraction measurements. *IEEE J. Oceanic Eng.* 23, 211–222.

Vagle, S., Chandler, P. and Farmer, D.M. (2005). On the dense bubble clouds and near bottom turbulence in the surf zone, *J. Geophys. Res.*, 110, C09018, doi:10.1029/2004JC002603.

Valembois, J. (1951). Methods used at the National Hydraulic Laboratory of Chatou (France) for measuring and recording gravity waves in models, *Gravity Waves. Proceedings of the NBS Semicentennial Symposium on Gravity Waves*, National Bureau of Standards on June 18-20, 1951, US Government Printing Office, Washington DC.

Van den Boomgaard, M.J.G. (2003). Wave focussing in a laboratory flume. MSc thesis. Delft University of Technology, Delft.

Van der Meer, J., Provoost, Y. and Steendam, G.J. (2012). The wave run-up simulator, theory and first pilot test. *Proceedings of the 33<sup>rd</sup> Int Conference on Coastal Engineering*, Santander, Spain. <http://journals.tdl.org/icce/index.php/icce/index>

Van der Molen, W. (2006). Behaviour of Moored Ships in Harbours. PhD Thesis. Delft University of Technology, The Netherlands, 140p. ISBN-10:90-9021264-7.

Van der Molen, W. and Moes, H. (2009). General characteristics of South African ports and the safe mooring of ships. *Proc. of the 28th Annual Southern African Transport Conference*, Pretoria, South Africa, July 6-9, pp.308-314. ISBN: 978-1-920017-39-2.

Van der Molen, W. and Wenneker, I. (2008). Time-domain calculation of moored ship motions in nonlinear waves. *Coastal Engineering*, Vol.55, N°5, pp.409-422.

Van der Werff, S. and Haase, A. (2012). Influence of the Ice Concentration on the Ice Loads on the Hull of a Ship in a Managed Ice Field, *Proceedings of 31<sup>st</sup> International Conference on Ocean, Offshore and Arctic Engineering OMAE 2012*, July 1-6, 2012, Rio de Janeiro, Brazil, [OMAE2012-83927].

Van der Werff, S. (2012). *Dynamic positioning in Ice – Assessment of hull forces induced by managed ice fields*, TU Delft, Master thesis, June 2012.

Van Gent M.R.A. (1995). *Wave interaction with permeable coastal structures*, Communications on hydraulic and geotechnical engineering, Faculty of Civil Engineering, TU Delft, The Netherlands, ISSN 0169-6548



Van Gent (2002). Wave runup at dikes with shallow foreshores. *J. of Waterway Port and Ocean Eng.* 127 (5).

Vanneste D. & Troch, P (2010) Experimental Research on Pore Pressure Attenuation in Rubble Mound Breakwaters, *Proc. 32nd International Conference on Coastal Engineering*, ASCE, <http://journals.tdl.org/icce/index.php/icce/index>.

Van Os, A. (2010). A short history of experimental hydraulic research in the Netherlands and beyond. HYDRALAB report.

Van Thiel de Vries, J. 2009. Dune erosion during storm surges. PhD thesis – TU Delft. Deltares Select Series, Volume 3.

Veltcheva, A.D. (2002). Wave and group transformation by a Hilbert spectrum. *Coastal Engineering Journal*, 44(4), pp. 283–300.

Veltcheva, A.D., Cavaco, P. and Soares, C.G. (2003). Comparison of methods for calculation of the wave envelope, *Ocean Eng.*, 30, 937–948, doi:10.1016/S0029-8018(02)00069-0.

Veltcheva, A.D., Guedes Soares C. (2004). Identification of the components of wave spectra by the Hilbert Huang transform method. *Appl Ocean Res.* 26: 1-12.

Veltcheva, A.D. (2005). An application of HHT method to the nearshore sea waves. In: Huang N, Attoh-Okine NO, editors. *The Hilbert\_Huang transform in engineering*. CRC Press; p. 97-119.

Wanek, J.M., Wu, C.H. (2006). Automated trinocular stereo imaging system for three-dimensional surface wave measurements. *Ocean Engineering* 33 (5–6), 723–747.

Wang, Y.S. (1984). Discussion of a fine grain model ice. *Proc. IAHR Symposium on Ice*, Hamburg, Germany, Vol. III, p. 552.

Weeks, W.F. and Anderson, D.L. (1958). An experimental study of strength of young sea ice. *Trans. Am. Geophys. Un.*, 39(4): 641-647.

Wenneker, I., Borsboom, M.J.A., Pinkster, J.A. and Weiler, O.M. (2006). A Boussinesq-type wave model coupled to a diffraction model to simulate wave-induced ship motion. *Proc. 31st PIANC Congress*. Estoril, Portugal. May.

Whitehouse, R., Grass, T., Simons, R. and Howell, R. (1995). Evaluation of the UK Coastal Research Facility. Proceedings of the *30th MAFF Conference of River and Coastal Engineers*, Keele University 5-7 July 1995, pages 7.2.1 - 7.2.11.

Wiegel, R.L. (1955). Laboratory studies of gravity waves generated by the movement of a submerged body. *Trans. AGU* 36, 759–774.

Wilkie MJ, & Young GAJ. (1952) Pneumatic tide generator, *The Engineer*, July.

Woo, S.-B. and Liu, P.L.F. (2004). Finite Element Model for Modified Boussinesq Equations, II: Applications to Nonlinear Harbor Oscillations, *J. Waterway, Port, Coast and Ocean Engineering*, Vol 130, (1), pp17-28.

Yalin, M.S. (1971). *Theory of Hydraulic Models*. Macmillan.

Yim, S.C., Cox, D.T. and Park, M.M. (2009). Experimental and Computational activities at the Oregon State University NEES Tsunami Research Facility, *Science of Tsunami Hazards*, Vol. 28, No. 1, 2009, page 1-14.

Yim S, Yeh H, Cox D, & Pancake C. (2004) A shared-used large-scale multidirectional wave basin for tsunami research. *Proc. 13th World Conf. on Earthquake Engn.* Vancouver; Paper 1517.

Zelt, J.A. and Skjelbreia, J.E. (1992). Estimating incident and reflected wave fields using an arbitrary number of wave gauges. *Proc. 23<sup>rd</sup> ICCE*, Venice. pp777-788.

Zhang, H. and Schäffer, H.A. (2007). Approximate Stream Function wavemaker theory for highly non-linear waves in wave flumes. *Ocean Engineering* 34, pp 1290-1302

Zhang, H. and Schäffer, H.A. (2005). Waves in numerical and physical wave flumes – a deterministic combination. *Coastal Engineering* 2004: pp. 43-55.

Zhang, H., Schäffer, H.A. and Jakobsen, K.P. (2007). Deterministic combination of numerical and physical coastal wave models. *Coastal Engineering* 54, pp 171-186.

Zhang, Q. and van der Werff, S. (2012). Image Processing for the Analysis of an Evolving Broken-Ice Field in Model Testing, *Proceedings of the 31<sup>st</sup> International Conference on Ocean, Offshore and Arctic Engineering OMAE 2012*, July 1-6, 2012, Rio de Janeiro, Brazil, [OMAE2012-84117].

Zufelt, J.E. and Ettema, R. (1996). Model Ice Properties. CRREL Report 96-1. U.S. Army Cold Regions Research and Engineering Laboratory Hanover, NH, USA

## 10 Appendix A, Contributors to the report

The following people have contributed text to the report

<i>Name</i>	<i>Organisation</i>
James Sutherland	HR Wallingford
William Allsop	HR Wallingford
Daniel Donnai	HR Wallingford
Karl-Ulrich Evers	HSVA
Jens Kirkegaard	DHI
Stefan Schimmels	LUH
Maike Paul	LUH
Karunya Ramachandran	LUH
Marc Le Boulluec	Ifremer
Jeremy Ohana	Ifremer
Carl Trygve Stansberg	MARINTEK
Bas Hofland	Deltares
Panayotis Prinos	Aristotle Uni Thessaloniki
Francisco Taveira Pinto	FEUP, Porto
Ramon Gutierrez-Serrat	CEDEX
Rudiger von Bock und Polach	Aalto University
Ove Tobias Gudmestad	University of Stavanger

In addition, the scope, structure and contents of the report were discussed at a Foresight study workshop during the large HYDRALAB event in Catania, attended by the following people:

<i>Name</i>	<i>Org</i>
James Sutherland	HR Wallingford
Karl-Ulrich Evers	HSVA
Jens Kirkegaard	DHI
Stefan Schimmels	LUH
Jeremy Ohana	Ifremer
Thomas Galtier	Ifremer
Carl Trygve Stansberg	MARINTEK
Bas Hofland	Deltares
Panayotis Prinos	Aristotle University of Thessaloniki
Vincenzo Marletta	University of Catania
Xavier Gironella	UPC
Mark Healey	University College Cork (MARINET)
Francisco Taveira Pinto	FEUP, Porto
Ramon Gutierrez-Serrat	CEDEX

## 11 Appendix B Catenary mooring

A catenary mooring of an homogeneous line (with a zero bending stiffness and with an infinite axial stiffness modulus) as shown in Figure 11.1 can be described using the following equations.

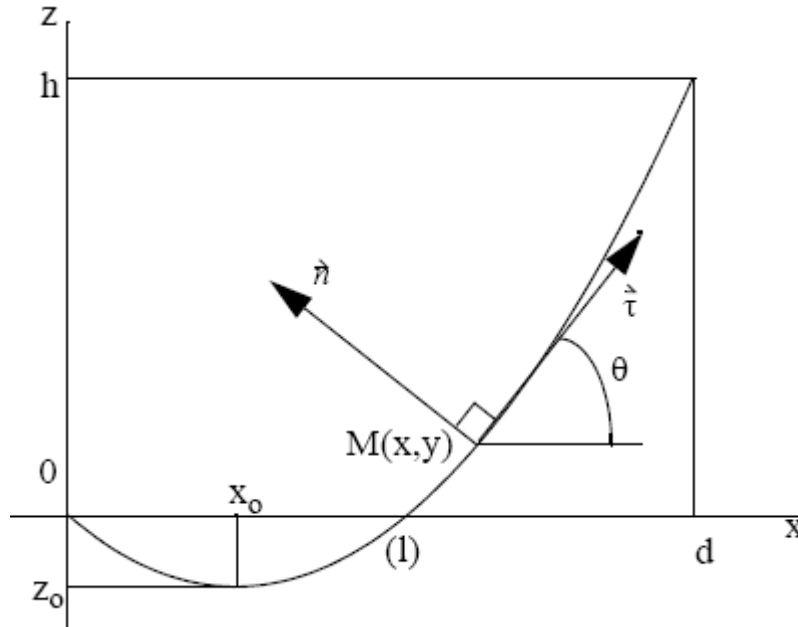


Figure 11.1 Catenary shape parameters of a line

3D coordinates (z vertical):  $x, y, z$

Catenary shape in (x, z) plane :

$$z - z_0 = \frac{T_0}{w} \left[ \cosh \frac{w}{T_0} (x - x_0) - 1 \right]$$

Linear weight :  $w$

Horizontal tension :  $T_x = T_0$

Vertical tension :  $T_z$

Tangent and normal vector :  $\vec{\tau}, \vec{n}$

Between end points

horizontal distance :  $d$

vertical distance :  $h$

length :  $l$

Non dimensional variables :

$$X = \frac{w}{T_0} x$$

$$Z = \frac{w}{T_0} z$$

$$S = \frac{w}{T_0} s$$

$$L = \frac{w}{T_0} l$$

$$D = \frac{w}{T_0} d$$

$$H = \frac{w}{T_0} h$$

$$Z - Z_0 = \cosh(X - X_0) - 1$$

$$S - S_0 = \sinh(X - X_0)$$

$$\frac{dZ}{dX} = \sinh(X - X_0) = \tan \theta = \frac{T_z}{T_x}$$

$$\frac{d^2 Z}{dX^2} = \cosh(X - X_0)$$

$$\tau_x = \frac{1}{\cosh(X-X_o)} \quad \tau_z = \tanh(X-X_o)$$

$$\frac{T_x}{T_o} = 1 \quad \frac{T_z}{T_o} = \sinh(X-X_o) \quad \frac{T}{T_o} = \cosh(X-X_o)$$

For the particular case of a bottom laying catenary line with its touch down point at  $x_o = z_o = 0$ :

Vertical tension at top :  $\frac{T_z}{T_o} = L$   $T_z = \varpi l$

Radius of curvature at the touch down point :  $R_o = \frac{T_o}{\varpi}$

Stiffness matrix in the mooring line plane :

$$\begin{bmatrix} dT_x \\ dT_z \end{bmatrix} = \begin{bmatrix} K_{xx} & K_{xz} \\ K_{zx} & K_{zz} \end{bmatrix} \begin{bmatrix} dx_e \\ dz_e \end{bmatrix} \quad \alpha = \frac{\varpi}{D \sinh D + H^2 - L^2}$$

$$K_{xx} = \frac{\varpi}{\alpha} \sinh D \quad K_{xz} = K_{zx} = \frac{\varpi}{\alpha} H \quad K_{zz} = \frac{\varpi}{\alpha} \left[ \frac{\alpha \sinh D + H^2 D}{L^2 - H^2} \right]$$

For lines composed of different segments, a simple algorithm can be used to ensure the continuity of the tension at consecutive end points.



## 12 Appendix C Foresight Study on the Physical Modelling of Wave and Ice Loads on Marine Structures

James Sutherland  
HR Wallingford, Howbery Park, Wallingford, Oxfordshire OX10 8BA, UK.  
Email: j.sutherland@hrwallingford.com

Karl-Ulrich Evers,  
Hamburgische Schiffbau-Versuchsanstalt GmbH (HSVA), Bramfelder Stasse 164, Hamburg, D-22305, Germany. E-mail: Evers@hsva.de

Paper published in the Proceedings of the 2013 IAHR World Congress, Chengdu, China.  
ISBN 978-7-89414-588-8.

**ABSTRACT:** The measurement of wave and / or ice loads on coastal and maritime structures can play an important role in their final design. The number and range of man-made structures that are subject to these loads is increasing – from offshore oil and gas facilities, through ships and, renewable energy devices, to breakwaters, quay walls, bridges and tunnels. This paper summarises the results of a Foresight Study, available from [www.hydralab.eu](http://www.hydralab.eu), which reviewed techniques for making physical model measurements of wave and ice loads on marine structures, summarised their weaknesses and outlined the advances in modelling techniques that the authors expect to see. The short-term developments that are expected include improvements in efficiency by the development of sampling schemes (so that shorter tests may be run) and the improvement of techniques for computing the low-frequency response of floating structures. They also include improvements in wave generation by improving techniques for producing focussed waves over varying bathymetry and in the presence of structures, improving shallow water wave generation using phase-resolving numerical wave models and developing novel forms of tsunami wave generation. We anticipate improvements in instrumentation, including the application of tactile pressure sensors to measure spatially-varying loads, the development of active (servomotor-based) transducers to reproduce non-linear responses and increases in the spatial coverage of optical and acoustic instruments. There will be improvements in access to data, including the sharing of meta-data over the semantic web and the transfer of data from remote experiments. The longer-term changes that are anticipated include (i) the development of composite models with full two-way coupling between numerical and physical models in real time, (ii) increased use of physical models with CFD, (iii) improved treatment of uncertainty, partly achieved through (iv) the provision of much more detailed datasets due to improvements in sensor size, resolution, sampling frequency and spatial coverage, (v) the development of the active laboratory, with many more computer-controlled non-linear devices, (vi) development of simulators to reproduce single phenomena (such as wave run-up or overtopping) in a controlled manner in the field and (vii) the development of more open science, with citations for publically-available data that can be found, described and downloaded over the web.

**KEY WORDS:** HYDRALAB, physical modelling, force, structure, foresight study.

### 1 INTRODUCTION

Mankind has built structures in, around, under or over water since the days of the earliest piers, bridges and enclosed harbours (C 2,500 BC). From offshore oil and gas facilities, through ports, terminals, marinas, quays and breakwaters, to groynes, bridges and pipelines, the number and range of man-made structures that interact with the hydraulic environment is increasing. There is a long history of conducting experimental tests of the interactions between water or ice and structures. The 20th century saw the development of many of the great

hydraulics and hydrodynamics laboratories that continue to use physical modelling as a design tool for river, coastal and marine structures. Indeed, the prevalence of hydraulics laboratories in Universities and Research Institutes across the world is testimony to the continued importance and influence of physical model testing in hydraulics today.

The study of wave or ice loads on man-made structures is an important sub-set of physical hydraulic modelling. Moreover, increasing development at the coast, the opening of new shipping routes in Arctic waters, the continued development of oil and gas facilities and the installation of shoals of renewable energy devices means that there is a continuing (and possibly even increasing) need for research and consultancy work on wave and ice forces on free-floating, moored and coastal structures.

The project HYDRALAB-IV has commissioned three Foresight studies into (i) water (including ice) and structures, (ii) water and environmental elements and (iii) water and sediments, each of which has developed a vision of how the physical modelling of water and the elements around it may evolve and has indicated the areas where the greatest changes are likely to occur. Each study has also identified what the possible consequences are for the development of our hydraulic laboratories, including instrumentation and facilities. All three foresight studies will be published on the HYDRALAB web site [www.hydralab.eu](http://www.hydralab.eu).

This paper summarises the foresight study into water (including ice) and structures (Sutherland and Evers, 2013) concentrating on the changes in facilities, instrumentations and techniques that are envisioned in the short-term (perhaps five years and generally based on on-going developments) and long-term (perhaps 10-15 years) which are more speculative. Due to the focus of the laboratories involved, the study is mainly confined to coastal and marine structures, where waves or ice loads are of greatest concern. The Foresight study (Sutherland and Evers, 2013) also contains sections on the following topics, which are not summarized here:

- Review of topics, which introduces four main classes of problems, (i) ships in harbours, (ii) floating structures in deep water, (iii) response of fixed structures to waves and currents, and (iv) response of structures to ice. The issues that are of greatest importance are described for each class of problem. The section ends with some observations on the trends observed in the modelling of particular topics.
- Establishing the correct environment, which is split into two main sub-sections: (i) establishing the correct hydrodynamic environment and (ii) establishing the correct ice environment. The former includes methods for producing waves, winds and currents, a summary of standard measurement techniques (for measuring surface elevation and velocity) and a section on measuring the air content in breaking waves. The latter includes descriptions of how ice sheets are produced, the measurement of ice properties and the modelling of different ice conditions (such as brash ice and ice ridges).
- State of the art in modelling techniques. This section is split into two main areas: (i) Model construction and (iii) Measuring and analysis techniques for modelling the forces on structures.
- Shortcomings, where limitations in our present methods are discussed.

## 2 SHORT-TERM DEVELOPMENTS

Improvements in techniques are anticipated over the next few years, although it is likely to take several more years for some of these techniques to achieve wide-spread use. The anticipated short-term advances are described in the sub-sections that follow. They have been arranged

into four categories: improvements in (i) the efficiency of testing, (ii) wave generation, (iii) instrumentation and (iv) access to data.

## **2.1 Improvements in efficiency**

### **2.1.1 Sampling schemes**

Long test series of several thousand waves have to be run in order to determine the response of a structure to high return period events. Davey et al (2008, 2010) applied an importance sampling technique to decrease the duration of a test run (overtopping over a vertical breakwater) by a factor of two to five. The development of other sampling schemes would allow shorter test series to be run for a wider range of structures and responses. Advances will come through the application of techniques to new cases and comparisons between different approaches.

### **2.1.2 Quadratic transfer functions**

Moored ships or other floating structures respond around their natural modes. The drift velocity of a free-floating body can be approximated by a simple model based on the equilibrium between the drift forces and drag forces. The drift forces are calculated from the second order quadratic transfer functions (QTFs) at zero frequency, taking into account their variations with the velocity through the wave drift damping (le Boulluec et al, 2008). Drag forces are tuned by a drag coefficient and a development of the square velocity. Side by side interaction involves precise modelling of the berthing lines and fenders (Lécuyer et al, 2012). Incremental advances are expected that will allow the calculation of QTFs to be undertaken more easily and with greater accuracy, while application of different methods to the same case(s) will point to the strengths and weaknesses of each approach.

## **2.2 Wave generation**

The ability to generate accurate representations of realistic sea states is a pre-requisite for many tests, so equipment manufacturers and facility operators are always looking to improve their wave generators. Three areas where wave generation is expected to improve within a few years are described below.

### **2.2.1 Coupling of Boussinesq model to wave paddle in shallow water**

Waves are typically generated in relatively deep water and then propagate up an artificially steep slope to an area where the bathymetry is realistic and can produce the desired wave characteristics at the structure. A smaller geometric length scale could be used in the same facility (or a smaller facility could be used at the same scale) if waves with the correct non-linear characteristics could be generated in intermediate to shallow water depths. Zhang and Schäffer (2005) originally coupled a Boussinesq wave model and a wave paddle to account for linear dispersion and shallow water non-linearities. Local wave phenomena – evanescent modes – are also taken into account so the elevation at the moving paddle can be computed. There is renewed interest in developing this approach for three dimensional sea states and different wave models.

### **2.2.2 Generation of tsunami-like waves**

Most piston paddles are limited in their ability to generating realistic tsunami waves by their stroke. One way to address this is to construct a flume with a long stroke. Wedges and landslides have also been used. Another approach is to use a pneumatic tsunami generator (Rossetto et al, 2011) which can generate controlled and stable simulation of extremely long waves led either by a crest or a trough (depressed wave). This pneumatic tsunami generator has been improved by the use of a computational fluid dynamics (CFD) model to test potential improvements, with only the best improvements being constructed and tested in the laboratory. More use of CFD models in the design of equipment and experiments is to be expected (see also Section 3.2).

### 2.2.3 Focused wave generation

In order to design safe and economic floating and non-floating structures along the coast and offshore, it is essential to model freak waves and other extreme wave patterns. This can be achieved in the laboratory using wave focusing techniques. Most of these use a linear back transformation from the target wave to the paddle, so non-linear effects and the effects of varying topography are neglected. Self-correcting techniques (Chaplin, 1996, Schmittner et al., 2009, Hofland et al. 2010) have proved promising in correcting for non-linear effects over a flat bathymetry. Fernández et al. (2013) have developed a self-correcting technique that uses a second order wave profile as the target signal at the focal point, is efficient and has been tested in a numerical wave tank for constant and variable water depth. The testing of such approaches to a range of non-linear applications over varying bathymetry in the laboratory and numerical wave tanks will increase confidence in the use of these techniques.

## 2.3 Improvements in instrumentation

### 2.3.1 Spatial variation of pressure

Traditionally, pressure measurements are conducted using an array of pressure transducers placed in the middle of the structure where the maximum pressures are commonly assumed to occur. In recent years the number of pressure sensors typically used has increased, with deployments of 16 to 32 becoming more common, due to advances in computers, data acquisition and sensor technology. Total forces are calculated by integrating the point measurements by assuming uniform pressure distribution between the sensors. For more complex studies the pressure distribution is significantly less well known and the calculated resultant force may vary quite considerably from the actual force (Alderson and Allsop 2007). Hence, there is a requirement to develop pressure measurement systems with high spatial and temporal resolution. This is already occurring through the application to hydraulics of technologies developed elsewhere and these developments are likely to continue. Two examples are given below.

Matrix based tactile sensors, such as those by Tekscan (2003) are attractive when there is a need to measure the pressure distribution with very high spatial resolution. A sensor consists of two thin sheets, which have electrically conductive electrodes deposited in varying patterns (Figure 1 left). The intersection of these rows and columns creates a sensing cell called a 'sensel'. The resistance of each sensel varies inversely with applied load. Stagonas et al. (2011) achieved simultaneous mapping of the horizontal and vertical distribution of wave impact pressures at the face of a vertical seawall in a small scale model, while Ramachandran et al (2013) present results from tests in a large-scale wave flume (Figure 1, right) and experiments have also been conducted on ice loads on a model lighthouse.

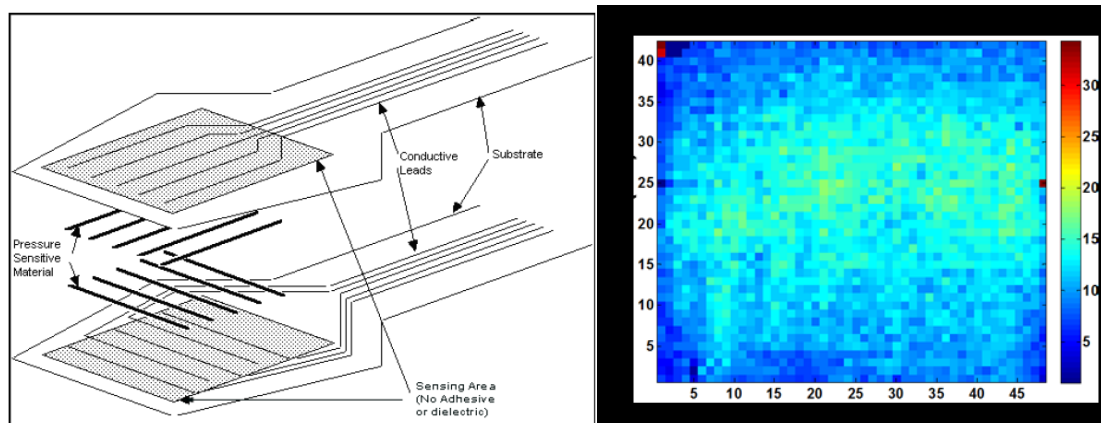


**Figure 1** Sensel arrangement (Tekscan, 2003, left) and spatial distribution of wave impact pressure (right, courtesy of Forschungszentrum Küste)

Tactile sensors have a lower sampling frequency than pressure sensors and only 8 bit digital output (0-255 scale) which lead to uncertainties in the results. For example, the 48 column by 42 row sensor used by Ramachandran et al. (2013) has a scanning rate of 680 Hz, which is not sufficient to entirely capture the peak impact pressures resulting from breaking waves. Further, simultaneous measurements of lower hydrostatic and impulsive peak pressures become quite challenging due to the lower output resolution (8 bits system). It may be several years before we see the size, sampling rate and resolution that would see tactile sensors acquiring a clear advantage over pressure sensors.

An alternative innovative approach to the development of pressure sensor arrays is to adopt the small sensors used by divers (of order 5mm in each direction). Eight have recently been deployed in a ring around a 70mm diameter cylinder. The test section was constructed using a 3D printer – another innovative technique which will be used more frequently in the future.

### 2.3.2 Active transducers

One aspect of floating structure physical modelling which has seen little change in decades is the representation of model elements (such as mooring lines and fenders) with nonlinear responses to applied loads. For such elements it is common practice to include an item of known stiffness e.g. a coil spring or length of metal, which gives a linear response to the applied load. The modeller can combine linear responses, through the introduction of stops, to better replicate the real non-linear system. This approach becomes increasingly complex to implement and tune where the load response is highly non-linear, such as in the buckling and recovery of a fender at high loads or the rapid irreversible extension of mooring lines prior to breaking.

An active transducer in the form of a servomotor will be capable of reproducing any elasticity curve on a physical model. The control capabilities of modern servomotors connected to programmable logic controllers allows for the accurate monitoring and control of both the torque being developed by the servomotor and the position of the servomotor's shaft (Figure 2). Assuming a linear relationship between the requested and delivered load, it is possible to adjust the torque of the servomotor dependent upon the shaft's position which essentially allows the replication of any elasticity characteristic likely to be required on a physical model. With changes in the hardware attached to the servomotor this system should be capable of modelling any part of a model for which precise deflection or extension under load is important.

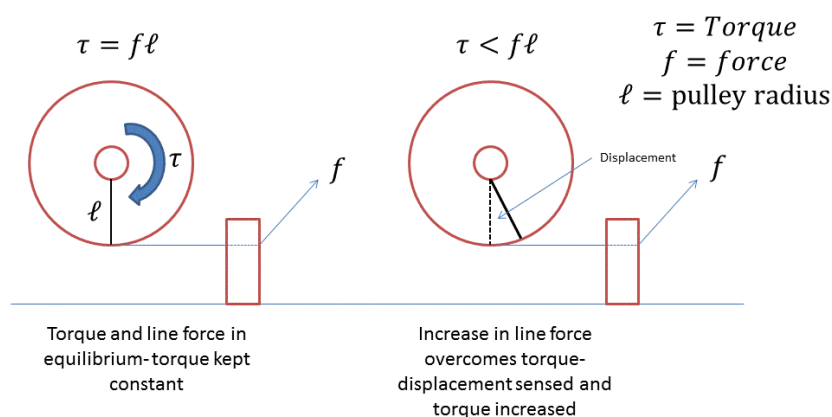


**Figure 2** Principles of an active transducer, illustrated by a mooring line

### 2.3.3 Optical or acoustic measurements of water surface

Physical models usually give the best description of non-linear wave processes, but this information cannot presently be obtained from the basins and flumes at the same spatial



resolution as numerical models. However, in the last decades a number of techniques have been developed whereby surfaces can be measured quickly and accurately. Stereo photography using digital CCD cameras can give a digital representation of a surface area after some post-processing. Laser scanners are used to scan 3D topographic data with more than 100,000 points per second and have been used for wave measurement in the field and in the laboratory (e.g. Blenkinsopp et al, 2010; Allis et al 2011). Range cameras (for instance used in the XBox game computer) can directly measure distances at about 10,000 points using a CCD chip that measures the phase of reflected infrared light. However, making these techniques robust for the hydraulic laboratory will require some work. The data processing must become fast and reliable (comparable to the development of numerical techniques), and the water surface must be visualized in an easy, not-too-intrusive, way. If these obstacles are overcome, it seems likely that we will be able to measure the water surface using these techniques relatively soon. This may lead to new analysis methods and parameters.

#### *2.3.4 Extension of optical / acoustic kinematics measurements to 3D volumes*

The development of acoustic and optical measurement techniques for measuring kinematics has led to improved understanding of the flows around structures. The extension of these techniques from measuring at a point to measuring profiles and eventually to measuring volumes will lead to increased information being obtained, which will inform our understanding of the reflection, refraction and diffraction of waves and flows around structures.

### **2.4 Improvements in access to data**

There are two main stages to ensuring that data can be re-used: finding a data set and transferring it. Ensuring that the data can be found and identified as useful and trustworthy by scientists and engineers who were not involved in collecting the data implies an increased use of meta-data. Within HYDRALAB ([www.hydralab-eu](http://www.hydralab-eu)) methods are being developed to share the meta-data collected on some projects over the world wide web. File-based data transfer is sometimes inefficient but offers a well utilised and simple structure for sharing data from a variety of sources.

## **3 LONG-TERM DEVELOPMENTS**

The short-term developments in the previous section indicate a trend towards specialisation in more complex, nonlinear phenomena, resolved at smaller scales. In this section, we propose changes that are likely to occur over a longer timeframe (perhaps 10 – 15 years). These technological developments will require innovation to bring us to a higher level of knowledge, which will allow physical modelling of wave and ice interactions with coastal and marine structures to remain a central part of the design and verification of these structures for many years to come. They have been split into four main sections covering improvements in techniques, instrumentation, facilities and openness.

### **3.1 Improvements in techniques**

#### *3.1.1 Development of composite models*

Composite modelling involves the combined use of more than one modelling tool (commonly a physical model and a numerical model) to address a complex problem (Gerritsen et al. 2011, Gerritsen and Sutherland 2011, Sutherland and Barfuss, 2011). One type of composite model is a hybrid model - where a physical model and a numerical model are run simultaneously and pass information between themselves in real time. True hybrid models (with two-way exchange of information) are rare and most test set-ups allow the sequential running of models and the one-way flow of information. The reasons for this include the difficulties in (i) running a numerical model synchronously with the physical model, (ii) passing information between models and (iii) getting the physical model to respond to the input from the numerical model. These difficulties are gradually being overcome, opening the realistic possibility that within a few years the full two-way coupling of numerical and physical models in real time will be achieved.

The starting point may be to use active transducers in a physical model, where the non-linear characteristics of the mooring line (for example) may be determined in advance. To advance from there, new technologies must be employed. For example, the reproduction of part of a mooring line may require an active transducer that varies its position, as well as its force/extension characteristics. That may require the use of a numerical model to calculate far field effects outside the physical model, with an active mooring line mounted on actuators at the interface between the physical and numerical models. Another potential development would be of a hexapode (6 dof motion mechanism) to enable the study of multi-parametric loads in relation to motions, eg full added mass or damping matrix. Two plates and 6 actuators have already been used by IFREMER to simulate the motion of a sea state.

### *3.1.2 Learning from CFD*

The development of Computational Fluid Dynamics (CFD) model code has put us in a position where CFD wave flumes and wave basins are being developed. This will draw the physical and CFD modelling communities together as both communities will be addressing similar problems, such as nonlinear wave generation and the absorption of reflected wave energy at the wave maker. The physical modelling community must be prepared to monitor developments in CFD and look for ways to implement the most promising approaches.

### *3.1.3 Treatment of uncertainty*

The increases in the volumes of data being collected and an improved awareness of risk (and hence uncertainty) are likely to lead to improvements in methods to define the uncertainty in measurements. Techniques will be developed to put uncertainty limits on measurements and to use measurements with uncertainty. It is common practice to compare predictions to measurements by assuming that the measurement is error-free. We will move towards analysis procedures that take into account the error in measurements.

Increases in spatial and temporal resolution, plus the increasing ability to measure over profiles or within volumes will lead to an increased capacity to measure the properties of turbulent flow fields. This is likely to lead to a better understanding of the role of turbulence and we will start to address more thoroughly questions such as: when is turbulence important and how do we characterise it?

## **3.2 Improvements in instrumentation: towards the active laboratory**

Sensors will reduce in size, increase in resolution and increase in sampling rates. The development of physical modelling facilities has already benefited tremendously from the increases in computer speeds, which has allowed more devices, such as wave paddles, to be controlled at higher speeds than before. The recent development of Ethernet technology (which can communicate over 1,000 channels at 1,000 Hz) has meant that communication speeds around the laboratory are substantially higher than could be achieved using RS232 or other cables.

The use of non-intrusive optical and acoustic methods will become more common and will cover larger areas. For example we may expect to see the use of optical techniques to measure surface elevations over a high-density spatial array of points at sampling rates of tens of Hertz. New materials, such as ferrofluids and other coatings, will be developed to measure shear stress, so that maps of shear stress distributions that vary in time over a surface will be produced.

The development of active transducers for mooring lines has been described above, while the active absorption of reflected waves (Schaffer and Klopman, 2000) is included in many modern wavemaker systems. Other potential applications of the active technology to the modelling of floating structures include breakaway tests (of the snapping of a mooring line) and recover

and constant tension winches, fenders, static and dynamic wind and current loading. Modern high performance embedded PC's are capable of running control logic for multiple servomotors with a cycle frequency measured in kHz, so several devices can be operated simultaneously alongside traditional wave gauges and other instruments. In the future we are likely to see laboratory set-ups featuring many more active systems (each with its own control loop).

### 3.3 Facility developments

Advances in wave generation and data collection are likely to continue in incremental steps. The mechanical designs of common wavemaker types (piston and flaps) are likely to remain substantially the same as they are today, with the development of new generation techniques for tsunamis adding diversity to the portfolio of options. Wave generation software will improve, including developments for focussed waves.

Both wind generation and current generation methods are relatively simplistic, with little control over changes in the spatial distribution or time-variation of wind or currents in many facilities. The cost of control systems has dropped significantly, so the development of spatial variations in wind or current fields may therefore come from the installation of many, smaller capacity pumps or fans, rather than through the manipulation of the output from a single unit.

Hydraulic and geotechnical engineering are generally taught separately at universities and their research studies have also been conducted separately. Geotechnics plays an important role in dike erosion (driven by wave overtopping) and also in the response of offshore foundations (such as wind turbine monopoles) which are excited by wave impacts. Greater links between hydraulic and geotechnics research will be developed to address these (and similar other) issues. This is likely to require specialized (or hybrid) facilities.

Whether or not the strength of a coastal structure can be modelled at small scale depends on the structure considered. Materials like grass on clay cannot be modelled easily on a smaller scale. Thus one can only perform tests of the materials on real dikes, or on parts moved to a large (or prototype) scale facility like the Delta Flume (Netherlands) or the GWK (Germany). Recently, simulators of a single process, such as wave overtopping, have been constructed in order to undertake controlled tests in the field (van der Meer et al, 2012, Steendam et al, 2013). Both wave run-up and overtopping simulators could be used to generate forces on a structure.

### 3.4 Open Science

An era of more open science is emerging, comprising: open source software, open software architecture, open access to data, open access publication and open collaboration (or networked science). There has been a rise in the use of open source numerical model codes and open software architecture, which can incorporate component models from different code bases using an interface standard such as OpenMI (<http://www.openmi.org/>). Meanwhile the importance of open access to public sector research has been recognised by the EC (2011) and there is a commitment to increasing access to data and publications within the EC's Horizon2020 research programme. Technologies for allowing open access to data from experiments are also being developed. Moreover, we are in an era of increasingly open scientific collaboration using the web.

The move towards open science is on-going but faces many difficulties. Nielsen (2011) predicts that it will only take place when we learn to value openness and the sharing of models and data as much as our publication and citation records. This will be assisted by the development of methods to assign a Digital Object Identifier, or DOI to datasets. DataCite (<http://datacite.org/>) for example, allocates DOIs that link to a public web page with meta-data about the associated dataset and a direct link to the data itself. This allows a dataset to receive a citation in a paper or report. The allocation of DOIs to quality physical model datasets will support researchers by

helping them to find, identify and cite these datasets with confidence. The inclusion of citations to data in the metrics produced by organisations such as the Web of Science would increase the citation records and h-indices of researchers who produce much-used datasets, which would change the culture of science to recognise the importance of sharing data.

It therefore seems highly likely that DOIs will start to be allocated to hydraulic datasets that are collected as part of research projects and that making data publically accessible will become a more common requirement of research organisations (such as the European Commission). This will lead to the development of shared datasets, which will help to create a free market in data, which every member of the community has equal access to. This will require protocols and standards to be developed, published, accepted and used. There will, for example, be benefits to enhancing the richness of information about shared data. This extra information will enable any interested party to judge the suitability and quality of the data. In order to do this we need to develop (and ideally consolidate) metadata standards and ontologies. Scientists and engineers will have to get used to the routine generation and use of metadata.

There is likely to be a move towards the standardisation of data, which is tending to occur at two levels: the structure of the data and its technical implementation. Definitions of data structure are independent of the file encoding. For example, ISO19115 outlines the data structure of spatial metadata with its XML encoding given in ISO19139. The supporting (use and discovery) metadata can be given in separate files to the values themselves. This is exhibited in formats such as CSML, NetCDF and XDMF, which offer a binary file type (such as HDF5) for high volumes. Also, directives such as INSPIRE provide a legal and technical framework for data interoperability. It includes specifications for the data, discovery, use and download services and is aimed at making the finding, using and sharing of data easier across the EU. However, for any practitioner wishing to offer a dataset to the wider community, the set of standards on offer is incomplete, overlapping and highly esoteric.

There is a role here for impartial, international organisations, such as International Association of Hydro-Environment Research and Development (IAHR) to provide repositories of (or links to) datasets that can become the de-facto standard for benchmarking tests.

#### **4 CONCLUSIONS**

Physical modelling has been the foundation of hydraulic and hydrodynamic studies for the past century and a half, particularly when it comes to the analysis of forces on structures and their interactions with waves, currents or ice. The complex, nonlinear phenomena involved in these interactions have been reproduced in the laboratory by increasingly sophisticated techniques for the reproduction of environmental conditions. The techniques used to measure the hydraulic, hydrodynamic and ice conditions and the resulting forces on structures have also improved immensely during this time. This has always meant that the most detailed studies of wave, flow and ice interactions with structures have been carried out in the laboratory, where conditions are controlled and experiments can be repeated. Field measurements, although more expensive and less controlled, have also played an important part in establishing knowledge about these interactions.

Improvements in numerical models, particularly computational fluid dynamics (CFD) codes, mean that these can now be used to determine forces on structures in relatively simple flow cases. CFD codes are being used at research organisations to model more and more complex structures and flow cases, such as waves breaking over structures. As the number of cases modelled increases, and more knowledge is gained in how to apply these models, they will be able to undertake more and more studies that previously could only be undertaken by a physical model. This does not, however, signal the end of physical modelling. Rather, it is likely to signal the start of a new era where numerical and physical modelling are used in collaboration

to address complex problems. There is a range of ways in which physical and numerical models can be combined (Sutherland and Barfus, 2011) including:

- Traditional nesting where a detailed physical model site within a regional numerical model;
- Numerical modelling can assist in the design of physical models;
- Numerical pre-modelling can provide information about potential problems associated with the theoretical design or proposed design changes to a structure, thereby reducing the number of physical modelling configurations that need to be tested.
- Modelling the model can allow a numerical model to be calibrated or corrected using the physical model results. The calibrated or corrected numerical model is then available to undertake additional model runs that would be too time consuming in a physical model or were only considered after the physical model has been decommissioned.

Clever combinations of physical and numerical modelling will be used in the design and testing of complex structures subject to extreme conditions for many years to come.

Laboratories have developed active feedback systems for absorbing re-reflected waves at wave paddles over the last twenty years (Schaffer and Klopman, 2000). The concept of the active transducer has now been extended to the reproduction of non-linear mooring lines. The same concepts and control systems could be applied to other phenomena, such as the snapping of a mooring line, constant tension winches, fenders or static and dynamic wind and current loading. Therefore we are likely to see the development of laboratories with many more active control systems.

The increases in computer power, the development of Ethernet technologies for transferring data and the shrinking of electronics mean that physical models have been able to make more and more detailed measurements at finer resolution and higher frequencies. This has allowed more detailed investigations of increasingly complex phenomena to be undertaken. This trend will continue and new measuring techniques will be developed, allowing physical measurements at a greater spatial density. We anticipate the use of more remote sensing (optical and acoustic). The improved spatial and temporal resolution of measurements will allow more detailed analysis of complex (often turbulent) phenomena; provide more data to validate numerical models and drive their development; allow the design of structures to be refined more than ever before; and generate unprecedented volumes of data.

The increased volume of data being generated will provide opportunities for this community and create additional obligations (especially when funding organisations begin to require open access to data as well as publications). Greater value will come from the sharing and re-use of data. This will require organisations to ensure that their data can be understood and read by others and comes with sufficient supporting information to indicate its quality. This is likely to drive moves towards common standards for meta-data and data and increased use of semantic web technologies for data discovery (although there is never likely to be a single standard for data). In an era when more data sets are public, we are likely to see a rise in data driven modelling and may gain benefits from the re-analysis of multiple data sets (as occurs in medicine, for example) which may reveal more information than any single data set. These developments will require this community to engage more with software developers.

Physical modelling of the interactions between structures and waves, flows or ice will continue to develop and will remain a core component of studies in this field for decades to come. There



will be an increased focus on non-linear phenomena, as numerical modelling takes over more of the modelling of shallow water flows and non-broken waves. There will therefore be an increasing emphasis on smaller spatial and temporal scales and on working with CFD models. The increasing specialisation in testing equipment and facilities makes it likely that there will be a reduction in the number of facilities with the capability to undertake the most advanced testing. There will therefore be a continued, and potentially increasing, demand for access to these facilities from regions and countries that do not possess such facilities. There is therefore a clear role for international funding organisations, such as the European Commission, in coordinating the access to and development of the largest facilities, in order to meet these needs.

## ACKNOWLEDGEMENT

The work described in this publication was supported by the European Community's 7th Framework Programme through the grant to the budget of the Integrating Activity HYDRALAB IV, Contract no. 261520. We acknowledge the contributions to the foresight study (Sutherland and Evers, 2013) by colleagues from HR Wallingford, HSWA, DHI, Forschungszentrum Küste, IFREMER, MARINTEK, Deltares, Aristotle University of Thessaloniki, University of Porto, CEDEX, Aalto University and the University of Stavanger. © HR Wallingford, 2013

## References

- Allis M.J., Peirson W.L. and Banner M.L., 2011. Application of LiDAR as a Measurement Tool for Waves. *Proceedings of the Twenty-first (2011) International Offshore and Polar Engineering Conference*. Maui, Hawaii, USA.
- Alderson J.S. & Allsop N.W.H., 2007. Comparisons of observed pressure integrated and directly measured global force measurements on caisson breakwater models *Proceedings of Coastal Structures 2007*, Venice. World Scientific, 249–258.
- Blenkinsopp C.E., Mole M.A., Turner I.L. and Peirson W.L., 2010. Measurements of the time-varying free-surface profile across the swash zone obtained using an industrial LIDAR. *Coastal Engineering* 57, 1059–1065.
- Chaplin J.R., 1996. On frequency-focusing unidirectional waves. *International Journal of Offshore and Polar Engineering* 6 (2).
- Davey T., Bruce T. and Allsop, N.W.H., 2008. Getting more from physical modelling – measuring extreme responses using importance sampling. *Proceedings 31st International Conference on Coastal Engineering*, 3058-3070.
- Davey T., 2010. *Modelling of extreme individual overtopping events at vertical seawalls*. PhD thesis. University of Edinburgh.
- European Commission, 2011. *Open Data, an engine for innovation, growth and transparent governance*. Communication from the Commission to the European Parliament, the Council, the European Economic and Social Committee and the Committee of the Regions, COM(2011) 882 final, Brussels.
- Fernández H., Schimmels S. and Sriram, V., 2013. Focussed wave generation by means of a self-correcting method. *Proceedings of the 23rd Int Ocean (Offshore) and Polar Engineering Conference*, ISOPE 2013, Anchorage, USA.
- Gerritsen H., Sutherland J., Deigaard R., Mutlu Sumer B., Fortes J.E.M., Sierra, J.P. and Schmidtke U., 2011. Composite modelling of the interactions between beaches and structures. *Journal of Hydraulic Research*. 49: sup1, 2-14.
- Gerritsen H. and Sutherland J., 2011. *Composite Modelling*. In Frostick, McLelland and Mercer (Eds), Users guide to physical modelling and experimentation: experience of the HYDRALAB Network. CRC Press/Balkema, Leiden, the Netherlands, 171 – 219.
- Hofland B., Kaminski M.L. and Wolters G., 2010. Large scale wave impacts on a vertical wall. *Proceedings 32nd International Conference on Coastal Engineering*. Shanghai, China.

Le Boulluec M., Forest B. and Mansuy E., 2008. Steady drift of floating objects in waves, experimental and numerical investigation. *Proceedings 27th International Conference on Offshore Mechanics and Arctic Engineering* (OMAE2008) Estoril, Portugal.

Lécuyer B., Ledoux A., Molin B., Le Boulluec M. and Heguiapal B., 2012. Hydro-Mechanical Issues of Offloading Operations Between a Floating LNG Terminal and a LNG Carrier in Side-by-Side Configuration. *Proceedings 31st International Conference on Offshore Mechanics and Arctic Engineering*. Rio de Janeiro, Brazil.

Nielsen M., 2011. *Reinventing discovery: the new era of networked science*. Princeton University Press. 280pp.

Ramachandran K., Schimmels S., Stagonas D. and Müller G., 2013. Measuring wave impact on coastal structures with a high spatial and temporal resolution – tactile pressure sensors a novel approach. *Proceedings 35th IAHR Congress*, Chengdu, China.

Rossetto T., Allsop N.W.H., Charvet I. and Robinson D., 2011. Physical modelling of tsunami using a new pneumatic wave generator. *Coastal Engineering*, 58, 517-527.

Schäffer H.A. and Klopman G., 2000. Review of multidirectional active wave absorption methods. *Journal of Waterway, Port, Coastal and Ocean Engineering*, pp 88-97.

Schmittner C., Kosleck S. and Hennig S., 2009. A Phase-Amplitude Iteration Scheme for the Optimization of Deterministic Wave Sequences. *Proceedings 28th International Conference on Ocean, Offshore and Arctic Engineering*. ASME.

Sutherland J. and Evers K.-U., 2013. *Foresight study on the laboratory modeling of wave and ice loads on coastal and marine structures*. HYDRALAB Deliverable D2.3. Available from [www.hydralab.eu](http://www.hydralab.eu).

Stagonas D., Müller G., Batten W. and Magagna D., 2011. Mapping the temporal and spatial distribution of experimental impact induced pressures at vertical seawalls: a novel method. *Proceedings 5th International Short Conference on Applied Coastal Research*. RWTH Aachen University, Germany.

Steendam GJ, Van der Meer J., van Steeg P., Van Hoven A. and Van der Meer G., 2013. Simulators as hydraulic test facilities at dikes and other coastal structures. *Proceedings of Coasts, Marine Structures and Breakwaters 2013*. Institution of Civil Engineers. Edinburgh.

Sutherland J. and Barfuss S., 2011. Composite Modelling, combining physical and numerical models. *Proceedings 34th IAHR World Congress*, Brisbane, Australia, 4505-4512, CD-ROM.

Tekscan, 2003: *I-Scan Equilibration and Calibration Practical Suggestions* (Rev.A). Tekscan, Inc. South Boston, USA. Available online at <http://www.tekscan.com/sensor-technology>, checked on 25/06/2013.

Van der Meer J., Provoost Y. and Steendam G.J., 2012. The wave run-up simulator, theory and first pilot test. *Proceedings of the 33rd International Conference on Coastal Engineering*, Santander, Spain. <http://journals.tdl.org/icce/>

Zhang H. and Schäffer H.A., 2005. Waves in numerical and physical wave flumes – a deterministic combination. *Coastal Engineering* 54(2) 43-55.